An in vitro study of the failure of short-fibre reinforced composite post and core restoration of endodontically treated teeth

Fawzia Salim AlZahrani

BDS, MDSc

Thesis submitted for the degree of Doctor of Philosophy

Adelaide Dental School, The University of Adelaide

June 2019

TABLE OF CONTENT

LIST OF FIGURES

LIST OF TABLES

LIST OF ACRONYMS

Bis-GMA	Bisphenol-A diglycidyl dimethacrylate
Bis-EMA	Bisphenol-A ethoxylated dimethacrylate
BMP	Bitmap
CT	Computed Tomography
EGDMA	Ethylene glycol dimethacrylate
ETT	Endodontically treated teeth
E-glass	Electrical -glass
FRC	Fibre Reinforced Composite
FOD	Fibre Orientation Distribution
GPa	Gigapascal
IPN	Interpenetrating Polymer Network
l_f	Fibre length
l_{fc}	Critical fibre length
l_{fo}	Optimal fibre length
mm	Millimetre
N	Newtons
n	Number of specimens per group (group size)
PFC	Particulate Filled composite
PMMA	Polymethyl methacrylate
ROI	Region of Interest
SD	Standard Deviation
SEM	Scanning Electron Microscope
Semi-IPN	Semi-Interpenetrating Polymer Network
SFRC	Short-Fibre Reinforced Composite
TEGDMA	Triethylene glycol dimethacrylate
TIIF	Tag Image File Format
UDMA	Urethane dimethacrylate
V_f%	fibre volume fraction
Wt_f%	fibre weight fraction
l/d	Aspect ratio: ratio of the fibre length to fibre diameter
µm	Micrometre

INTRODUCTION

In deep caries and trauma cases a tooth can lose a significant amount of coronal structure, and as a result might require root canal treatment (RCT). For the resultant endodontically-treated tooth (ETT) to satisfy its functional and aesthetic requirements, it should receive a well-designed, full-coverage crown as a final restoration. Commonly, prior to crown insertion, the missing tooth structure is reconstructed with a foundation restoration consisting of a post and core to provide sufficient anchorage for the crown.

Clinicians can choose from a range of alternative materials for post fabrication. In recent times, aesthetic, tooth-coloured, fibre-reinforced composite (FRC) posts have been developed to overcome the disadvantages of their metallic predecessors. The most recent potential addition to the restorative treatment options for ETT is a short-FRC (SFRC) post and core build up. This material consists of a semi-interpenetrating fibre network (semi-IPN) with randomly-orientated, discontinuous, short, E-glass fibres. The first commercially-available products of this type were introduced as bulk-fill restorations. Based on an assessment of physico-mechanical parameters of SFRC as a bulk-fill material, it was hypothesized that this material had the potential to sustain intraoral stresses and to function as a post and core restoration (Garoushi et al., 2013b). Subsequently, three studies have investigated SFRC as a post and core restoration in ETT (Bijelic et al., 2013; Forster et al., 2017; Nagas et al., 2017). They concluded that under static load application ETT restored with a SFRC post and core had a superior load bearing capacity compared with teeth restored with alternative materials.

To date, there is insufficient data on the fracture resistance and mode of failure of the ETT restored with SFRC as a post and core, particularly when applying a mechanical testing protocol that reflects the real clinical situation. Therefore, this research aims to fill this gap in our knowledge by investigating the failure of ETT restored with the SFRC as a post and core restoration under cyclic fracture resistance test protocol, followed by evaluating the mode of failure. Moreover, this research presents structural analyses of SFRC posts and cores before and after failure utilizing two analytical research tools; micro-Computed Tomography (micro-CT) and Scanning Electron Microscopy (SEM).

THESIS ABSTRACT

Statement of problem: There is insufficient data on the failure of ETT restored with SFRC as a post and core restoration.

Objectives: To comprehensively analyse the failure of ETT restored with SFRC as a post and core by conducting the following investigations: (1) analysis of the internal structures of SFRC posts and cores using micro-CT; (2) evaluation of failure load and failure mode of ETT restored with SFRC as a post and core after subjecting the teeth to fracture resistance testing and (3) analysis of the fractured surfaces of SFRC using SEM (fractography).

Methods: Extracted premolars were divided randomly into three groups (15 teeth/group); control group of untreated teeth (C), ETT restored with SFRC posts and cores(XFP), and ETT restored with prefabricated FRC posts (PFP). Teeth in XFP group and PFP group received RCT and were restored with posts and cores and ceramic crowns. Qualitative and quantitative analyses of SFRC posts and cores (XFP group) were performed using a micro-CT scanner and associated software. All groups were thermocycled and subjected to a gradual cyclic fracture resistance test followed by failure mode evaluation. Fractured XFP specimens were imaged using SEM for fractographic analysis.

Results: The control group had the highest mean failure load (1209.20N±126.65). The mean failure load of the XFP group (731.25N±86.33) was significantly higher ($P < 0.0001$) than the mean failure load of PFP group (373.85N±64.21). While all teeth in XFP group had restorable failures, four specimens (27%) in PFP group had non-restorable root fractures. Voids were detected inside SFRC post and core build-ups and at the interface between the posts and dentine. Voids were distributed evenly inside SFRC posts. 88.2%±2.6 of the voids were smaller than 100μm^3. For every 1% increase in the post voids, the mean failure load of teeth restored with SFRC posts increased by 53.9N. Fractographic analysis indicated that fibre orientation and distribution influenced the failure of ETT restored with SFRC posts.

Conclusions: Endodontically-treated premolars restored with SFRC posts and cores demonstrated high failure load and favourable failure modes. The presence of voids and alteration in fibre orientation and distribution can affect the failure of ETT restored with SFRC posts and cores.

DECLARATION

I certify that this work contains no material which has been accepted for the award of any other degree or diploma to Fawzia AlZahrani in any university or other tertiary institution and, to the best of my knowledge and belief, contains no material previously published or written by another person, except where due reference has been made in the text.

I certify that no part of this work will, in the future, be used in a submission in my name for any other degree or diploma in any university or other tertiary institution without the prior approval of the University of Adelaide and where applicable, any partner institution responsible for the joint award of this degree.

The author acknowledges that copyright of published work contained within this thesis (as listed below*) resides with the copyright holder of this work.

I give permission for the digital version of my thesis to be made available on the web, via the University's digital research repository, the Library Search and also through web search engines, unless permission has been granted by the University to restrict access for a period of time.

Fawzia Salim AlZahrani

Dated …19…/…8…/…2019…….

* AlZahrani, F. and Richards, L. (2018) 'Micro-CT evaluation of a novel periodontal ligament simulation technique for dental experimental models', Archives of Orofacial Science, 13(2).
* Figure 6.1 on page 108 of this thesis was obtained from Abouelleil et al. 2015.
* Figure 6.2 on page 108 of this thesis was obtained from Bijelic et al. 2016
* Figure 6.3 on page 109 of this thesis was obtained from Shouha, Swain and Ellakwa, 2014
* Figure 6.10 on page 119 of this thesis was modified from Karger-Kocsis & Friedrich 1988
* Figure 6.16 on page 126 and Figure 6.17 on page 127 of this thesis was modified from Roulin-Moloney, 1989

ACKNOWLEDGEMENTS

Before I begin to thank anyone or anything, I would like to thank the PhD I spent years working on to finally present this thesis. To say that the PhD journey was all fun and smiles would be a tremendous lie. It was one of the most challenging, gruelling and strenuous experiences in my life. Despite the many days I spent studying and investigating and the nights I spent worrying and thinking, I would not trade these past few years of hard work for nothing. I can never forget that the PhD was also the most beneficial and enlightening adventure in my life. However, I would not have been able to complete this work, to grow and learn, if it were not for the many people who constantly supported, and willingly guided me throughout the way.

First and foremost, I thank God for giving me the opportunity and the strength to accomplish this research study. Undertaking a higher-degree study abroad has been always one of my precious dreams. I am grateful to the Saudi government represented by the Saudi Arabian Cultural Mission in Canberra and Prince Sultan Medical Military City in Riyadh that helped me to peruse my dream and sponsored my scholarship to study in Australia.

I am truly grateful to my principle supervisor, Professor Lindsay Richards. Over the last few years, Professor Lindsay offered an untiring encouragement, support and guidance. He would always enlighten me to challenge my thinking and view issues from different perspectives. However, he would never instruct me directedly. He always has the right motivating story for every situation! I also appreciate his help in maintaining serenity and positivity when I tend to stray far from them. For all of that and more, I will be forever indebted to him. I must also give special thanks to my supervisors, Associate Professor James Dudley and Dr Sarbin Ranjitkar for providing valuable advice and heartfelt support.

It is a pleasure to acknowledge Adelaide Dental School for such pleasant and educational research experience that I had during my PhD studies. I must thank administrative and technical staff in Adelaide Dental Laboratory and Adelaide Dental Simulation Clinic, namely Victor Marino, Lucy Ludlow and Penny Tsoutouras for assisting me and providing me with the requisite materials and resources. Gratitude is also

due to academic and non-academic staff in Adelaide Dental School for their continuous support and sincere wishes.

I am thankful to Ms Ruth Williams, Dr Agatha Labrinidis and Dr Lisa Anne O'Donovan in Adelaide Microscopy department for their assistance and thorough training on Micro-CT scanner and software and SEM. I am also grateful to Ryan Quarriington and Dr. Clare Jones from Adelaide Engineering School for assisting me in the Instron machine programming. I truly appreciate the assistance and patience of Suzanne Edwards in Adelaide Health and Technology Assessment department during data statistical analyses.

To my friends; Zainab, Ruba, Mariam and Belinda. Thank you for your support, well-wishes, texts, phone calls, rides and stress-less dinners. Thank you for taking care of me and being there whenever I needed a true friend.

To my family. I am grateful to my parents who implanted in me ambition and eagerness to learn and grow. My kids; Mishari, Leena and Rayan, what an enriching life experience we had together in Australia during the PhD journey! It was elevating on many levels, but mostly it brought us closer together as a family. Thank you for listening to me and giving me advice. You even were parenting me sometimes! Finally, my husband, Abdullah, thank you for encouraging me to peruse my dreams and being always there to support me and take care of me. Thank you for believing in me even when I lose faith in myself. Thank you for being in my life.

CHAPTER 1

Background and Aims

This chapter presents a literature review to document the development of non-metallic fibre-reinforced composite (FRC) posts as alternatives to metallic posts, the development of the contemporary short-fibre reinforced composites (SFRC) and their application as post and core systems. This chapter concludes by defining the aims of the thesis.

1.1 Endodontically Treated Teeth (ETT)

An endodontically treated tooth (ETT) is a tooth that has received Root Canal Treatment (RCT) to manage acute or chronic pulpitis resulting from dental caries and/or trauma (Shillingburg and Kessler, 1982). Successful RCT starts with complete canal cleaning and shaping in order to decontaminate the pulp, followed by root canal obturation (Schilder, 1966). When performed properly, RCT should eliminate infection and protect the tooth and surrounding structure from microbial spread (Gulabivala and Ng, 2004).

According to Morgano and Brackett (1999), after successful endodontic and restorative treatment, an ETT should resume its normal function. However, the biomechanical changes and structural strength of ETT are controversial subjects in the literature. Some investigators have indicated that ETT are brittle due to compositional alterations following endodontic treatment. The brittleness of ETT has been attributed to moisture loss (Helfer et al., 1972; Kishen and Asundi, 2005; Jameson et al., 1993), collagen content alteration (Ferrari et al., 2004, Moreira et al., 2011) and blood supply impairment (Baraban, 1967). Other group of researchers have suggested that the ability of ETT to resist fracture is affected, not by the compositional alterations, but by the coronal and radicular dentine loss due to deep caries, trauma, previous restorations and root canal treatment procedures (Steagall et al., 1980; Larson et al., 1981; Trope et al., 1985; Sedgley and Messer, 1992; Assif and Gorfil, 1994; Reeh et al., 1998; Bier et al., 2009). On the other hand, other investigators have concluded that there are no significant structural or mechanical differences between ETT and vital teeth (Fusayama and Maeda, 1969, Lewinstein and Grajower, 1981, Rivera et al., 1988, Papa et al., 1994).

1.2 Restoration of ETT

Despite the disagreement on the biomechanical changes in ETT, the restoration of the missing tooth structure immediately after RCT is mandatory for the tooth to resume masticatory and aesthetic functions (Morgano, 1996) and to prevent coronal micro-leakage (Wu et al., 1998; Ng et al., 2006).

Restorative options for ETT varies from conservative access cavity restoration to a complete coverage (artificial crown placement) depending on the amount of missing tooth structure. Crown placement is indicated in ETT with substantial coronal tooth loss due to deep caries, trauma or previous complex restorations.

Before crown placement, a foundation or core restoration is required to reconstruct the missing coronal structure. The core restoration restores the coronal geometry that provides retention and resistance requirements for the crown (Rosenstiel et al., 2006).

Different guidelines for core restoration material selection and design have appeared in the literature (Shillingburg et al., 1970; Christensen, 1996; Smith and Schuman, 1997; Fernandes et al., 2003; Schwartz and Robbins, 2004; Rosenstiel et al., 2006). The guidelines are based on the overall prosthetic treatment plan, the material's physical and mechanical properties, tooth location in the dental arch (anterior vs posterior) and the amount of intact remaining tooth structure. Considering the aforementioned guidelines, different restorative protocols have been suggested, of which, post and core restoration is an option.

1.3 Post and core restorations

Post and core restorations are often used to restore ETT with extensive loss of coronal tooth structure. This approach involves placement of the post in the canal to support the core restoration followed by a full crown or fixed partial denture (PDF). Posts and cores are constructed separately or as a single unit utilizing different materials and techniques.

1.3.1 Rationale of the post placement

According to the Glossary of Prosthodontic Terms, the post is "usually made of metal that is fitted into a prepared root canal of a natural tooth. When combined with an artificial crown or core, it provides retention and resistance for the restoration" (The Academy of Prosthodontics, 2005). Although this definition does

not reflect the versatility of the currently available post and core systems, it outlines the post's main function. The post is inserted in the canal to provide retention and anchorage for the core restoration, when adequate coronal tooth structure is not available to support the core (Cheung, 2005; Schwartz and Robbins, 2004). Additionally, an ideal post should aim to preserve tooth structure and disperse intraoral forces in a strategic pattern within the radicular dentine in order to avoid increasing tooth susceptibility to fracture (Sokol, 1984; Sorensen and Martinoff, 1984a; Assif et al., 1993; Asmussen et al., 1999; Yenisey and Kulunk, 2008).

The functions of posts are affected by factors such as post length, diameter, design, surface configuration and material composition (Sokol, 1984; Holmes et al., 1996; Stockton, 1999; Cheung, 2005). In terms of material composition, posts are generally categorized as metallic or non-metallic.

1.4 Metallic posts

1.4.1 Classifications of metallic posts

A Metallic post was traditionally the standard of dental care for the restoration of ETT (Perel and Muroff, 1972, Shillingburg et al., 1970). Metallic post can be either custom-fabricated (cast post and core) or prefabricated.

Guidelines for fabricating a cast post and core are well documented (Lloyd and Palik, 1993; Shillingburg et al., 1997; Rosenstiel et al., 2006) and involves either a direct (auto-polymerizing acrylic resin pattern) or indirect (root canal impression) duplication of the prepared canal morphology into a one piece post and core pattern, which is cast in either gold (precious) alloy, base (non-precious) metal alloys or silver-palladium alloys (Dale and Moser, 1977). Cast post and core is generally indicated in ETT with minimal sound coronal structure available to support the crown (Bergman et al., 1989; Morgano and Milot, 1993; Smith and Schuman, 1997), and in cases where adjustment of tooth alignment to accommodate the adjacent teeth is required (Schwartz and Robbins, 2004; Rosenstiel et al., 2006). The indirect techniques are also an efficient way to fabricate multiple posts and cores with minimal chair-side time (Schwartz and

Robbins, 2004). However, the construction of such posts includes two clinical visits, additional laboratory work and extra fees. Additionally, the cast post and core fabrication procedure necessitates temporary restoration placement, which might increase the risk of root canal contamination (Fox and Gutteridge, 1997).

To avoid additional chair-side time and the laboratory stage and temporisation, prefabricated metal posts have been developed. Prefabricated posts are cemented or screwed into the root canal followed by core construction using amalgam, resin composites or resin-modified glass-ionomer. Prefabricated metal posts are available in different structural compositions, designs and surface configurations to suit different clinical situations. The metal composition of a prefabricated post can include different pure metals or alloys such as, stainless steel, pure- titanium, titanium-based alloys, platinum-gold-palladium and chromium-based alloys (Shillingburg et al., 1997; Rosenstiel et al., 2006). There are two surface configurations of the prefabricated metal posts; serrated posts (active) that engage the canal walls and smooth posts (passive) that are retained in the canal by a luting agent. In terms of designs, prefabricated post is either tapered or parallel sided. It has been suggested that the prefabricated post's design, composition and surface configuration can influence the longevity of the restored ETT, therefore, proper prefabricated metal post selection is paramount.

1.4.2 Limitations of metallic posts

Increasing numbers of practitioners have moved away from the use of metallic posts due to their unavoidable biological, mechanical and aesthetic properties. Both custom-fabricated and prefabricated metallic posts are generally dark-coloured, which restrict their use in highly aesthetic areas. Metal deterioration and release of corrosion by-products is a common long-term disadvantage of metallic posts (Angmar-Mansson et al., 1968; Derand, 1971; Arvidson and Wroblewski, 1978). It is believed that corrosion by-products accumulate inside the root and exert pressure between the post and canal walls and eventually lead to root fracture (Angmar-Mansson et al., 1968; Rud and Omnell, 1970; Petersen, 1971; Arvidson and Wroblewski, 1978). Moreover, corrosion by-products have been detected in the dentinal tubules (Silness et al., 1979) and gingival tissue surrounding teeth restored with metal posts

(Arvidson and Wroblewski, 1978), which has been related to the development of tissue irritation, hypersensitivity and allergic or toxic reactions (Frykholm et al., 1968; Christensen, 2004).

More than forty years ago, it was widely believed that placement of a stiff metal post strengthened the ETT (Perel and Muroff, 1972; Kantor and Pines, 1977;Trabert et al., 1978; Sapone and Lorencki, 1981). But, more recent studies have challenged this believe and confirmed the tendency of metal posts to increase the chance of irreversible root fracture (Lovdahl and Nicholls, 1977; Guzy and Nicholls, 1979; Assif and Gorfil, 1994; Sorensen and Martinoff, 1984b; Trope et al., 1985; Cormier et al., 2001; Akkayan and Gulmez, 2002). In this regard, it has been speculated that the poor mechanical performance of metallic posts is due to disparity in physical properties, namely the modulus of elasticity, between the metal posts (ranges between 53 GPa – 200 GPa) and dentine (15 - 40 GPa), which hinders the uniformity of stresses distribution in the restored ETT (O'Brien, 2002; Kinney et al., 2003; Torbjorner and Fransson, 2004; Dietschi et al., 2007; Dietschi et al., 2008). Finite element analyses (FEA) have demonstrated that the stresses accumulated around the metal post circumferentially and apically, which might protect the tooth's cervical structure but leads to catastrophic root fracture below cemento-enamel junction (Eskitascıoglu et al., 2002; Asmussen et al., 2005; Boschian Pest et al., 2006; Rodriguez-Cervantes et al., 2007).

Placement techniques of threaded, prefabricated metal posts can also introduce undue stresses during threading and tapping. When poorly placed (off centred), serrated post can cause uneven internal stresses distribution and root fracture (Standlee et al. 1972; Standlee and Caputo 1992).

Precise adaptation is an advantage of cast post techniques compares with the prefabricated post alternatives. However, some technical issues during cast post fabrication can lead to undesirable outcomes. For example, it has been suggested that the presence of undetected casting defects (nodules) on the surface of the cast post can affect post adaptation and act as a wedging point with possible root fracture (Morgano and Milot, 1993).

Since non-resinous cements (zinc phosphate, glass ionomer and poly carboxylate) are traditionally used to cement metallic posts, the bonding depends on mechanical interlocking between the post and dentine (Hanson and Caputo, 1974; Jokstad and Mjor, 1996). Therefore, insertion of a wider and longer post was a common practice to improve the retention of the non-adhesively bonded metallic post (Standlee et al., 1972; Standlee et al., 1978; Sorensen and Martinoff, 1984a). The undue removal of tooth structure associated with this approach weakens the ETT and possibly results in root perforation and disturbance of apical seal with further compromise of ETT prognosis (Sokol, 1984; Mattison et al., 1984; Hunter et al., 1989).

Metal posts have shown inconsistent clinical performance results, which further complicates the clinician decision. In a 25-year clinical follow up study, ETT restored with cast post and core had a similar survival rate to crowned vital teeth (Valderhaug et al., 1997). Comparable results were documented in other retrospective (Roberts, 1970; Turner, 1982; Bergman et al., 1989; Mentink et al., 1993) and prospective (Ellner et al., 2002) research. On the other hand, after reviewing the clinical records of 1273 ETT, Sorensen and Martinoff (1984b) found that regardless of the tooth location in the mouth, teeth restored with cast post and core had significantly higher failure rate when compared to teeth crowned without post placement. Compared to prefabricated metal posts, cast posts and cores have demonstrated both similar (Salvi et al., 2007) and lower survival rates (Sorensen and Martinoff, 1984a; Torbjorner et al., 1995).

1.5 Non-metallic posts

Athey, defines a "system" as “any set of components working together for the overall objective of the whole” (Athey, 1982). In a dental context "biomimetics" is a term that refers to “mimicking or recovery of the biomechanics of the original tooth by the restoration” (Magne and Douglas, 1999). Combining the two concepts, planning the restoration of ETT should be based on the compatibility of the restoration with the dentine to work as one system. The compatibility needs to be on mechanical, biological and aesthetic levels. Ideally, the post and core material should induce no adverse biological reaction, it should also be

tooth-coloured or translucent, especially with the increasing demand for all-ceramic crown restorations. In addition, post and core materials should be of similar physical properties to each other and to dentine (Akkayan and Gulmez, 2002; Lassila et al., 2004; Torbjorner and Fransson, 2004).

Assessment of the structural, mechanical and functional properties of the teeth has led to the development of restorative systems that mimic teeth nature. In this context, non-metallic posts, namely Fibre Reinforced Composite (FRC) posts, were introduced and perceived by clinicians as an alternative post material to the traditional metallic predecessor. FRC posts are composite resin intra-radicular posts that characterized by improved mechanical, aesthetic and bonding properties.

1.6 Composite resin

Dental composite resin is composed of inorganic phase of reinforcing fillers within an organic phase of monomer matrix that polymerizes during application and a silane coupling agent that bind the filler to the matrix. Additional chemicals such as polymerization reaction initiators, pigments and stabilizers are added to the matrix.

Classically, matrix in dental composite is dimethacrylate-based; e.g. Bis-GMA (bisphenol-A glycidyl dimethacrylate), Bis-EMA (bisphenol-A ethoxylated dimethacrylate) and UDMA (urethane dimethacrylate) and diluted with TEGDMA (triethylene glycol dimethacrylate) or EGDMA (ethylene glycol dimethacrylate) to control matrix viscosity (Ferracane, 2011; Bayne and Thompson, 2013).

The reinforcing phase in dental composite is essentially silica-based fillers that are modified by other ions such as lithium, boron or yttrium to achieve desirable properties such as easier manufacturing and improved radiopacity (Bayne and Thompson, 2013). During the last sixty years, the *particle-filler* geometry, content, morphology and distribution have been subjected to continuous modifications, which resulted in the development of a wide range of Particulate Filler Composite (PFC) with variable physical and mechanical properties, consistencies and application techniques (Figure 1.1). Therefore, dental composite can be classified according to:

- consistency: into flowable and condensable,
- insertion technique: into injectable or packable (applied with hand instrument),
- application technique: into indirect and direct (further classified as incremental or bulk-fill*),
- polymerization method: into light-cured, self-cured and dual-cured,
- filler size: into macro-filled, midi-filled, micro-filled, nano-filled and hybrid (mixed ranges of particle sizes) (Figure 1.1).

During the evolution of different composite formulations, the reinforcing fillers have been modified to improve the mechanical properties, polymerization shrinkage, aesthetics and wear resistance of composites as well as to broaden their clinical applications (Ilie and Hickel, 2009). In this context, the interest in FRC that are reinforced with *fibre-fillers* has increased.

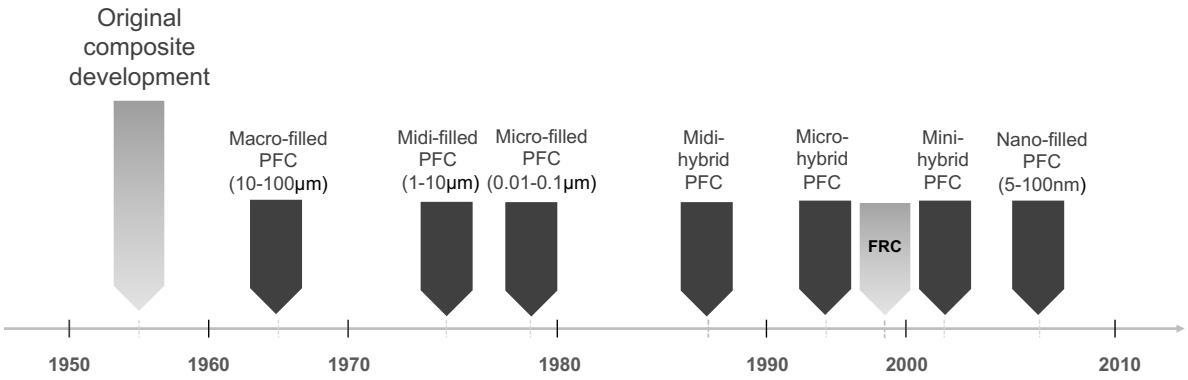

Figure 1.1: The historical evolution of dental composite based on reinforcing fillers alterations (Ferracane, 2011 and Bayne and Thompson, 2013).

** Bulk-fill are newly introduced composite resins that are applied as a bulk of 4mm or more to simplify the restorative procedure and reduce the chair-time and drawbacks of incremental application*

1.7 Fibre Reinforced Composites (FRC)

Fibre reinforced systems are naturally available in structures such as wood, which is reinforced with short cellulose fibres and in bone and dentine, which are reinforced with collagen fibres. Hence, the idea of fibre reinforcement was applied in many man-made products where high static and dynamic strength and fracture toughness are desired. FRCs have functioned successfully in a range of industrial applications such as aerospace systems, marine and automotive industries, building constructions, medical applications, furniture and sports equipment. Industrial FRC gained popularity due to their strength, adaptability to conventional manufacturing technique and low fabrication cost.

In dentistry, the concept of fibre reinforcement was first introduced and used in acrylic removable denture bases in early sixties (Smith, 1962). However, due to handling and technical difficulties in combining the fibres into the resin systems, the availability of dental FRCs for clinical application was delayed until late nineties (Meiers and Freilich, 2000; Vallittu, 1996; 1997b).

When first used in the acrylic base of removable dentures, the reinforcing fibres were found to be superior to conventional metal wire reinforcement (Vallittu, 1996). Thereafter, the reinforcing fibres were successfully combined with dimethacrylate resins and particulate filler composites (Vallittu, 1997a , Meiers and Freilich, 2000). An improved understanding of the FRC led to the development of a wide range of FRC-based dental materials that are now used in different dental disciplines (Vallittu, 2018) including fixed prostheses (Freilich et al., 1998), implant prostheses (Meiers and Freilich, 2006), orthodontics (Rantala et al., 2003), periodontics (Meiers et al., 1998), endodontics (Goldberg and Burstone, 1992) and restorative dentistry (Fennis et al., 2005).

1.7.1 Structure of FRCs

FRCs are essentially polymer matrix with embedded reinforcing fibre-fillers connected via a silane coupling agent.

Polymer matrix: consists of a cross-linked polymer matrix, which is a resin-based composite such as epoxy resin or dimethacrylate-based materials (Lamichhane et al., 2014; Tanner and Le Bell, 2016).

Recently, a new FRC matrix has been developed by mixing the cross-linked resin with a linear poly methyl methacrylate (PMMA) non-crosslinked resin to create a multiphasic polymer blend known as a semi-Interpenetrating Polymer Network (semi-IPN) (Vallittu, 1995b; Sperling and Mishra, 1996). On the molecular level, the two polymers in the semi-INP polymer are partially interwoven but are not chemically bonded to each other, and upon setting reaction, a well interlocked structure is established (Sperling and Mishra, 1996). The function of the matrix is to absorb and transfer the stresses to the reinforcing fibres and protect the fibres from surrounding moisture in the oral cavity (Tanner and Le Bell, 2016).

Reinforcing fibres: fibres of a variety of types, geometry (length and diameter), orientations and quantity are incorporated into the matrix in different FRCs. When FRCs are in function, the following fibre-related factors contribute to the reinforcement efficiency of the fibres and the structural, mechanical, physical and optical properties of the FRCs:

1.7.2. Fibre-related factors

1.7.2.1 Fibre length

Reinforcing fibres in FRC can be long (continuous) or short (discontinuous), which is further described as micrometre-scale or millilitre-scale fibres. The use of long fibres in dental composite is justified by the superior reinforcement achieved along their long axis (Vallittu, 1999). Short discontinuous fibres have been introduced recently to reinforce dental composites that are known as short-FRCs (SFRCs). However, the short-fibres length (l_f) needs to exceed a critical fibre length (l_{fc}) to offer an effective reinforcement (Petersen, 2005). The critical fibre length is the minimum length that allow efficient transfer of the load from the matrix to the fibres (Norman and Robertson, 2003), which for SFRC has been estimated to be as much as 50 times the diameter of the fibres (Batdorf, 2012; Petersen, 2005). Short-fibres with a subcritical length have ineffective reinforcement (Hull and Clyne, 1996; Callister and Rethwisch, 2007)

Additionally, the ratio of the fibre length to fibre diameter (l/d), which is given as a number and known as fibre aspect ratio, is another parameter that has an influence on the reinforcement efficiency of FRC (Lee,

1992; Vallittu, 2015). The higher the aspect ratio, the greater is the strength of FRC (Lee, 1992). On the contrary, in the FRC with low aspect ratio, the fibre ends create discontinuity in the matrix, act as stress concentration, and consequently weaken the composite (Shouha et al., 2014). The lowest limit for efficient fibre aspect ratio in dental SFRC has been determined to be 5.2, whereas the highest aspect ratio that assure a significant improvement in the mechanical properties ranges between 68 and 640 (Kardos, 1985; Shouha et al., 2014).

1.7.2.2 Fibre orientation

The reinforcing fibres can be oriented in a unidirectional (aligned) manner, where the fibres are parallel to each other, or they can be in a bidirectional orientation (woven, knitted or braided). Fibres can also be multidirectional (randomly oriented) in three or two dimensions (Bateman et al., 2003; Vallittu, 2009).

The mechanical properties of the FRC are affected by the orientation of the fibres in relation to the direction of the applied stresses. Hence, FRC can be classified as isotropic or anisotropic (Murphy, 1998). FRC with unidirectional fibres are described as anisotropic, which means that the material possesses different properties in different directions. In other words, the material provides maximum reinforcement when the stresses are exerted along the long axis of the fibres and the reinforcement reduces when the stresses are perpendicular to the long axis of the fibres (Khan et al., 2015). On the other hand, FRC with randomly oriented fibres in three dimensions (3D) are isotropic. Isotropic material provides the same mechanical properties regardless the applied stresses direction. However, if the fibres are randomly oriented in two dimensions (e.g. transversely oriented) the isotropic properties are changed to anisotropic properties (Zhu et al., 1997). Finally, bidirectional FRCs are orthotropic with same properties in one direction of the fibres and different properties in the other direction (Khan et al., 2015).

The theoretical estimate of the mechanical strength magnitude of FRC –based on fibre orientation– is described as Krenchel's factor (Krenchel, 1964). Krenchel's factor scales the efficiency of fibre reinforcement from 0 to 1 (Figure 1.2). Unidirectional fibres attain the highest Krenchel's factor =1 (100%) when the stresses are in the direction of the fibre's long axis and reaches the lowest value (Krenchel's

factor=0) when the stresses are perpendicular to the fibres' long axis. Other fibres orientations have variable Krenchel's factor values that ranges between 0.2 to 0.5. For example, bidirectional fibres can achieve reinforcement in two directions with Krenchel's factor 0.5 (50%) or 0.25 (25%), and randomly oriented fibres provides same reinforcing properties in all directions with Krenchel's factor of 0.38 (38%) when oriented in 2D and 0.2 (20%) when oriented in 3D (Chong and Chai, 2003).

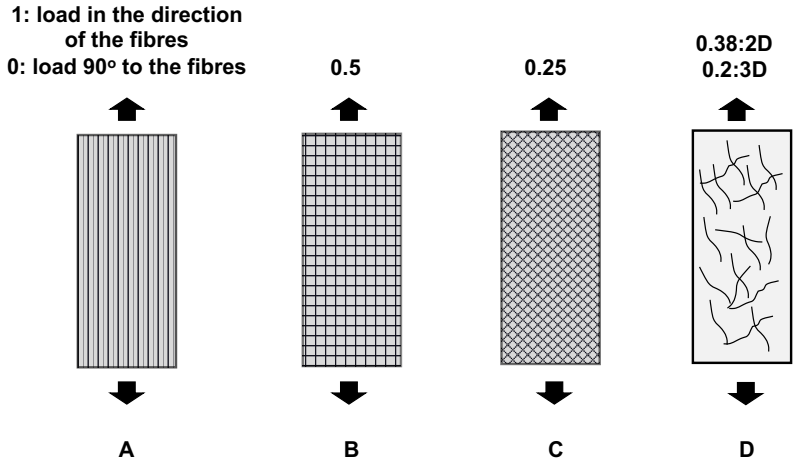

Figure 1.2: Reinforcing efficiency (Krenchel's factor) for different fibres orientation; A: Unidirectional, B: Bidirectional (0/90), C: Bidirectional (45/45) and D: Random orientation (arrows indicate the direction of the load) (modified from Tanner and Le Bell, 2016).

1.7.2.3 Fibre impregnation

Effective impregnation is achieved when the matrix is completely contacting all surfaces of reinforcing fibres. Fibre impregnation is accomplished during FRC manufacturing process, and it is essential for durable adhesion between the fibres and the matrix and therefore effective transfer of the load from matrix to fibres and optimal mechanical performance and longevity of dental restorations (Vallittu, 1995b; 2009). The complete degree of impregnation can be obtained easier if the fibres are pre-impregnated either with polymer, monomer or with a combination of both (Vallittu, 1997b; Lastumaki et al., 2002). Strong adhesion between the fibres and the polymer matrix is further enhanced by pre-treatment of the fibres with silane coupling agents (Vallittu, 1993)

Failure to achieve successful impregnation (e.g. due to resin high viscosity or polymerization shrinkage) might lead to failure to reach the theoretically-calculated mechanical strength values of FRC (Vallittu,

1998b; 2009). The degraded mechanical properties in such cases have been explained by fibre debonding and voids formation as a result to incomplete impregnation. Voids might increase the chance of water sorption, which results in hydrolytic degradation of the resin or discoloration of the composite due to microbial invasion (Miettinen and Vallittu, 1997). Moreover, voids can act as oxygen reserves, which might affect the complete polymerization process (Lastumaki et al., 2003). Consequently, to overcome the problem of incomplete impregnation, pre-impregnated fibres with the linear poly methyl methacrylate (PMMA) has been introduced (fibre-resin prepregs) (Vallittu, 1998b; 1999).

1.7.2.4 Fibre quantity

Fibre quantity in FRC is expressed in fibre volume (V_f%) or fibre weight (Wt_f%) fractions, which indicate the fibre volume and weight in relation to matrix volume and weight, respectively. Fibre weight can be measured by simply weighing the fibres during manufacturing of an FRC product. Fibre weight fraction can be converted to volume fraction using a mathematical formula when the densities of the fibres and the matrix are known. The FRC product developers measure the fibre volume fraction for more control of the structural performance of the material (Vallittu, 2015).

Although it has been found that increasing the fibre volume increases the mechanical properties of the FRC material (Norman and Robertson, 2003), the fibre volume fraction should not exceed a critical fibre volume fraction limit, which ranges between 45-65% (Vallittu, 1994; Lassila et al., 2005; Ilie and Hickel, 2009). Excessive fibre inclusion can create defects/flaws in the matrix and affect the impregnation of the fibres with the matrix and, consequently, the transferability of the load from matrix to fibres (Lassila and Vallittu, 2004).

1.7.2.5 Fibre type

As part of the development of FRCs, several reinforcing fibres have been used. Initially carbon/graphite fibres were used to reinforce composites. Despite the strong reinforcement guaranteed by carbon fibres, their black colour and complicated manufacturing technique limit their dental applications (Torbjorner et al., 1996).

Ultrahigh molecular weight (UHMW) polyethylene fibres are one of the strongest available reinforcing fibres (Gutteridge, 1992; Murphy, 1998). Nevertheless, their clinical use is limited also due to technical difficulties in bonding to the dental polymers as well as their high affinity to microbial adhesion in the oral environment (Gutteridge, 1992; Tanner et al., 2003).

Currently, glass fibres are predominantly used to reinforce composites in both industrial and dental applications. For dental FRCs, the composition and the mechanical and optical characteristics of glass fibres support their compatibility with dental polymers (Murphy, 1998; Tanner and Le Bell, 2016). Glass fibres have high mechanical strength, low cost, transparent aesthetic appearance, and most importantly a surface composition that permits adequate adhesion to the polymer matrix (Vallittu, 1993; 1996; Ellakwa et al., 2002). Glass fibres are formed by mixing and heating raw materials (sand, kaolin, limestone and colemanite) at a temperature of 1600°C. The liquid glass mass is then transformed into filaments, from which the fibres are processed.

The first generation of glass fibres used in dentistry required the dentist/technician to manually add resin and bonding agent to the nonimpregnated fibres. The second generation were preimpregnated with resin by the manufacturer. The second generation glass fibres were first produced in 1999 by Vallittu, who introduced the pre-impregnation of the fibres to overcome the technical challenges with the first generation and to improve the fibres adhesion to the polymer matrix.

There are different types of glass fibres classified according to their structural composition, mechanical and chemical properties (Vallittu, 1998a; 1998b):

- A-glass (Alkali),
- C-glass (Chemically resistance),
- D-glass (Dielectric),
- E-glass (Electrical),
- R-glass (Resistance), and
- S-glass (High strength).

E-glass fibres is the most commonly used to reinforced dental composites, followed by S-glass fibres.

1.8 Glass FRC in dentistry

The glass FRCs are used in different applications in dental practice. Glass FRC periodontal splints are used as an alternative to the metal wire splints (Hoeppner et al., 2011). Glass FRC is used also for both active and passive orthodontic appliances (Burstone and Kuhlberg, 2000) and as implant supra-structures (Meiers and Freilich, 2006). In fixed prosthodontics, glass FRC is used for direct (Freilich et al., 1998; Vallittu, 2001) and indirect (Meiers and Freilich, 2006) fabrication of fixed partial dentures (FPD).

In restorative dentistry, FRC was used as a substructure that is covered with a PFC surface layer to create bilayered composite restorations (Garoushi et al., 2007a; Garoushi et al., 2007b). One of the restorative applications of glass FRC is the restoration of ETT (Garoushi et al., 2013a). This includes using glass FRC as a core restoration (Tuncer et al., 2013; Kemaloglu et al., 2015) and/or as a root canal post material (Newman et al., 2003; Mannocci et al., 2008; Bijelic et al., 2013; Abduljawad et al., 2016).

1.9 Glass FRC as a root canal post system

Since the development of glass FRCs, and with the growing interest in aesthetic dental restorations during the past decades, progress has been made toward optimizing their mechanical and handling properties and introducing them as a potential post material for ETT. This has been achieved through manipulating the size, quantity and orientation of the glass fibres as well as changing the matrix formulations. As a result, different glass FRC post systems have been introduced: prefabricated FRC posts, individually-formed FRC posts and short-FRC (SFRC) posts (Figure 1.3).

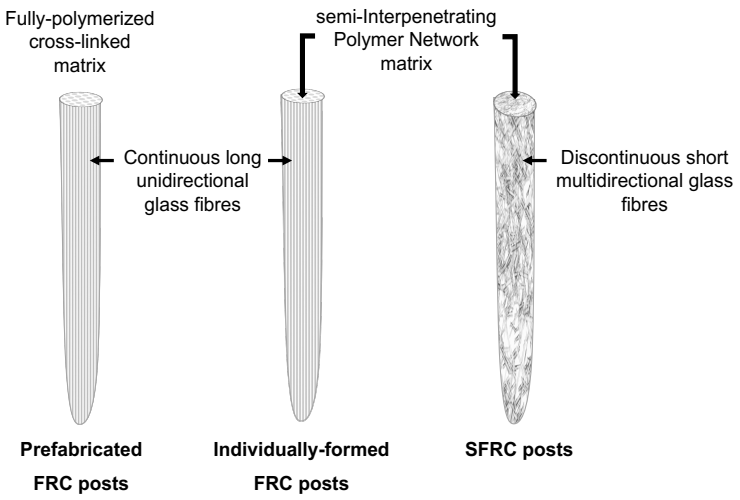

Figure 1.3: Schematic demonstration of glass FRC root canal post systems showing the difference in the matrix and reinforcing glass fibres.

1.9.1 Prefabricated glass FRC post

The concept of incorporating reinforcing fibres into the resin matrix to produce intra-radicular post has been demonstrated primarily in the prefabricated FRC posts. Prefabricated FRC posts were first produced and used clinically in 1989 in France (Composipost, C-Post™). The first scientific article on FRC posts was published in 1990, by Duret et al. (Duret et al., 1990), and in 1998, the first long-term clinical study on that post system was published (Fredriksson et al., 1998).

The prefabricated FRC post consists of high volume fraction of closely packed long continuous unidirectional fibres embedded in a fully-polymerized (cross-linked) matrix of epoxy resin or a combination of epoxy and dimethacrylate resins (Lamichhane et al., 2014). The first prefabricated FRC post contained dark carbon/graphite fibres. It was popular until glass reinforced prefabricated posts were introduced (Goldberg and Burstone, 1992). Since then, a wide variety of prefabricated glass FRC posts manufactured in several compositions, designs, dimensions, translucencies, and therefore variable mechanical and physical properties, have become available. Prefabricated glass FRC posts are cemented to the canal using composite resin luting cements. Subsequently, a core is constructed using a variety of composite resin materials.

1.9.1.1 Advantages of prefabricated glass FRC posts

When compared to metallic posts, prefabricated glass FRC posts are biologically, mechanically and aesthetically compatible with tooth structure. Prefabricated glass fibre posts have been primarily promoted for their modulus of elasticity that is compatible with the dentine when compared to metallic posts (Table 1.1). This compatibility has been reported to allows slight post flexion during function, which presumably dissipate stresses and reduces the likelihood of unfavourable tooth failure (Fokkinga et al., 2004; Galhano et al., 2005; Boschian Pest et al., 2006; Varvara et al., 2007).

Additionally, when compared to metallic posts, prefabricated FRC posts have demonstrated, high flexural strength (Stewardson et al., 2010) and high fatigue resistance (Wiskott et al., 2007). However, it is noteworthy that variable physical and mechanical properties have been reported for different prefabricated glass FRC posts with different dimensions, designs, compositions and manufacturing qualities (Seefeld et al., 2007, Freedman and Jain, 2008).

Table 1.1: Elastic modulus of human dentine, prefabricated FRC and metallic posts

Material	**Elastic modulus** (GPa)		**Reference**
Dentine		15-40*	O'Brien, 2002; Kinney et al., 2003; Ziskind et al., 2011; Zhang et al., 2014.
Prefabricated glass FRC post		15-24	Lassila et al., 2004; Plotino et al., 2007; Zicari et al., 2013.
		40	Pegoretti et al., 2002.
		29-46	Mallick, 2007.
Metallic post	Titanium	66-110	O'Brien, 2002; Plotino et al., 2007; Dietschi et al., 2007; Goracci and Ferrari, 2011.
	Stainless steel	109-202	
	Gold	53-108	O'Brien, 2002; Pegoretti et al., 2002; Plotino et al., 2007.

*Values vary based on dentine location, tooth type and dry/moist environment.

The use of adhesive systems and resin cements allows bonding the prefabricated FRC posts to dentine (Love and Purton, 1998). It has been suggested that adhesively bonded post (using resin cements) together with a composite resin core, creates a homogenous unit, which might further contribute in the homogeneity of stresses distribution in ETT (Mendoza et al., 1997; Mezzomo et al., 2003).

The prefabricated FRC post is translucent and has been described as a “fibre-optic light guide” that carries the light deep into the root canal (Strassler, 1999; Bassi, 2001; Milnar, 2010). In addition to enhanced aesthetics, light transmitting translucent post can enhance the post retention and ultimately the final structural integrity of the restored ETT (Pitel and Hicks, 2003). Nevertheless, studies have documented that some light was transmitted through the translucent FRC post up to a depth of 10mm (Teixeira et al., 2006) but not at the apical third of the root (Galhano et al., 2008), which suggests that this proposed advantage may be limited.

1.9.1.2 Limitations of prefabricated glass FRC posts

One of the shortcomings of the prefabricated FRC posts is the fact that they are manufactured to a predetermined shape and diameter that rarely adapt well to the root canal anatomy. Therefore, they are centrally positioned in the neutral axis of the canal. The consequences of this limitation are summarized in figure 1.4.

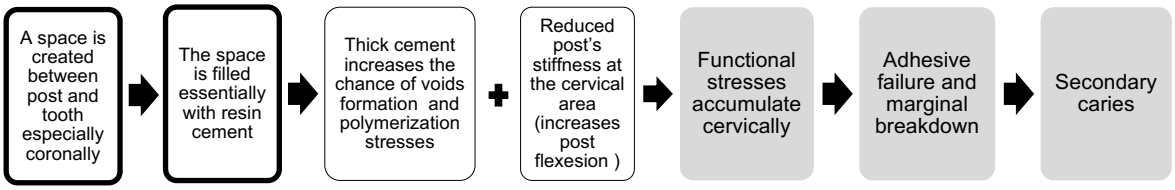

Figure 1.4: Possible consequences of imprecise adaptation of prefabricated FRC post to canal walls. (Tanner and Le Bell, 2016).

The second disadvantage of prefabricated FRC posts is related to the inner structure of the post. The matrix is highly cross-linked (polymerized to a high degree of conversion) and allows no inter-diffusion bonding between the post and the adhesive cement or resin-based core materials (Lastumaki et al., 2003; Monticelli et al., 2004; Sadek et al., 2007). Therefore, the post’s retention to dentine and core material is described as a mechanical interlocking, not a chemical bonding. However, manufacturers continuously introduce surface features and recommend chemical and mechanical pre-conditioning to improve the adhesion of the post to tooth structure and core material (Sahafi et al., 2002; Monticelli et al., 2006; Perdigao et al., 2006).

The fibres in the prefabricated glass FRC post are arranged in a continuous longitudinal manner. Therefore, under intraoral loading conditions, the post possess its maximum strength and mechanical performance when the load is along the fibres' long axis, but when the load is perpendicular to the fibres, the reinforcement efficiency of the post is reduced (anisotropy) (Vallittu, 2015). Importantly, intraoral loads are multidirectional.

1.9.1.3 Studies on prefabricated glass FRC posts

The data for prefabricated FRC posts derived from in vitro studies are variable, especially when reporting the mechanical performance of the posts under stresses (Cormier et al., 2001; Akkayan and Gulmez, 2002; Hu et al., 2003; Giovani et al., 2009; McLaren et al., 2009). The variable results in these reports are ascribed to variability in design (cylindrical or tapered), surface characteristics (smooth-sided, threaded or serrated) and dimensions of the tested posts. Additionally, different manufacturers produce prefabricated FRC posts with different fibre/matrix ratio, fibre diameter, and fabrication quality. Moreover, there is lack of consistency in testing protocols, such as nature of load (static/dynamic), load direction and angle, which hampers the assessment and comparison of the reported results and conclusions.

The reports on the fracture resistance of ETT restored with prefabricated glass FRC posts in comparison to metal posts were inconclusive. Higher failure load has been reported in metal posts (Newman et al., 2003; Qing et al., 2007; McLaren et al., 2009), and in FRC posts (Barjau-Escribano et al., 2006; Hayashi et al., 2006) while other reports have found no significant difference in failure loads between metal and FRC posts (Hu et al., 2003; Fokkinga et al., 2006a). However, dental clinicians predominantly appreciate a restoration that have high probability of tooth-repairability in cases of failure, to avoid extracting the tooth and complicating the treatment plan. In this regard, in a review conducted by Fokkinga et al. (2006), they concluded that ETT restored with FRC posts have more restorable failures than metal posts (prefabricated and cast posts).

Although several systematic reviews have been reported on FRC posts, all agreed that it is difficult to compare the clinical studies due to inconsistencies in sample selection and the baseline evaluation

protocol such as RCT quality evaluation, remaining tooth structure (e.g. ferrule effect) and presence/absence of parafunctional habits (Soares et al., 2012; Dikbas and Tanalp, 2013). Nevertheless, over reasonably long follow-up periods in both retrospective (Signore et al., 2009; Ghavamnasiri et al., 2011) and prospective (Naumann et al., 2005a; Naumann et al., 2005b; Zicari et al., 2010; Schmitter et al., 2011; Naumann et al., 2012; Gbadebo et al., 2014) clinical studies, prefabricated FRC post showed favourable clinical performance with high survival rates (65%- 98%-follow-up period of 2 -7 years) and a more repairable root fracture when compared to metal post.

Finally, in finite element analyses (FEA), prefabricated FRC posts demonstrated high stresses in the cervical region due to post flexibility and lowest stresses inside the root (Pegoretti et al., 2002; Boschian Pest et al., 2006).

1.9.2 Individually-formed glass FRC post

Although several attempts have been undertaken to improve the bonding between the prefabricated glass FRC post and the adhesive cements through chemical treatments of the post, neither the chemical pre-treatment modalities nor the adhesive monomers were able to penetrate the fully polymerized matrix of the prefabricated glass FRC posts (Le Bell-Ronnlof et al., 2004; 2005). Hence, an intra-radicular post with a partially polymerized matrix was developed. This was achieved by manufacturing a glass FRC material consisting of a semi-IPN matrix that is reinforced with continuous longitudinal fibres. Among the dental applications of this glass FRC material is the restoration of ETT where the FRC is used to construct individually-formed posts (Fokkinga et al., 2006a; Abo El-Ela et al., 2008; Yang et al., 2008; Ozcan and Valandro, 2009,). For individually-formed post construction, multiple strips of the material are cut and adapted to fit the post space depth and width, then polymerized in situ. This is followed by composite core build up.

1.9.2.1 Advantages of individually-formed glass FRC posts

Since both prefabricated and individually-formed posts are essentially glass FRC material, they have common basic advantages over metallic posts. However, compared with prefabricated FRC posts, individually-formed FRC posts have the advantage of being fabricated to fit canal configuration and dimensions without undue root structure removal. Unlike prefabricated FRC post, the individually-formed post is closely adapted to canal walls in the cervical area of the root, which has been found to improve the load bearing capacity (Le Bell-Ronnlof et al., 2011). It has been demonstrated that when the reinforcing fibres are placed closer to outer dentine rather than the centre of root canal, the resultant configuration closely simulates the biomechanics of the natural tooth (Guzy and Nicholls, 1979; Torbjorner, 2000). Additionally, closely adapted posts minimize the cement thickness, thus minimizing polymerization stresses.

The presence of the linear phase in the crosslinked matrix has been found to provide greater toughness (Lassila et al., 2004) and improved inter-diffusion bonding of individually-formed FRC posts (Kallio et al., 2001; Lastumaki et al., 2002; Mannocci et al., 2005). The linear polymer phases act as an adhesion facilitator. Some dental resin-based bonding agent monomers can diffuse into that linear phase and dissolve it, forming a secondary-IPN (Mannocci et al., 2005; Vallittu, 2009). This results in an inter-diffusion bonding between the post and the adhesive cement (Vallittu, 2009; Wolff et al., 2012).

1.9.2.2 Limitations of individually-formed glass FRC posts

Clinically, the build-up procedure of individually-formed post is technique sensitive (Terry et al., 2001). Similar to prefabricate FRC posts, individually-formed posts have an anisotropic nature.

1.9.2.3 Studies on individually-formed glass FRC posts

Compared to metal posts, contradictory results have been reported on the in vitro mechanical performance of individually-formed glass FRC posts (Lassila et al., 2004; Fokkinga et al., 2006a; 2006b, Abo El-Ela et al., 2008; Yang et al., 2008,; Ozcan and Valandro, 2009; Davis et al., 2010; Le Bell-Ronnlof et al., 2011). While, improved flexural strength has been reported for individually-formed FRC posts by

Lassila et al. (2004), low flexural strength has been reported by Davis et al. (2010) and Yang et al. (2008). In contrast to Ozcan and Valandro (2009) , Abo El-Ela et al. (2008), have reported higher failure load of ETT restored with individually-formed FRC post compared to metal posts. On the other hand, Fokkinga et al.(2006a and 2006b), Le Bell-Ronnlof et al. (2011) and Yang et al. (2008) found no significant difference between the fracture resistance of metal posts and individually-formed FRC posts.

Favourable failure mode has been demonstrated by utilizing individually-formed FRC posts (Fokkinga et al., 2006a; 2006b, Yang et al., 2008; Le Bell-Ronnlof et al., 2011), whereas Davis et al. (2010) have identified both favourable and unfavourable failures mode in ETT restored with individually-formed FRC posts.

Unfortunately, long term clinical evaluation of ETT restored with individually-formed posts is not available yet.

1.9.3 Short-Fibre Reinforced Composite (SFRC) posts

Recently, a glass FRC with modified fibre orientation and length was developed. It is a composite material with discontinuous millimetre-scale reinforcing E-glass fibres that are randomly oriented in a semi-IPN matrix, and it is known as short-fibre reinforced composite (SFRC). It was first introduced to the dental market as a restorative filling material in high stress-bearing areas to overcome the disadvantages of PFC restorations and has recently been promoted as an intra-radicular post material.

1.9.3.1 Development of SFRCs

PFCs are increasingly selected by clinicians to restore anterior and posterior teeth due to their bonding ability, aesthetics and low cost (da Veiga et al., 2016). However, the success of PFC in high stress-bearing areas is limited by commonly occurring secondary caries and restoration fracture (Demarco et al., 2012; Heintze and Rousson, 2012; Opdam et al., 2014). In this respect, it has been demonstrated that PFC bulk fractures were more frequent than caries and were associated with early failures (Brunthaler et al., 2003; Rodolpho et al., 2011).

In a recent systematic review conducted by Heintze et al. (2017), they have correlated the clinical fracture of composite restorations to the material's fracture toughness. Fracture toughness is a mechanical property reflecting the ability of a brittle material to resist catastrophic crack propagation under an applied load through efficient load transfer from the matrix to the reinforcing fillers (Kim and Okuno, 2002). Hence, fracture toughness is influenced by the material's composition. In this regard, the PFC (reinforced with particle-fillers) has been acknowledged as structurally different from dentine (reinforced with collagen fibres), which might affect the fracture toughness of PFC (Manhart et al., 2000). Therefore, the idea of reinforcing restorative composite with fibre-fillers to resemble dentine microstructure has evolved, and consequently a variety of restorative SFRCs have become available. Generally, restorative SFRCs are reinforced with discontinuous randomly oriented short-glass fibres and are available in packable or flowable consistencies. They are recommended to restore large cavities in vital and non-vital teeth.

Early attempts to reinforce restorative composite with discontinuous short-glass fibres were not completely successful and some products have been withdrawn from the market (Van Dijken and Sunnegardh-Gronberg, 2006; Al-Turki et al., 2007; Drummond et al., 2009). Investigators have correlated the materials' poor clinical performance mainly with quantity, geometry and aspect ratio (length to diameter ratio) of the reinforcing fibres (Van Dijken and Sunnegardh-Gronberg, 2006).

Bearing in mind that for efficient transfer of load from matrix to fibres the reinforcing short-fibres length (l_f) needs to surpass the critical fibre length (l_{fc}), the earlier SRFC products, on reflection, probably have not fulfilled this requirement (Petersen, 2005; Batdorf, 2012). The fibres in the earlier SFRC formulations were described as micrometre-scale fibres (60 - 200μm) with a diameter that is less than 9μm, therefore, such formulations were speculated to be sub-optimally reinforced and not capable of providing adequate strength and toughness. Hence, restorations constructed using earlier SFRC formulations showed clinical problems such as progressive wear and surface roughness and high failure rate mainly due to restoration bulk fracture (Van Dijken and Sunnegardh-Gronberg, 2006).

Also, the earlier SFRC products were described as low aspect ratio composites (l/d ranges between 6 and 22). Although their aspect ratio is above the lowest aspect ratio limit for dental SFRC, which is 5.2

(Kardos, 1985; Shouha et al., 2014), it has been found that a higher aspect ratio improves the strength, fracture toughness and reinforcing efficiency in SFRCs (Lee, 1992; Petersen, 2005).

The efforts to develop a reinforced restorative composite continued and were documented in a series of in vitro studies conducted primarily by Garoushi and groups of researchers. They tested different experimental SFRC formulations through incorporating longer fibres (millimetre-scale glass fibres), in higher aspect ratio and in different quantities to semi-IPN matrix until they reached the formula of the contemporary restorative SFRC. Their early experimental formulations were prepared by adding Bis-GMA-TEGDMA impregnated millimetre-scale glass fibres (1-6 mm in length and 0-22 V_f%) to PMMA (Garoushi et al., 2006). They concluded that there is no significant difference in reinforcing capacity with embedded fibres lengths from 2mm to 5mm. Additionally, since longer fibres were associated with more challenging handling of the material, 2mm fibre length were considered as the upper limit of the reinforcing millimetre-scale glass fibres.

Subsequent studies were carried out to test the mechanical properties of the new millimetre-scale SFRC experimental formulation in various restorative applications in comparison to PFC. In these studies, the new SFRC was tested using a bi-layered restoration approach that consists of SFRC bulk-filled substructure and a cover layer (1-2mm) of PFC. In this context, experimental SFRC was used to repair fractured incisors and the results revealed a significant increase of the load bearing capacity (Garoushi et al., 2007a; 2007b). Similar observations were identified when experimental SFRC was used as a single crown restoration (Garoushi et al., 2007c), 3-unit fixed partial dentures (Garoushi et al., 2007d) and for post and core construction (Garoushi et al., 2009).

Physical and biological properties of the experimental SFRC were also evaluated. Studies have revealed an acceptable depth of cure, reduced polymerization shrinkage and microleakage for the experimental SFRC specimens (Garoushi et al., 2008a; 2008b). The experimental SFRC also have shown similar bacterial adhesion (Streptococcus mutans) to that of PFC in spite of rougher SFRC surface (Lassila et al., 2009).

The experimental millimetre-scale SFRC demonstrated a significant improvement in mechanical properties, namely; fracture toughness (14 $MNm^{-1.5}$), compressive strength (129 MPa) and load bearing capacity (1584 N) in comparison to PFC (2 $MNm^{-1.5}$, 112 MPa and1031N) (Garoushi et al., 2011). The authors concluded that these findings supported the use of the new SFRC as a bulk-fill restoration in the posterior region.

The first commercial millimetre-scale SFRC (Xenious, StickTeck Ltd, Turku, Finland) was manufactured and launched for clinical application in Finland in 2011. With the promising results of the in vitro studies, in 2012, Garoushi et al. reported a short term (12 months follow up) study to investigate the clinical performance of the commercial millimetre-scale SFRC. The material was used to restore complex cavities (class I and II) in vital and non-vital posterior teeth as a bulk-fill restoration. The results were promising with lack of caries and restoration fracture, however, five out of 37 teeth exhibited marginal leakage with one case of post-operative pulpal sensitivity.

In 2013, the name of the millimetre-scale SFRC material was changed to everX Posterior™ (StickTeck Ltd, Turku, Finland) and launched globally. everX Posterior is a millimetre-scale SFRC consisting of Bis-GMA (bisphenol-A diglycidyl dimethacrylate) and TEGDMA (triethylene glycol dimethacrylate) crosslinked polymers with a linear polymer of PMMA (polymethyl methacrylate) creating a semi-IPN matrix. It is reinforced with high aspect ratio discontinuous, randomly oriented millimetre-scale short E-glass fibre fillers with diameter of 16-17μm and length ranges between 0.3 mm and 2 mm (according to the manufacturer) and inorganic particulate fillers (Appendix 1). Since then, everX Posterior has been recognized primarily as a packable bulk-fill SFRC restorative material. Although, different packable and flowable bulk-fill SFRC have been commercialized since then, to the author's knowledge, everX Posterior is the only bulk-fill SFRC with *millimetre-scale* E-glass reinforcing fibres in a *semi-IPN matrix*.

1.9.3.2 Studies on everX Posterior SFRC as a bulk-fill restoration

everX Posterior SFRC has attracted the interest of a number of researchers and has been the focus of both laboratory and clinical studies. In these studies, the mechanical properties of everX Posterior SFRC has been compared with either micro-filled or nano-filled PFC. everX Posterior SFRC was evaluated as a direct onlay restoration (Garoushi et al., 2013a) and as a complex restoration (Frater et al., 2014; Soares et al., 2018). It has been concluded that the mechanical performance of everX Posterior SFRC is superior to PFC in high stress bearing areas. Similar findings were reported when everX Posterior SFRC was used to restore complex cavities in endodontically treated premolars (Kemaloglu et al., 2015; Bilgi et al., 2016; Gurel et al., 2016; Eapen et al., 2017; Gaintantzopoulou et al., 2018) and molars (Ozsevik et al., 2016; Yasa et al., 2016; Garlapati et al., 2017; Tekce et al., 2017). On the other hand, some studies found no significant differences between PFC composite and everX Posterior SFRC when used for complex restoration in molars (Rocca et al., 2015) and premolars (Atalay et al., 2016; Barreto et al., 2016).

Clinically, everX Posterior SFRC has been evaluated in a number of case-reports. In these reports, everX Posterior SFRC was used to restore structurally compromised ETT molars as a bulk-fill restoration. Case-reports indicated that SFRC provided coronal reinforcement and seal and conserved tooth structure (Shah et al., 2016; Soares et al., 2016; Yadav et al., 2016).

1.9.3.3 Structural and physico-mechanical properties of everX Posterior SFRC

The reported studies on everX Posterior SFRC have addressed the performance of this new SFRC in relation to its structural and physico-mechanical properties:

everX Posterior *physico-mechanical properties:* Under mechanical testing, everX Posterior SFRC showed significantly improved mechanical properties (Table 1.2) including flexural strength, flexural modulus, fracture toughness and compressive strength when compared to PFC and other bulk-fill restorative composite resins (Garoushi et al., 2013b; Belli et al., 2014; Leprince et al., 2014; Abouelleil et al., 2015;

Bijelic et al., 2015b; Bijelic et al., 2016; Tsujimoto et al., 2016c; Garoushi et al., 2017). Additionally, everX Posterior SFRC showed improved static and fatigue fracture resistance when compared to PFC and other bulk-fill composite resin restorations in ETT and non-ETT teeth (Bijelic et al., 2015b; Ozsevik et al., 2016; Eapen et al., 2017; Garlapati et al., 2017).

In a recent study conducted by Garoushi et al. (2017), they evaluated the mechanical properties of all of the currently available SFRCs (micrometre-scale SFRCs: Alert, EasyCore, Build-It, TI-Core, millimetre-scale SFRC: everX Posterior™). everX Posterior demonstrated significantly higher fracture toughness (2.4MPa$^{1/2}$) than other materials (1.3-1.8 MPa$^{1/2}$) and comparable flexural strength (120MPa) to other materials (90-125MPa).

Table 1.2: Mechanical properties of everX Posterior SFRC as reported in various studies

Reference	Flexural strength (MPa)	Flexural modulus (GPa)	Fracture toughness (MPa$^{1/2}$)	Compressive strength (MPa)
Garoushi et al., 2013b; 2016	124.3	9.5	2.9	-
Belli et al., 2014	110.7	12.2	2.2	-
Leprince et al., 2014	101	8.3	-	-
Goracci et al., 2014	201			
Abouelleil et al., 2015	153	14.6	3.1	-
Bijelic et al., 2015b	107		2.6	247
Bijelic et al., 2016	119	12.6	2.4	235
Tsujimoto et al., 2016c	124.3	9.5	3.1	
Garoushi et al., 2017	120	-	2.4	-

The ability of a restorative material to resist fracture is of a vital importance especially in stress-bearing areas. Dental materials with adequate fracture toughness can hinder the fracture propagation, which reduces the chance of restoration bulk fracture and results in a more “graceful” restoration failure and a more favourable outcome for the tooth. It has been claimed that there is no other composite material has a fracture toughness greater than the reported value of everX Posterior SFRC (Garoushi et al., 2017). The high fracture toughness of everX Posterior SFRC has influenced the fracture behaviour of the restored teeth. Favourable failure behaviour of teeth restored with everX Posterior SFRC has been more frequently reported (Garoushi et al., 2013a; Frater et al., 2014; Kemaloglu et al., 2015; Bilgi et al., 2016;

Gurel et al., 2016; Eapen et al., 2017; Garlapati et al., 2017; Soares et al., 2018) than the unfavourable failure behaviour (Rocca et al., 2015; Barreto et al., 2016; Yasa et al., 2016; Tekce et al., 2017)

Another factor that might influence early or late restoration failure is compatibility of the mechanical properties of the restorative material to dentine (Donovan et al., 2017). everX Posterior SFRC modulus of elasticity is reported to range between 8.3-14.6 MPa, which is close to the reported values of the dentine (Table 1.3). Similarly, the reported flexural strength, fracture toughness and compressive strength values of everX Posterior SFRC match those reported for human dentine.

Table 1.3: Comparison between everX Posterior SFRC and dentine mechanical properties

	everX Posterior SFRC*	**Dentine**
Elastic modulus (GPa)	8.3-14.6	18-25 (Kinney et al., 2003)
Fracture toughness ($MPa^{1/2}$)	2.4 - 3.1	1.13 - 2.02 (Iwamoto and Ruse, 2003)
Flexural strength (MPa)	101-201	213 (Plotino et al., 2007)
Compressive strength (MPa)	235-247	297.1 (Craig and Peyton, 1958)

* Details on the reported values and references were presented in table 1.2

Polymerization stability, microleakage, depth of cure, light transmission and bonding performance are among the most frequently investigated physical characteristics of SFRCs (Garoushi et al., 2018). everX Posterior SFRC exhibited lower polymerization shrinkage and polymerization shrinkage-induced stresses compared to other bulk-fill and conventional composites (Garoushi et al., 2013b; 2015a Tsujimoto et al., 2016c). Restricted polymerization shrinkage has been attributed to the material's composition (semi-IPN and randomly oriented short-fibres) and to the bulk-fill application technique (Tezvergil et al., 2006; Garoushi et al., 2008b; 2015a Vallittu, 2009; 2015). Low polymerization shrinkage is crucial for marginal integrity and microleakage control and to avoid subsequent secondary caries, post-operative sensitivity and restoration failure (Demarco et al., 2012).

Lower microleakage of everX Posterior SFRC has been documented when compared to other bulk-fill and conventional composite restorations (Garoushi et al., 2015a; Patel et al., 2016; Patnana et al., 2017). In contrast, other studies have reported similar microleakage in both everX Posterior SFRC and other bulk-fill and PFC materials (Al Sunbul et al., 2016; Miletic et al., 2016)

Depth of cure of everX Posterior SFRC was similar to some bulk-fill materials but significantly higher than conventional composite resin (Garoushi et al., 2013b; Tsujimoto et al., 2016c). Depth of cure is the maximum depth of the material that guarantees adequate light intensity for complete polymerization through the composite restoration increment. The depth of cure of the everX Posterior SFRC (4 – 5 mm) as a bulk-fill restoration has been found to be twice that of conventional composite (Garoushi et al., 2013b; Li et al., 2015; Omran et al., 2016; Tsujimoto et al., 2016c, Miletic et al., 2017). Deeper cure has been explained by the translucency and the fibre content of SFRC (Garoushi et al., 2015b; Donovan et al., 2017; Miletic et al., 2017). The irregular inner structure of SFRC due to the presence of different light propagation media (resin matrix and short random fibres) enhances light transmission and reflection (Vallittu, 2015). According to Le bell et al (2013), light conduction and scattering is better in fibre-reinforced composite compared to conventional composite. Additionally, E- glass, which present in SFRC structure, has been found to enhance the light scattering after polymerization initiation (Vallittu, 2015). Adequate light cure penetration has been found to affect the mechanical properties, colour stability, biocompatibility and clinical longevity of restorations (Ferracane and Greener, 1986; Tanaka et al., 1991). Improved light transmission qualities are also advantageous when curing inaccessible posterior restorations due to difficult light unit placement in close contact with the restoration. Additionally, increased depth of cure to 4-5mm allows application of thicker increments, which saves time and simplifies management.

Reports on bonding performance of everX Posterior SFRC to dentine are conflicting. Durable bonding to dentine (improved shear bond strength) compared to PFC, has been reported for everX Posterior SFRC (Tsujimoto et al., 2016a). In this study, Tsujimoto et al (2016a) suggested that the superior mechanical properties of everX Posterior SFRC have influenced the bond durability. In contrast, everX Posterior SFRC bonding performance was found to be similar to PFC using similar adhesive resins (Tsujimoto et al., 2016b; Nagas et al., 2017).

Interlayer bonding strength of everX Posterior SFRC has been also evaluated and compared to PFC. Bijelic et al. (2015a) evaluated the effect of the presence of an oxygen inhibition layer formed on the surface of everX Posterior SFRC and conventional composite to estimate the interlayer bond strength.

The oxygen inhibition layer formed on everX Posterior SFRC surface after polymerization was thicker than that formed on conventional composite. They attributed the results to the difference in the composition of both materials. However, the interlayer bond strength in everX Posterior SFRC was similar to that of conventional composite. Interestingly, everX Posterior SFRC showed evidence of interlayer bonding even with the absence of oxygen inhibition layer (Bijelic et al., 2015a). Reliable interlayer bonding in the presence and absence of oxygen inhibition layer is useful in clinical repair of fractured restoration when new composite is added to the old one.

everX Posterior *SFRC structural properties:* The mechanical and physical behaviour of everX Posterior SFRC was attributed to the matrix and fibres of SFRC and their reciprocal interaction.

The elastic properties of the semi-IPN polymer matrix in SFRC have been assumed to absorb polymerization shrinkage-induced stresses during polymerization (Vallittu, 2009). Additionally, the presence of the linear phase (PMMA) reduces the brittleness of the cross-linked phase and consequently contributes in the material's improved toughness competency (Bijelic et al., 2016).

The linear polymer (PMMA) and the cross-linked polymer (Bis-GMA and TEGDMA) are not bonded chemically, which permits monomer inter-diffusion bonding. Microscopically, the monomers of the new resins (repairing, veneering composite or luting cement) swell the soluble phase (PMMA) of the semi-IPN allowing penetration of the new resins into the swelled phases of the matrix. During polymerization, the new resin monomer locks into the swelled PMMA phases and an IPN-bonding result (secondary-IPN) (Lastumaki et al., 2003; Keulemans et al., 2017). However, the structural integrity of the matrix might be interrupted by the presence of flaws such as porosity, cracks, resin rich regions and contamination, which are not uncommon in heterogenous structures.

The reinforcing fibres in SFRC are similar to collagen fibres in dentine, which make them both flexible, tough and able to resist crack-growth (Nalla et al., 2003). However, fibre-related properties such as length, aspect ratio, quantity and orientation have an influence on the reinforcing and toughening mechanism of SFRC.

In everX Posterior SFRC, the fibre length is described as a range of 0.3 to 1.9mm. However, different fibres length values have been reported by different manufacturers (Garoushi et al., 2013b; Abouelleil et al., 2015; Bijelic et al., 2016). The gradual fibre length range is influenced by the manufacturing process, which might lead to fibre breakage during fabrication (Mortazavian and Fatemi, 2015b).

For effective reinforcement, the discontinuous short-fibre length must exceed a critical fibre length (l_{fc}) and match an optimal fibre length (l_{fo}). Critical fibre length of glass fibres has been calculated to be as much as 50 times the fibre's diameter (Vallittu, 2015). The diameter of currently used reinforcing glass fibres in SFRCs is 16 –18 μm, therefore the critical fibre length has been estimated to range between 0.75 – 0.9 mm according to Vallittu, 2015. In everX Posterior SFRC, the critical fibre length was measured to be between 0.85 and 1.09 mm (Bijelic et al., 2016). Optimal fibre length (l_{fo}) is estimated to be approximately 1.2 times the critical fibre length, and in SFRCs, optimal fibre length has been estimated to range between 1.0-1.5 mm (Li et al., 1991; Wetherhold and Jain, 1992). The optimal fibre length for everX Posterior SFRC was measured to be approximately 1.15 mm (Bijelic et al., 2016). Therefore, the range of efficiently reinforcing fibre length in everX posterior SFRC is between 0.85-1.15mm ($l_{fc} \leq$ fibre length$\leq l_{fo}$).

Interestingly, microscopic analysis of everX Posterior SFRC revealed specific reinforcement functions carried by fibres of different lengths (Bijelic et al., 2016). While, the shortest fibres (represent 18% of the total fibres content) act as particulate fillers, the longest fibres (1.1-1.9mm) that exceed the optimal fibre length (11% of the total fibres content) will either break or behave as continuous fibres. Both fibre length range have no actual reinforcing functions. The remaining fibres (71% of the fibre content) range between 0.4-1.0mm. Fibres in this range can effectively encounter the load and act as a crack propagation stopper through their ability to stretch, pull out and bridge between crack edges (Garoushi et al., 2007e; 2013b, Bijelic et al., 2016). Thus, fibres that range between 0.4-0.7mm tend to pull-out (short embedded segment of the fibre) and continue to carry the load, whereas the fibres that range between 0.8-1.0mm tend to bridge between the crack edges. This is known as toughening mechanism, which results in slowing crack

propagation, blunting the sharp crack and reducing stress concentration at crack tip in SFRCs (Kim and Watts, 2004).

everX Posterior is described as a high aspect ratio SFRC compared to the earlier SFRC products. High aspect ratio fibres have a high ratio of the fibre length to its cross-sectional diameter and are associated with a significant improvement in the flexural strength. The measured aspect ratio in everX Posterior ranges between18 and 112 (Bijelic et al., 2016), which is above the lower limit of the aspect ratio in SFRCs (5.2) and within the range of the recommended high aspect ratio (68-640), as concluded by Shouha et al., 2014.

In the same study, Shouha et al., 2014 have also conclude that fibre volume fraction of 5% is associated with poor mechanical performance, and10% fibre volume loading provides the best mechanical performance in SFRCs, which is in agreement with other studies (Norman and Robertson, 2003; Berger et al., 2007). Nevertheless, higher fibre volume increases the tendency of the fibres to cluster, which can adversely affect the fibre-matrix interfacial bond, result in voids formation and eventually decrease the mechanical strength of SFRCs (Karacaer et al., 2003). Fibre volume fraction in everX Posterior™ is 7.2%, which is within the reported efficient fibre volume range (Bijelic et al., 2016).

Microscopically, the random orientation of the short-fibres in everX Posterior™ was described as 3D X-orientation, hence the inclusion of the letter 'X" in the trade name of the material. Random fibre orientation has been strongly correlated with multidirectional broader reinforcement and with the toughness characteristics of everX Posterior™ (Bijelic et al., 2013; Garoushi et al., 2007e; 2013b). Additionally, unlike long aligned fibres, the random orientation reduces the chance of fibres debonding, which improves the load bearing capacity (Brighenti and Scorza, 2012a).

Although 3D multidirectional orientation is known originally to provide an isotropic reinforcing effect (Krenchel's reinforcing factor of 0.2), the homogeneity of the 3D orientation distribution in SFRCs is uncertain. It has been found that fibre orientation distribution (FOD) in SFRCs is influenced by fibre geometry and quantity, viscoelastic behaviour of the matrix, fabrication process, the insertion method

(injectable vs packable), manipulation technique and size of the cavity, leaving FOD difficult to predict or measure (Zhu et al., 1997, Mortazavian and Fatemi, 2015b, Bijelic et al., 2016). Change of the fibre orientation from 3D orientation to 2D orientation with anisotropic behaviour (Krenchel's reinforcing factor of 0.38) has been reported (Vallittu, 2014; Bijelic et al., 2016; Nagata et al., 2016; Keulemans et al., 2017; Vallittu and Ozcan, 2017). 2D orientation is created during packing of SFRC, where the longest discontinuous fibres aligned transversely.

1.9.3.4 everX Posterior SFRC as a root canal post

Based on the aforementioned efficient mechanical and physical properties of everX Posterior SFRC as a bulk -fill restoration in high stress bearing areas, it has been hypothesized that everX Posterior SFRC materials can sustain the load conditions as an intra-radicular post (Garoushi et al., 2009). During the early stages of everX Posterior SFRC development, the experimental SFRC was evaluated as post and core restorations (Garoushi et al., 2009). The results showed that ETT restored with experimental SFRC had both a high failure load and a favourable fracture pattern.

To date, three studies have assessed the commercially available everX Posterior SFRC as an intra-radicular post. One study evaluated the bond strength of everX Posterior SFRC to canal dentine (Nagas et al., 2017), while the other studies evaluated the fracture strength of everX Posterior SFRC posts in anterior (Bijelic et al., 2013) and posterior teeth (Forster et al., 2017)

Bijelic et al. (2013) reconstructed severely damaged ETT incisors with SFRC* as a core only, as a core on individually-formed FRC post and as a whole post and core system. They compared it to a PFC core with and without an individually-formed FRC post. After subjecting the teeth to static load, they found that all SFRC restorative combinations had a higher fracture strength than PFC restorations. Amongst all SFRC restorative combinations, the core restoration alone without post placement had the highest fracture load. However, SFRC post placement was associated with more favourable fracture patterns.

** From now on in this thesis, the shorter term "SFRC" will be used to refer to everX Posterior: "randomly oriented discontinuous, millimetre-scale E-glass reinforcing fibres in semi-IPN matrix", unless specification of the trade name is required.*

They attributed the enhanced reinforcement not only to the randomly orientated fibres in SFRC, but also to the homogeneity of the post and core as one assembly constructed of the same material.

In another reported study of endodontically-treated premolars with more conservative access cavity design, SFRC was applied as a coronal restoration with and without a post of the same material (Forster et al., 2017). They compared it to intact premolars and to conventional coronal composite with and without prefabricated FRC post. Restoring ETT with SFRC resulted in higher facture strength under static load in comparison to other restorative reconstruction techniques. However, teeth restored with SFRC had more catastrophic failures than teeth restored with prefabricated FRC post and intact teeth.

Nagas et al. (2017) assessed SFRC post push-out bond strength before and after cyclic loading and compared it to prefabricated FRC post. The results showed that the SFRC post had a bond strength comparable to that of a prefabricated FRC and cyclic loading had no effect on the bond strength in both post systems. They commented that the fibres in both restorative materials might absorb all the stresses and consequently preserved the adhesive bond to root canal dentine.

1.10 Failure of restored ETT

When restoring an ETT with a post and core, the ultimate clinical goal is to restore functional and aesthetic characteristics of the tooth and to minimize the chances of early and non-restorable failures. Therefore, the selection of the appropriate post and core material should be based on the ability of the material to withstand the physical, mechanical and biological conditions to which they will be exposed in the oral environment. Post and core should preserve tooth structure, be easy to handle and come at a reasonable cost. Additionally, when the ETT is to be restored with all ceramic crown, the aesthetic characteristics of the post and core material is a significant additional consideration.

Post space preparation for the SFRC is conservative. Firstly, because extra modification of the canal to fit the post is not required, and secondly, because the adhesive bonding of the SFRC to dentine diminishes the need for increasing the post length for extra retention and strength. In addition, everX Posterior is supplied in transparent shade, which satisfies aesthetic requirements when this is a consideration.

ETT restored with SFRC as a post have been shown to withstand intraoral stresses in posterior and anterior region and fracture in a favourable manner (Bijelic et al., 2013). This is supported by the fact that SFRC is constructed in the root with close adaptation to the canal dentine walls rather than being placed centrally in the root, which is the case with prefabricated posts. Mechanically, SFRC adaptation to canal walls is advantageous in terms of reinforcement of the root against cervical tensile stresses (Le Bell-Ronnlof et al., 2011).

Similarities between SFRC and dentine physico-mechanical properties enable homogenous load distribution within the root. SFRC post and core provides a mono-phasic assembly that is adhesively bonded to dentine, which also contributes to improved mechanical support.

1.11 Statement of problem

Tooth fracture is the most serious type of failure in restored ETT. Intraorally, tooth fracture commonly results from repeated functional or parafunctional forces (Dietschi et al., 2008). Therefore, it seems realistic to design fracture resistance tests that replicate oral conditions in terms of the nature of the load (cyclic load) and temperature (thermocycling). Both cyclic loading and thermocycling have not been considered in the previous SFRC post and core fracture resistance investigations.

As demonstrated earlier, structural composition of SFRC has affected the mechanical behaviour of teeth restored with SFRC as bulk-fill restorations. Nevertheless, there is very little data on the effect of such factor on the mechanical behaviour of ETT restored with SFRC as post and core restorations.

1.12 Aims of the thesis

The general aim of this thesis is to analyse the failure of ETT restored with SFRC as directly-layered post and core restorations. In the series of studies presented in this thesis, failure load and failure mode of ETT restored with SFRC post and core restorations will be evaluated after subjecting the teeth to cyclic fracture resistance testing protocol. Internal structure of SFRC will be analysed using two research tools; micro-Computed Tomography (micro-CT) and Scanning Electron Microscopy (SEM).

The first hypothesis: restoring ETT with SFRC post and core restoration improves the fracture strength and reduces the incidence of catastrophic failure of ETT.

The second hypothesis: the structural composition of SFRC has an impact on the mechanical behaviour of ETT restored with SFRC posts and cores restorations.

The detailed aims are:

1. To perform qualitative and quantitative three-dimensional analysis of SFRC posts and cores structure using micro-CT.

2. To evaluate fracture strength (failure load) of extensively-damaged, endodontically-treated premolars restored with SFRC posts and core sand ceramic crowns and compare it to fracture strength of sound premolars and ETT restored with prefabricated FRC posts.

3. To evaluate the failure mode of ETT restored with SFRC posts and cores, prefabricated FRC posts and sound premolars.

4. To investigate the relationship between SFRC structural analysis (micro-CT results) and the failure of ETT restored with SFRC posts and cores.

5. To evaluate the fractured surface (fractography) of SFRC posts and cores using SEM and correlate the findings to the failure of ETT restored with SFRC posts and cores.

CHAPTER 2

General material and methods

This chapter describes the materials used in this project and introduces the general methodology. However, in Chapters 3, 4,5 and 6, more experiment-related details will be presented related to the specific investigation described in each chapter.

2.1 Project outline

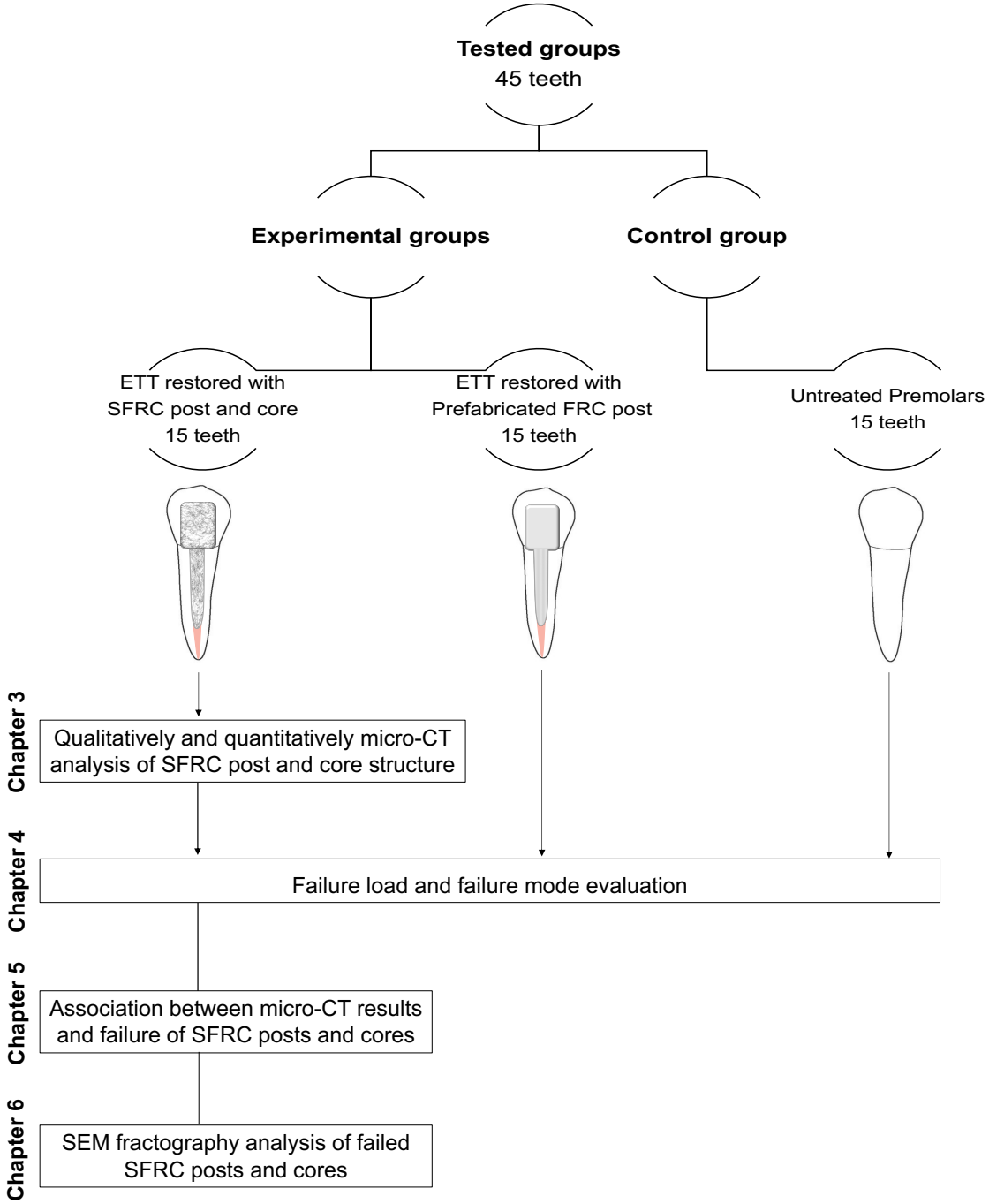

Figure2.1: Project outline presents tested groups, investigations and corresponding chapters

2.2 Specimen preparation

Single-rooted, human permanent premolars were selected for this study. Premolars were selected for two reasons; firstly, the endodontically treated premolars are more prone to root fracture (Testori et al., 1993) and secondly, structurally compromised endodontically treated premolars require post placement to support the core restoration due to inadequate size of the pulp chamber (Schwartz and Robbins, 2004). The total number of specimens was calculated using power analysis software (G*Power 3.1.9.2, Faul, Erdfelder, Lang, & Buchner, 2007) as a result, forty-five premolars were collected.

Root length and mesiodistal and buccolingual tooth dimensions were measured using digital caliper (Sidchrome; Vic, Australia). Root length was measured from the labial CEJ to root apex. Mesiodistal and buccolingual tooth dimensions were measured cervically at the CEJ. The included teeth had a mean root length of 14 ± 0.5mm, a mean mesiodistal dimension of 5.3± 0.3 mm and a mean buccolingual dimension of 7.4 ± 0.2mm. The teeth were visually inspected for restorations, caries or visible defects. The teeth were also examined with loups (magnification x25) to rule out the presence of any defects or cracks. Periapical radiographs of the teeth were examined to ensure the presence of straight, single canals, completely formed apices and to rule out the presence of previous RCTs or calcifications.

Teeth were thoroughly washed in running water followed by cleaning from calculus, deposits and any attached soft tissue using an ultrasonic scaler (TITANUS-E; TKD, Calenzano, Italy). Teeth were then stored in 1% aqueous thymol solution.

Teeth were randomly distributed into three groups (n=15); a control group (C) of sound premolars and two experimental groups (Table 2.1). Experimental group 1 (XFP) received RCT and were restored with SFRC (everX Posterior™; GC, Tokyo, Japan) posts. Experimental group 2 (PFP) received RCT and were restored with prefabricated glass FRC post (RelyX™; 3M ESPE, MN, USA). Prefabricated FRC was selected as it represents the traditional aesthetic chair-side restoration for structurally compromised endodontically treated premolar. One operator performed all specimen preparations.

Table 2.1: Specimen distribution, restorative procedures and materials used in the tested groups

Groups			Restorative procedures				
			RCT	Post space	Post	Core	Crown
Experimental groups	Group 1 (XFP)	n=15	Yes	10 mm post length	SFRC (everX Posterior™; GC, Tokyo, Japan)	SFRC (everX Posterior™; GC, Tokyo, Japan)	IPS e.max CAD
	Group 2 (PFP)	n=15	Yes	10 mm post length	Prefabricated glass FRC post (ø = 1.6 mm) (RelyX™; 3M ESPE, MN, USA)	Core build up composite (Multicore; Ivoclar Vivadent, Schaan, Liechtenstein)	(Ivoclar Vivadent; Schaan, Liechtenstein)
Control group(C)		n=15	Received no restorative treatment				

2.2.1 Control group preparation

The premolars in control group were untreated and received no preparation at this stage.

2.2.2 Experimental groups' preparation

Teeth in the experimental groups were decoronated, then received RCT, post space preparation, cervical tooth structure preparation and post and core build up before conducting the first investigation.

Coronal sectioning (decoronation):

The crowns of the experimental groups were sectioned leaving the cervical third to simulate trauma cases or structurally compromised endodontically treated premolars that are indicated for post and core restoration (Schwartz and Robbins, 2004).

A reference line was marked with a graphite pencil at a height of 3 mm coronal to the labial CEJ of the teeth. The marking was based on the digital calliper measurements. Each tooth was then decoronated by sectioning the occlusal and the middle thirds, at the reference line, perpendicular to the long axis of the teeth (Figure 2.2). The sectioning was performed with slow speed sectioning machine (IsoMet1000; Bueler, Illinois, USA) with water coolant. The resultant coronal tooth surface was flat and smooth.

Figure 2.2: premolar before and after decoronation using the slow speed sectioning machine

Root canal treatment:

For root canal preparation, canals were cleaned and shaped using both rotary and hand instrumentation (0.06-degree taper, NiTi files). The working length was determined by subtracting 1.0 mm from the root length measured by introducing a size 10 K-file (Dentsply Maillefer; Ballaigues, Switzerland) until it was visible through the apical foramen. The root canal instrumentation continued sequentially using rotary instrument (ProTaper; Dentsply Maillefer, Ballaigues, Switzerland) to achieve stranded canal width of size 40 file. Canal instrumentation started from No.15 initial file to No. 40 apical master file. During instrumentation, saline solution was used to irrigate the canals. Canals were then dried using paper points (Dentsply Maillefer) and obturated with gutta-percha cones (Dentsply Maillefer) and root canal sealer (AH26; Dentsply Maillefer). Excess gutta-percha at the canal orifice was cut using a heated plugger. Teeth were then stored in distilled water in a refrigerator (Titley et al. 1998).

Post space preparation:

The post space was initially prepared using Gates Glidden drills (Gates Glidden; Dentsply Maillefer), from size 1 to size 4 under water cooling at low-speed handpiece, to prepare a 10 mm post space measured from the flat coronal surface. The final post space enlargement was performed using size 2 post space

drill (Red post drill, ø = 1.6 mm, RelyX) provided with the corresponding size 2 prefabricated glass FRC post (Red post, size 2, ø = 1.6 mm, RelyX). The drill was used to standardize the post space diameter in both experimental groups. Saline was used to irrigate the canals and to clean debris during post space preparation.

The posts used in this study are bonded to the canal walls; therefore, conservative post space dimensions that are half of the root length (Nissan et al., 2001) and not exceeding one third of the root width (Stern and Hirshfeld, 1973) were selected to preserve radicular tooth structure and apical seal. Additionally, increasing the post length might reduce the efficiency of light transmission and the quality of resin polymerization at the deeper regions of the post (Teixeira et al., 2008).

Cervical tooth structure preparation:

The remaining coronal structure was prepared circumferentially to create gingival finish line and a ferrule effect. It has been found that incorporation of 2 mm ferrule above the CEJ provides resistance form for structurally compromised ETT (Sorensen and Engelman, 1990; Terry et al., 2001, Akkayan, 2004)

A reference line was first marked with graphite pencil at a height of 1mm coronal to the labial CEJ. Using diamond rotary cutting instrument (komet 8877; Komet Dental, Lemgo, Germany) mounted to a high-speed hand piece under water-cooling, and the coronal structure was prepared circumferentially following the marked reference line. This resulted in a 2 mm ferrule height and a 1 mm rounded shoulder finish line width (Rosenstiel et al., 2006). Any inter-specimen variation was minimized by standardization of the coronal structure measurements, which was controlled with digital caliper.

Post and core restorations:

Prior to post and core fabrication in the experimental groups, the post space and the remaining coronal tooth structure were etched using 37% phosphoric acid for 15 seconds, rinsed with water and dried with paper points. Dual-cure resin cement (RelyX™ Unicem; 3M ESPE, MN, USA) was applied for both experimental groups according to the manufacturer's instructions.

Group 1(XFP): SFRC post and core

SFRC posts (everX Posterior™; GC) were fabricated directly into the post space by condensing and polymerizing increments of SFRC into the canals using blunted endodontic plugger. To fabricate the SFRC post, a thin layer (approximately 1.00 mm thick) of SFRC was first condensed vertically to ensure proper post material adaptation at the deepest region of the post space. The first increment was light polymerized (XL 3000; 3M ESPE, MN, USA) for 40 seconds, the subsequent increments were introduced to the canal and condensed both laterally and vertically to ensure maximum adaptation of the post to the canal walls. Each increment was light polymerized for 40 second during which the light cure tip was placed in a direct contact with the canal orifice. A 2mm coronal extension of the SFRC post was built to act a junction between the post and the core build up. The SFRC cores were fabricated immediately.

For standardization of the core build up, a model was constructed into a predetermined core height, mesiodistal and buccolingual dimensions. The core model was constructed to obtain a properly contoured core with minimal variations between the specimens. First, a wax pattern representing the core was fabricated then cast into copper-aluminium alloy. Using the cast model, plastic translucent moulds were obtained using soft flexible plastic plates (Drufosoft®; Dreve Dentamid, Unna, Germany) under vacuum.

For direct core build up procedure, the translucent plastic moulds were bulk-filled with SFRC and positioned to overlay the post's coronal extension while supported by the cervical finish line (Figure 2.3). The core was light polymerized (XL 3000; 3M ESPE) for 40 seconds in all directions (occlusal, buccal, lingual, mesial and distal) while light source was placed in close contact the plastic mould. The plastic mould was removed with a surgical blade after complete polymerization of the core build-up material.

Figure 2.3: Plastic mould filled with composite material, positioned over the post's coronal extension and supported by the cervical finish line.

Group 2 (PFP): Prefabricated glass FRC post and core

Tapered prefabricated glass FRC post (Red post, size 2, ø = 1.6 mm, RelyX) was used in this study. The prefabricated glass FRC post has a standard length of 16 mm, therefore, the post was shortened to the required length (leaving 2mm coronal extension) using a diamond disc (Komet 2979, Komet Dental) mounted to a slow speed handpiece with water coolant.

The post was cemented into the respective post space using a dual-cure resin cement (RelyX™ Unicem; 3M ESPE) according to the manufacturer's instructions. The cement was introduced into the canal and the post was inserted immediately. During cementation, hydraulic pressure was released by slight twisting followed by withdrawal of the post, which was then gently reinserted in the canal, allowing the excess cement to vent. Finger pressure was maintained on the coronal extension of the post while removing excess cement and curing. The post was light cured for 40 seconds.

A dual-cure core build up composite (Multicore®; Ivoclar Vivadent, Schaan, Liechtenstein) was used to fabricate the cores on the prefabricated glass FRC posts. The same steps followed to fabricate the direct cores in group 1(XFP) specimens were applied in group 2 (PFP) specimens.

2.3 Statistical analysis

Specific data analysis methods applied in each part of this study were based on the consultation with Data, Design and Statistics Services in Adelaide Health Technology Assessment Department. Details of the statistical analysis related to each study will be presented in the respective chapter.

CHAPTER 3

Micro-CT analysis of SFRC posts and cores

This chapter describes the study conducted to qualitatively and quantitively evaluate SFRC posts and cores structure using micro-CT. The chapter includes a brief introduction, methodology of micro-CT imaging and analyses, results and discussion.

3.1 Introduction

The heterogeneous nature of SFRCs can influence the manufacturing and handling of the material, which might result in development of local or distributed defects in the matrix and/or fibres (Greenhalgh, 2009). Fibre degradation, anomalies or variation in the quantity, orientation, distribution and length are examples of possible defects in the fibres of SFRCs. The matrix might demonstrate a predominance of resin-rich regions, contamination or void entrapment.

Voids are regions in composite matrix unfilled with polymer and fibres (Mehdikhani et al., 2018). They are inherent defects in restorative composites that can be entrapped during manufacturing process. Mulder et al. (2017) have reported voids that ranges between 0.04 and 1.14% in ampules of bulk-fill composite, and Fano et al. (1995) have reported voids that range between 0.05 and 1.4% in freshly-extruded composite material. Additionally, voids can be created during clinical manipulation of the material. Composite insertion technique has been correlated with void introduction both within the structure of the restoration and between the restoration and the cavity walls (Opdam et al., 1996a; Opdam et al., 2002).

Voids have been reported within the structure of SFRC restorations (Shouha et al., 2014; Bijelic et al., 2016; Patel et al., 2016; Garoushi et al., 2017) and at SFRC restoration-dentine interfaces (Tuncer et al., 2013; Patel et al., 2016).

During SFRC manufacturing process, E glass-fibres are pre-impregnated and saturated with resin to create resin-fibre prepregs (Vallittu, 2014). Effective impregnation should assure complete contact between the resin matrix and all surfaces of every glass-fibres for effective fibre reinforcement (Vallittu, 1995b; 2009). Failure to achieving complete impregnation, can lead to void formation (Vallittu, 1995a; 1995b; Miettinen et al., 1999; Fonseca et al., 2016).

Incomplete impregnation in SFRC can occur due to high viscosity of the resin matrix, uneven fibre distribution or polymerization shrinkage (Vallittu, 1995a; 1995b; 1997b, Miettinen et al., 1999; Karacaer et al., 2003; Fonseca et al., 2014; Fonseca et al., 2016). Uneven fibre distribution might create areas of clustered fibres with increased risk of poor wetting of the fibres and void formation (Fonseca et al., 2014;

Shouha et al., 2014). On the other hand, areas with low fibre quantity will increase the risk of creating matrix-rich regions that facilitate air bubbles entrapment (Miettinen, Narva and Vallittu 1999; Guo et al. 2012; Fonseca et al. 2016;). Polymerization shrinkage of composite can create slits between the matrix and the fibres and disturb complete fibre impregnation (Solnit, 1991; Vallittu, 1994; Vallittu et al., 1994; Karacaer et al., 2003). Highly viscous matrix hinders complete wetting of the fibres and intensifies difficulties in handling of composite, such as difficult packing and stickiness of the material to the instrument, which might lead to void formation (Dietschi et al., 1995; Opdam et al., 1996b; Lagouvardos et al., 2015; Bijelic et al., 2016).

The presence of voids can adversely affect the clinical longevity of the dental composites. It has been reported that voids act as moisture or oxygen reservoirs, which might inhibit full polymerization, lead to hydrolytic degradation and eventually reduce the mechanical properties of composites (Vallittu, 1995a; 1998b; Miettinen and Vallittu, 1997; Karacaer et al., 2003; Fonseca et al., 2014). Additionally, it has been suggested that voids between the restoration and the cavity walls might contribute to microleakage, secondary caries and postoperative sensitivity (Opdam et al., 1998; Totiam et al., 2007).

Since the presence of voids can be detrimental to a restoration's durability and since voids are inherent defects in dental composites, investigating voids in dental restorations has attracted researchers' attention. In this regard, different techniques for void analysis and characterisation have been utilized. These include theoretical calculation (e.g. Archimedes theoretical versus actual density), microscopy and micro-Computed Tomography (micro-CT) analyses (Little et al., 2012). The theoretical calculation technique is a non-visual technique that provides limited data and requires an accurate knowledge of filler and matrix parameters for accurate calculations (ASTM, 1999; Kelly, 2000). Microscopy is limited to two-dimensional (2D) visual analysis and has the significant disadvantage of being destructive (Liu et al., 2006; Little et al., 2012). Micro-CT, on the other hand, is a non-destructive, three-dimensional (3D), visual, qualitative and quantitative analysis tool (Swain and Xue, 2009).

Micro-CT scanning uses rotating micro-focal X-rays to scan a fixed specimen. Subsequently, 2D images of the specimen's cross-sections dataset is projected in different planes (X, Y and Z). As a result, the

specimen's 3D structure is generated, visualized and analysed using the wide range of available micro-CT-related software. Micro-CT requires minimal specimen preparation and once the micro-CT images are collected and properly filed, they remain available for further analyses using scanner-specific software. Most importantly, for void characterisation in composites, micro-CT has been verified as the most reliable, reproducible (with low standard deviation) and accurate tool when compared to other void characterisation tools (Little et al., 2012).

Micro-CT has been used widely in dental research for different applications, such as geometrical analysis of dental structures (Olejniczak and Grine, 2006; Kim et al., 2007), pre- and post- endodontic treatment examinations (Peters et al., 2000; 2001), peri-dental implant assessment (Park et al., 2005), mineral concentration analysis, Finite Element Model (FEM) generation (Magne, 2007) and restoration parameters evaluation including void analysis within the structure of composites (Elbishari et al., 2012; Nazari et al., 2013; Lagouvardos et al., 2015; Dunn, 2016) or at the composite-dentine interfaces (Kakaboura et al., 2007; Sun and Lin-Gibson, 2008; Sun et al., 2009a; 2009b, Papadogiannis et al., 2009; Lagouvardos et al., 2015). However, there is lack of reports that analyse or characterise voids in the structure of SFRC restorations, and most importantly when SFRC is used as a post and core.

Aims of this study:

To analyse the structure of SFRC post and core and characterise voids within the structure of SFRC posts and cores and at the post-dentine interfaces.

3.2 Material and methods

The ETT restored with SFRC posts and cores (XFP group, n=15) were evaluated in this study. XFP group specimens were scanned, immediately after SFRC post and core fabrication, for qualitative and quantitative analyses using micro-CT scanner and software (SkyScan 1076; Bruker microCT, Kontich, Belgium) (Table 3.1). One operator performed all qualitative and quantitative analyses of the specimens.

Table 3.1: Summary of the instruments and software used for micro-CT imaging and analyses of SFRC posts and cores

Instrument	Function	Evaluation performed
SkyScan 1076 scanner	Acquires images of the tooth using predetermined parameters	-
SkyScan NRecon software version 1.6.9.4	Reconstruct the projected images of each tooth	-
SkyScan Data Viewer software version 1.5.1.2	Display the reconstructed images in three orthogonal views	Qualitative analysis of SFRC posts and cores
SkyScan CTAn software version 1.14.4.1	Create surface rendered models	Quantitative analyses of SFRC posts and cores: to calculate the content of voids according to their; - **Location:** voids within the post, within the core and at the post-dentine interfaces. - **Distribution:** voids in coronal, middle and apical thirds of the post. - **Size:** small, medium and large voids.
SkyScan CTVol software version 2.2.3.0	3D model construction	Construction of colour-coded 3D models

3.2.1 Micro-CT scanning

Before scanning, the specimen was fixed to a foam holder that facilitated proper positioning of the teeth in the CT scanner. The foam holder containing the tooth was then fixed to a 33mm-diameter carbon-composite bed inside the micro-CT scanner (SkyScan 1076; Bruker microCT) chamber. The long axis of the tooth was parallel to the scanning tube floor. To prevent teeth from drying inside the chamber during the scanning procedure, teeth were covered with a wet cotton gauze (Carrera et al., 2015).

Predetermined acquisition parameters were set and saved to be applied in each scan to ensure consistency of scanning procedure for all specimens. The selected parameters and reasoning of selection

are presented in Table 3.2. All scanning parameters were set with the assistance of a SkyScan scanner specialist.

Multiple X-ray images (cross-sections) were acquired by the scanner, and the images were recorded in each rotation. The 3D projected raw images (cross-sections) were saved as a Tag Image File Format (TIFF) file.

Table 3.2: Selected acquisition parameters for micro-CT scanning (applied for all scanning procedures in this project)

Acquisition Parameters	Value	Justification
Filter (mm)	1.0 Aluminium	Recommended when scanning calcified structures for better contrast.
Resolution (µm)	9	To improve the spatial resolution and image sharpness, although demanding a longer scanning and reconstruction time (Dowker et al., 1997, Peters et al., 2000). This number also represent the images voxel (3D pixel)
Rotation step (degree)	0.7	It represents the rotation degree at which CT scanner camera captures the image. The smaller the number, the more images are to be captured, however with a longer scanning duration.
Rotation(degree)	180^0	To balance long scanning duration, the scanning was undertaken with 180^0 rotation instead of 360^0, which assists in controlling the total scanning time.
Frame averaging	2	Two frames were averaged to produce single image in order to minimize the undesirable background noise and enhances the image details (Neves et al., 2014)
Voltage (KV)	100	Recommended by the manufacturer for long and thick tissue.
Current (mA)	100	

3.2.2 Micro-CT images reconstruction

SkyScan NRecon software (Bruker microCT), version 1.6.9.4 was used to reconstruct and combine the projected images (resolution 1204 X 1012 pixels) of each specimen. After importing (TIIF) files to the NRecon software, one cross-section was previewed to set the parameters in order to ensure maximum contrast and visualization of different parts of the images. These parameters include; smoothing = 3, beam-hardening correction = 30%, misalignment compensation = - 1.0 and thresholding ranging between 0 and 0.08. The same parameters were used for all cross-sections of all scanned specimens to create Bitmap format (BMP) files.

3.2.3 Micro-CT images analyses

3.2.3.1 Qualitative analysis

Data Viewer software (Bruker microCT), version 1.5.1.2 was used to display the reconstructed images in three orthogonal views (coronal, sagittal and trans-axial). Using this software, the reconstructed BMP images dataset was retrieved, displayed in different planes and saved to allow initial qualitative analysis of the SFRC post and core structure.

3.2.3.2 Quantitative analysis

Two software programs were used for quantitative analyses; CTAn software (Bruker microCT), version 1.14.4.1 and CTVol software (Bruker microCT), version 2.2.3.0.

Using CTAn software, the saved BMP image dataset was opened and the Region of Interest (ROI) for the post and core was created. ROI allows the collection of all cross-sections of a specific area or region into one folder for further evaluation and analyses. The ROI for the core is delineated to include trans-axial cross-sections of the core starting from the X-ray image that shows a coronal full diameter of the core (representing the top of ROI) and ends at the cross-section where the core ends, and post starts (representing the bottom of ROI). The top of ROI for the post is the next X-ray image to the core's ROI bottom until the cross-section where the post ends. The ROI for the post and the core was saved separately.

For proper and consistent void analysis, binary images of the ROIs, with a predetermined thresholding, were created and saved. Based on grey values, voids/air spaces were represented as black areas and solid posts/core structures were represented as white areas in the binary image. The voids trapped between the post and the dentine was calculated by subtracting two cylindrical ROIs. The cylindrical ROI of the post was subtracted from the cylindrical ROI that include post and surrounding dentine walls.

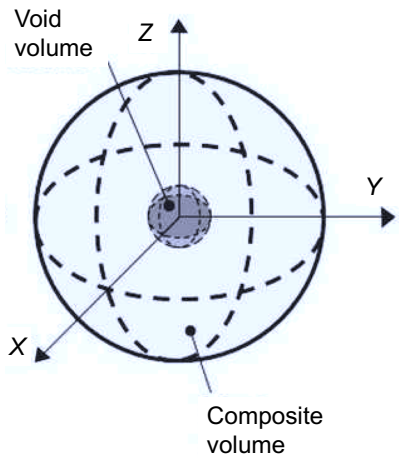

Figure 3.1: Void volume fraction measures the volume of the void in relation to the surrounding structure volume (Modified from Santos et al., 2018).

The quantitative analysis was conducted in this study to calculate void content in SFRC posts and cores. The void content was expressed in void volume and void volume fraction. While void volume (in mm^3) indicates the total void volume irrespective of the surrounding structures, void volume fraction (in percentage) measures the total void volume in relation to the solid composite volume in a specific ROI (Figure 3.1).

CTAn software was used to calculate the void content in SFRC posts and cores based on the following void characterisations:

A. Void location:

Voids were located in the core and in the post. According to their location in the post, two void types were identified: closed voids and open voids (Figure 3.2). Closed voids enclosed completely within the structure of the post, and open voids enclosed partially by the post as they are located at the post-dentine interface. Considering void location, the following void measurements were performed:

- Closed voids volume and volume fraction.
- Open voids volume and volume fraction.
- Core voids volume and volume fraction.

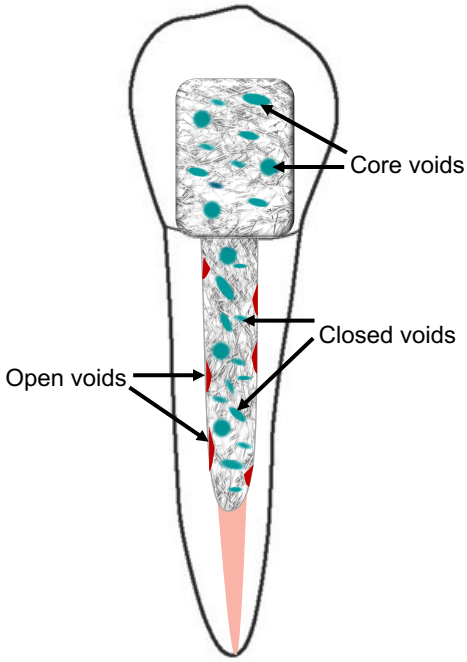

Figure 3.2: Schematic diagram showing void location; core voids, closed and open voids

Open voids have been calculated to evaluate post adaptation to canal walls. Closed voids were used to evaluate the homogeneity of SFRC post structure; therefore, further analyses of closed voids size and distribution have been conducted.

B. Void distribution:

Closed void content in the coronal, middle and apical thirds of the post were calculated. To define the coronal, middle and apical thirds in a SFRC post, the total number of the cross-sections of the post was divided by three in each post's ROI dataset. Each third represented a post section. For void distribution, the following void measurements were performed:

- Closed void volume and volume fraction in the coronal third.
- Closed void volume and volume fraction in the middle third.
- Closed void volume and volume fraction in the apical third.

C. Void size:

Closed voids inside SFRC posts were classified into three sizes; small voids (<100 μm^3), medium voids (100 μm^3 ≤ voids ≤500 μm^3) and large voids (> 500 μm^3). The percentage of each size in SFRC posts has been calculated.

CTVol software was used to create colour-coded 3D models of SFRC posts. CTVol and CTAn software programs were used to create a video to present the colour-coded closed voids in three-dimensions (video 3.1)

For each analysis, a task list was created in CTAn software to include the detailed tasks (e.g. thresholding, despeckling, ROI shrink-wrap) required to perform the 3D analysis and create an MS Excel file with the relative measurements. The task lists were saved to allow consistency between specimen analyses.

3.2.4 Statistical analysis

Descriptive statistics (mean ± SD) were calculated for volume and volume fraction for core voids, closed and open voids in the posts; voids in apical, middle and apical thirds and for the percentage of small, medium and large size voids. Linear mixed-effects models were used to account for clustering on void location, distribution and size. These models have been used to detect:

- Statistically significant differences in volume and volume fraction:
    - Between closed voids and open voids.
    - Between closed voids and core voids.
    - Between closed voids in coronal, middle and apical thirds.
- Statistically significant differences between small, medium and large closed voids percentage.

Post-hoc analyses based on pairwise comparisons were carried out subsequently. All statistical tests were performed with SAS 9.4 software (SAS Institute Inc., Cary, NC, USA) with a probability of less than 5% taken to indicate statistical significance.

3.3 Results

3.3.1 Qualitative analysis results

Data Viewer software images (in three planes; coronal, sagittal and trans-axial) allowed an initial assessment of the SFRC posts and cores structural homogeneity and adaptation to canal walls (Figures 3.3 and 3.4). The images indicate that the posts are well adapted to canal walls, however, the homogeneity of the post build up is interrupted by voids.

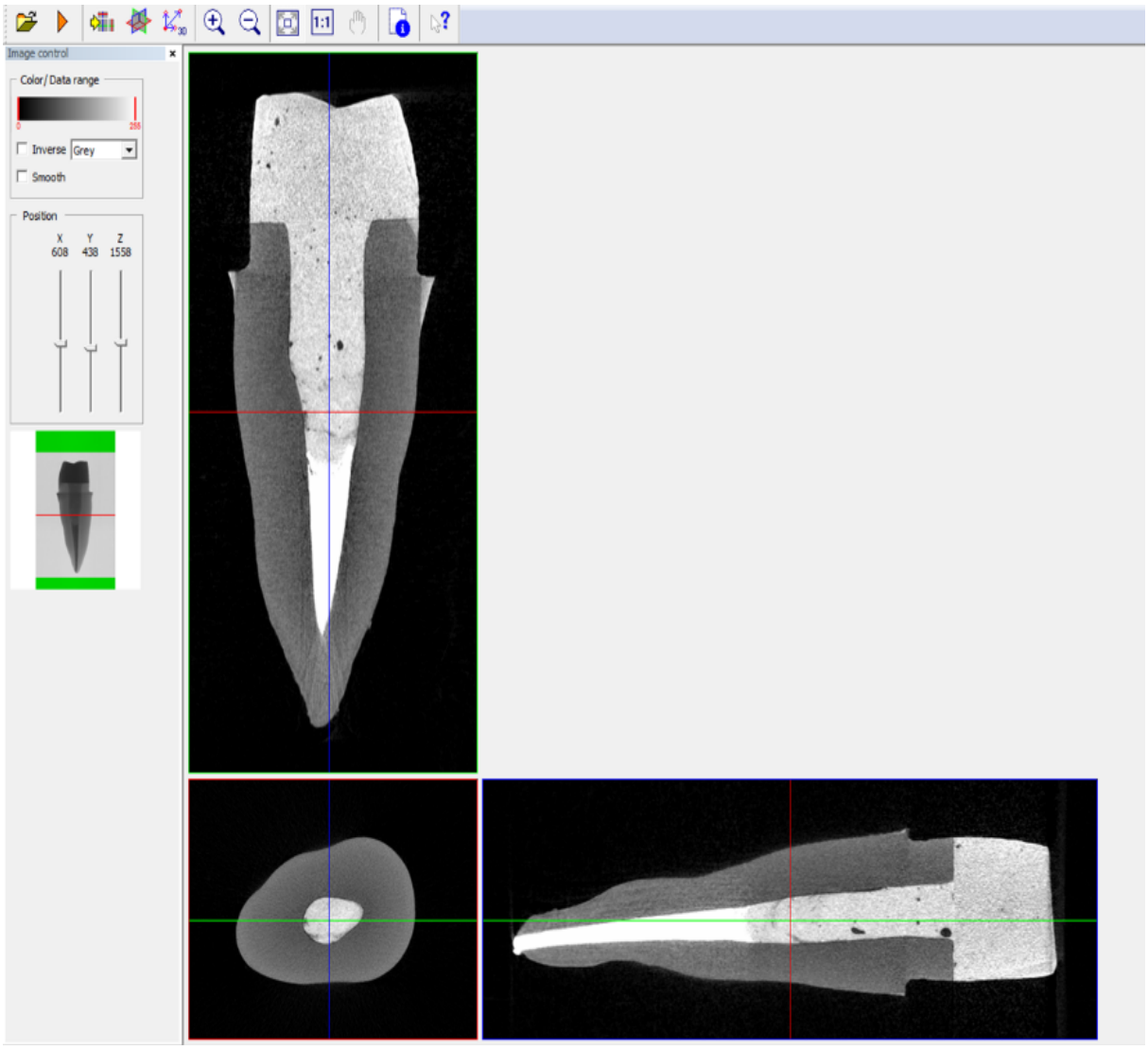

Figure 3.3: Data Viewer software images of SFRC post and core showing a scanned tooth in three planes; coronal, sagittal and trans-axial.

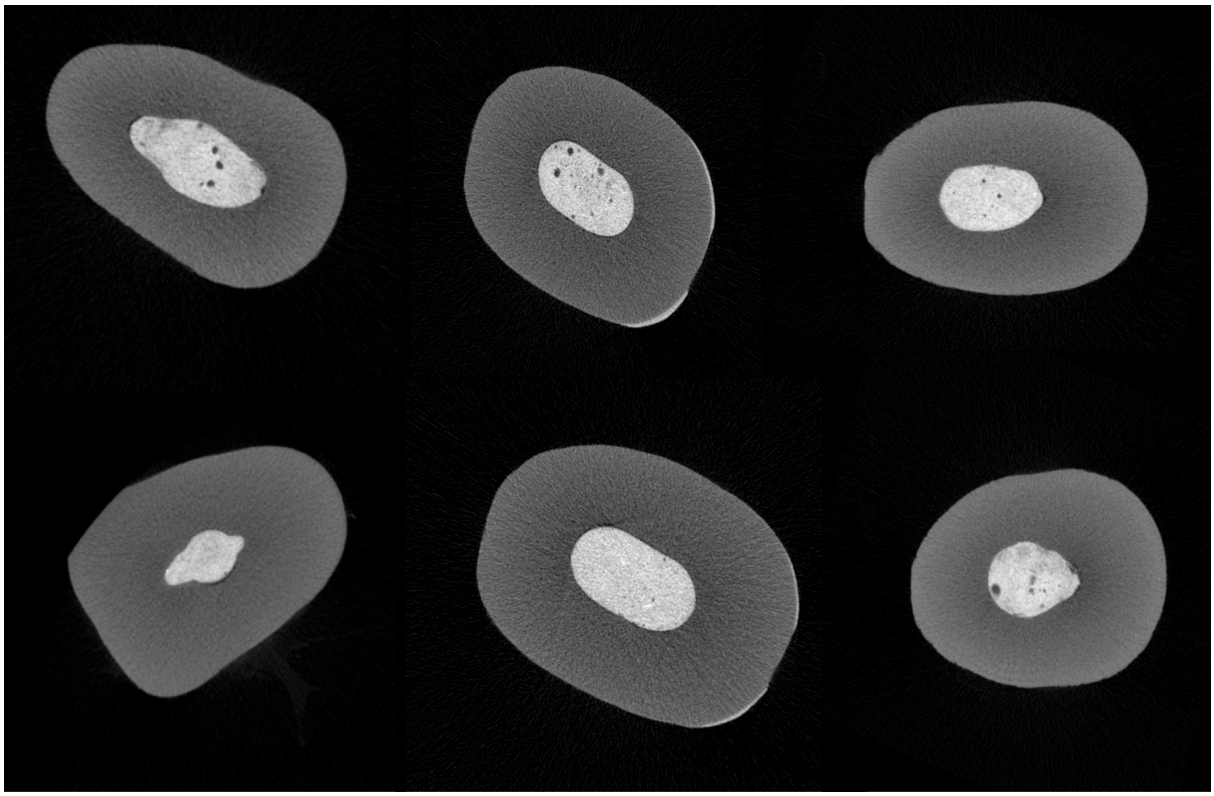

Figure 3.4: Multiple trans-axial images of different teeth created using Data Viewer software. The images indicate that the posts build ups follows the anatomical shape of the canal, however, the homogeneity of the posts build ups is interrupted by voids.

3.3.2 Quantitative analysis results

Void location:

Table 3.3 shows the descriptive statistics for the volumes and volume fractions of closed voids* and open voids**. For closed voids, the mean volume (± SD) was 0.7 mm^3± 0.2, and the mean volume fraction (± SD) was 2.82% ± 1.2. For open voids, the mean volume (± SD) was 0.3 mm^3±0.2 and the mean volume fraction (± SD) was 1.4%±0.8 (Figure 3.5).

Linear mixed-effects models indicated significant differences between open and closed voids in volume and volume fraction (Appendix 2, section 2.1). The mean volume (estimate=0.3, 95% confidence interval (CI): 0.5, 0.2, P-value=0.0009) and volume fraction (estimate=1.4, 95% CI: 2.1, 0.7, P-value=0.0007) of closed voids was significantly higher than open voids.

Table 3.3: Descriptive statistics for volume and volume fraction of open and closed voids (n=15)

Voids in SFRC post	**Voids volume** (mm^3)				**Voids volume fraction** (%)			
	Minimum	Maximum	Mean	SD	Minimum	Maximum	Mean	SD
Closed voids	0.3	1.3	0.7[a]	0.2	1.3	4.9	2.8[b]	1.2
Open voids	0.0	0.7	0.3[a]	0.2	0.0	2.8	1.4[b]	0.8

Same superscript letters over means indicate significant difference at 0.05 confidence level:
a: means are significantly different at P-value=0.0009.
b: means are significantly different at P-value=0.0007.

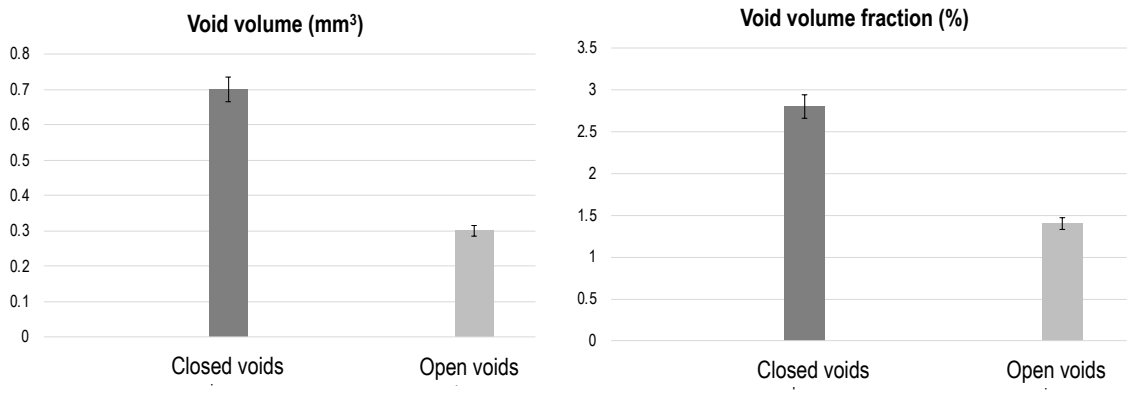

Figure 3.5: Mean volume and volume fraction of open and closed voids in SFRC posts (n=15)

**Voids within post structure*
***Voids at post-dentine interface*

Table 3.4 shows the descriptive statistics for the volumes and volume fractions of cores voids and closed voids (Figure 3.6). While, there was no significant difference in the mean voids volume between the closed voids and core voids, the mean volume fraction of closed voids was significantly higher than core voids (estimate= 2.0, 95% CI: 2.6, 1.4, P-value <0.0001) (Appendix 2, section 2.1)

Table 3.4: Descriptive statistics for volume and volume fraction of core voids and closed voids (n=15)

	Voids volume (mm^3)				**Voids volume fraction** (%)			
	Minimum	Maximum	Mean	SD	Minimum	Maximum	Mean	SD
Closed voids	0.3	1.3	0.7	0.2	1.3	4.9	2.8[a]	1.2
Core voids	0.1	1.4	0.6	0.3	0.2	1.8	0.8[a]	0.4

Same superscript letters over means indicate significant difference at 0.05 confidence level (P-value <0.0001).

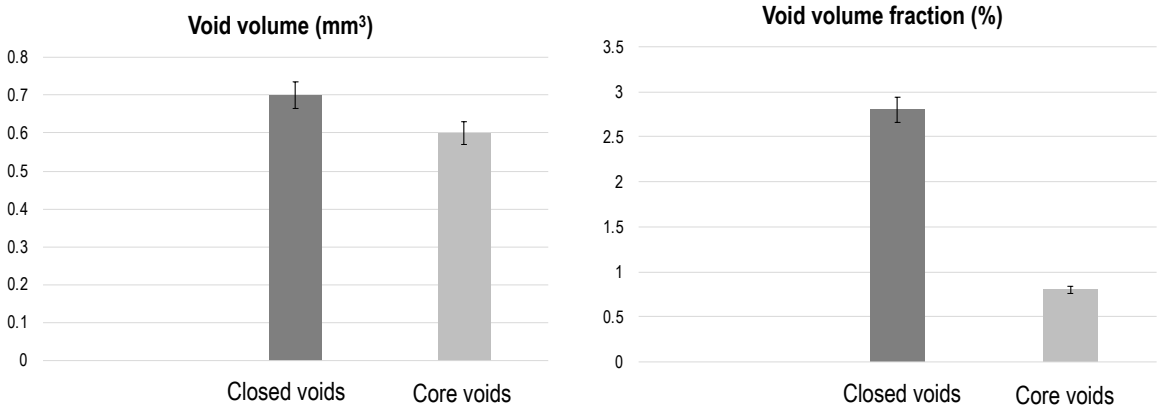

Figure 3.6: Mean volume and volume fraction of core voids and closed voids (n=15)

Void distribution:

Table 3.5 shows the descriptive statistics for closed void volumes and volume fractions in the three posts sections. The mean void volume (± SD) in coronal third was 0.3 mm^3 ±0.2, and in middle and apical third was 0.2 mm^3 ±0.1. The mean void volume fraction (± SD) in coronal third was 3.4%±1.7, in middle third was 2.7% ±1.4 and in apical third was 3.3% ±1.6 (Figure 3.7).

Linear mixed-effects models indicated a significant difference in void volumes between the three sections at 0.05 confidence level (Appendix 2, section 2.2). Void volume in coronal third was significantly greater than middle (estimate= 0.11, 95% CI: 0.02, 0.19, P-value=0.0134) and apical thirds (estimate= -0.14, 95% CI: -0.26, -0.03, P-value=0.0164).

Table 3.5: Descriptive statistics for volumes and volume fractions of voids in coronal, middle and apical thirds of SFRC posts (n=15)

SFRC post sections	**Void volume** (mm^3)				**Void volume fraction** (%)			
	Minimum	Maximum	Mean	SD	Minimum	Maximum	Mean	SD
Coronal third	0.1	0.6	0.3[ab]	0.2	1.2	6.3	3.4	1.7
Middle third	0.1	0.5	0.2[a]	0.1	0.9	5.2	2.7	1.4
Apical third	0.0	0.6	0.2[b]	0.1	0.9	6.0	3.3	1.6

Same superscript letters over means indicate significant difference at 0.05 confidence level
a: means are significantly different at P-value=0.0134.
b: means are significantly different at P-value=0.0164.

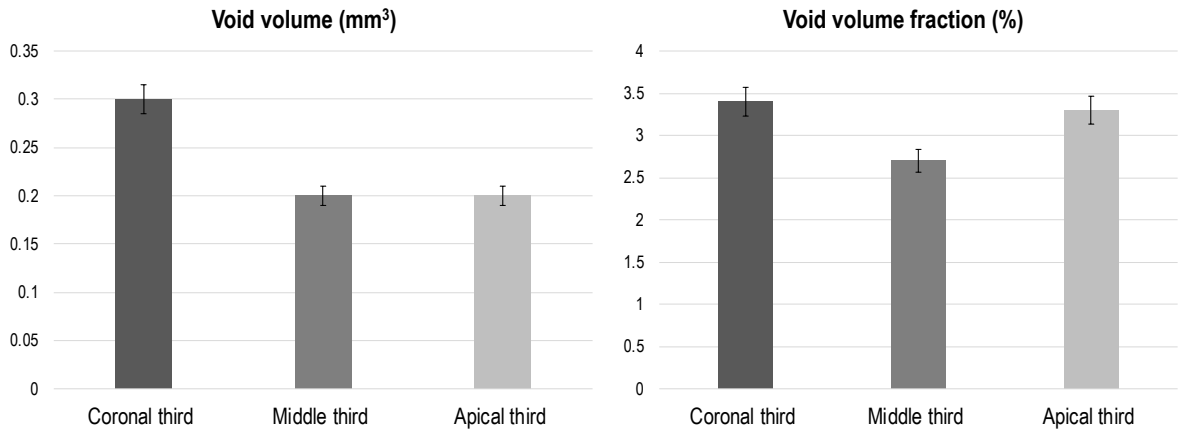

Figure 3.7: Mean volume and volume fraction of voids in coronal, middle and apical thirds of SFRC posts (n=15).

Void size:

Table 3.6 shows the number and percentage of small, medium and large voids in SFRC posts. The percentage of small voids was the highest (88.2%± 2.6, ranges between 84.4% and 92.3%) compared to medium (8.7%± 2.3, ranges between 5.2 % and 13.5%) and large (3%± 0.9, ranges between1.9% and 5.2 %) voids (Figure 3.8). Linear mixed-effects models indicated significant differences between small, medium and large voids number and percentage (P-value<0.0001) (Appendix 2, section 2.3).

Figure 3.9 shows colour-coded models of the void sizes created using CTVol software. Unlike small and medium voids, large voids were of irregular shapes. Small voids represent the highest void content and were evenly distributed along the length of the post together with medium voids. Large voids did not have a typical distribution pattern; however, largest voids located mainly in the middle third (Appendix 3: shows 3D models of all specimens).

Table 3.6: Number and percentage of small, medium and large voids in SFRC posts (n=15)

Void size	**Number**				**Percentage**			
	Minimum	Maximum	Mean	SD	Minimum	Maximum	Mean	SD
Small voids (<100 µm³)	147	477	328.5[a]	90.6	84.4	92.3	88.3[b]	2.6
Medium voids (100 -500 µm³)	18	52	31.5[a]	9.8	5.2	13.5	8.7[b]	2.3
Large voids (> 500 µm³)	5	19	11.2[a]	4.4	1.9	5.2	3.0[b]	0.9

Same superscript letters over means indicate significant difference at 0.05 confidence level:
a: means are significantly different at P-value<0.0001.
b: means are significantly different at P-value<0.0001.

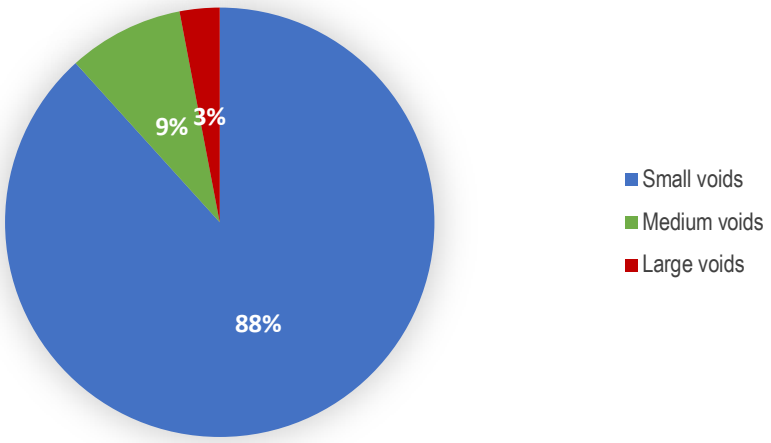

Figure 3.8: Percentage of small, medium and large voids in SFRC posts (n=15).

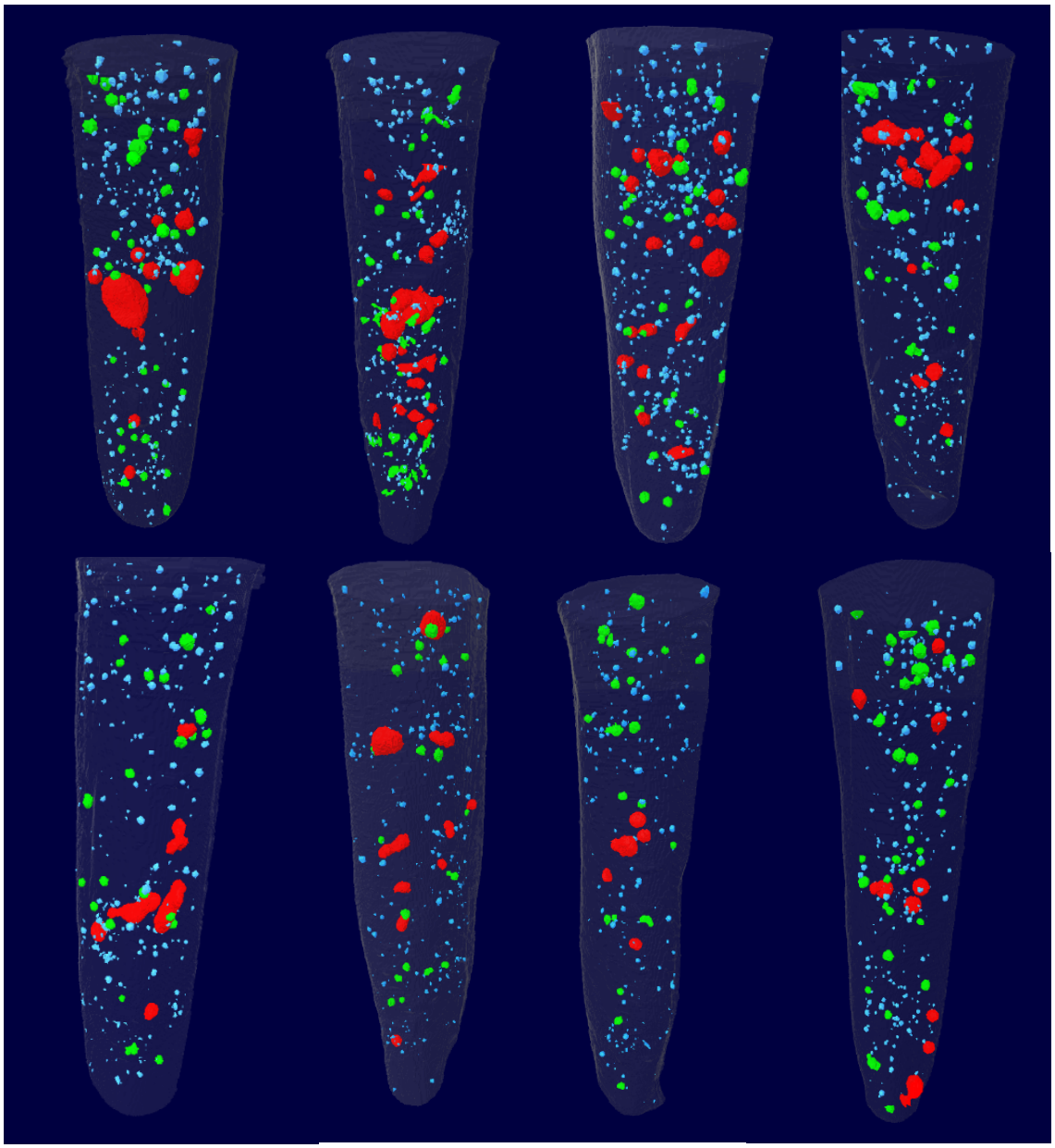

Figure 3.9: Colour-coded models of closed voids in different specimens. Red=large voids, green=medium voids and blue=small voids. Small voids represent the highest void content. Both small and medium voids are evenly distributed along the length of the post and have relatively regular round shapes. Large voids did not have a typical shape or distribution pattern.

3.4 Discussion

In this study, micro-CT was used for void analysis and characterisation in SFRC posts and cores. Micro-CT rendered models were initially visualized to assess post and core structures and design an appropriate analytical approach using micro-CT software. Although micro-CT is a non-destructive, comprehensive and reproducible analysis method, the scanning process was time consuming and required large computer data storage. The specimens required scanning times between 2-3 hours per specimen, and the data were stored in files that occupied storage size ranges between 10-12 gigabytes per specimen.

Void content in composite restorations have been calculated using different methods with inconsistent results. Void content of 9.4% has been calculated by SEM micrographs (Ogden, 1985), 1.2-28.4% by point counting in photographs (Skjorland et al., 1982) and 0.7- 5.1% by micro-CT (Lagouvardos et al., 2015; Dunn, 2016).

Despite its efficiency for comprehensive visualization and characterisation of voids in dental composites, micro-CT has not been applied previously to analyse voids in SFRC restorations, possibly due to the time and labour-intensive investment. Voids in SFRC have only been demonstrated in SEM micrographs with a lack of void analysis reporting (Shouha et al., 2014; Bijelic et al., 2015a; Garoushi et al., 2017). In addition to the invasive nature of SEM methods, the void interpretation using this method is limited and imprecise (Uzun et al., 2016).

Mehdikhani et al. (2018) emphasised on the importance of considering void characteristics such as size, shape, distribution and location for accurate void analysis. This study have considered those characteristics in void analysis in SFRC posts and cores.

Micro-CT structural analyses, in this study, indicated that all specimens had voids within the post and core and at the post-dentine interface. The void volume fraction in the posts ranged between 1.3-4.9% and in the cores between 0.2-1.8%. The combined mean volume fraction of the voids in posts and cores was 3.6%. To the knowledge of the author, a critical void content has not been defined in composites for dental applications. However, Ghiorse (1993) suggested that –apart from advanced composite applications–

voids levels of 5% can be tolerated. For example, in dynamic aerospace composites, Ghiorse indicated that void content above 1% is not allowed.

The results presented here indicate that the void volume fraction in the post (closed voids) is significantly higher than the core. This difference might suggest the influence of different application techniques on void formation. In this study SFRC was incrementally applied into the post spaces to build the posts. The post build up was technique sensitive and required careful insertion and manipulation of each increment to ensure maximum adaptation of the post material to the surrounding dentine and to the previous SFRC layer. On a microstructural level, over manipulation during incremental application might alter the fibre distribution (Bijelic et al., 2013; 2016), and as a result, areas of clustered or of dispersed fibres might be created with the possibility of void creation (Fonseca et al., 2014; 2016; Shouha et al., 2014).The challenging manipulation of SFRC inside the post space is influenced by difficult accessibility and the material's viscosity.

Highly viscous composite is associated with compromised handling characteristics, including difficult packing and malleability and stickiness of the material to instruments (material pull-back), which might lead to interlayer void formation (Dietschi et al., 1995; Opdam et al., 1996b; Lagouvardos et al., 2015; Bijelic et al., 2016). In this study, during post fabrication, SFRC tended to stick to the packing instrument, resulting in over manipulation and air bubble entrapments between the layers. This is in accordance with other research conducted by Bijelic et al on everX Posterior™ SFRC where a high viscosity of SFRC was reported (Bijelic et al., 2015a ; 2016).

Viscosity of resins is affected by filler quantity, geometry, shape and aspect ratio (Choi et al., 2000a; Al-Sharaa and Watts, 2003, Lee et al., 2006, Kaleem et al., 2009, Elbishari et al., 2011). It has been demonstrated that the viscosity of dental composites increases as the filler quantity increases, and for the same filler quantity, the viscosity increases progressively when sphere; grain; plate and rod-shaped fillers are compared. For rod-shaped fillers such as glass fibres, as the aspect ratio (length/diameter) increases, the viscosity increases. In this regard, Elbishari et al. (2011 and 2012) have evaluated the effect of filler size on the viscosity and handling properties of composites and on void formation. They concluded that

as the fillers increased in size, the viscosity (Elbishari et al., 2011) and void content increased (Elbishari et al., 2012). Lagouvardos et al., (2015) have investigated the relationship between viscosity and void volume fraction in composite and have found the highest void volume fraction of 2.7% in highly viscous composite.

The cores, on the other hand, were constructed as bulk-fill restorations. A recent micro-CT analysis of porosity in bulk-fill composite in comparison to incrementally applied composite conducted by Dunn et al. (2016) found that the incremental placement technique resulted in significantly greater porosity than the bulk-fill technique. The difference in the cavity size between the post and the core might also contribute to increased interlayer void content in the post in comparison to the core. It has been found that insertion of highly viscous composite in small cavities (1.0-1.5 mm) is associated with difficult manipulation and internal void formation (Lagouvardos et al., 2015).

The micro-CT trans-axial images revealed close adaptation of the posts to the canal walls. Regardless the anatomical variability of the canals, the SFRC post adhered to the canal wall and followed the shape of the respective canal (Figure 3.4). Minimizing the discrepancy between the post and the canal walls is desirable. A post that is well adapted to the surrounding dentine , distributes the stresses uniformly within the canal (Anchieta et al., 2012, Lazari et al., 2013) and reduces the thickness of the cement (Grandini et al., 2005a), which controls void formation (Grandini et al., 2005a, Rengo et al., 2014), microleakage (Milutinovic-Nikolic et al., 2007) and cement polymerization shrinkage stresses (Choi et al., 2000b; Ferracane, 2005).

To have an insight into post adaptation, the volume and volume fraction of air spaces entrapped at the post-dentine interface was measured and categorized as open voids. The results indicate that the mean volume fraction of the open voids at post-dentine interfaces was 1.4%, which is below a reported post-dentine gap (1.9-3.3%) measured by Papadogiannis et al. (2009) using micro-CT.

The open voids between the SFRC post and the dentine might be created as a result to composite's handling characteristics (e.g. viscosity and wettability) or incremental application technique. However, the

effect of both factors on composite adaptation to cavity walls is controversial. It has been reported that highly viscous composites are associated with inadequate restoration adaptation to the cavity walls (Opdam et al., 1996a; Peutzfeldt and Asmussen, 2004). On the contrary, Jordan and Suzuki (1992) have recommended a highly-viscous, condensable composite for good wall adaptation. In the current study, it seems that the viscosity of SFRC has negatively influenced SFRC interlayer adaptation more than SFRC-to-dentine adaptation. This was evident in higher closed void (voids inside the post) content compared to open voids (voids at post-dentine interface) content.

As discussed earlier, incremental application has been linked to interlayer void development in composite restorations, however, this link has not yet been clearly established between incremental technique and restoration adaptation to cavity walls. Alternatively, application technique has been linked to polymerization shrinkage and gap formation at the restoration-dentine interface. While some researchers favour the incremental technique over the bulk-fill method to control polymerization shrinkage and gaps at restoration-dentine interface (Yamazaki et al., 2006; Park et al., 2008; Kwon et al., 2012), other researchers have favoured the bulk-fill technique (Abbas et al., 2003; Bicalho et al., 2014; Rosatto et al., 2015) or have found no significant difference between the two application techniques (Kuijs et al., 2003, Tuncer et al., 2013; Silva de Assis et al., 2016).

Although quantifying polymerization shrinkage in SFRC is beyond the scope of this project, there is lack of evidence that incrementally-built-post have negatively affected polymerization shrinkage or adaptation of the post to dentine. In this context, lower polymerization shrinkage of SFRC has been reported compared to PFC and other bulk-fill composite restorations (Garoushi et al., 2013b; 2015a, Tsujimoto et al., 2016c).

The CTAn software results have indicated that, the coronal third of the post had significantly higher void volumes compared to middle and apical thirds. Nevertheless, there was no significant difference in void volume fraction between the three sections. In other words, the highest void volume in coronal third might be explained by the highest composite volume in that particular section compared to middle and apical

thirds. A contradicting result was reported by Lagouvardos et al (2015) who found that the deepest part of the restoration had the most interlayer voids, especially when thick-consistency composite was used.

In this study, there were significantly fewer large voids (3 %) inside SFRC posts compared to small and medium voids. Small voids percentage, on the other hand, was significantly the highest (88.3%), which agrees with Ogden et al., (1985) who found that the vast majority of voids detected in SEM micrographs were 50 μm or less in different composite products.

As shown in the colour-coded models (Figure 3.9), large voids can be of elongated or irregular shape and were scattered unevenly in the post with the largest voids located mostly in the middle third. Small and medium voids, on the other hand, tended to be regular and round in shape and distributed evenly in all sections of the posts.

To interpret void characteristics in the SFRC post and core, a strand (ø = 1.8 mm, I= 14mm) of freshly extruded SFRC material was scanned and analysed using micro-CT and related software (Figure 3.10). Non-manipulated material had voids volume of 0.2 mm^3 and voids volume fraction of 0.9%, which is within the range of void volume fraction (0.05-1.4%) reported by Fano et al. (1995) in raw composite.

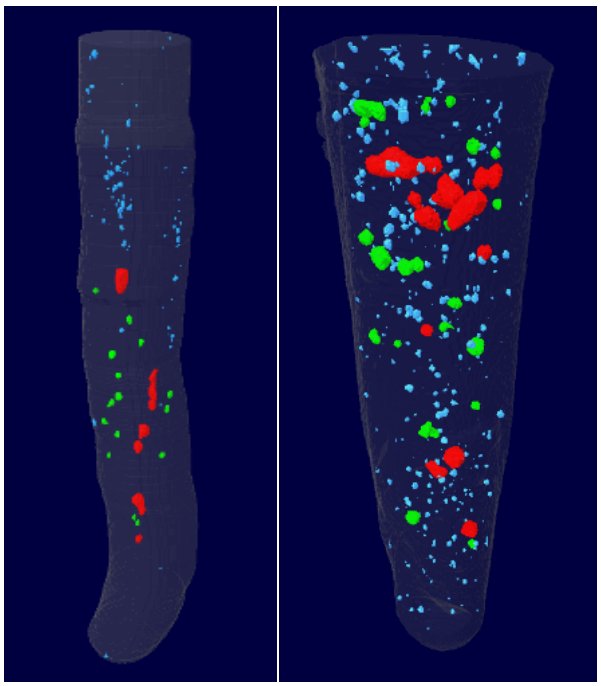

Figure 3.10: Colour-coded model of a freshly extruded SFRC material and SFRC post and core. Both models have small, medium and large voids, however, voids become larger when SFRC material is inserted inside the post space.

The percentage of small (81.3%), medium (13.4%) and large (5.3%) voids in the raw material is in accordance with the mean void percentage of each size in SFRC posts. Also, similar to SFRC post, small and medium voids in the raw SFRC material were of regular round shapes and large voids were of irregular elongated shapes. These findings illustrate the fact that small, medium and large voids might be created during the manufacturing process with the shape of the large voids affected by the process of extruding the material through the narrow nozzle. The very large voids in the post were absent in the raw material. This might indicate that the largest voids that were present in the post were created during material insertion and condensation inside the post space (Ironside and Makinson, 1993).

One of the challenges in studies such as this is that micro-CT scanning and analysis requires meticulous setting of the scanner and software parameters in order to obtain reliable images and data to facilitate accurate interpretation of the voids. Micro-CT scanning generates a dataset of 2D projected images, which are reconstructed to form grayscale cross-section images datasets. Binarization of grayscale images is necessary prior to analysis to allow differentiation between the subjects (voids) from the background (composite). This step is critical and could influence interpretation of the results. Factors such as image noise, scaffold composition (different materials with overlapping X-ray attenuation values) and beam hardening can affect thin structures (e.g. voids walls), resulting in lower X-ray density for these structures (Bartos et al., 2018). Additionally, it must be noted in this study, the pixel size was 9µm in the micro-CT images, therefore, voids smaller than that threshold might not have been detected.

According to many reports, the presence of voids is detrimental to the structural integrity and mechanical properties of composites (Vallittu, 1995a; Miettinen & Vallittu, 1997; Karacaer et al., 2003; Fonseca et al., 2014). Other reports have indicated that voids might potentially have a positive effect on composite performance under load (Alster et al., 1992; Rengo et al., 2014). However, there are no reports to support either conclusion in relation to voids in SRFC. Therefore, the next two chapters will evaluate the failure of ETT restored with SFRC posts and cores (Chapter 4) and investigate whether or not voids in SFRC influence the failure of ETT restored with SFRC posts and cores (Chapter 5).

CHAPTER 4

Failure load and failure mode evaluation of ETT restored with SFRC posts and cores

---

This chapter describes an investigation of the fracture strength of ETT restored with SFRC posts and cores in comparison to sound teeth and ETT restored with prefabricated FRC posts after subjecting the teeth to cyclic fracture testing

It includes an introduction, material and methods (describing experimental and control groups preparation and fracture resistance test protocol), results (failure load and failure mode) and discussion.

4.1 Introduction

For decades, restorative modalities for ETT including posts and cores, have been the subject of dental investigations. Clinical and laboratory-based research have been conducted to evaluate and compare different post systems. For any material to satisfactorily function as a post and core, it should minimize the possibility of tooth failures that are catastrophic, early in service or at a low functional load. The consequence of such failures is more complicated when the ETT is an abutment for a fixed or removable partial prosthesis. In this context, fracture resistance testing in response to masticatory (dynamic) and traumatic (static) loads has been conducted to evaluate failure load and failure mode of ETT restored with different post systems.

Fracture resistance testing of ETT restored with glass FRC posts has been reported in the literature, including prefabricated FRC posts, individually-formed FRC and SFRC posts. Conflicting results on the mechanical performance ETT restored with prefabricated FRC posts (Maccari et al., 2007; Ambica et al., 2013; Pereira et al., 2014; Abduljawad et al., 2016; Habibzadeh et al., 2017) and individually formed FRC posts have been reported (Fokkinga et al., 2006a; Bonfante et al., 2007; Abo El-Ela et al., 2008; Ozcan and Valandro, 2009).

SFRC has been promoted recently as a post system and the fracture resistance of ETT restored with SFRC as post and core has been evaluated in a limited number of in vitro studies (Garoushi et al., 2009, Bijelic et al., 2013, Forster et al., 2017). These studies demonstrated that ETT restored with SFRC have high fracture strength. ETT restored with SFRC posts demonstrated higher failure load than prefabricated FRC posts (Bijelic et al., 2013; Forster et al., 2017) and individually-formed FRC posts (Garoushi et al., 2009). Bijelic et al. (2013) and Garoushi et al. (2009) have indicated that failures of ETT restored with SFRC posts are restorable, but Forster et al. (2017), have reported higher incidences of non-restorable failures in ETT restored with SFRC posts in comparison to prefabricated FRC posts.

In the abovementioned studies, the conclusions were based on monotonic static compressive testing of ETT restored with SFRC. However, restorative failures in the oral cavity are more likely induced by

repetitive functional/parafunctional forces in a thermally changing, aqueous environment rather of being induced by a single, high load incident. These conditions are ideally simulated by thermomechanical loading that involves thermocycling (aging) and dynamic loading (fatigue) protocols (Naumann et al., 2005c; Amaral et al., 2007; Dietschi et al., 2008; Naumann et al., 2009; Sterzenbach et al., 2012; Morresi et al., 2014; Blumer et al., 2015).

Different protocols for dynamic fatigue loading have been described for fracture resistance testing. Nevertheless, the testing protocols lack standardization and have been modified from time to time. Dynamic loading protocols differ in terms of loading parameters such as frequency, direction and magnitude of the applied forces and the number and duration of the cycles. Also, protocols with or without simultaneous thermocycling and with or without additional static load-to-failure have been described.

In 1990, Krejci introduced a chewing simulator in which the load is applied over a large number of cycles (up to 1,200, 000 cycles) to simulate up to 5 years of clinical service. This was the first and remains the most frequently available method for dynamic testing, yet it is time consuming and expensive. Different versions of chewing simulator using different loading chamber designs, loading cycles, loading devices and forces have been developed by researchers.

A simplified and economic dynamic loading using universal mechanical testing apparatus was introduced by Isidor and Brondum (1992). They described intermittent dynamic loading in universal mechanical testing machine, where cyclic loading is applied at a frequency of 2 cycles/second and a magnitude that is constant in all cycles. Although the loading parameters of this protocol have been modified by different researchers, the main disadvantage is lack of consistency. It has been observed that the intermittent loading frequently continues for a long period without failure, hence, the test is discontinued, which complicates statistical interpretation (Isidor et al., 1995).

Gradual cyclic loading was introduced by Strand et al in 1995. This is a modification of the intermittent loading in which the load is applied in cycles with a gradual increase in the loading magnitude in each cycle (Strand et al., 1995). For example, if the load commences at 50N, after certain number of cycles,

the load is increased to 100N and continues for the same number of cycles before it raised to 150N. The load gradual elevation continues until the specimen fails.

Naumann et al. (2005c) compared different loading protocols applied to restored ETT. They found that gradual cyclic loading and a chewing simulator provide equivalent results. However, for realistic testing conditions, they considered gradual cyclic protocol as a simplified, economic and time-saving alternative to the use of a more complex chewing simulator.

Thermocycling has been found to be an effective artificial ageing method (Morresi et al., 2014). Thermocycling is achieved by subjecting the specimen to repeated cycles of hot and cold temperature to reproduce thermal changes in oral cavity. It is either applied prior to or simultaneously with the dynamic loading. During thermocycling, hot water accelerates restorative material hydrolysis, and the thermal expansion coefficients variation between dental tissues and restorative materials generates contraction/expansion stresses (De Munck et al., 2005). Again, thermocycling lacks technical standardization with a wide range of temperature extremes, transfer times between temperatures and dwell times (Morresi et al., 2014). However, the International Standards Organization (ISO) has published a standard protocol for thermocycling that involves 500 cycles in each bath of 5–55 ^{o}C with a dwell time ≥ 20 s (ISO, 2003).

When investigating failure of dental composite restorations, it seems that thermomechanical testing is a realistic tool to evaluate fracture resistance and long-term mechanical properties of composites (Lohbauer et al., 2003). Thermomechanical testing simulates closely the intraoral functional conditions. Also, fatigue fracture has been found to be the most common reason for composite failure (Kohler et al., 2000; Burke et al., 2001). Cracks in fractured composite are initiated and promoted by dynamic loading and water exposure (Lohbauer et al., 2003). Dynamic loading initiates a crack that grow slowly, and water exposure accelerates the crack propagation through weakening of the matrix or degradation of matrix-filler interfacial bonding (Drummond, 1989; Braem et al., 1995).

The crack growth and fracture behaviour in SFRCs are even more complex due to the complexity of SFRC microstructural constituents such as fibre size, orientation and distribution (Mortazavian and Fatemi, 2015a; 2015b). Therefore, it seems that thermomechanical-testing better evaluates SFRC failure behaviour.

Failure of SFRC as a bulk-fill restoration has been reported using different fracture testing protocols. While some studies have evaluated the fatigue failure of SFRC in chewing simulators with (Rocca et al., 2015; Barreto et al., 2016) and without subsequent static load-to-failure (Soares et al., 2018), other studies have performed static failure tests (Atalay et al., 2016; Garlapati et al., 2017). There is, however, lack of data on the failure of ETT restored with SFRC posts and cores under thermomechanical loading protocol.

Considering the previously mentioned test designs, and to provide a reliable simulation of the oral environment, this study applied the standard ISO thermocycling and a gradual cyclic fracture resistance testing protocols to evaluate the failure of SFRC post and cores.

After conducting fracture resistance tests on ETT restored with posts and cores, mode of failure is commonly evaluated, which gives an insight into the location, severity and restorability of the fracture. Mode of failure is generally assessed by visual inspection of the teeth, radiographic image analysis or microscopic observation. However, in this project, micro-CT was utilized for a non-destructive and comprehensive mode of failure evaluation of fractured ETT.

Aims of this study:

To evaluate failure load and failure mode of ETT restored with SFRC posts and cores in response to a thermomechanical fracture resistance testing, and to compare the failure of ETT restored with SFRC post and core to the failure of ETT restored with prefabricated FRC post and sound premolars.

4.2 Material and methods

Both control (sound premolars, n=15) and experimental groups (restored ETT, n=30) were subjected to fracture resistance testing (Figure 4.1).

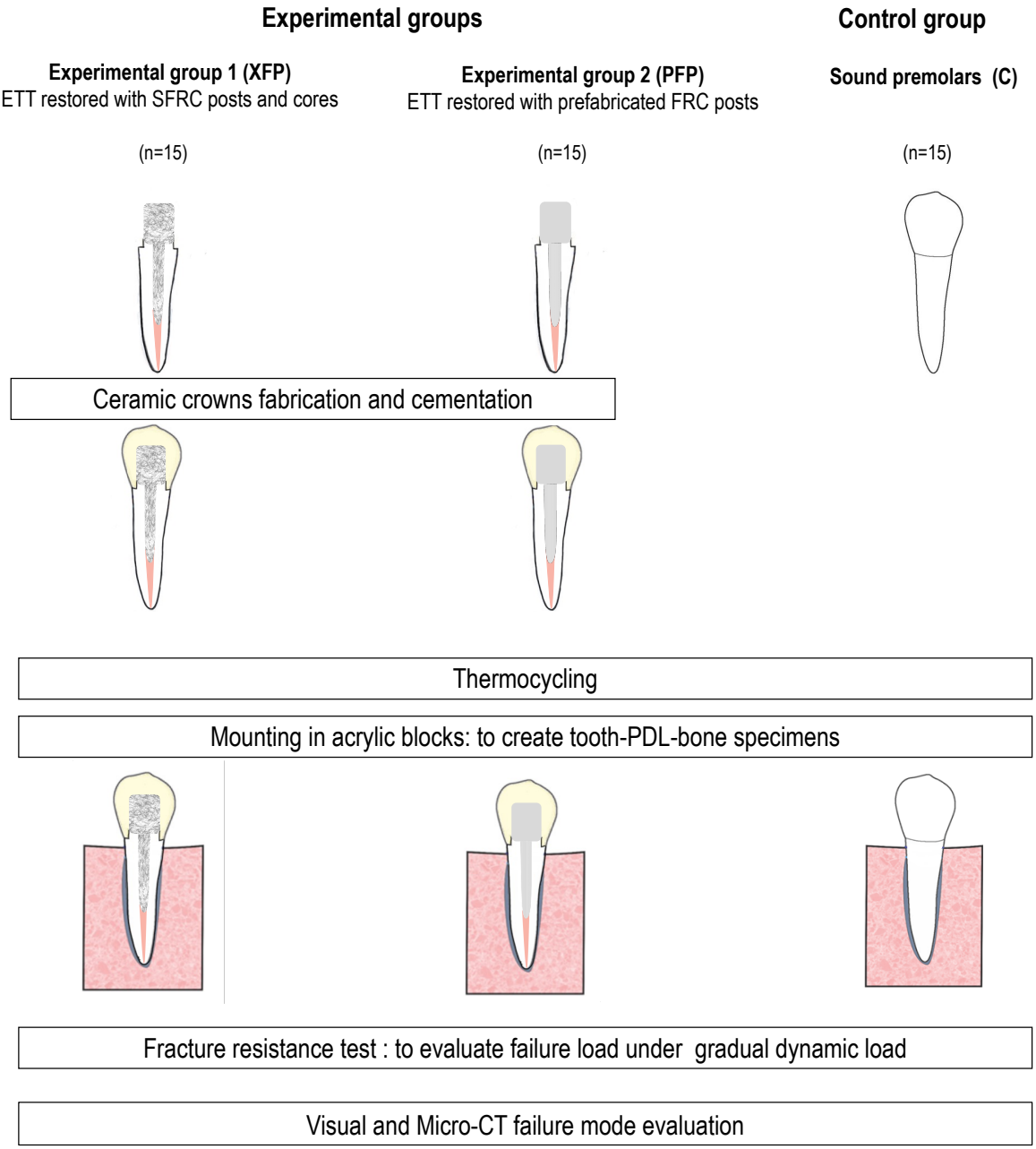

Figure 4.1: Summary of the fracture resistance testing protocol for tested groups (n=45)

In this study, experimental group 1 (XFP): ETT restored with SFRC posts and cores, and group 2 (PFP): ETT restored with prefabricated FRC posts, received ceramic crowns. Then, all teeth in experimental and control groups were thermocycled, mounted in acrylic resin blocks with simulated PDL in preparation for gradual dynamic fracture resistance test. Finally, teeth were inspected visually and using micro-CT images to evaluate mode of failure.

4.2.1 Ceramic crowns fabrication and cementation

When testing post systems, it has been argued that crown placement creates a ferrule effect, which will overpower the tested post system (Barkhordar et al., 1989; Sorensen and Engelman, 1990; Assif et al., 1993; Libman and Nicholls, 1995). However, for extensively damaged ETT, crown placement on a post and core is recommended to restore aesthetics and function (Sorensen and Engelman, 1990; Butz et al., 2001; Torbjorner and Fransson, 2004; Naumann et al., 2005c). In the current project, ceramic crowns were selected for aesthetic full coverage of the extensively damaged endodontically treated premolars to simulate clinical management of such teeth (Butz et al., 2001; Naumann et al., 2005c).

Ceramic crowns were fabricated for teeth in the experimental groups. A digital scanner (inEos X5; Dentsply Sirona, NC, USA) was used to directly scan the cores in both experimental groups. The crown thickness (1.5mm), height (8mm), marginal thickness (1.0mm) and cement space thickness (30μm) were all standardized through the scanner software (inLab SW 15.0.; Dentsply Sirona, NC, USA).

The crowns were then milled (inLab MC XL; Dentsply Sirona, NC, USA) from A4 shade ceramic blocks (IPS e.max® CAD; Ivoclar Vivadent, Schaan, Liechtenstein). All crowns were visually evaluated to ensure complete seating and marginal adaptation to their respective specimens, with no external or internal adjustments. The crowns were cleaned in distilled water and cemented using dual cure resin cement (RelyX™; 3M ESPE, MN, USA) according to the manufacturer's instructions. The crowns were seated, and finger pressure was maintained during the light polymerization (XL 3000; 3M/ESPE) which was applied circumferentially for 40 seconds.

4.2.2 Thermocycling

Teeth in all groups were aged by thermocycling following the standardized protocol outlined in the most recent International Organization for Standardization ISO/TR 11405 (ISO, 2003). Teeth were subjected to 500 cycles between two water baths of 5°C and 55°C. The specimens were immersed in each bath for 30 seconds (dwell time) (De Munck et al., 2005; Siso et al., 2007).

4.2.3 Teeth mounting in acrylic resin blocks

All teeth were then mounted in acrylic resin blocks to represent the alveolar bone. However, prior to mounting in the resin blocks, the PDL was simulated around the roots. This was to create tooth-PDL-bone specimens (Figure 4.2).

4.2.3.1 PDL simulation

Teeth in all groups were coated with multiple coats of latex rubber (Rubber-Sep®, Kerr Dental, CA, USA) to simulate the PDL. This PDL simulation technique was developed as part of this project (AlZahrani and Richards, 2018) (paper is attached in Appendix 4). This technique ensures uniform and continuous thickness of the simulated PDL around the roots as well as consistency of the PDL reproduction among teeth in all groups. Uniformity and reproducibility of this technique in comparison to another commonly used PDL simulation technique was confirmed through micro-CT scan evaluation (AlZahrani and Richards, 2018).

Figure 4.2: A tooth-PDL-bone specimen

4.2.3.2 Alveolar bone simulation

Teeth with the simulated PDL layer were mounted in auto-polymerizing acrylic resin contained in cylindrical brass mould (AlZahrani and Richards, 2018).

4.2.4 Fracture resistance testing

All teeth were subjected to gradual dynamic fatigue loading until failure occurred. A Universal testing machine (Instron 8874) with a 1.0 KN load cell was used to for fracture resistance test. A custom-made mounting apparatus was utilized to fix the tooth-PDL-bone specimen to the base of the Instron machine (Figure 4.3). The mounting apparatus was fabricated with a deep centre corresponding to the brass cylinder dimensions to allow stabilization of the block. Two stainless steel screws were added to secure the specimen in the mounting apparatus. To avoid slippage of the mounting apparatus, it was further stabilized in position below the loading device using fixing accessories (Figure 4.3).

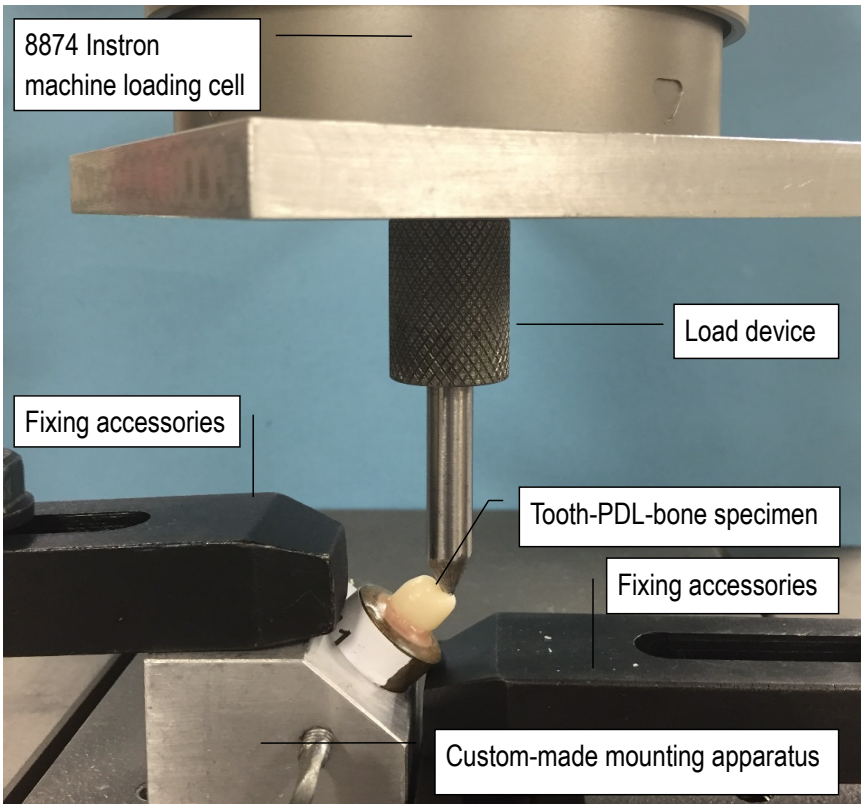

Figure 4.3: A tooth-PDL-bone specimen mounted into the Instron 8874 universal testing machine

Gradual dynamic fracture resistance testing was then commenced applying the following guidelines:

a. Load position: The load was applied on the non-functional cusp as they have been demonstrated to show weaker resistance to fracture than functional cusps (Cavel et al., 1985; Khera et al., 1990).

b. Load direction: The mounting base was manufactured to allow loading of the teeth at an angle of 45°to the long axis of the tooth (Loney et al., 1995; Butz et al., 2001; Naumann et al., 2005c; Mangold and Kern, 2011; Zicari et al., 2012; Nie et al., 2013). This load direction represents the worst-case scenario in the fracture resistance of ETT and has been considered appropriate for evaluating the mechanical behaviour of post restorations (Zicari et al., 2012).

c. Load device: The load was applied using a cylindrical-shaped stainless-steel rod with a 2.00 mm diameter round terminus attached to the crosshead grip of the Instron machine (Salameh et al., 2007; Mohammadi et al., 2009; Nie et al., 2013).

d. Load parameters: The gradual dynamic loading protocol proposed by Naumann et al. (2005c) was applied in this study. The loading protocol was designed to start with loading force of 10-50 N with frequency of 0.5 Hz and for 100 cycles. The applied force was then increased in steps of 50N in each loading level. The testing protocol was designed to be automatically discontinued when the tooth fails, which was indicated by loading device vertical displacement due to dislocation of the fractured tooth. The load-to-failure was recorded.

4.2.5 Failure mode evaluation

Teeth were inspected visually and using micro-CT (experimental groups) for comprehensive evaluation of the mode of failure. Prior to micro-CT scanning, the teeth with the surrounding acrylic were released from the brass moulds to avoid metal artefacts in the projected images. The teeth were then scanned using the micro-CT scanner (SkyScan 1076; Bruker microCT) with the same acquisition and dataset reconstruction (SkyScan NRecon software, version 1.6.9.4) parameters used in the pre-fracture scanning procedure described in Chapter 3. Data Viewer software (Bruker microCT, version 1.5.1.2) and CTAn

software (Bruker microCT, version 1.14.4.1) were used for qualitative analysis and classification of failures modes in experimental groups. The following failure modes were identified:

I. **Restorable:** which is further classified into;

- Crack/chipping of the crown (natural or ceramic).
- Decementation of the ceramic crown.
- Decementation of ceramic crown with post and core.
- Restoration bulk fracture (with/without tooth fracture above CEJ).

II. **Non-restorable:** Deep tooth fracture (below CEJ)

4.2.6 Statistical analysis

The descriptive statistics for the failure loads were calculated. Univariate linear regression and post-hoc multiple pairwise comparisons were conducted to detect significant differences in the mean failure load and failure mode between groups at 0.05 level of significance. All statistical analyses were performed using software: SAS 9.4 (SAS Institute Inc., Cary, NC, USA).

4.3 Results

4.3.1 Fracture resistance test results

The descriptive statistics for the failure load are summarised in Table 4.1. The mean failure load (± SD) for teeth restored with SFRC posts (XFP group) is 731.25±86.33N. The highest mean failure load was recorded for the control group (1209.2±126.65N), while the lowest was recorded for teeth restored with prefabricated FRC posts (373.86±64.21N) (Figure 4.4).

Univariate linear regression analyses were conducted to detect significant differences in the mean failure load between groups. Assumptions of a linear regression were upheld for all the models. Significant overall differences in the mean failure load were revealed between groups (P-value <0.0001) (Table 4.1). Post-hoc multiple pairwise comparisons were conducted (Appendix 5). They indicated that the failure load of control group was significantly higher than the failure load of teeth in both experimental groups. The failure load of teeth in XFP group (teeth restored with SFRC post) was significantly higher than PFP group (teeth restored with prefabricated FRC post).

Table 4.1: Descriptive statistics for the failure load in control and experimental groups (n=45)

Group	n	Mean (N)	SD	Minimum Load	Maximum Load
Control group	15	1209.20*	126.65	975.21	1377.5
XFP group	15	731.25*	86.33	577.94	876.45
PFP group	15	373.86*	64.21	276.82	456.19

* means are significantly different at P-value<0.0001.
XFP: ETT restored with SFRC post, **PFP**: ETT restored with prefabricated FRC post

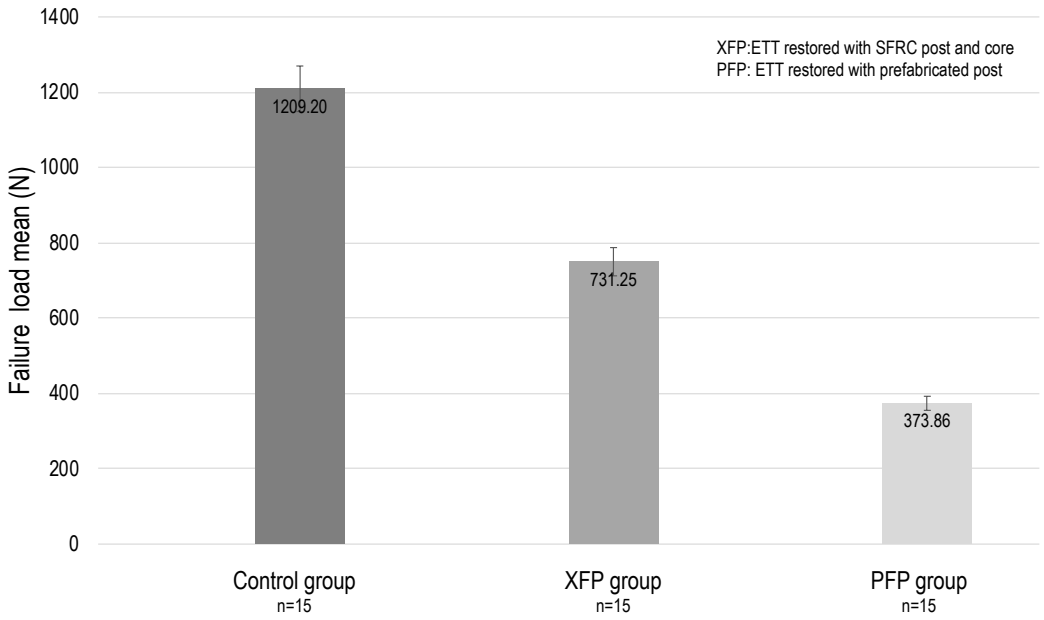

Figure 4.4: The mean failure load of experimental and control groups (n=45)

4.3.2 Failure mode evaluation results

Table 4.2 shows the number of failed specimens in each failure mode class. All of the failures in control and XFP groups were restorable. While all teeth in control group failed by chipping of the crown, five teeth in each experimental group failed by crack/chipping of the cemented ceramic crown with intact posts and cores. The PFP group had five specimens with decemented ceramic crowns, while in the XFP group, four specimens failed similarly. Only one specimen failed by complete decementation of the restorative system (ceramic crown with the post and core), and this mode of failure was observed only in PFP group. Six specimens in XFP group failed by restoration bulk fracture with/without restorable tooth fracture above CEJ. On the other hand, four specimens in PFP group failed by non-restorable tooth fracture that extends deeply into the root (Figure 4.5).

Table 4.2: Number of failed specimens in each failure mode class

Failure mode		**Control group**	**XFP group**	**PFP group**
Restorable	Crack/chipping of the crown (natural or ceramic)	15	5	5
	Decementation of the ceramic crown	0	4	5
	Decementation of ceramic crown with post and core	0	0	1
	Restoration bulk fracture (with/without tooth fracture above CEJ)	0	6	0
Non-restorable	Deep tooth fracture (below CEJ)	0	0	4
Total		15	15	15

XFP: ETT restored with SFRC post, **PFP**: ETT restored with prefabricated FRC post.

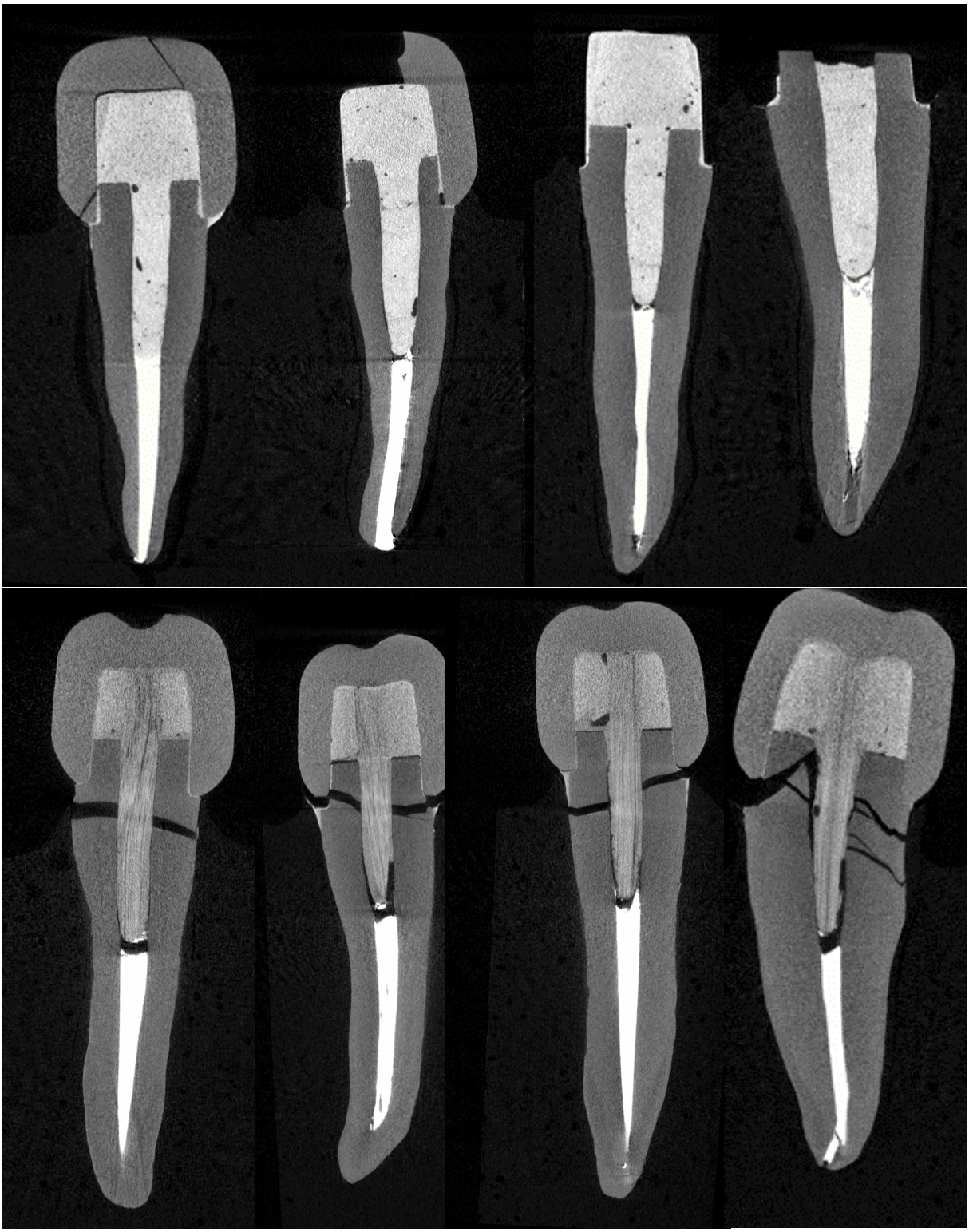

Figure 4.5: Micro-CT images of the failed experimental groups; top images: restorable failures in XFP group: from left to right; crack in the ceramic crown, chipping of the ceramic crown, decementation of ceramic crown and restoration bulk fracture with intact tooth structure. Bottom images: non-restorable failures in PFP group.

Using cross-tabulation, a statistically significant difference in the mode of failure was found between test groups (Fisher's Exact Test P-value = 0.0123) (Appendix 6). While none of the teeth in XFP group and control group had non-restorable failures, 27% of the specimens in PFP group had non-restorable tooth fracture (below CEJ). In PFP group, 7% of the specimens failed by complete decementation of the post, while teeth in XFP group never failed by decementation of the post system. In XFP group, 40 % of the specimens had bulk fracture of the restoration (Table 4.3).

Table 4.3: Percentage of failures in test groups (n=45)

Mode of failure		**Percentage of failure (%)**		
		Control group (n=15)	**PFP group** (n=15)	**XFP group** (n=15)
Restorable	Crack/chipping of the crown (natural or ceramic)	100	33	33
	Decementation of the ceramic crown	0	33	27
	Decementation of ceramic crown with post and core	0	7	0
	Restoration bulk fracture (with/without tooth fracture above CEJ)	0	0	40
Non-restorable	Deep tooth fracture (below CEJ)	0	27	0

XFP: ETT restored with SFRC post, **PFP**: ETT restored with prefabricated FRC post

4.4 Discussion

It is advisable to conduct a fracture resistance test that simulates the intraoral environmental, structural and functional conditions to improve the clinical applicability of the test results. Therefore, a PDL was simulated, aging and fatigue loading were performed in this study. Nevertheless, teeth are exposed intraorally to complicated 3D loading conditions that involve compression, tension and shear, which are difficult to simulate simultaneously in laboratory studies. Hence, unidirectional load is usually applied to assess a specific aspect of a restorative material (mechanical, physical, biological or chemical) to simplify testing condition (Bayne and Thompson, 2013). Although the load direction was standardised in this study, the control teeth were not restored and as a result there would be some slight variation in the loading angle as there would be clinically. Premolars in this study has been decoronated to simulate an extreme but not unusual clinical situation encountered in ETT, and a "ferrule" was incorporated to embrace and protect the circumference of the root (Sorensen and Engelman; 1990, Assif et al., 1993; Isidor et al., 1999).

This study has demonstrated that ETT restored with SFRC posts and cores failed at a mean failure load of 731.25N±86.33. A similar failure load (727.98N±287.37) was reported by Forster et al. (2017) and a lower failure load (490.5N±288.6) was reported by Bijelic et al. (2013). Both studies tested ETT restored with SFRC posts and cores under static load. However, Forster et al. evaluated endodontically treated premolars with conservative access cavity and with a simulated PDL, while Bijelic et al. evaluated extensively damaged incisors without a simulated PDL. Presence of a simulated PDL in Forster et al. study and the difference in the amount of remaining tooth structure compared to Bijelic et al. study might have influenced the stresses distribution and fracture strength results.

While all ETT restored with SFRC posts had restorable failures in the current study, Forster et al. and Bijelic et al. have reported non-restorable fractures for SFRC restored ETT. This might be explained by the traumatic static load applied by Forster et al. and Bijelic et al. and the lack of ferrule effect in the study by Bijelic et al.

Testing human teeth is associated with inherent complications due to size variability. In spite of this uncontrolled variation, significant differences were demonstrated in this study. The results have indicated that sound premolars had higher fracture strength (1209.2N±126.65) compared to restored ETT, which is in accordance with other studies (Ambica et al., 2013; Forster et al., 2017). In unrestored teeth, occlusal load dissipates over a large volume of tooth structure (enamel and dentine), which results in minimal overall stresses and tooth deformation (Bayne and Thompson, 2013). In restored teeth, the load transfers from the restoration directly to dentine due to partial or complete loss of enamel, which results in decreased fracture resistance (Bayne and Thompson, 2013). Furthermore, loss of coronal or intra-radicular dentine in the preparation for a post and core restoration might compromise the dentine's fracture strength (Kinney et al., 2003, Meira et al., 2009). Ambica et al. (2013) have reported a 22% reduction in ETT fracture strength compared to 16% in sound teeth after cyclic loading.

FRC posts have been introduced with the claim that they are manufactured to have an elastic modulus of 15-46 GPa (Lassila et al., 2004; Mallick, 2007; Plotino et al., 2007; Zicari et al., 2013) that is comparable to the modulus range reported for dentine (15 - 40 GPa)(O'Brien, 2002; Kinney et al., 2003; Ziskind et al., 2011; Zhang et al., 2014). Although controversial, the similarity in elastic modulus between the post and dentine has been speculated to reduce the chances of root fracture (Drummond, 2000; Cormier et al., 2001; Fokkinga et al., 2004; Asmussen et al., 2005; Galhano et al., 2005). In this context, root fracture occurred in four teeth in the experimental groups in this study. Other failure modes such as loss of marginal seal, core fracture and post fracture or loss of retention are predicted to occur more frequently in ETT restored with FRC posts, which is in accordance with the current study (Lambjerg-Hansen and Asmussen, 1997; Torbjorner and Fransson, 2004).

The mechanical behaviour and mode of failure of ETT restored with prefabricated FRC posts were different from ETT restored with SFRC posts in this study. ETT restored with SFRC posts showed superior fracture strength compared to ETT restored with prefabricated FRC posts, which is in accordance with other studies (Bijelic et al., 2013; Forster et al., 2017). While factors such as post length, core and crown dimensions and remaining tooth structure were standardized in this study, there were differences in post

adaptation, diameter and structural composition between the tested posts, which might explain the difference in the mechanical behaviour between ETT restored with SFRC posts and prefabricated FRC posts.

The SFRC posts have multidirectional discontinuous E-glass fibres in a semi-IPN matrix, while prefabricated FRC posts contain unidirectional continuous E-glass fibres surrounded by a fully polymerized (cross-linked) matrix. Fibre orientation can influence the efficiency of fibre reinforcement (Murphy, 1998). Continuous unidirectional fibres in the prefabricated FRC post give anisotropic mechanical strength in the direction of the fibres (Chieruzzi et al., 2014). However, the loads in this study were applied at 45 degrees to the long access of the tooth and hence the post's fibres. This might reduce the Krenchel's factor below 1 (when the load is in the direction of the fibres) because the load is at an angle to the fibres (Krenchel, 1964). In comparison, multidirectional fibres give isotropic mechanical strength with equal reinforcement in all directions with Krenchel's factor varying between 0.2 and 0.38, depending on whether the fibres were randomly oriented in 2D or 3D (Vallittu, 2014). Additionally, the randomly oriented short E-glass fibres in SFRC posts absorb and dissipate crack energy and slow crack propagation (Frater et al., 2014; Bijelic et al., 2015b). Finally, it has been speculated that the presence of the PMMA chain in the matrix of SFRC post reduces the stresses formation at the matrix-fibre interface (Lassila et al., 2004) and improves the material's toughness competency (Bijelic et al., 2016).

The adaptation of prefabricated FRC posts to the surrounding dentine was variable in comparison to SFRC post as shown in figure 4.6. Among the advantages of minimal discrepancy between the post and the canal wall is uniform stresses distribution within the canal (Anchieta et al., 2012; Lazari et al., 2013). The variations in the adaptation of prefabricated FRC post might have affected the stresses transfer from the posts to the surrounding dentine and resulted in differences in the facture strength and failure mode between the posts. The root cross-section images (Figure 4.6) have also shown that the diameter of SFRC post is larger than the diameter of prefabricated FRC post. Lassila et al. (2004) have found a direct relationship between increased post diameter and the fracture strength in ETT, presuming that excess post-space preparation is avoided (Lassila et al., 2004).

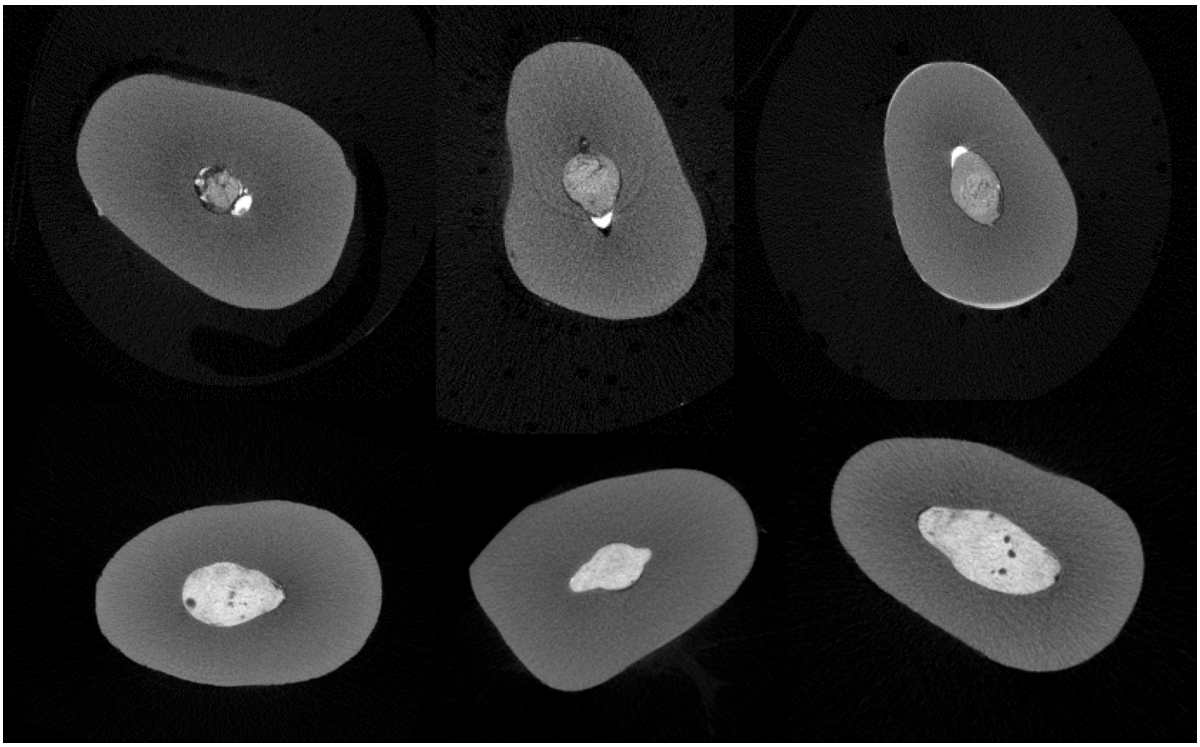

Figure 4.6: Trans-axial micro-CT images of root cross-sections showing adaptation of the prefabricated FRC posts (top) compared to SFRC posts (bottom).

The posts and the cores used in this study are composite resin materials that are bonded to the reconstruct ETT. In the case of prefabricated FRC posts, the matrix is fully cross-linked; therefore, the bonding between the post and the core and between the post and the adhesive cement is mainly mechanical (Love and Purton, 1996; Al-harbi and Nathanson, 2003). As a result, interfacial stresses might be created between the reconstructive components (cement-post-core), which might interrupt the uniformity of stress distribution throughout the restoration and adversely affect the fracture strength of the ETT (Bitter and Kielbassa, 2007; Chieruzzi et al., 2014). SFRC post contains a non-cross-linked polymer (PMMA), which allows penetration of the SFRC core monomers into the post and create inter-diffusion bonding between the post and the core that is known as secondary-IPN (Sperling and Mishra, 1996; Lastumaki et al., 2002; Le Bell-Ronnlof et al., 2007; Vallittu, 2009; Wolff et al., 2012; Kallio et al., 2014). The resultant mono-block-SFRC restoration might contribute in the improved integrity of the post and core structure and homogenous load transfer in the ETT restored with SFRC posts and cores.

Post adaptation, diameter and structural composition have also influenced the failure mode of ETT restored with SFRC compared to ETT restored prefabricated FRC posts as demonstrated in the micro-CT images (Figure 4.5). Non-restorable root fractures and complete post decementation were present only in ETT restored with prefabricated FRC posts. It appears that prefabricated FRC post were not able to maintain their structural integrity and displaced as they flexed during cyclic loading. Post flexion interrupted the integrity of post-cement-tooth system and resulted in adhesive failure and post decementation in that group (Bayne and Thompson, 2013).

By way of contrast, Forster et al. (2017) have found a higher percentage of unfavourable failures in ETT restored with SFRC posts and cores in comparison to ETT restored with prefabricated FRC posts. However, they have also reported 42% non-restorable failures in ETT restored with prefabricated FRC post, while in the current study, prefabricated FRC post group had 27% non-restorable failures. Higher percentage of non-restorable failures in Forester et al. study can be explained by the destructive loading protocol.

Although documented intraoral loads vary widely (ranges between 10 N to 500 N) (Helkimo et al., 1977, Bates et al., 1975), under the simulated conditions in the present study, the fracture strength of ETT restored with SFRC post (731.25N±86.33) is greater than commonly-reported intraoral loads. Additionally, the failure load of ETT restored with SFRC was approximately 60% of the failure load of the sound premolars (1209.2±126.65) reported in this study.

On the other hand, failure load of ETT restored with prefabricated FRC post reported in this study (373.86±64.21) was approximately 30% of the failure load of the sound premolars. Various conclusions have been reported on the mechanical behaviour of teeth restored with prefabricated FRC posts due to variability of the commercially available prefabricated FRC posts in terms of dimensions, designs, structural compositions and physico-mechanical properties (Maccari et al., 2007, Ambica et al., 2013, Pereira et al., 2014, Abduljawad et al., 2016, Habibzadeh et al., 2017). Hence, conclusive comparison between the mechanical behaviour of prefabricated FRC post used in this study and other studies is almost impossible.

Other studies have investigated SFRC as a core restoration (with no post) in ETT (Kemaloglu et al., 2015; Bilgi et al., 2016; Gurel et al., 2016; Eapen et al., 2017). It has been found that ETT restored with SFRC restorations have higher fracture strengths and higher rate of repairable fractures in comparison to other composite restorations.

One of the factors that might influence the fracture strength of ETT restored with SFRC, and has not been discussed above, is the presence of voids in the structure of SFRC. While, all SFRC posts and cores contained variable percentages of voids in the range of 1.5 - 6.7 %, (see Chapter 3), SFRC posts and cores have shown adequate fracture strength compared to sound premolars, and superior fracture strength compared to prefabricated posts. Therefore, the association between the presence of voids and the fracture strength of SFRC is questionable. Chapter 5 will investigate and discuss the effect of voids sizes, location, and distribution on the fracture strength of SFRC posts and cores.

CHAPTER 5

Effect of void size, location and distribution on the failure of ETT restored with SFRC posts and cores

This chapter describes the relationship between voids (size, location and distribution) and the failure load of ETT restored with SFRC posts and cores using the statistical results presented in Chapter 3 (micro-CT quantitative analysis) and Chapter 4 (failure load).

5.1 Introduction

The application of mechanical load results in a progressive or acute failure of dental restorations. Restoration failure is further affected by the existence of structural defects that initiate or accelerate the failure process. Voids are among the common defects described in the structure of dental composites. While it has been commonly demonstrated that voids can negatively affect the physical and mechanical properties of composites (De Gee, 1979; McCabe and Ogden, 1987; Vallittu, 1995a; 1998b ; Huysmans et al., 1996; Miettinen and Vallittu, 1997; Opdam et al., 2002; Karacaer et al., 2003; Evans, 2006; Purk et al., 2007), other reports have demonstrated that the presence of voids in dental composites might be advantageous (Alster et al., 1992; Feilzer et al., 1993; Rengo et al., 2014).

Long-term adverse effects of voids on composite longevity have been described. Voids can act as a moisture or oxygen reservoir that might inhibit complete polymerization and lead to hydrolytic degradation of composite (Vallittu, 1995a; 1998b; Miettinen and Vallittu, 1997). They can also act as stress concentration areas (Chung et al., 2004; Grandini et al., 2005b; de Silva et al., 2015) and either initiate or promote crack propagation (Evans, 2006; Drummond, 2008; Baudin et al., 2009; Garoushi et al., 2017). As a result, voids can degrade the mechanical properties of composite such as compressive strength (Karacaer et al., 2003), flexural strength (Huysmans et al., 1996) and fatigue resistance (McCabe and Ogden, 1987; Evans, 2006).

On the other hand, some reports have failed to demonstrate any significant association between the presence of voids and physical and mechanical properties of composite such as fracture toughness (Elbishari et al., 2012) and bacterial adhesion (Skjorland et al., 1982). Moreover, a few reports have demonstrated that presence of voids in dental composites is not harmful per se. In fact, it has been shown that voids can potentially decrease (Alster et al., 1992; Feilzer et al., 1993) or absorb (Rengo et al., 2014) the stresses developed in composite.

Voids in dental composites have been investigated using a range of methods including micro-CT (Kakaboura et al., 2007; Sun and Lin-Gibson, 2008; Papadogiannis et al., 2009; Sun et al., 2009a; 2009b, Elbishari et al., 2012; Nazari et al., 2013, Lagouvardos et al., 2015; Dunn, 2016). However, the association between the mechanical performance of dental composites and characteristics of voids, such as distribution, location and size, have rarely been addressed in in vitro dental studies (Evans, 2006; Sun et al., 2009b; Elbishari et al., 2012; Shouha et al., 2014). According to Costa et al. (2005) void features such as size, shape, and distribution are determining factors in the mechanical behaviour of reinforced composites.

Importantly, there is lack of studies that define the critical void content, size, or location that might affect the mechanical performance of dental composites. Interestingly, investigations of this type, are common in engineering and in industrial research (Tang et al., 1987; Boey, 1990; Gurdal et al., 1991; Ghiorse, 1993; Suarez et al., 1993; Chambers et al., 2006; Sisodia et al., 2015). For example, in the industrial context, Ghiorse (1993) reported that for every 1% increase in the void content in carbon/epoxy composite, the flexural strength and flexural modulus drops by 10% and 5%, respectively. Tang et al. (1987) and Boey et al. (1990) reported a threshold of 3-4% of voids content after which the mechanical strength of composite remains consistent.

In Chapter 3, micro-CT analyses were conducted to quantify voids in different locations (closed voids, open voids and core voids), of different sizes (small, medium and large) and according to distribution (in coronal, middle and apical thirds) in SFRC posts and cores (XFP group). In Chapter 4, fracture resistance testing was conducted and failure load for ETT restored with SFRC posts and cores was calculated. Therefore, investigating and quantifying the relationship between voids and fracture strength would appear to be a logical next step toward a better understanding of the failure of SFRC.

Aim of this study:

The aim of this study is to investigate the relationship between void location, size and distribution and the fracture strength of ETT restored with SFRC posts and cores.

5.2 Statistical Analysis

Univariate linear regression modelling was undertaken to detect significant associations between failure load and void size, location and distribution in SFRC posts and cores. The following predictors of failure load were individually modelled:

- Core void volume and volume fraction.
- Open void volume and volume fraction.
- Closed void volume and volume fraction.
- Coronal third void volume and volume fraction.
- Middle third void volume and volume fraction.
- Apical third void volume and volume fraction.
- Small void percentage.
- Medium void percentage.
- Large void percentage.

Assumptions of a linear regression were satisfied for all of the models by inspection of scatter plots and histograms of residuals and predictors. All statistical tests were performed with SAS 9.4 software (SAS Institute Inc., Cary, NC, USA) with a probability of 0.05 taken to indicate statistical significance.

5.3 Results

Table 5.1 presents the descriptive statistics of the failure load and the predictor's micro-CT measurements for XFP group (ETT restored with SFRC posts and cores, n=15).

Table 5.1: Failure load and micro-CT measurements for each linear regression predictor for the XFP group

Predictors		n	Mean	SD	Min	Max	Median	Lower Quartile	Upper Quartile
	Failure load		**731.25**	**86.33**	**577.94**	**876.45**	**743.21**	**676.18**	**804.68**
Void location	Core voids volume	15	0.6	0.3	0.1	1.4	0.5	0.8	0.4
	Core voids volume fraction	15	0.8	0.4	0.2	1.8	0.7	1.0	0.6
	Closed voids volume	15	0.7	0.2	0.3	1.3	0.6	0.9	0.4
	Closed voids volume fraction	15	2.8	1.2	1.3	4.9	2.7	3.9	1.9
	Open voids volume	15	0.3	0.2	0.0	0.7	0.3	0.5	0.1
	Open voids volume fraction	15	1.4	0.8	0.0	2.8	1.4	0.5	2.1
Void distribution	Coronal third voids volume	15	0.3	0.2	0.1	0.6	0.3	0.2	0.4
	Coronal third voids volume fraction	15	3.4	1.7	1.2	6.3	2.7	2.1	5.5
	Middle third voids volume	15	0.2	0.1	0.1	0.5	0.2	0.1	0.3
	Middle third voids volume fraction	15	2.7	1.4	0.9	5.2	2.3	1.6	3.5
	Apical third voids volume	15	0.2	0.1	0.00	0.6	0.1	0.1	0.2
	Apical third voids volume fraction	15	3.3	1.6	0.9	6.0	2.9	1.9	4.7
Void size	Small voids percentage	15	88.3	2.6	84.4	92.3	88.3	85.9	90.3
	Medium voids percentage	15	8.7	2.3	5.2	13.5	8.6	6.5	10.3
	Large voids percentage	15	3.0	0.9	1.9	5.2	2.9	2.2	3.6

5.3.1 Effect of void location on the failure load of SFRC posts and cores

The results from the linear regression modelling of the relationship between void location and the failure load of SFRC posts and cores are presented in Tables 5.2 and 5.3.

Core voids and open voids had no statistically significant effect on failure load. Closed void volume (Table 5.2) and volume fraction (Table 5.3) were the only predictors –among other locations– that had a statistically significant effect on the failure load (P-value<0.0001).

In the post, for every 0.1 mm^3 increase in closed voids volume, the mean failure load increased by 22.7N** (estimate= 22.7, 95% confidence interval (CI): 13.1, 32.2, P-value<0.0001) (Figure 5.1) and for every 1% increase in closed void volume fraction, the mean failure load increased by 53.9N (estimate= 53,9, 95% CI: 29.0, 79.0, P-value<0.0001) (Figure 5.2).

Table5.2: Univariate linear regression modelling of the relationship between failure load and the volume of voids in different locations (n=15)

Void location		**Voids volume** mean ±SD (mm^3)	**Estimate**	**95% confidence interval** Lower	Upper	**P-value**
SFRC core		0.6±0.3	41.3	-88.6	171.1	0.5332
SFRC post	**Closed voids**	0.7±0.2	227.0	131.3	322.7	<0.0001*
	Open voids	0.3±0.2	-9.1	-207.1	189.0	0.9285

* Significant positive effect on the failure load of SFRC posts and cores at 0.05 confidence level
Closed voids: voids within post structure.
Open voids: voids at post-dentine interface.

Table 5.3: Univariate linear regression modelling of the relationship between failure load and the volume fraction of voids in different locations (n=15)

Voids location		**Voids volume fraction** mean ±SD (%)	**Estimate**	**95% confidence interval** Lower	Upper	**P-value**
SFRC core		0.8±0.4	34.0	-64.8	132.9	0.5000
SFRC post	**Closed voids**	2.8±1.2	53.9	28.9	78.9	<0.0001*
	Open voids	1.4±0.8	-59.5	47.3	27.3	0.8239

* Significant positive effect on the failure load of SFRC posts and cores at 0.05 confidence level

** Calculated for every 0.1 mm^3 closed void volume.

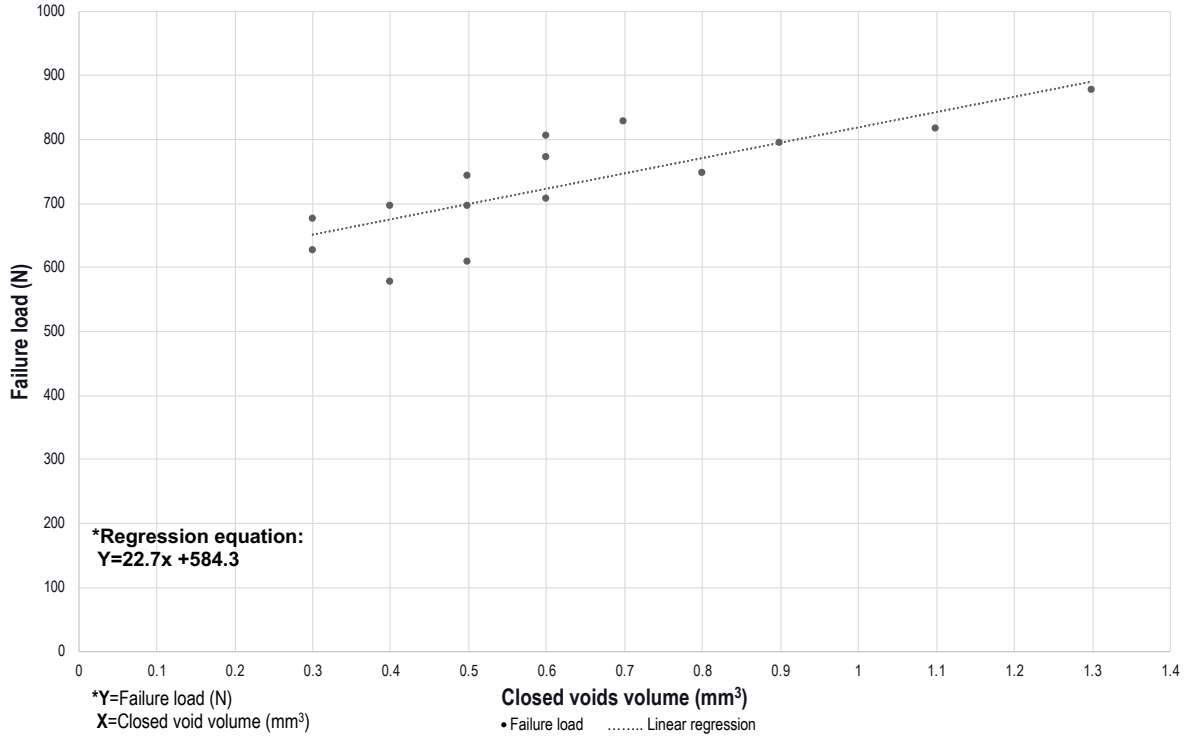

Figure 5.1: Scatter plot of failure load versus closed voids volume in SFRC posts (n=15)

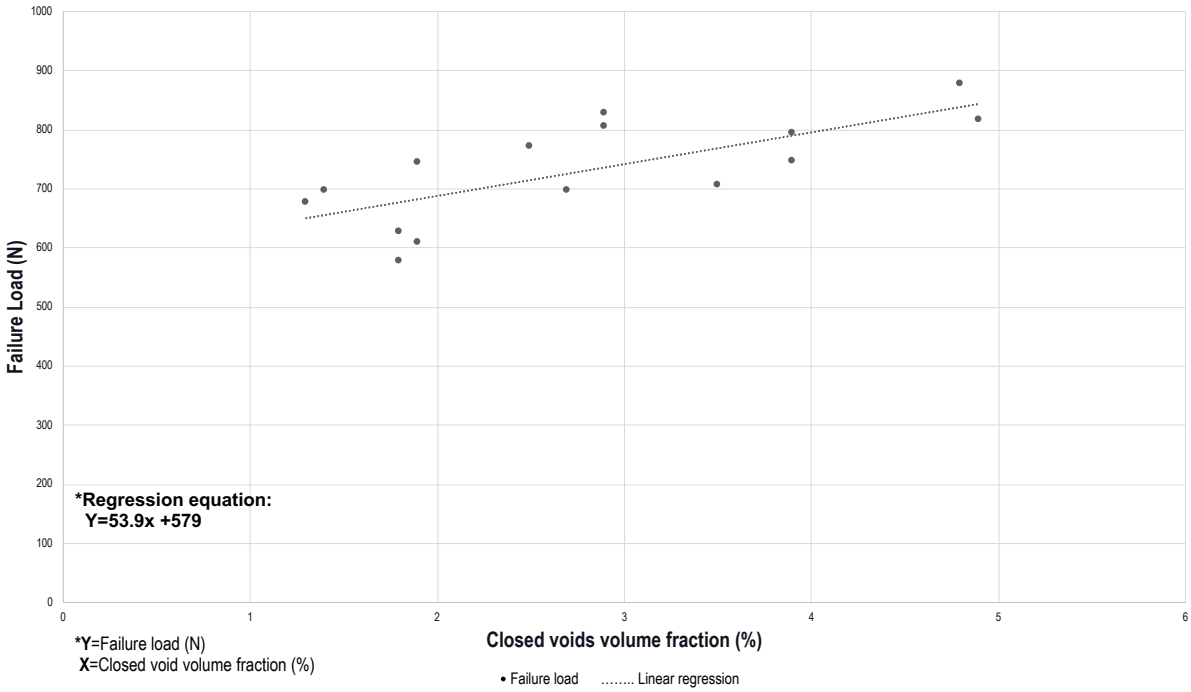

Figure 5.2: Scatter plot of failure load versus closed voids volume fraction in SFRC posts (n=15)

5.3.2 Effect of void distribution on the failure load of SFRC posts and cores

The effect of void distribution on the failure load of SFRC posts and cores is presented in Tables 5.4 and 5.5. The volume and the volume fraction of voids in the coronal (Figure 5.3 and 5.4), middle (Figure 5.5 and 5.6) and apical (Figure 5.7 and 5.7) thirds had a statistically significant positive effect on the failure load of SFRC posts and cores.

Table 5.4: Univariate linear regression modelling of the relationship between failure load and the void volume in three SFRC post sections (n=15)

Void distribution	Voids volume mean ±SD (mm^3)	Estimate	95% confidence interval Lower	Upper	P-value
Coronal third	0.3±0.2	312.0	86.9	537.2	0.0066*
Middle third	0.2±0.1	487.8	197.5	778.2	0.001*
Apical third	0.2±0.1	284.7	25.5	543.9	0.0313*

* Significant positive effect on the failure load of SFRC posts and cores at 0.05 confidence level

Table 5.5: Univariate linear regression modelling of the relationship between failure load and the void volume fraction in three SFRC post sections (n=15)

Void distribution	Voids volume fraction mean ±SD (%)	Estimate	95% confidence interval Lower	Upper	P-value
Coronal third	3.4±1.7	30.6	9.3	51.9	0.0049*
Middle third	2.7±1.4	39.9	15.9	64.1	0.0011*
Apical third	3.3±1.6	26.2	2.4	50.1	0.0310*

* Significant positive effect on the failure load of SFRC posts and cores at 0.05 confidence level

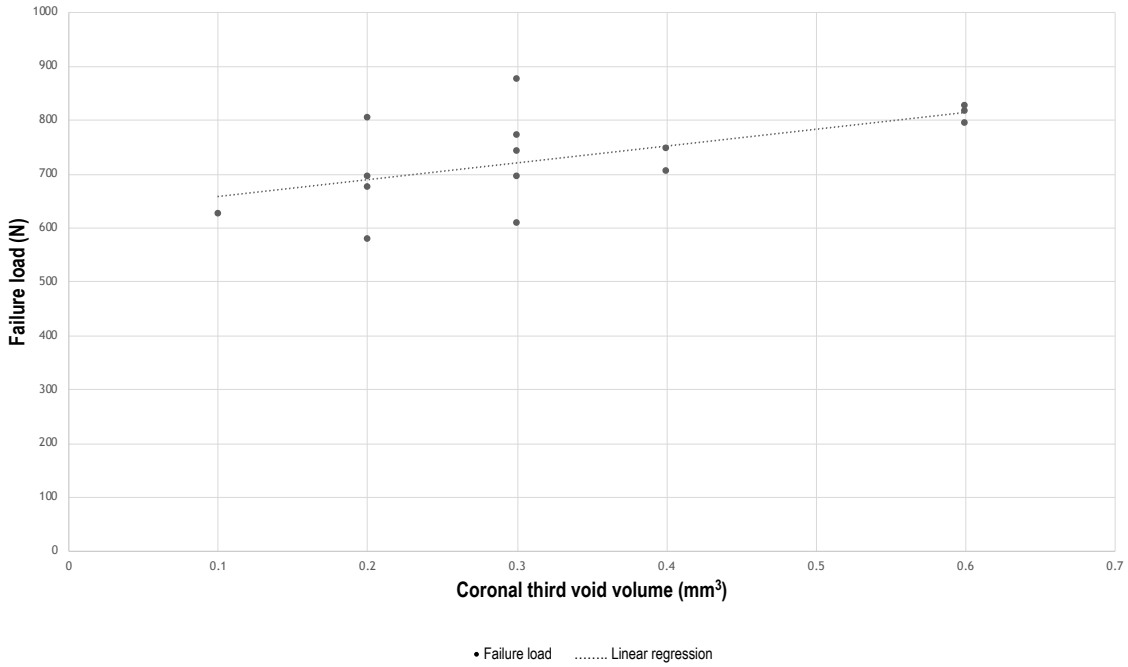

Figure 5.3: Scatter plot of failure load versus coronal third void volume in SFRC posts (n=15)

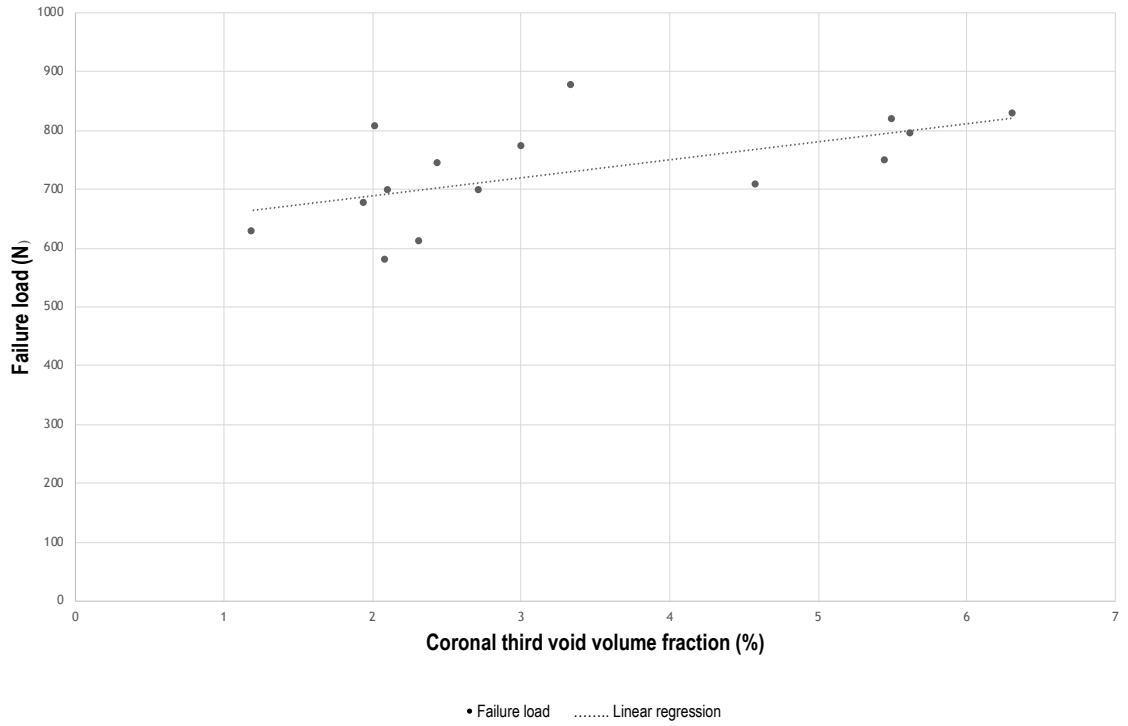

Figure 5.4: Scatter plot of failure load versus coronal third void volume fraction in SFRC posts (n=15)

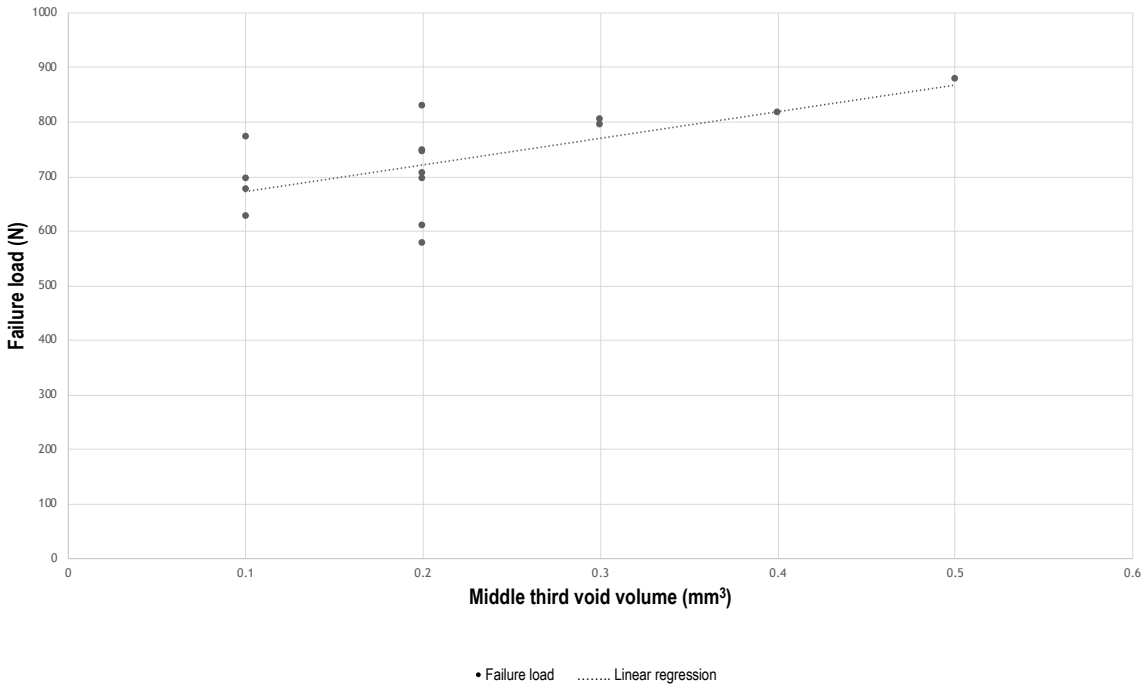

Figure 5.5: Scatter plot of failure load versus middle third void volume in SFRC posts (n=15)

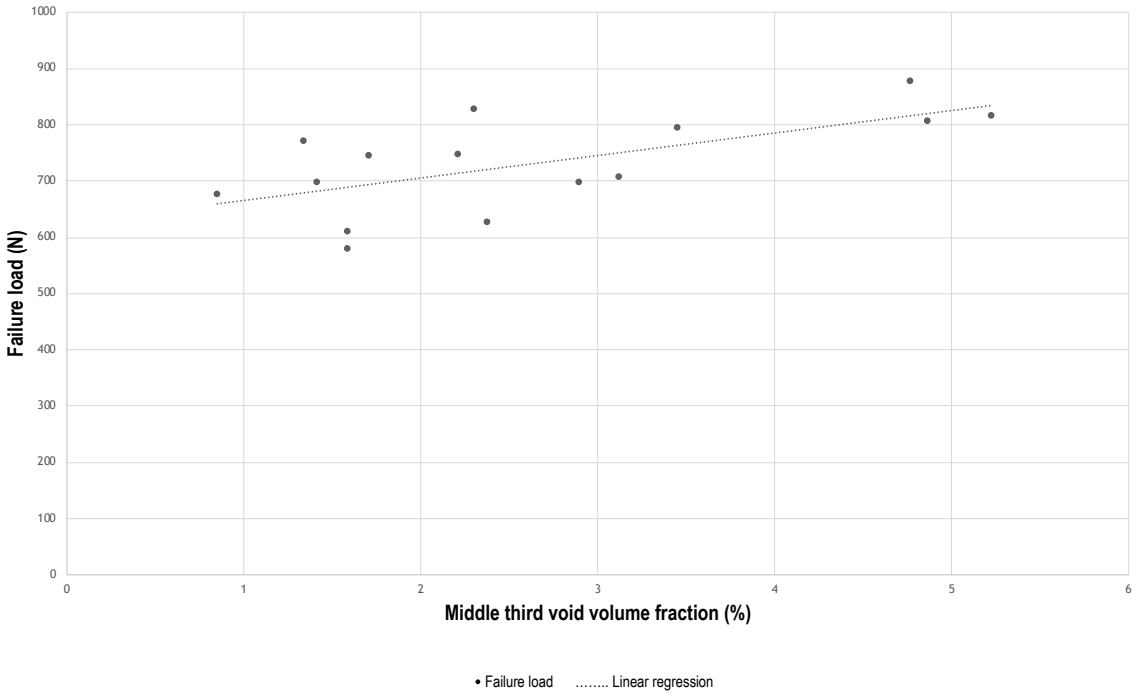

Figure 5.6: Scatter plot of failure load versus middle third void volume fraction in SFRC posts (n=15)

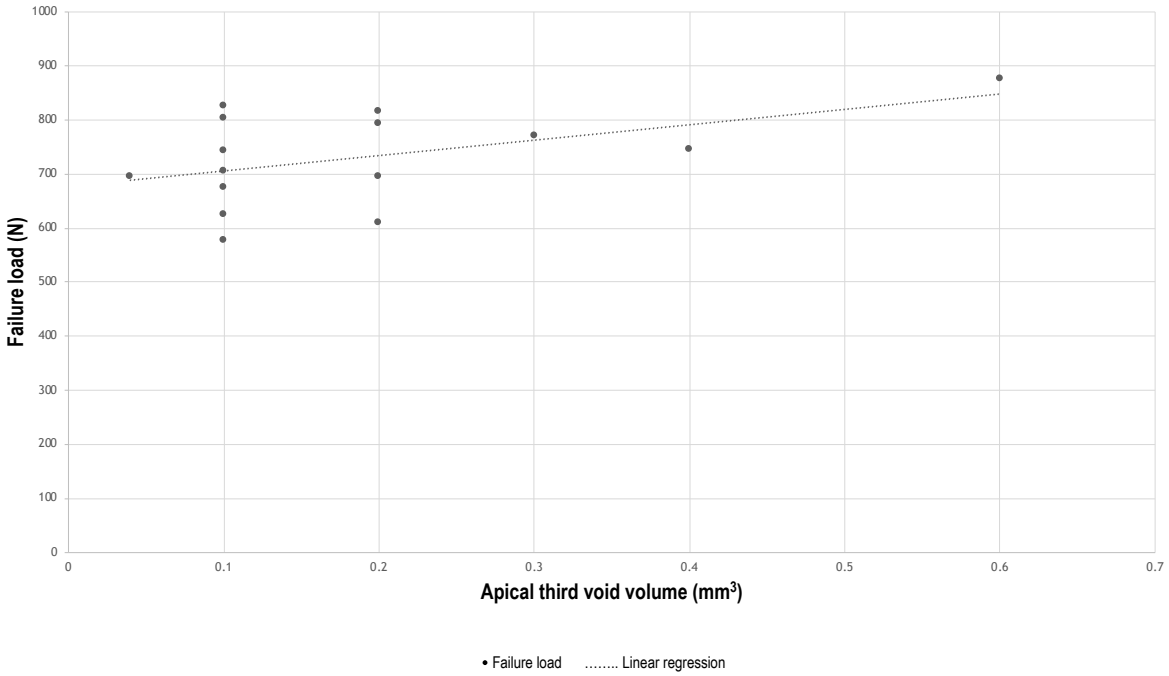

Figure 5.7: Scatter plot of failure load versus apical third void volume in SFRC posts (n=15)

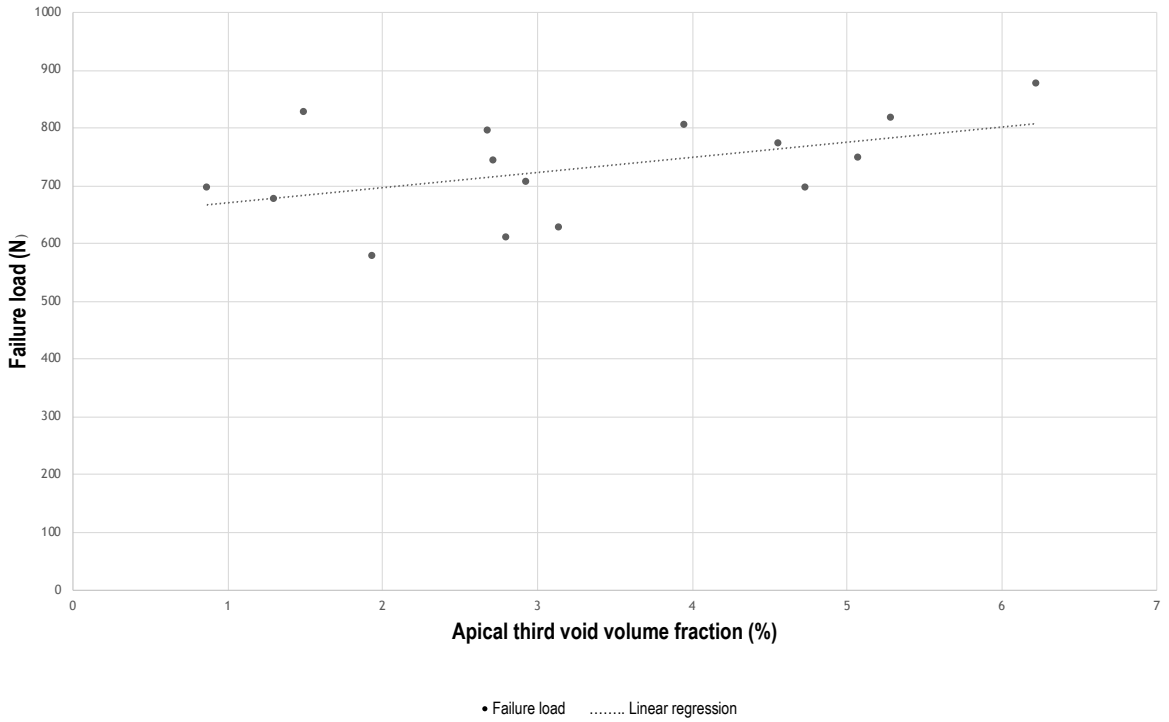

Figure 5.8: Scatter plot of failure load versus apical third void volume fraction in SFRC posts (n=15)

5.3.3 Effect of void size on the failure load of SFRC posts and cores

The relationship between void size (small, medium and large voids) and the failure load of SFRC posts and cores is summarised in Table 5.6. No significant relationship between void size and the failure load was evident.

Table 5.6: Univariate linear regression modelling of the relationship between failure load and the percentage of voids size in SFRC post (n=15)

Void size	**Voids percentage** mean ±SD (%)	**Estimate**	**95% confidence interval** Lower	upper	**P-value**
Small voids (<100 µm)	88.2±2.6	3.7841	-12.2486	19.8169	0.9733
Medium voids (100 µm -500 µm)	8.7±2.3	-3.8102	-22.3464	14.7259	0.9173
Large voids (> 500 µm)	3±0.9	-9.4820	-57.1094	38.1454	0.7161

5.4 Discussion

Composite resins are brittle materials. Their fracture behaviour is influenced by acting stresses, fracture strength (against the applied load), fracture toughness, material composition and presence of internal flaws (microcracks, voids, etc.) (Baudin et al., 2009; Ferracane, 2013). SFRC restorations exhibited significantly higher fracture toughness and compressive strength when compared to PFC and other bulk-fill restorative composite resins (Garoushi et al., 2013b; Belli et al., 2014; Leprince et al., 2014; Abouelleil et al., 2015; Bijelic et al., 2015b; 2016, Tsujimoto et al., 2016c; Garoushi et al., 2017). However, micro-CT analyses conducted in this project and micrographs presented in other studies have confirmed the presence of voids in the structure of SFRC (Tuncer et al., 2013; Shouha et al., 2014; Bijelic et al., 2016, Patel et al., 2016; Garoushi et al., 2017).

Although voids have been recognized as having the potential to increase stresses under fatigue loading (Evans, 2006, Baudin et al., 2009), the magnitude of the effect of voids on the mechanical performance of dental composites has not been described in the literature. This study investigated the relationship between characteristics of voids (size, distribution and location) and the failure load of ETT restored with SFRC posts and cores.

The results indicated that core voids and open voids had no significant effect on the fracture strength of the ETT, whereas, the closed voids regardless their distribution can positively affect the fracture strength of ETT restored with SFRC posts and cores.

Open voids represent the entrapped air between the post and the dentine, and it gives an insight into the adaptation of the post to the prepared root canal. It seems that the small volume and volume fraction of open voids did not contribute significantly to the failure mechanism of the ETT restored with SFRC posts, at least under the simulated conditions of the present study. Perhaps more important than actual voids at the restoration-dentine interface is the close adaptation of the post to the canal walls, which has been argued to promote uniform stresses distribution within the canal (Anchieta et al., 2012; Lazari et al., 2013)

The void size had no significant effect on the fracture strength of ETT restored with SFRC posts and cores. To some extent this may have been the result of the low variability in the void size between specimens. This is in agreement with Evans (2006) who measured the stresses around voids in PMMA acrylic and indicated that stresses around voids were insufficient to initiate crack –independent of the void size– unless the voids significantly reduce the overall cross-section.

In the contrary, Shouha et al. (2014) demonstrated a relationship between large voids (400μm) and poor mechanical performance of composite. However, such results were merely descriptive and represent the author's interpretation of the failure behaviour as displayed in the micrographs of fractured composite surfaces. It lacked any statistical analysis of the relationship between the failure behaviour and the size, number or distribution of voids in the restoration.

In this study, it was possible to quantify the relationship between the voids and the fatigue fracture strength in SFRC post and core restorations. To the knowledge of the author, there is no previously reported work describing this relationship for dental composites.

Interestingly, the results of this study have indicated that the voids and fracture strength have a positive relationship. The results have shown that for every 0.1 mm^3 increase in the volume of closed voids, the mean failure load increased by 22.7N, and for every 1% increase in the volume fraction of closed voids, the failure load of ETT increased by 53.9N.

Bearing in mind that in general industrial application void content of up to 5% has been reported to be tolerable (Ghiorse, 1993). Void percentage in the current study (1.3 - 4.9%, mean= 2.8%) might also be not only tolerable but could be actually absorbing the stresses and delaying the fracture of the specimen. A similar finding was reported by Rengo et al, (2014) who concluded that voids might act as stress absorber. Also, Alster et al. (1992) and Feilzer et al. (1993) have found that incorporation of porosities might be necessary to relief stresses in luting composite. Voids that are homogeneously distributed has been described by McMillan (2012) as “defender holes” that provide stress shielding and stress

concentration control. In this project, small voids were observed to be homogeneously distributed in SFRC posts.

In medical applications, for example in arthroplastic implants fixed by acrylic cements, the relationship between the voids in the cement and the initiation of fatigue failure was questioned (Ling and Lee, 1998). Ling and Lee (1998) presented evidence from several prospective clinical studies that pores have not initiated fractures and in some cases lack of voids led to irreversible failure that required revision. They finally suggested that porosity reduction in such application is not necessary or even harmful.

As mentioned earlier, voids in dental SFRC have been considered as a marginal factor and their formation and relationship to SFRC failure is not fully understood. Considering the evidence from the general industrial applications of FRC, the quoted values on the relationship between voids and composite strength are variable due to differences in specimen design, material composition, test methods and void calculation techniques. In this context, Mehdikhani et al. (2018) have commented that voids in composites are stochastic phenomena and their size, shape, and location suffer from complex statistical analyses.

The failure mode evaluation (Chapter 4) indicated that all specimens in XFP group failed favourably regardless the presence of voids and their size and distribution. Six specimens (40%) in XFP group had restoration bulk fractures and the void content was variable in those specimens. These results support the suggestion that the mechanical behaviour of SFRC is not necessarily directly and solely related to void content and that other factors might be involved. This imply that voids might contribute to the fracture strength of SFRC, but not to the fracture behaviour. In this context, Evans (2006) indicated that even in areas with large voids, cracks were initiated from other secondary stress concentrators. Also, Elbishari et al. (2012) found no correlation between the void content and the fracture toughness of FRC, and according to Boey et la. (1990) for acceptable mechanical testing of FRC, it is important to control not only the void content, but the fibre alignment.

In this study, SFRC was inserted incrementally into the post spaces, whereas the cores were constructed as bulk-fill restorations. Both techniques created voids inside the posts and the cores, yet, bulk fracture

accrued in the posts. This implies that there might have been other crack promoters in the post that influenced the failure of SFRC restorations.

Baudin et al. (2009) have reported that the strength values in composite resin are determined by the quality of the restoration application. It has been also suggested that SFRC insertion technique induces variations in the fibres orientation and distribution (Bijelic et al., 2016; Bocalon et al., 2016), which have been reported to alter fibre reinforcement, and hence the failure mechanism in response to cyclic loading (Lang et al., 1987; Roulin-Moloney, 1989; Jain and Wetherhold, 1992; Greenhalgh, 2009).

To better understand the failure in SFRC, a fractographic analysis was conducted to examine the fractured SFRC surfaces and provide an insight into the failure mechanism, failure origin(s) and crack promotor(s). This is presented in Chapter 6.

CHAPTER 6

Scanning Electron Microscope fractography

This chapter describes the fractographic analysis conducted on the ETT restored with SFRC that failed by bulk fracture of the posts and cores restoration.

6.1 Introduction

Fractography is the topographical examination of the fracture surface of a failed structure. It involves reporting the macro- and micro-structural alterations, failure origins and mechanisms. Scanning Electron Microscopy (SEM) is a powerful tool in fractographic analysis that is used in many scientific and industrial fields because of the ease of the procedure and sample preparation, and the versatility of acquired information. Fractography was introduced to dental research by Kelly et al. in 1989 (Kelly et al., 1989). It has been used to evaluate fracture surfaces of both dental structures (Nalla et al., 2003; Bajaj et al., 2006) and dental restorations (Draughn, 1987; Ferracane and Condon, 1992; Campos et al., 2015).

Research on dental SFRC has frequently included fractography to analyse the failed components of SFRC that were tested either as standard-shape test specimens (Fonseca et al., 2014; 2016; Abouelleil et al., 2015; Bijelic et al., 2016; Lassila et al., 2016; Garoushi et al., 2017; 2019) or as restorations (Rocca et al., 2015; Nagata et al., 2016; Barreto et al., 2016). In this context, SEM micrographs were utilized to evaluate the failure mode of SFRC (Rocca et al., 2015; Barreto et al., 2016) and to describe microstructural features such as fibre orientation and distribution (Bijelic et al., 2016; Lassila et al., 2016; Nagata et al., 2016; Garoushi et al., 2019) or fibre quantity and size (Lassila et al., 2016; Garoushi et al., 2017). SEM micrographs have also been used to address the fracture toughness and crack propagation arresting mechanisms in SFRC (Figure 6.1) and the fibre response to the crack propagation (Figure 6.2). Structural defects and imperfections, including voids, have been reported as incidental findings in the micrographs of SFRC restorations (Figure 6.3) (Shouha et al., 2014; Bijelic et al., 2016; Patel et al., 2016; Garoushi et al., 2017).

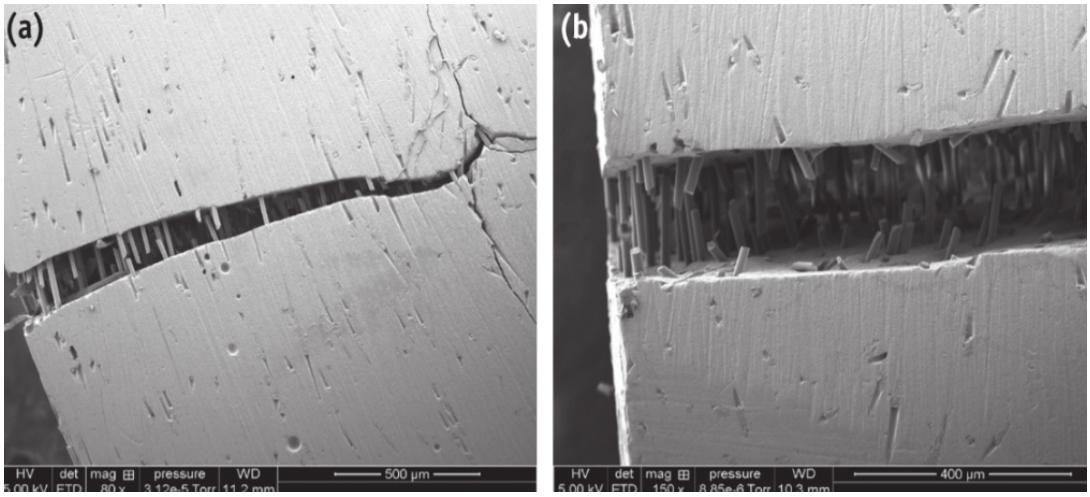

Figure 6.1: SEM images of a SFRC specimen after failure showing fracture toughness mechanism. (a) SEM micrograph showing pulled out and bridging fibres between the crack edges which resulted in arresting crack propagation; (b) Fiber orientation across the failure line at a higher magnification (Obtained from Abouelleil et al. 2015)

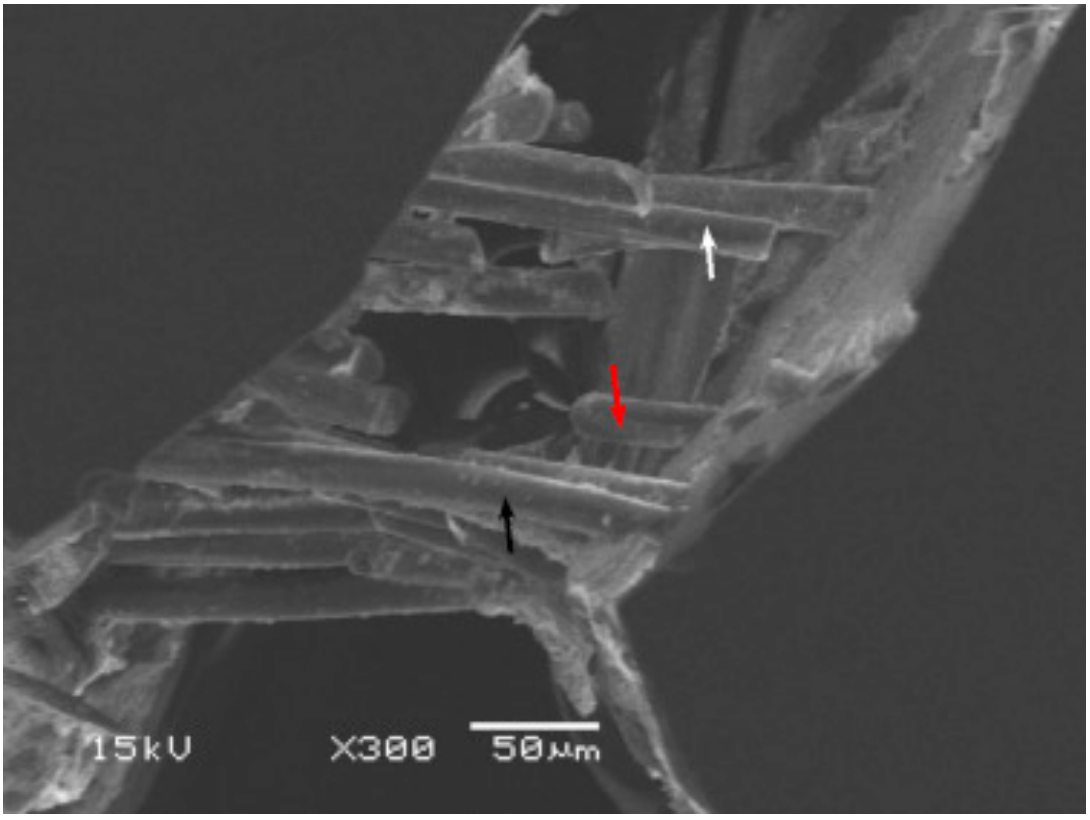

Figure 6.2: SEM image showing fibres response to the initiated cracks; fractured (red arrow), pulled out (white arrow) and bridging (black) fibres in SFRC (Obtained from Bijelic et al. 2016)

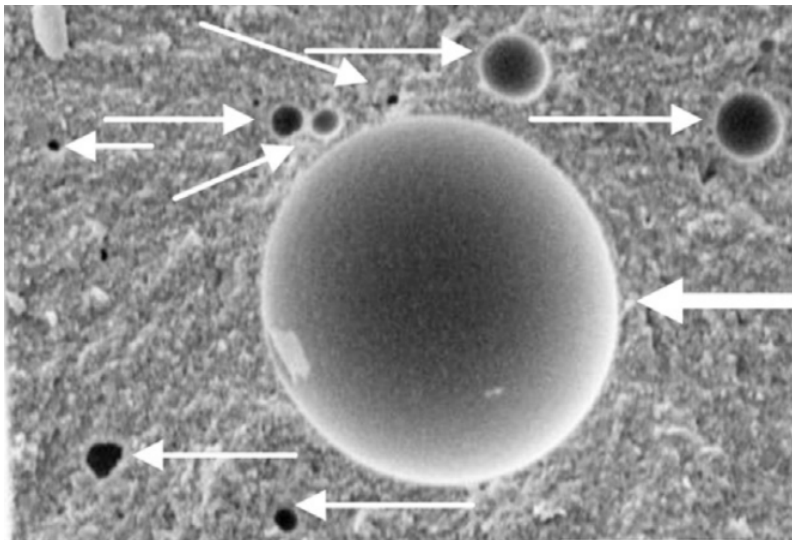

Figure 6.3: SEM image of SFRC showing voids of different sizes as demonstrated by Shouha, Swain and Ellakwa, 2014

Fractographic analysis of SFRC has revealed that the failure interpretation of such material is complex and affected by the microstructural composition (Mortazavian and Fatemi, 2015b). The reinforcing short-fibres have been recognized as a potential stress concentrator per se (Shouha et al., 2014; Lange, 2016) or as a result of modified fibre distribution, length, quantity, orientation and interfacial adhesion to the matrix (Dyer et al., 2004; Callaghan et al., 2006; Garoushi et al., 2009; Fonseca et al., 2016). Additionally, it has been reported that reinforcing fibres might change void location, shape, distribution and size, which might negatively affect the composite strength (Guo et al., 2009).

It has been reported that fatigue cracks predominantly proceed in three stages; crack initiation, slow crack propagation and fast fracture, with each step having identifiable fractographic manifestations. However, microstructural heterogeneities of SFRC might alter fractographic manifestations under cyclic loading (Lohbauer et al., 2003).

Interestingly, Mortazavian and Fatemi (2015b) have concluded that SFRC fatigue behaviour has not received adequate attention from researchers. They emphasised the need for analysis of the fatigue fracture behaviour of SFRC with the aim of better understanding processes such as crack initiation, growth

and arrest, and to assess the role of the structural components/imperfection in the fracture mechanism, which is one of the aims of this study. Understanding the fracture mechanisms and the involved structural factors allows future material improvements and better clinical service prediction.

Aims of this study:

To conduct SEM fractographic analysis of fractured SFRC posts and cores to:

- Describe the microstructural topography of the fracture post surface in terms of fibre distribution and orientation, matrix characteristics and structural flaws/imperfections.
- Identify the fractographic manifestations of fatigue failure on the matrix and the fibres.
- Identify the failure origin(s) and crack propagation process.
- Identify the failure mechanism(s).
- Correlate fractographic features with the fracture strength of SFRC posts and cores.

6.2 Material and methods

After cyclic loading, specimens in the XFP group that failed by bulk fracture of SFRC post and core restoration (n=6) (Figure 6.4) were examined under SEM (Quanta 450 FEG Environmental SEM, FEI, Oregon, USA) (Figure 6.5). The exposed SFRC post surfaces were coated with gold-palladium sputter prior to SEM analysis. Specimens were fixed on the SEM stage and images with magnifications up to x1600 were obtained. Image analysis software (ImageJ version 1.52a, NIH, Maryland, USA) was used to perform measurements on the SEM micrographs.

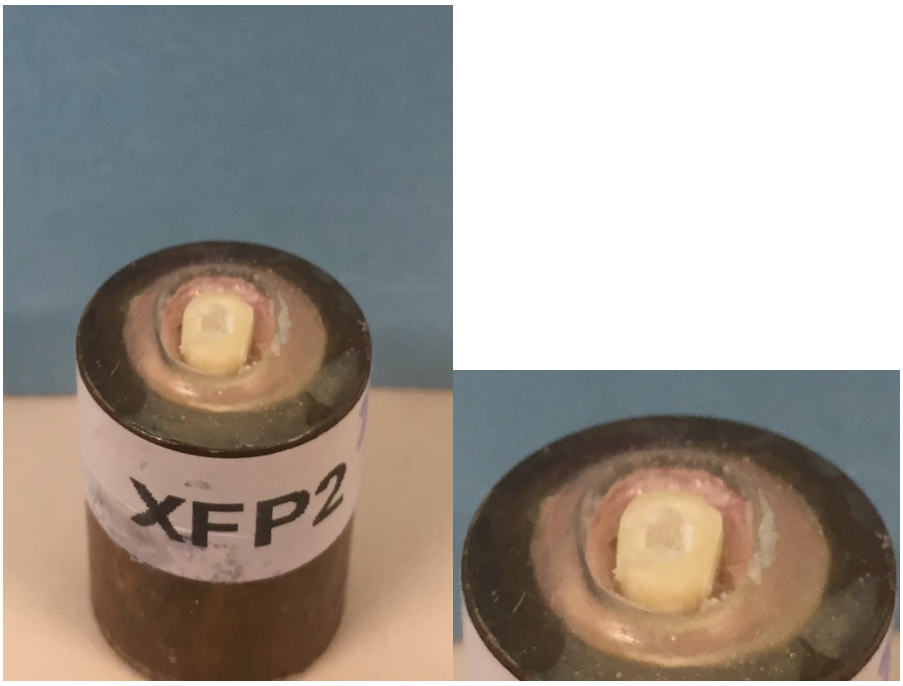

Figure 6.4: An XFP specimen (ETT restored with SFRC post and core) failed by bulk fracture of the post and core restoration

Figure 6.5: Quanta 450 FEG Environmental SEM

6.3 Results and discussion

The fractography results and discussion are arranged in the following sections:

6.3.1 Microstructural topography

6.3.2 Fatigue failure manifestations

A Matrix manifestations

B Fibre manifestations

B.1 Cohesive failure (fractured fibres)

B. 2 Adhesive failure (debonded fibres)

B. 3 Combined cohesive and adhesive failure

B. 4 Toughening mechanism

6.3.3 Failure mechanisms

A T-orientated fibre (T-cracks)

B L-orientated fibres (L-cracks)

6.3.4 Fracture origin(s) and crack propagation

6.3.5 Correlations between fractographic features and fracture strength of SFRC posts and cores

6.3.1 Microstructural topography

In this section, the general microstructural features of SFRC fracture surfaces including fibre distribution and orientation, matrix characteristics, and structural flaws and imperfections will be described (Figures 6.6 and 6.7).

The fractured surfaces shared general microstructural features that included heterogonous surfaces with rough matrix and multidirectional reinforcing glass fibres. However, fibre quantity, orientation and distribution varied among the specimens (Figure 6.6). While uniform fibre distribution was evident in some specimens (Figure 6.6 A), other specimens showed an uneven fibre distribution (Figure 6.6 B). Although the fibres were generally oriented in different directions, in some specimens, transverse fibre orientation was dominant (Figure 6.6 C and D). It has been shown that the stress induced during extruding viscous fibre-reinforced composites through the dispensing nozzle can change the fibres orientation (Braem et al., 1993; Shouha et al., 2014). In addition, as discussed earlier, SFRC application's technique during post build up required pressure exertion to ensure close adaptation of the highly viscous material to canal walls and to the preceding increment, which has been speculated to induce variation in the fibre arrangement and distribution (Bijelic et al., 2016; Bocalon et al., 2016).

The main defects and imperfections in the fracture surface of SFRC posts were voids in the matrix. Two forms of voids have been recognized in SEM images: regularly shaped and irregularly shaped voids.

Regularly shaped voids are well-defined half spheres of variable sizes with a smooth resin-rich internal surface (Figure 6.7 A and B). Fracture surfaces showed more small-scale than large-scale regularly shaped voids. Similar findings were reported by Shouha et al. (2014,) who described voids of variable sizes in micrographs of experimental SFRC formulations.

Irregularly shaped voids were characterized by textured internal surfaces (Figure 6.7C). It can be speculated that such voids represent the interlayer-entrapped air between composite increments. The textured surface represents the resin that has not been manipulated during packing, which has created a

thin resin film that is interrupted by pores exposing the underlying matrix of the preceding composite increment (Greenhalgh, 2009).

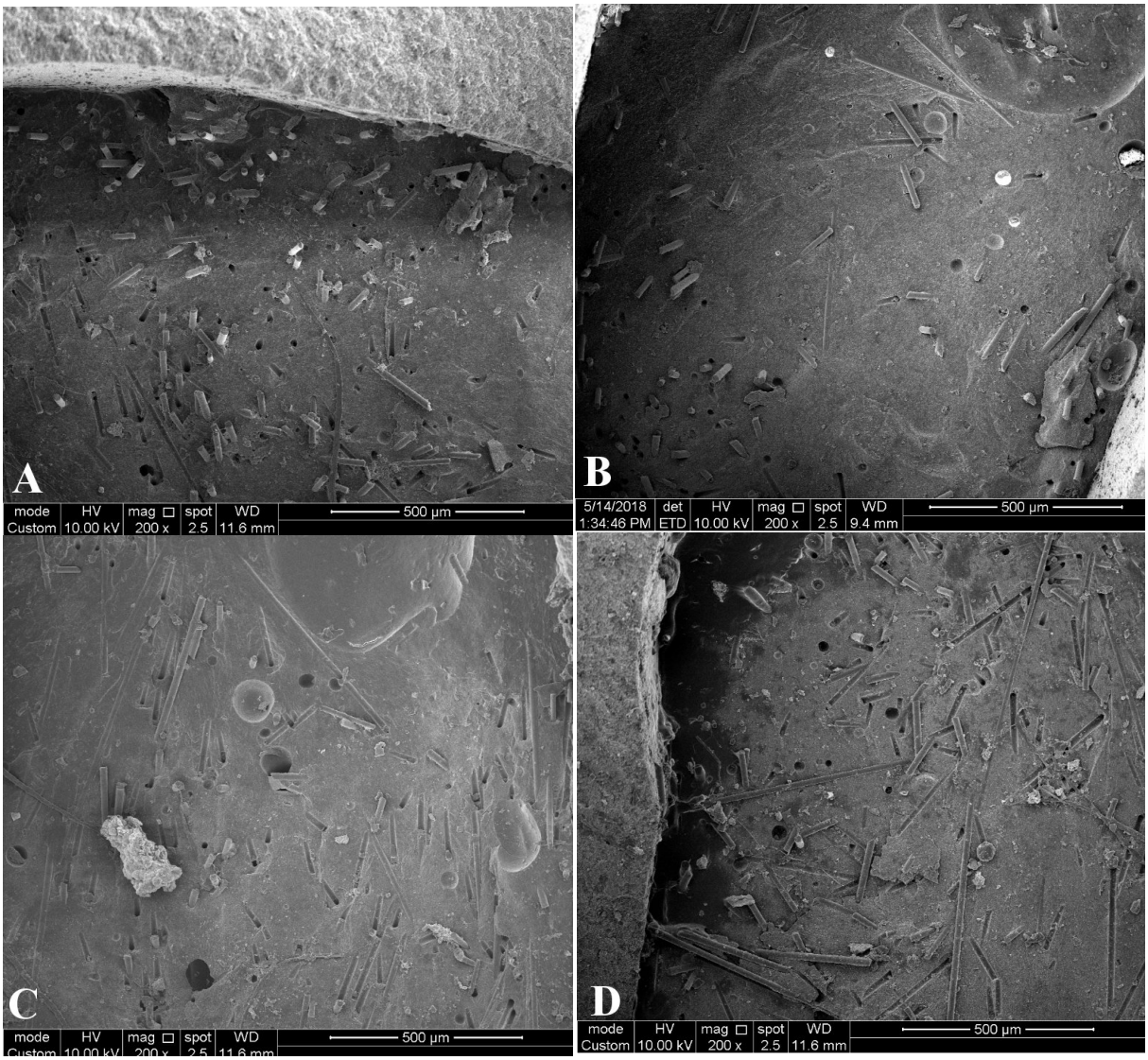

Figure 6.6: SEM micrographs (x200) of different fractured SFRC posts' surfaces showing variable fibres quantities, orientation and distribution:
(A) Even fibre distribution in multidirectional orientation;
(B) Low fibre quantity that are unevenly distributed;
(C) and (D) Even fibre distribution and dominantly in a transverse orientation.

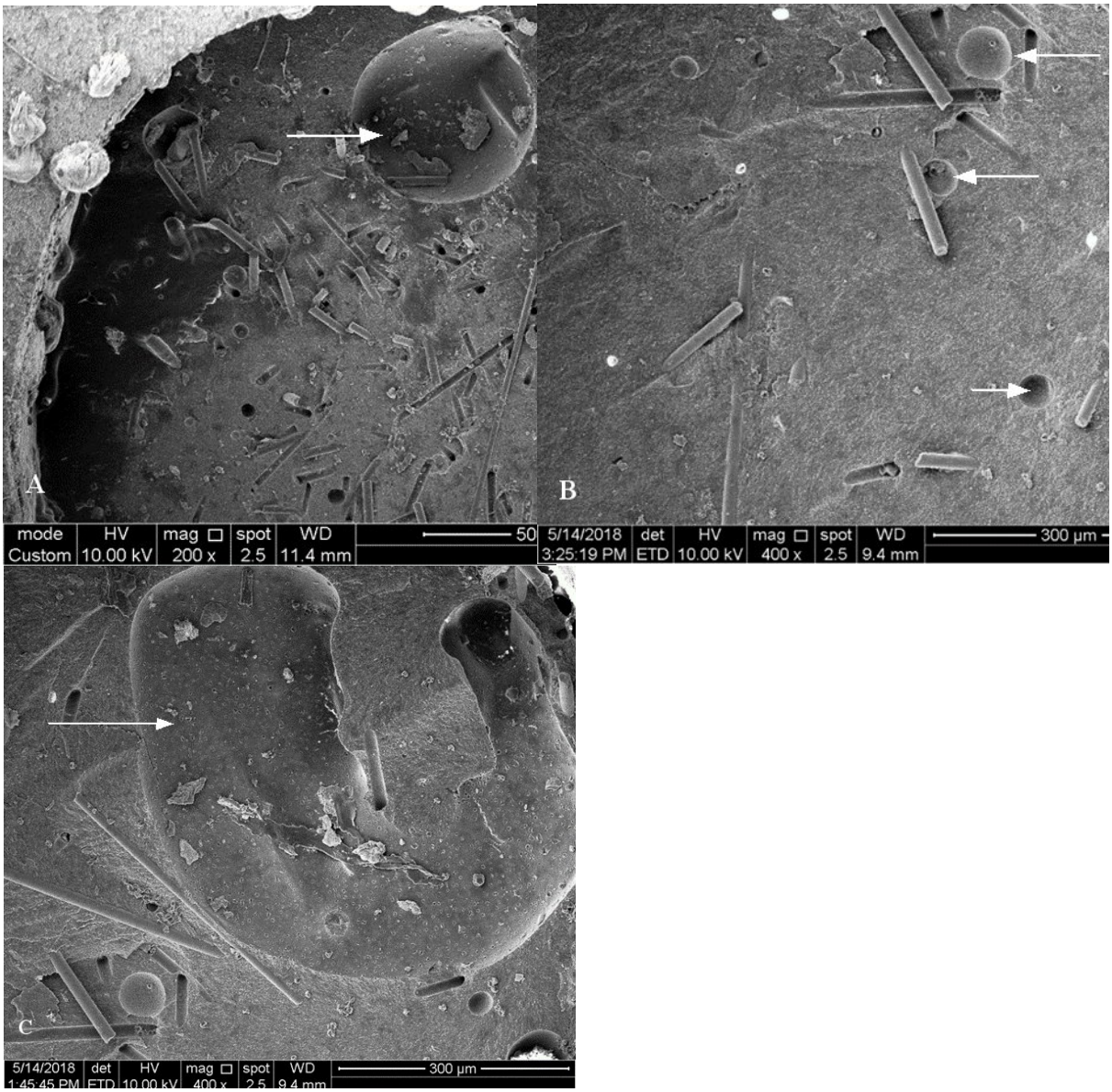

Figure 6.7: SEM micrographs showing voids of different sizes, shapes and distributions: (A) Arrow indicates a large-scale regularly shaped void (157.7µm in diameter); (B) Arrows indicate small-scale regularly shaped voids (27-50µm in diameter) and (C) Arrow indicates irregularly shaped void with textured internal surface.

6.3.2 Fatigue failure manifestations

It has been reported that a surface fractured under cyclic loading conditions develops fractographic features that differ from those resulting from static loading (Draughn, 1987; Greenhalgh, 2009; Quinn and Quinn, 2010). Microstructural failure caused by the cyclic loading protocol applied in this study was manifested in both the matrix and the reinforcing fibres.

A. Matrix manifestations

The effect of cyclic loading was evident as fatigue striations that were observed on the matrix of SFRC (Figure 6.8). Fatigue striations are fractographic features that appear as consecutive curved lines and imply the process of crack growth and arrest (Hiley, 1999; Hayes et al., 2015; Jollivet and Greenhalgh, 2015). Considering fatigue striations patterns, Greenhalgh (2009) has described two forms of crack propagation; normal fatigue crack propagation (NFCP) and retarded fatigue crack propagation (RFCP). While NFCP is characterized by regular striations on the fractured surface, RFCP is characterized by discontinuous crack growth bands (each band includes multiple fatigue cycles). RFCP is the pattern recognized on the fractured surface of SFRC and it indicates discrete crack growth increments after crack arrest that continued over a number of loading cycles (Greenhalgh, 2009). Spacing of the striations can indicate the load intensity, and curve of the striations can indicate crack growth direction (Figure 6.8). However, interpreting fatigue striations –especially if they are highly localized– is not straightforward in a heterogeneous surface such as in SFRC. This view has been endorsed by others in the literature (Lang et al., 1987; Jollivet and Greenhalgh, 2015).

The cracks in the matrix varied from microcracks to matrix deformation. It has been reported that the degree of SFRC matrix involvement during cycling loading is affected by the fibre orientation (Roulin-Moloney, 1989). For example, transversely aligned fibres (parallel to crack direction) can resist the early stages of loading. However, as the load grows in intensity and just prior to ultimate failure, the load is no longer carried by the fibres and the matrix will eventually deform (Figure 6.9 A). On the other hand, the

fibres that are perpendicular to crack path hinder crack growth and carry the load until the occurrence of ultimate failure with no extensive matrix deformation (Figure 6.9 B).

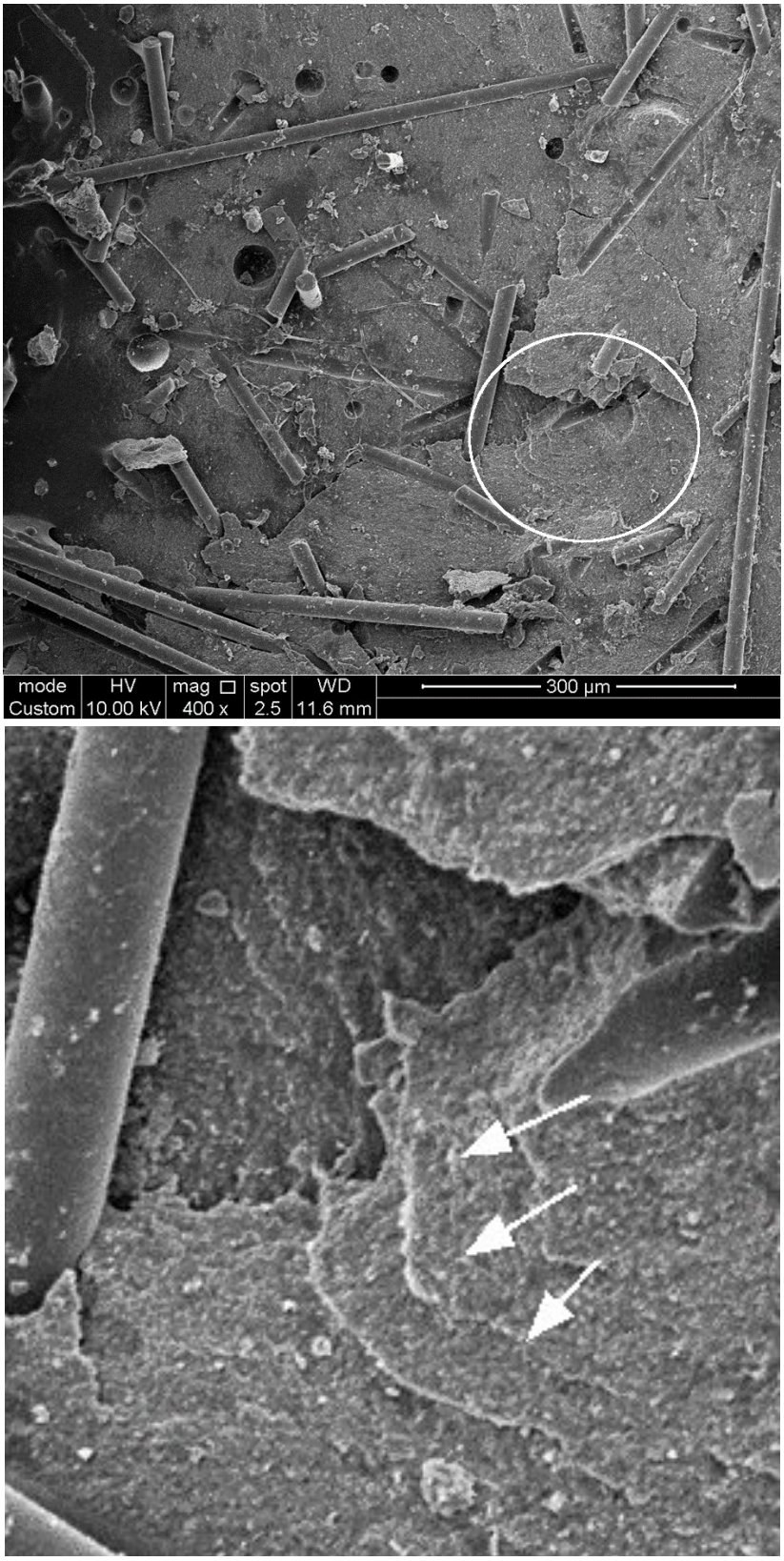

Figure 6.8: Top: SEM micrographs (x400) showing fatigue striations inside the circle. Bottom: enlarged fatigue striations. The curvature of the striations (arrows) might indicate the crack growth direction.

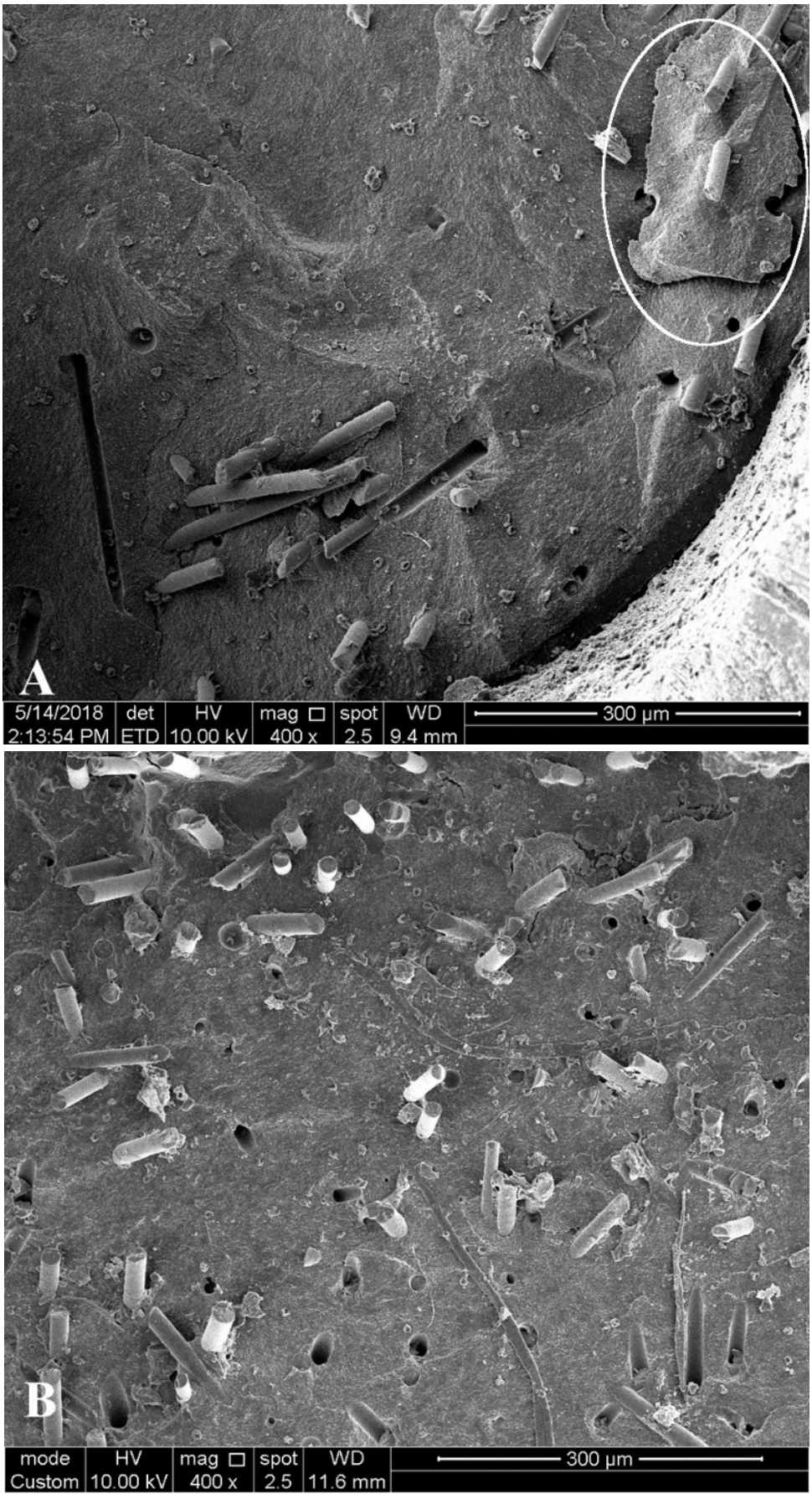

Figure 6.9: (A): SEM micrograph (x400) showing matrix deformation around transversely aligned fibres. (B): Lack of observable extensive deformation in the matrix that is dominated by fibres aligned perpendicular to the crack path.

B. Fibre manifestations

The reinforcing glass fibre response to cyclic loading is affected by the fibre orientation, length and matrix-fibre interfacial bond strength (Lang et al., 1987; Jain and Wetherhold, 1992; Greenhalgh, 2009). In relation to the fibres, four manifestations of cyclic load were observed (Figure 6.10): *cohesive failure* in which fibres fracture (discussed in section B.1 below); *adhesive failure* in which fibres debond (section B.2); failure involving a *combination* of both mechanisms (section B.3) and bridging fibres that indicate the *toughening mechanism* (section B.4)

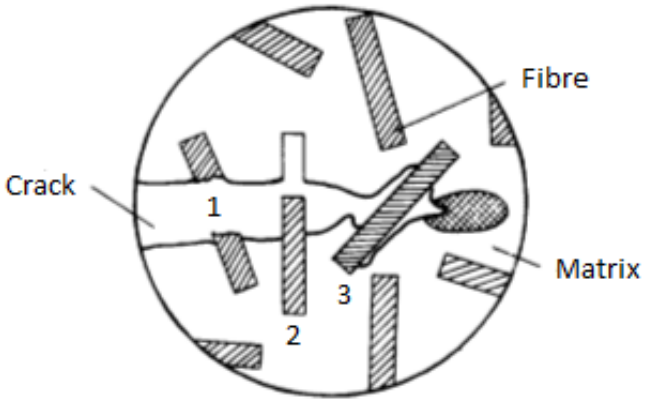

Figure 6.10: Schematic diagram (modified from Karger-Kocsis & Friedrich 1988) illustrates different fibres responses to load; (1) fractured fibre *(cohesive failure)*, (2) debonded fibre *(adhesive failure)* and (3) bridging fibre *(toughening mechanism)*

B.1 Cohesive fibre failure (fractured fibres)

As mentioned earlier, the everX Posterior™ SFRC tested in this project consisted of short E-glass fibres with a range of lengths between 0.3 and 1.9mm. This fibre range is above the critical fibre length (l_{fc}) of 0.85-1.09mm that is required for effective reinforcement (Bijelic et al., 2016)(Appendix1). Importantly, the fibres length should not exceed the optimal fibre length (l_{fo}) of 1.0-1.3 mm (Bijelic et al., 2016). Fibres exceeding the optimal fibre length (especially if they were of the order of twice the l_{fo}) might fracture under load or act as continuous fibres (Wetherhold and Jain, 1992).

Figure 6.11 is a SEM micrograph showing fractured fibres with multidirectional fracture patterns observed on the fractured fibres (as indicated by the arrows in figure 6.11). Such behaviour suggests that the crack consumed high energy to fracture well-adhered fibres, indicating effective fibre-matrix interfacial bond and reinforcement (Fonseca et al., 2016).

The typical radial pattern of mirror-mist-hackle regions was occasionally observed in high magnification SEM images on the fractured fibres (Figure 6.11) (Lang et al., 1987; Mecholsky, 1995; Greenhalgh, 2009). The mirror region indicates the crack origin. The mist and hackle regions develop as the crack fans out from the mirror region indicating the direction of crack propagation.

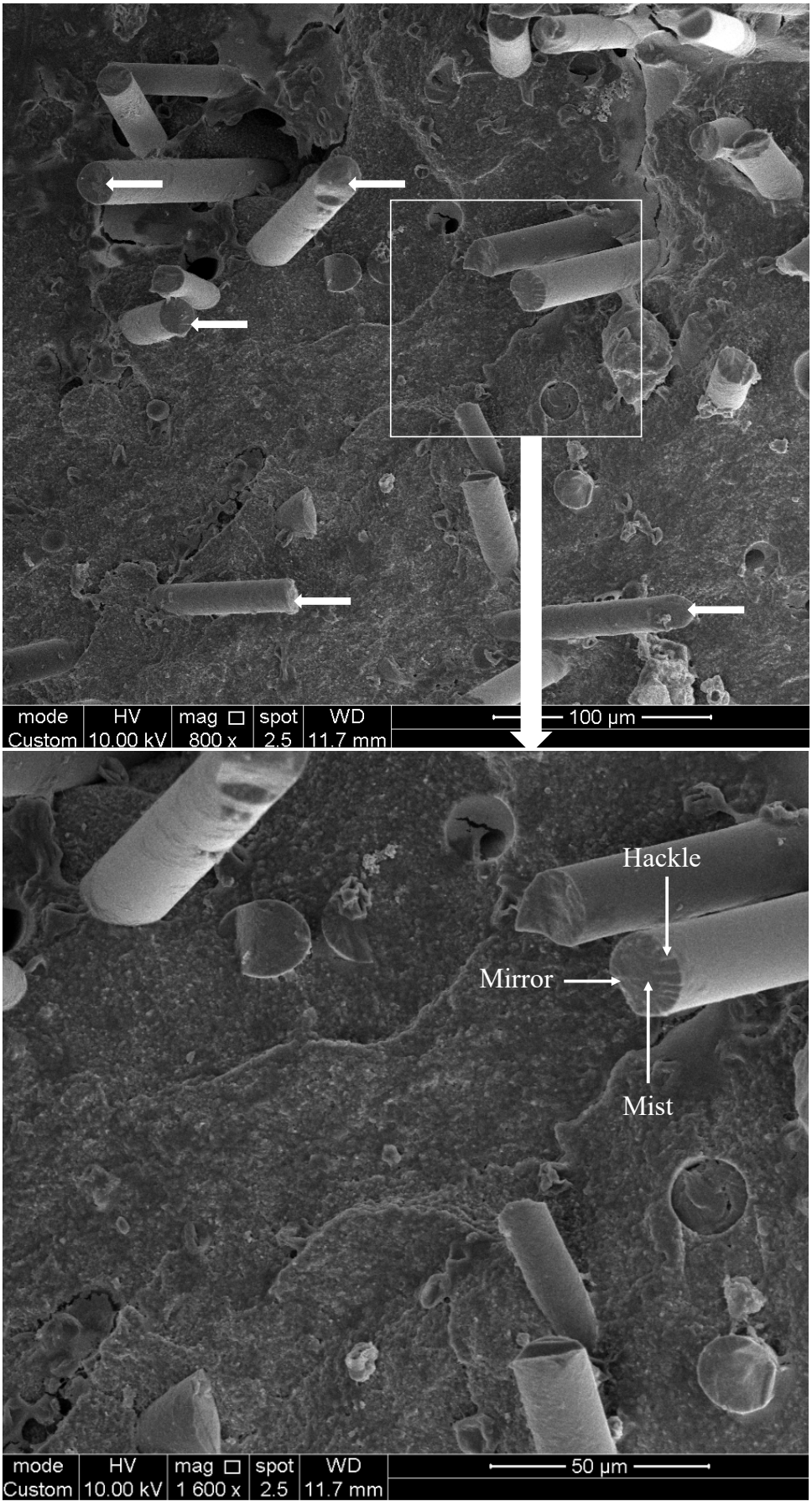

Figure 6.11: Top: SEM micrograph (x800) showing multidirectional fractured fibre surface (arrows) and a fractured fibre surface with the typical radial fracture pattern. Bottom: magnified fractured fibre surface (x1600). Note the radial pattern of mirror-mist-hackle on the fractured fibre.

B.2 Adhesive fibre failure (debonded fibres)

Debonded fibres detected in SEM images are essentially the transversely aligned longer fibres. The denuded fibres with attached pieces of resin indicate strong matrix-fibre interfacial bond and successful fibre reinforcement (Figure 6.12). As a result, the crack needed higher energy to propagate as it was resisted by the well-bonded fibres (Fonseca et al. 2016). On the other hand, a clean fibre surface (Figure 6.12) indicates poor interfacial bond and minimal contribution in crack propagation resistance (Roulin-Moloney, 1989).

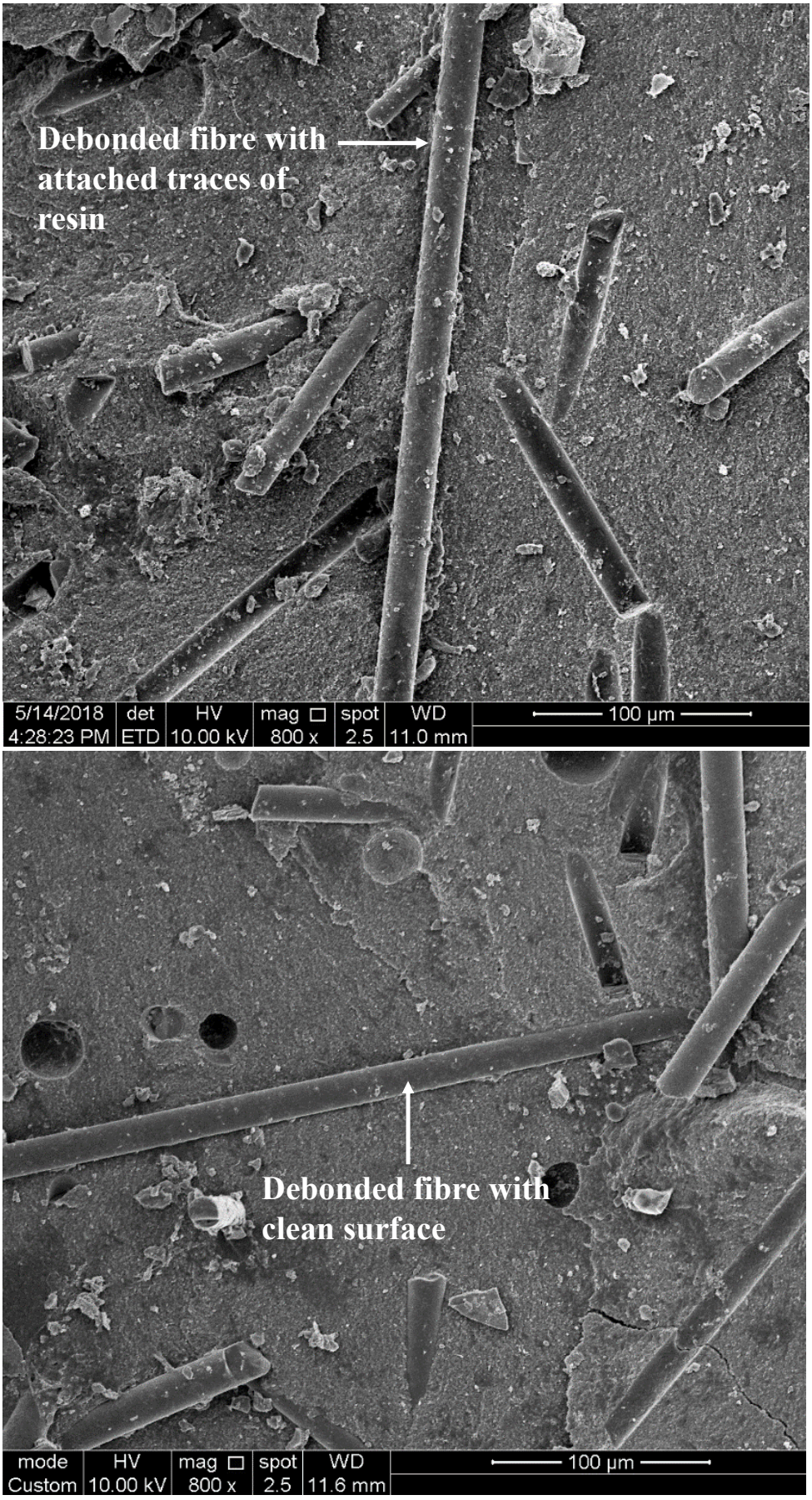

Figure 6.12: SEM micrographs (x800) showing debonded long transversely aligned fibres. Top: debonded fibre with attached traces of resin. Bottom: clean debonded fibre.

In SEM images some of the debonded fibres were dislocated leaving indentations on the matrix (Figure 6.13). According to Nicola et al. (2016), such fibres might cause deviation of the crack direction. It might be speculated that long transversely aligned fibres were incapable of stopping the crack, but they managed to deviate it instead. As a result, the fibres dislocated as the crack propagated. The crack deviation phenomenon is clinically effective when such fibres are closer to the cavity walls and deviate the crack away from the tooth structure, resulting in a favourable restorative failure (Rocca et al., 2015).

Figure 6.13: SEM micrographs (x800) showing indentation of debonded long, transversely aligned fibres (arrows).

B.3 Combination of adhesive and cohesive failures

Some fibres were neither transversely aligned nor perpendicularly aligned in relation to crack path. Such fibres, however, can be described as "misoriented" because they were unfavourably sloped in relation to the crack path (Figure 6.14). SEM images have shown that such fibres were first forced to debond (adhesive failure), leaving indentations on the matrix. Next, as the crack propagates to reach the embedded section of the fibre, the fibres fracture eventually (cohesive failure). However, this pattern was observed in the fibres that sloped against the direction of the crack, which might assist in deducing the crack propagation direction.

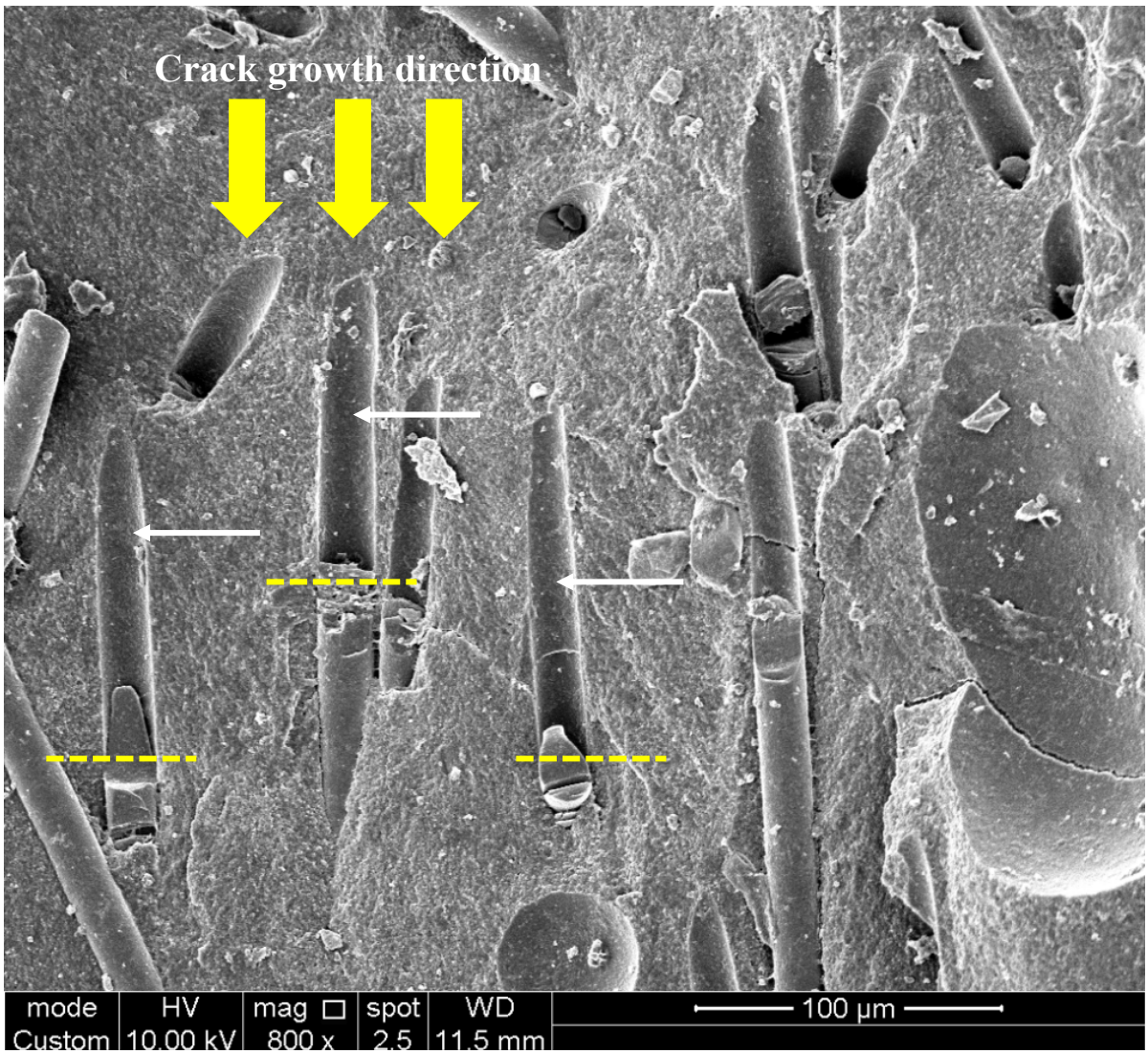

Figure 6.14: SEM micrographs (x800) showing fibres sloped against the crack propagation direction and responded by debonding, leaving indentation on the matrix (arrows) then fracture at their roots (yellow lines). Note aggressively deformed fractured surfaces of the fibres, which might indicate that the crack consumed high energy to fracture well-adhered fibres, indicating effective fibre-matrix interfacial bond and reinforcement.

B.4 Toughening mechanism (bridging fibres)

Bijelic et al. (2016) measured the E-glass fibre length in everX Posterior™ SFRC and found that 71% of the fibres varied between 0.4 and 1.0 mm, 11% varied between 1.1-1.9 mm and 18% were 0.3 mm. While, the shortest fibres in SFRC act as particulate fillers, the longest fibres, which exceeded the optimal fibre length, will either debond (transversely aligned), fracture or behave as continuous fibres (perpendicularly oriented). The rest of the fibres that are perpendicular to crack path and satisfy both critical fibre length and optimal fibre length guidelines are described as bridging fibres (Figure 6.15).

Bridging fibres can effectively encounter the load and act as a crack propagation stopper through their ability to stretch, pull out and bridge between crack edges, which is known as toughening mechanism (Garoushi et al., 2007e; 2013b; Bijelic et al., 2016).

When the crack propagates, the toughening mechanism is responsible for slowing the crack, blunting the sharp crack and reducing stress concentration at the crack tip in SFRC (Kim and Watts, 2004). However, the stretched fibres are rooted in crack edges with variable lengths (Figure 6.15). Eventually, as the crack propagates and bulk fracture accrues, the short embedded segment of the fibre will be pulled out and the long embedded segment will remain embedded in the matrix (Jain and Wetherhold, 1992; Wetherhold and Jain, 1992).

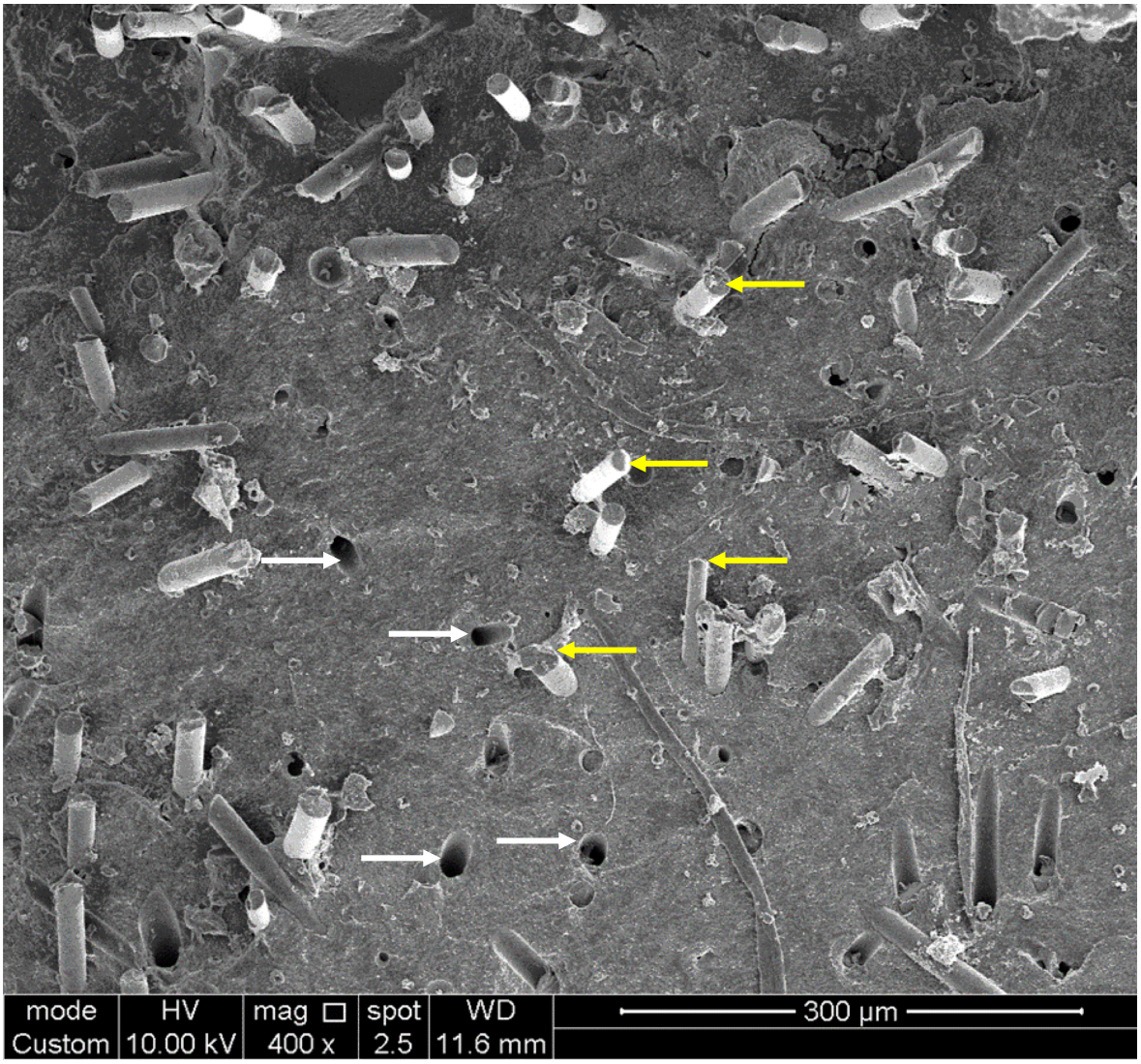

Figure 6.15: SEM micrographs (x400) showing the reinforcing fibres on the fractured surface after complete crack opening (restoration bulk fracture). White arrows: indicate the pulled-out fibres. The holes were holding the short-embedded segments of the reinforcing fibres while the long segment is embedded in the opposing crack edge. Yellow arrows: indicate the long-embedded segment of the stretched reinforcing fibres that is still bonded to the matrix.

6.3.3 Failure mechanisms

Failure of SFRC has been classified by Friedrich and Karger-Kocsis (1989) into two main mechanisms. The classification describes the fractographic observations of the fracture surface bearing in mind the fibre orientation in relation to the crack plane direction. Therefore, T-oriented-fibre (T-Crack) and L-oriented-fibre (L-Crack) fracture mechanisms were described (Figures 6.16 and 6.17). This classification epitomizes the SFRC fractographic observations presented in the preceding sections of this chapter. A combination of both fracture mechanisms has been observed in the fractured SFRC posts. However, the extent to which a particular mode is dominant depends on the orientation of the fibres in each specimen.

A. T-oriented-fibre fracture mechanism (T-cracks): describes failures when majority of the fibres are oriented perpendicular to the crack plane and are bridging the crack faces (Figure 6.16). T-cracks are associated with slow crack propagation, higher fracture energy and indicates higher fracture toughness (Friedrich and Karger-Kocsis, 1989).

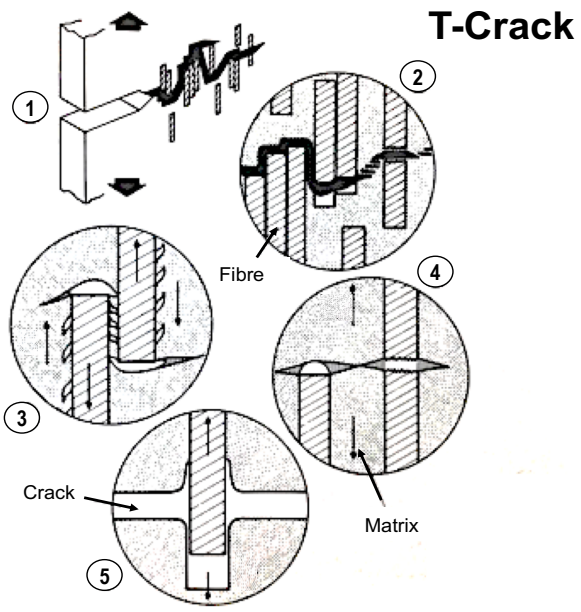

Figure 6.16: T-cracks can be manifested in one or more of the following fractographic features; (1) zig-zag crack profile, (2) short cracks between fibre ends or broken fibre, (3) and (4) crack formation at fibre ends or along their well bonded interfaces at the onset of fibre pull-out and (5) fibres debonding and pull-out (modified from Roulin-Moloney, 1989)

B. L-oriented-fibre fracture mechanism (L-cracks): describes failure when majority of the fibres are oriented parallel to the crack plane (transversely aligned fibres) (Figure 6.17). L-cracks are associated with faster fracture, lower fracture energy and fracture toughness (Friedrich and Karger-Kocsis, 1989).

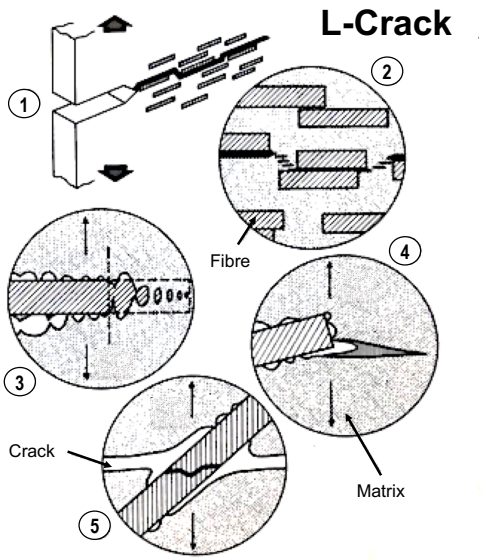

Figure 6.17: L-cracks can be manifested in one or more of the following fractographic features; (1) straight crack profile, (2) cracks between fibre bundles, (3) voids formation around the fibres and matrix rupture, (4) crack at fibre end and (5) debonding and fracture of misoriented fibres (modified from Roulin-Moloney, 1989)

6.3.4 Failure origin(s) and crack propagation

It has been reported that under cyclic loading conditions, fractures proceed in three stages; crack initiation, slow crack propagation and unstable crack growth (fast fracture) (Lohbauer et al. 2003). However, the heterogeneous nature of the SFRC causes variability in crack origin, speed and direction (Greenhalgh 2009).

There is general consensus that voids are recognized as crack initiators in brittle materials. In fractured SFRC specimens, two types of voids have been described in section 6.3.1. Neither void type was associated with cracks or fatigue striations in the adjacent matrix as shown in the SEM images (Figure 6.18, also refer to Figure 6.7), which supports the finding that voids are not stress-inducing factors in SFRC. Similar finding has been demonstrated by Evans (2006) who reported that stress concentration factor around voids in PMMA acrylic is insufficient to cause cracks. Hayashi and Takahashi (2017) have demonstrated that it is the fibre orientation rather than the void that affects the mechanical properties of FRC.

Contradictory findings were reported by Ogden (1985) who observed cracks passing through voids and linking the voids, which was interpreted as an evidence that voids are a source of weakness. Ogden, (1985) further commented that the internal void surface represents incompletely polymerized resin caused by oxygen inhibition, which will eventually degrade the composite structure. According to Greenhalgh (2009), cracks in the voids are post-failure cracks that are not contributing in the failure mechanism. Micro-cracks propagating through voids have been observed occasionally in the fractured surface of SFRC post (Figure 6.19).

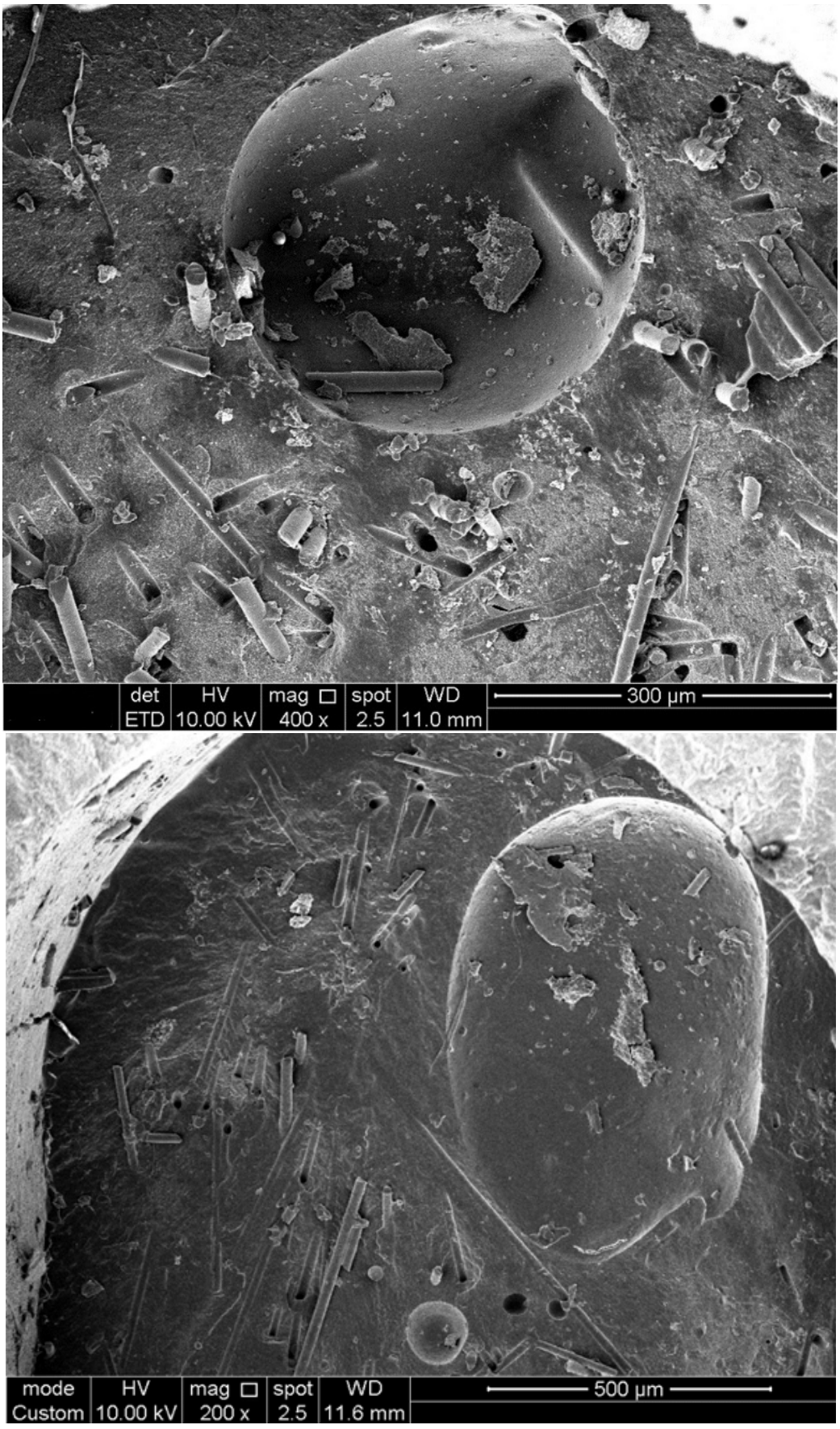

Figure 6.18: SEM micrographs (top x400 and bottom x200) showing voids of variable sizes with no cracks in the matrix adjacent to the voids.

Figure 6.19: SEM micrograph (x400) showing a crack passing through void (arrow)

On the other hand, regions with either low or high fibre content showed evidence of matrix micro-cracks and deformation in SEM images (Figures 6.20 and 6.21), which implies that these regions might be involved in the origin or growth of the crack. It can be assumed that closely collected fibre can exhibit areas with poor interfacial bonding, which might interrupt the reinforcing process of load transfer from matrix to fibres (Figure 6.20). Similarly, low fibre content might disturb the reinforcing process in SFRC (Figure 6.21). These same findings were described by Fonseca et al. (2016).

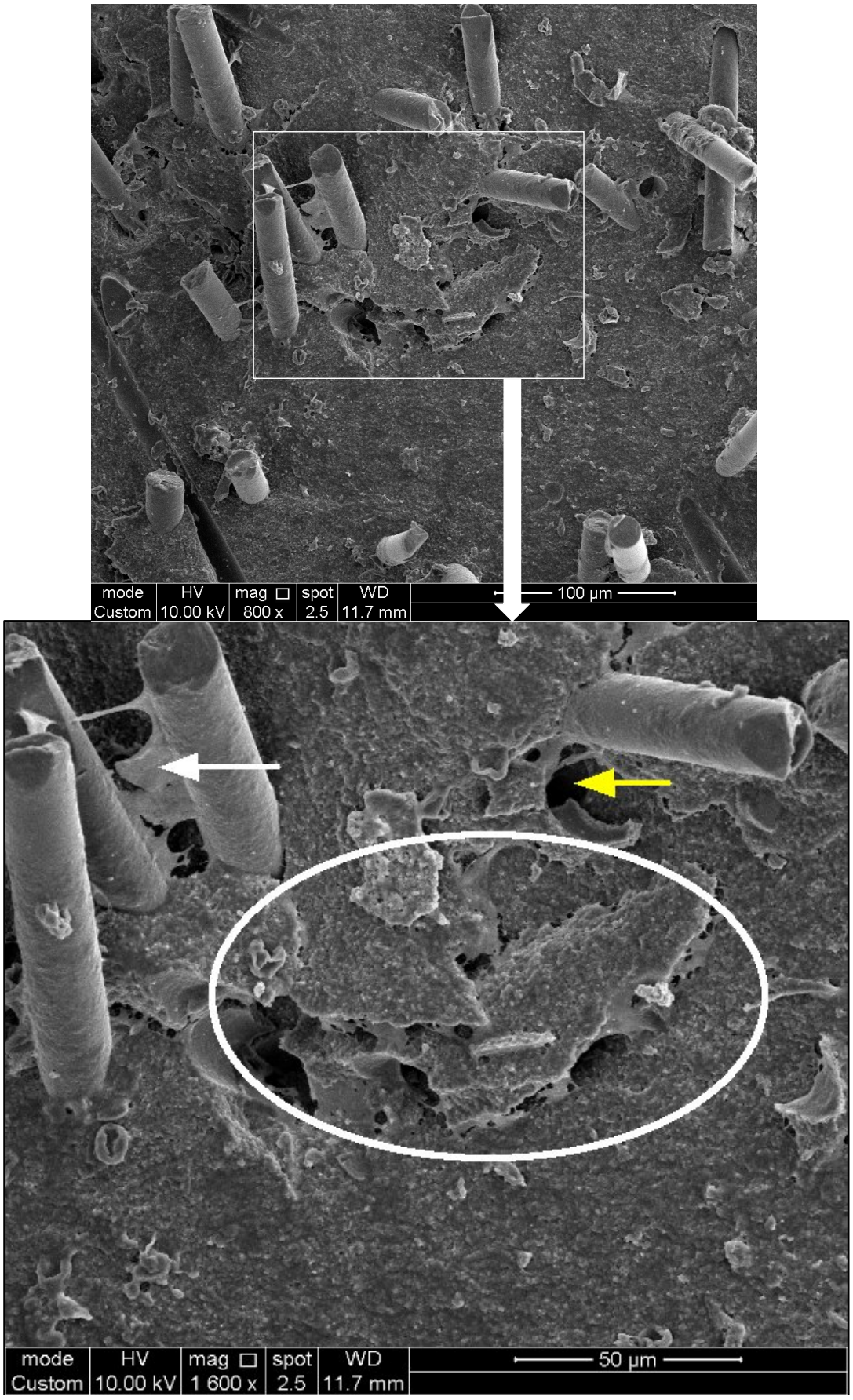

Figure 6.20: Top: SEM micrographs (x800) showing matrix deformation at area of closely packed fibres. Bottom: defected matrix magnified to x1600. Note the deformed matrix (oval), defected matrix-fibre interfacial bonding (white arrow) and void around the fibre (yellow arrow).

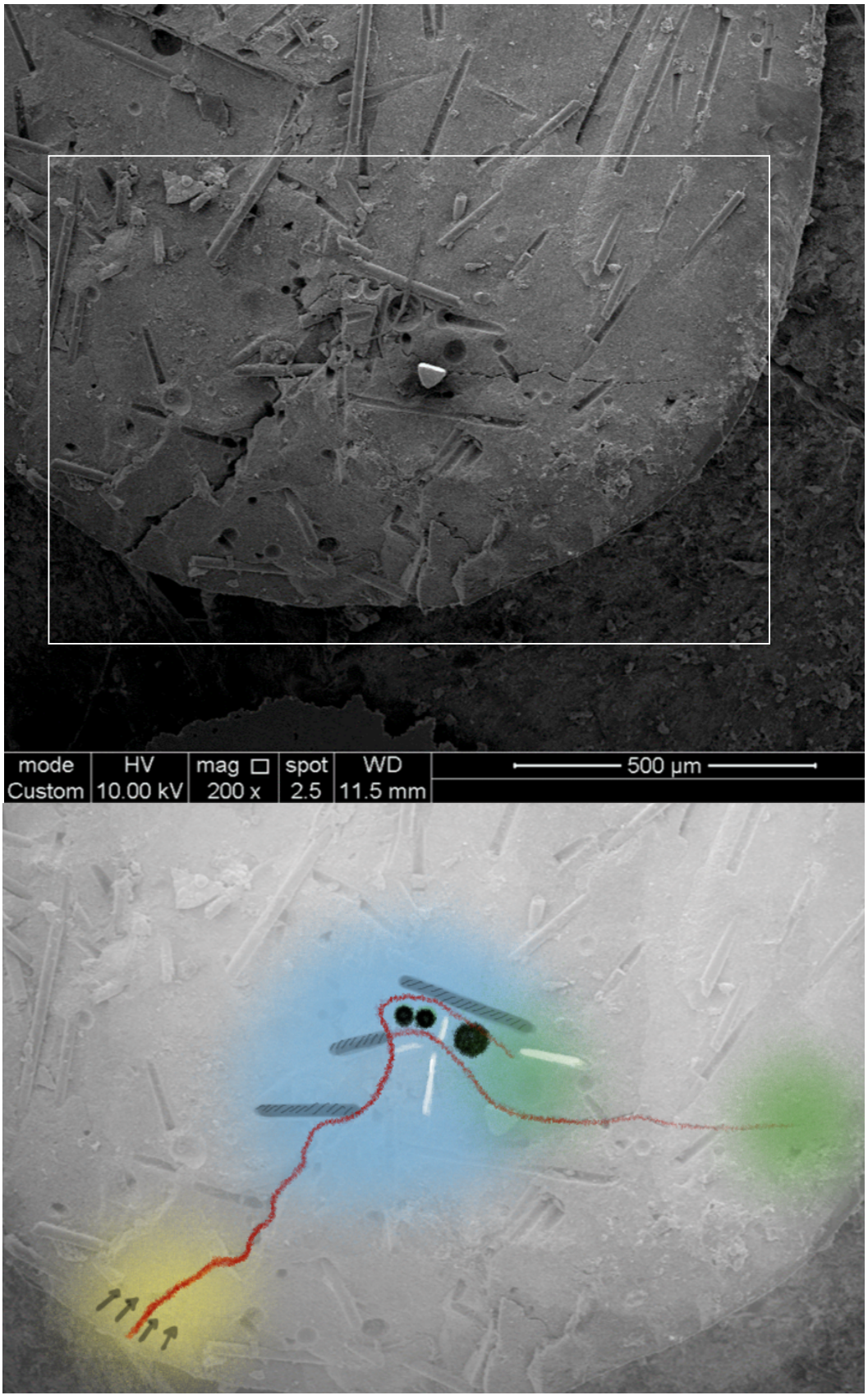

Figure 6.21: Top: SEM micrographs (x200) showing a crack (in the white rectangle) traced in the bottom figure. Bottom: The crack has initiated at an area of low fibre content (yellow-highlighted area). Crack faced an area of transversely oriented fibres and voids (blue-highlighted area). The crack then deviated and divided into two cracks. The crack energy dissipated and eventually arrested (green-highlighted areas).

Crack propagation direction and speed in SFRC is affected by heterogeneous nature of the material (Lang et al., 1987; Braem et al., 1994; Drummond, 2008; Greenhalgh, 2009). It is not uncommon, in such heterogeneous structures to observe cracks that have been redirected, curved or transformed into multiple secondary cracks (Figure 6.21). It has been demonstrated that crack deviation is an indication of efficient reinforcement (Rocca et al. 2015).

6.3.5 Correlation between fractographic features and fracture strength

Considering the previously presented micrographs and the failure load values of the fractured specimens, this section addresses the possible correlation between the micro-structural features and the fracture strength of SFRC.

SEM images of all specimens have shown voids of variable sizes that have not occupied a significant proportion of the post cross-section. However, SFRC posts that failed at a lower load displayed dominant transverse fibres orientation, uneven distribution, debonded fibres and lower fibres content in comparison to specimens fractured at a higher load value (Figure 6.22 A and B). On the other hand, in specimens fractured at high loading values, a relatively higher content of multidirectional fibres that are uniformly distributed were observed (Figure 6.22 C) (Appendix 7: SEM micrographs of all failed specimens).

SFRC with multidirectional fibres exhibits isotropic mechanical properties, whereas dominance of transversely aligned fibres, allows anisotropic properties to dominate (Brighenti et al., 2016). In other words, the SFRC post in such cases is transversally isotropic, which means that SFRC post will exhibit maximum reinforcement only when the load is applied along the long axis of the transversally oriented fibres. However, the load in this study was perpendicular to the transversely aligned fibres, which resulted in reduced reinforcement and lower failure load values in specimens with dominated transversely aligned fibres.

Specimens with low fibre content was associated with lower fracture strength in this study. On the other hand, higher fibre content was associated with higher fracture strength, which is an agreement with Fonseca et al. (2016). However, in addition to the fibre quantity, the uniform distribution of the fibres is crucial for dispersed reinforcement in the restorative structure. While clustering of the fibres can weaken the fibres' impregnation with the matrix, a region that lacks the fibres will have matrix-dominated properties (Hull and Clyne, 1996). In both situations, the reinforcement is disturbed.

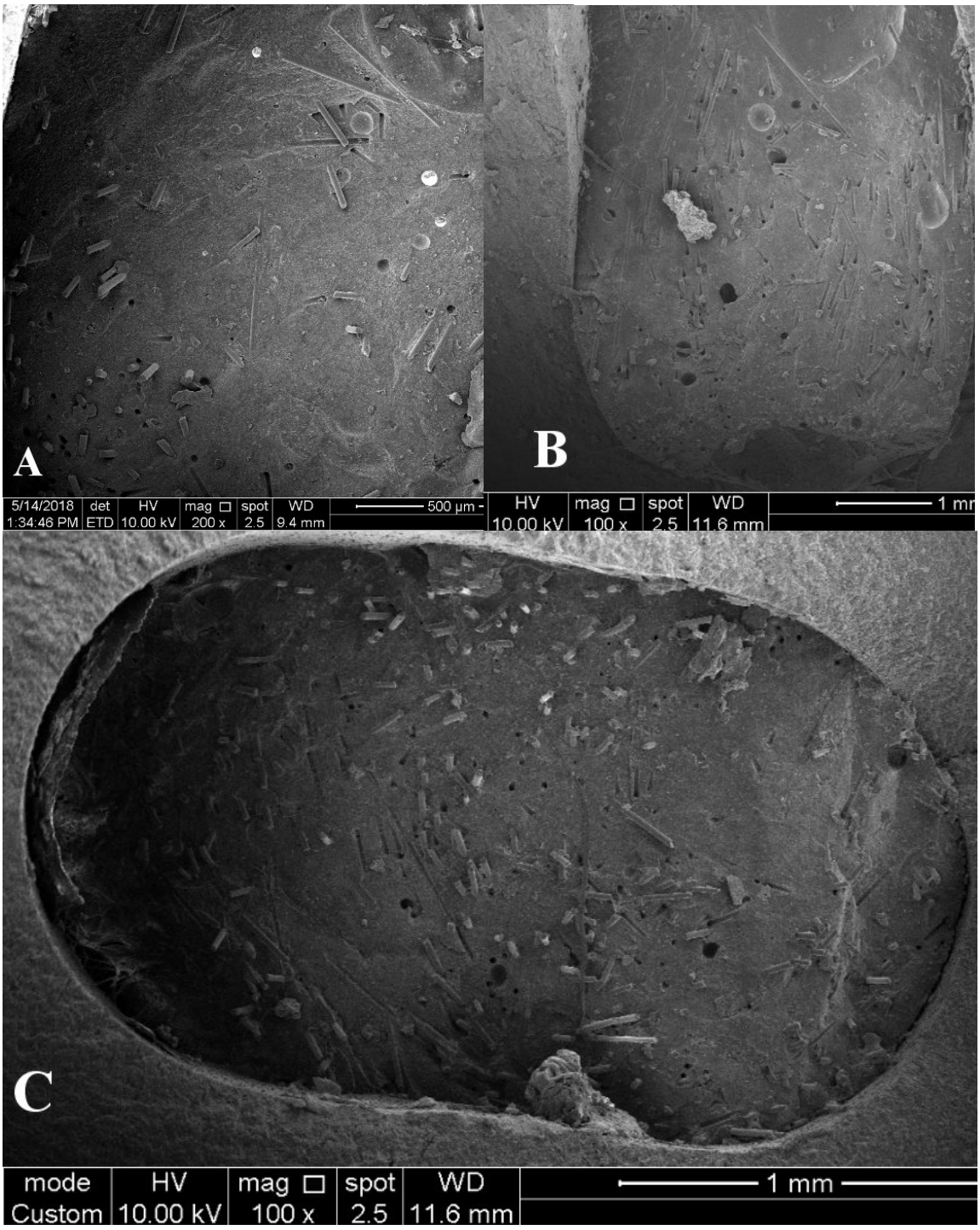

Figure 6.22: SEM micrographs of specimens scored low failure load (A and B) and high failure load values (C):
(A) SEM micrograph (x200) of a specimen failed at 609.3N showing a fracture surface with low fibre content and dominance of transverse fibre orientation that are unevenly distributed;
(B) SEM micrograph (x100) of a specimen failed at 577.9N showing a fracture surface with low fibre content and dominance of transvers fibres orientation and debonded fibres; and
(C) SEM micrograph (x100) of a specimen failed at 816.4N showing a fracture surface with uniform multidirectional fibres distribution that are present in higher quantity compared to (A) and (B).

Fibre orientation distribution in SFRC restorations is uncertain and strongly influenced by material structural properties (fibre geometry and quantity, and matrix viscosity), manufacturing process, application method (injectable vs packable), manipulation technique, and geometry of the restorative component (Zhu et al., 1997; Brighenti and Scorza, 2012b; Mortazavian and Fatemi, 2015b).

The reinforcement in SFRC is achieved through load transfer from matrix to fibres through fibre ends and along the matrix-fibre interface. The transferability depends on the fibre length and matrix-fibre interfacial bond strength (Mortazavian and Fatemi, 2015b). Although fibre length in SFRC is predetermined, the manufacturing process together with the application technique can alter the fibres length (Zhu et al., 1997; Mortazavian and Fatemi, 2015a; Bijelic et al., 2016). Thus, fibres that are shorter than the critical fibre length might negatively influence the strength of SFRC, firstly by altering the fibres' aspect ratio (length to diameter ratio), secondly by concentrating the stresses in the matrix at the broken fibres ends and thirdly by disturbing load transfer from matrix to fibres (Shouha et al., 2014).

Given the complexity of failure mechanisms in SFRC, mere acceptance that voids are a major influential factor on the mechanical properties of SFRC need to be re-evaluated. The short-glass fibres that primarily function as reinforcing elements, might act as weakening elements when their geometry, alignment or distribution are altered. Considered together, the fractographic evidence provides a valuable insight into the way in which short-glass fibres act and the circumstances under which they best contribute to increasing the fracture strength of SFRC. This will be expanded upon in the next chapter.

CHAPTER 7

General discussion and conclusions

This chapter presents a general discussion and clinical implications of the findings of the previous chapters. It also presents the limitations, future perspectives and conclusions of this project.

7.1 General discussion

Dentine is a natural composite that is composed of reinforcing collagen fibres in a hard inorganic mineral hydroxyapatite matrix. From a biomechanical perspective, the high aspect ratio of collagen fibres in dentine accounts for strength and toughness of the teeth. This balanced biological structure has inspired the search for dental materials that mimic tooth structure and restore not only the form but also the biomechanics of the tooth.

In contemporary restorative dentistry, designing a new material is driven by the "biomimetic" concept, in which material designers study the structure and physical function of the tooth to design improved restorative materials and techniques to restore teeth (Magne and Douglas, 1999). This biomimetic approach strives to restore the tooth with a "biomaterial" that is compatible with its biological, physical and mechanical properties.

Although particulate filled composite (PFC) has fulfilled aesthetic, cost and time-effectiveness requirements, some dental practitioners have been concerned about their clinical longevity in high stress bearing areas due to biomechanical incompatibility with the dentine. This has encouraged the formulation of a composite material that has a fibrous structure and physico-mechanical properties closer to dentin. However, incorporating fibres in the composite matrix needs to satisfy geometrical, alignment and quantity requirements for efficient fibre reinforcement of the restoration. As a result, high aspect ratio, discontinuous, randomly oriented, millimetre-scale SFRC was introduced. This SFRC has gone considerable way toward satisfying the requirements of biomimetic concept and has encouraged the extension of SFRC applications beyond merely restorative solutions to resto-endodontic techniques in which SFRC is used as a core or as a post and core in ETT.

The few promising in vitro results of SFRC as a post and core has encouraged the author to comprehensively analyse the failure of ETT restored with SFRC posts and cores in a common challenging scenario–extensively damaged endodontically treated premolars.

The results of this project have shown that ETT restored with SFRC posts and cores had almost twice the strength of comparable teeth restored with prefabricated FRC post, and similar rate of restorable failure (100%) as the sound, untreated premolars (Figure 7.1).

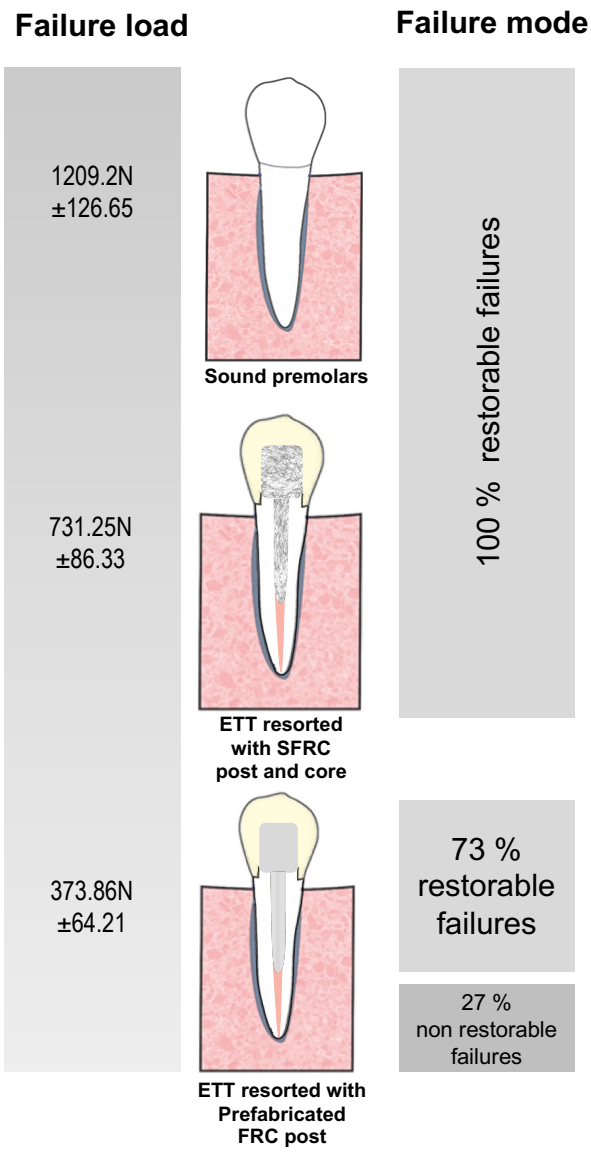

Figure 7.1: Summary of failure load and failure mode results of ETT restored with SFRC posts and cores in comparison to prefabricated posts and control group

Two previously reported studies have evaluated everX Posterior™ SFRC as a post and core restoration (Bijelic et al., 2013; Forster et al., 2017). Figure 7.2 presents the agreements and disagreements between those studies and the current project in regard to study protocols and results.

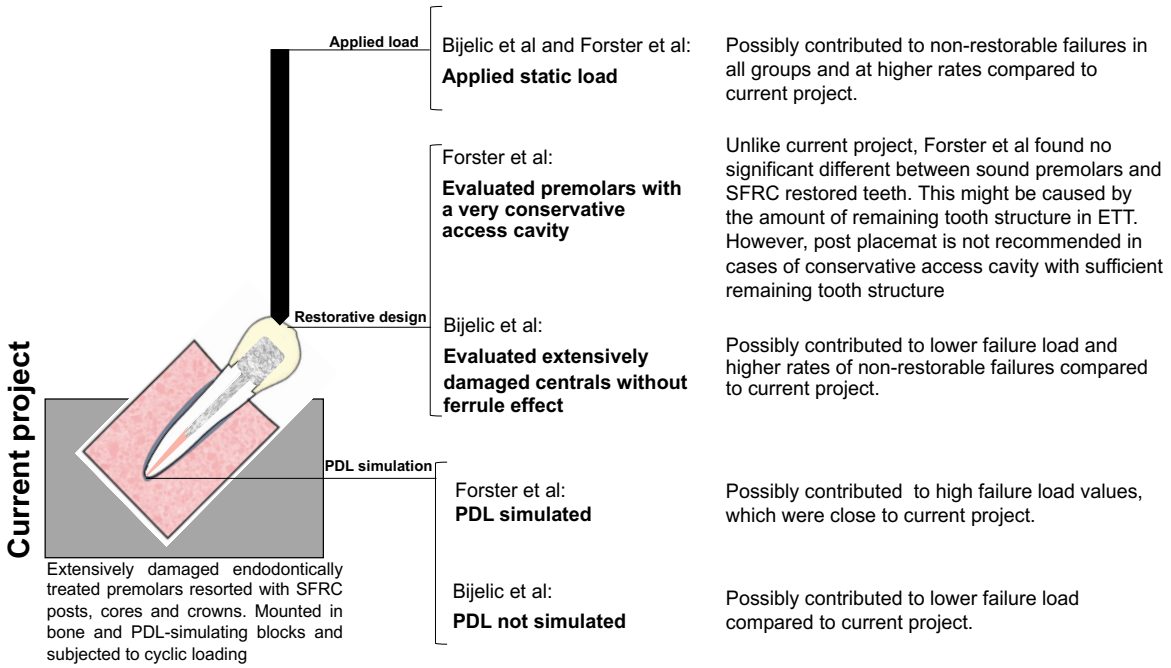

Figure 7.2: Agreements and disagreements between current project and other studies: Bijelic et al., 2013 and Forster et al., 2017.

Considering the fact that the structure of SFRC is complex, and for better understanding of the mechanical behaviour of SFRC as a post and core, it seemed logical to analyse the failure of SFRC at a microstructural level. Therefore, micro-CT and fractographic analyses were conducted.

The comprehensive failure analysis has indicted that the fracture strength and reinforcement effectiveness in SFRC might be affected by interrelated, external and internal factors. The external factors include; test mode and conditions. The internal factors are those related to microstructural components (matrix, fibres, matrix-fibre interfacial bond and defects) and mechanical properties of SFRC. Internal factors are further influenced by manufacturing-related factors, clinician-related factors and cavity-related factors.

Initial micro-CT evaluation of the SFRC structure have indicated that posts were well adapted to the canal walls, however, defects in the form of voids/porosity were present in the posts and cores. The presence of voids was explained by manufacturing-related factors (i.e. voids created during material fabrication or extruding viscous material through the provided dispensing nozzle) and aggravated by clinician-related

factors (e.g. overmanipulation). Figure 7.3 summarises the effect of different void locations on the fracture strength of SFRC post and core.

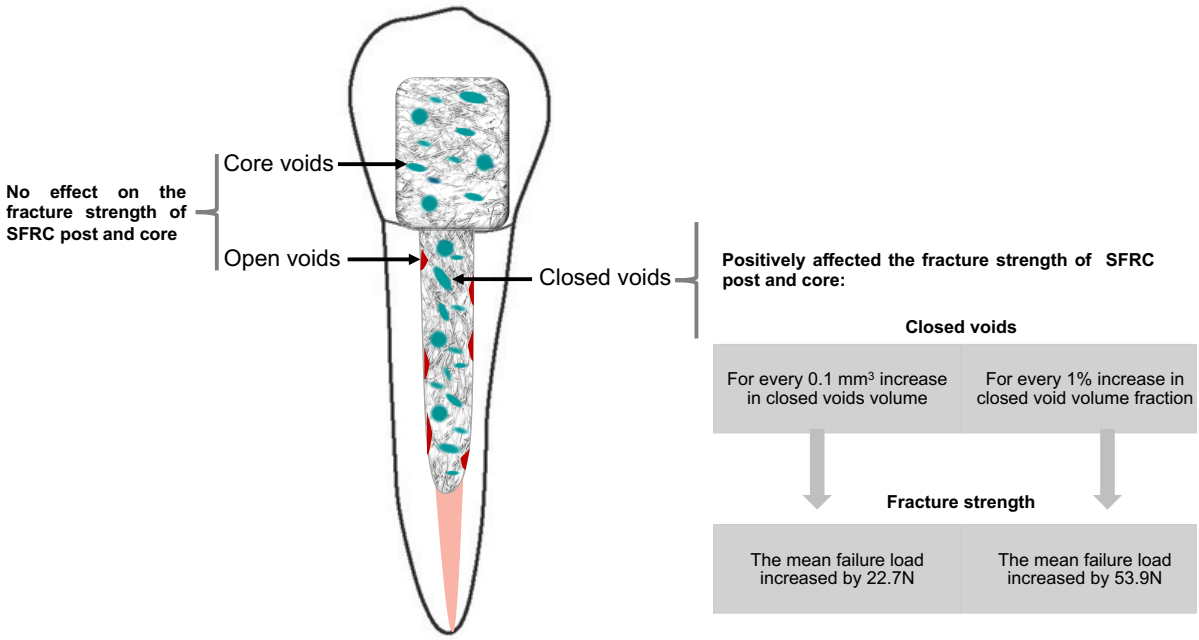

Figure 7.3: Effect of voids on fracture strength of SFRC posts and cores

Since the presence of voids has been shown to increase fracture strength in this project, it has been speculated that factors other than voids are acting to initiate and/or accelerate cracks in the structure of SFRC. This speculation is driven by the failure mode results, which indicated that all specimens failed favourably regardless the presence of voids, but almost one third of the SFRC specimens had bulk fracture of the restoration. Fractographic analysis have revealed some interesting results in this regard.

The first interesting fractographic observation was lack of evidence of fatigue failure (e.g. microcracks, fatigue striations) in the matrix close to voids. This might support the speculation that voids are not directly related to weakening SFRC structure.

The second fractographic observation, there was an inter-specimens and intra-specimen variations in the fibre quantity, length, orientation and distribution. This variation has resulted in differences in the mechanical properties of SFRC across the post ad core structure and variation of the mechanical

behaviour between specimens. Unfortunately, it is difficult to control or predict the fibre quantity, length or orientation distribution within a SFRC restorative structure. The variation in the fibre orientation and length and their distribution might be created as a result to manufacturer-related factors, clinician-related factors or cavity related-factors as shown in figure 7.4.

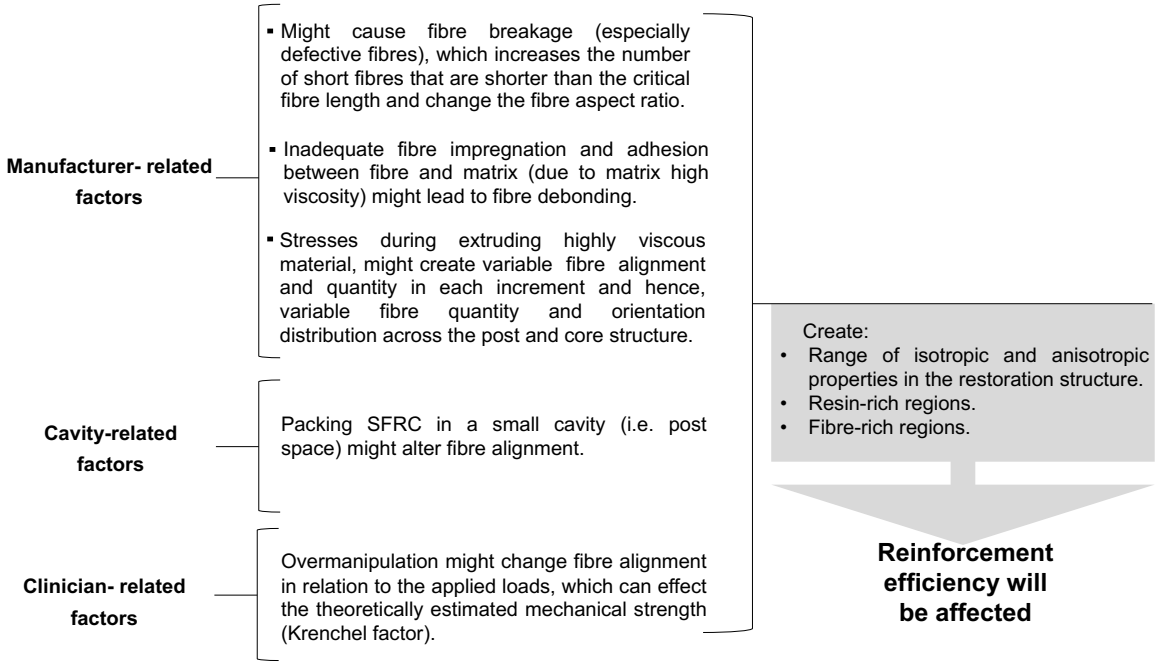

Figure 7.4: Possible reasons and consequences of variable fibre quantity, length, orientation and distribution in SFRC

7.2 Clinical implications and future perspectives

It would appear that voids and fibre-characteristic variations are inevitable in SFRC. In the early fibre-incorporation-for-reinforcement dental research conducted by Vallittu, the void presented in the final products were unexplained. According to Ironside and Makinson (1993), it is easy to incorporate porosities into composite restorations no matter how it has been handled (Ironside and Makinson, 1993). Similarly, the heterogeneous nature of SFRC makes it difficult to predict or control the consistency of fibre characteristics (length, orientation and distribution) across the whole restoration. However, every attempt should be made by the clinician to minimally manipulate SFRC during restoration construction and to preferably restrict its application to bulk-fill restorations in order to minimize fibre-characteristics variations.

A maximum void percentage of 4.9% was recorded in this project. A study testing the effect of intentionally introduced voids above that level in SFRC might show a negative relationship between void content and fracture resistance. To provide a broader perspective of the significance of the voids, it is also worth considering future studies analysing voids in SFRC in comparison to voids in other bulk-fill composites or PFC.

The improved mechanical performance of SFRC as a post and core reported in this study was achieved, in part at least, by the careful handling during post construction. This was demanding, technique sensitive and time consuming and, on reflection, is not going to be achieved by all operators in every clinical situation using currently available SFRC materials. Therefore, it seems entirely reasonable to use SFRC as a bulk-fill core restoration in ETT, with ample evidence supporting this application (Kemaloglu et al., 2015; Eapen et al., 2017; Gurel et al., 2016; Gaintantzopoulou et al., 2018).

In the future, consideration could be given to developing techniques for the use SFRC for the construction of shorter posts (4-5mm) where a bulk-fill technique, which avoids over manipulation, might be appropriate. An analysis of the strength and fracture mechanics of restorations of this type is another promising area for future research.

Furthermore, history has shown that as manufacturers continue to develop materials, there is continuous improvement in a range of properties including delivery systems and ease of manipulation. The promising results in this study should encourage manufacturers to pursue such modifications.

The demanding handling, unpredictable voids and fibre arrangement and distribution of SFRC were mainly caused by the material high viscosity. Few measures can be applied by the clinicians and/or manufacturer to counteract the viscosity of SFRC. For example; warming the increment prior to application, use of a sonicated delivery system and modifying the flowability and/or dispensing nozzle (use a larger diameter nozzle could be considered).

Interestingly, the group of researchers who contributed in the development of everX posterior™ SFRC are working now on new experimental formulations to develop a flowable SFRC (initially named as Exp-SFRC). With this new flowable composite, the authors reported promising results in regard to mechanical properties (flexural strength and fracture toughness) and failure behaviour in comparison to PFC (Lassila et al., 2018; Garoushi et al., 2019).

7.3 Limitations

This project aimed to understand the failure of SFRC as a post and core restoration using mechanical testing, micro-CT and fractographic analyses. Micro-CT scanning and analysis required meticulous setting of parameters, which might affect the accuracy of image interpretation. This risk was managed by working closely with imaging specialists. One operator has performed the analysis of micro-CT images and micrographs. This might introduce the possibility of operator bias. Also, due to lack of comparable studies that consider micro-CT void analysis, void-fracture strength relationship and fractography in dental SFRC, discussion of the results was limited in some situations.

7.4 Conclusions

Considering the conditions and limitations of the present project, both hypotheses presented in Chapter 1 were accepted; restoring ETT with SFRC as directly-layered post and core restorations improves the fracture strength and reduces the incidence of catastrophic failure of ETT, and the structural composition of SFRC have an impact on the mechanical behaviour of ETT restored with SFRC posts and cores.

The following are the specific conclusions of the studies presented in this project, which analysed the failure of endodontically treated premolars restored with SFRC posts and cores:

Chapter 3:

- Posts and cores constructed using SFRC has voids of variable sizes and distributions.
- The volume fraction of voids within the post that was incrementally-built was significantly higher than the volume fraction of voids within the core that was constructed using bulk-fill technique.
- SFRC resulted in a well-adapted posts to canal walls.
- The coronal third of the SFRC posts had the highest volume of voids compared to the middle and apical thirds.
- The percentage of small voids (<100 μm^3) in the SFRC posts was significantly greater than the medium voids (100 -500 μm^3) and large voids (> 500 μm^3).

Chapter 4:

- Sound untreated premolars had the highest fracture strength compared to ETT restored with SFRC posts and cores and ETT restored with prefabricated FRC posts.
- The fracture strength of ETT restored with SFRC posts and cores was significantly higher than the fracture strength of ETT restored with prefabricated FRC posts.

- All sound untreated premolars and ETT restored with SFRC posts and cores had favourable failure mode, whereas, unfavourable failure mode was reported only in ETT restored with prefabricated FRC posts.

Chapter 5:

- There was a positive relationship between the voids (in the range of 1.3-4.9%) in the SFRC posts and the fracture strength of ETT restored with SFRC posts and cores.
- For every 0.1 mm^3 increase in the void volume, the mean failure load of ETT restored with SFRC posts and cores increased by 22.7N.
- For every 1% increase in void volume fraction, the mean failure load of ETT restored with SFRC posts and cores increased by 53.9N.

Chapter 6:

- The glass-fibre length, orientation and distribution in SFRC restorations are unpredictable.
- There was no evidence that voids in SFRC restorations have initiated failures in ETT restored with SFRC posts and cores.

CHAPTER 8

Bibliography

Bibliography

Abbas, G., Fleming, G., Harrington, E., Shortall, A. and Burke, F. (2003) 'Cuspal movement and microleakage in premolar teeth restored with a packable composite cured in bulk or in increments', J Dent, 31(6), pp. 437-444.

Abduljawad, M., Samran, A., Kadour, J., Karzoun, W. and Kern, M. (2016) 'Effect of fiber posts on the fracture resistance of maxillary central incisors with class III restorations: An in vitro study', J Prosthet Dent, 118(1), pp. 55-60.

Abo El-Ela, O. A., Atta, O. A. and El-Mowafy, O. (2008) 'Fracture resistance of anterior teeth restored with a novel nonmetallic post', J Can Dent Assoc, 74(5), pp. 441-441e.

Abouelleil, H., Pradelle, N., Villat, C., Attik, N., Colon, P. and Grosgogeat, B. (2015) 'Comparison of mechanical properties of a new fiber reinforced composite and bulk filling composites', Restor Dent Endod, 40(4), pp. 262-270.

Akkayan, B. (2004) 'An in vitro study evaluating the effect of ferrule length on fracture resistance of endodontically treated teeth restored with fiber-reinforced and zirconia dowel systems', J Prosthet Dent, 92(2), pp. 155-62.

Akkayan, B. and Gulmez, T. (2002) 'Resistance to fracture of endodontically treated teeth restored with different post systems', J Prosthet Dent, 87(4), pp. 431-7.

Al Sunbul, H., Silikas, N. and Watts, D. (2016) 'Surface and bulk properties of dental resin-composites after solvent storage', Dent Mater, 32(8), pp. 987-997.

Al-harbi, F. and Nathanson, D. (2003) 'In vitro assessment of retention of four esthetic dowels to resin core foundation and teeth', J Prosthet Dent, 90(6), pp. 547-555.

Al-Sharaa, K. and Watts, D. (2003) 'Stickiness prior to setting of some light cured resin-composites', Dent Mater, 19(3), pp. 182-187.

Al-Turki, L. I., Drummond, J. L., Agojci, M., Gosz, M., Tyrus, J. and Lin, L. (2007) 'Contact versus flexure fatigue of a fiber-filled composite', Dent Mater, 23(5), pp. 648-653.

Alster, D., Feilzer, A., De Gee, A., Moli, A. and Davidson, C. (1992) 'The Dependence of Shrinkage Stress Reduction on Porosity Concentration in Thin Resin Layers', JnDent Res, 71(9), pp. 1619-1622.

AlZahrani, F. and Richards, L. (2018) 'Micro-CT evaluation of a novel periodontal ligament simulation technique for dental experimental models', Arch Orofac Sci, 13(2), pp. 93-102

Amaral, F., Colucci, V., PALMA-DIBB, R. and Corona, S. (2007) 'Assessment of in vitro methods used to promote adhesive interface degradation: a critical review', J Esthet Restor Dent, 19(6), pp. 340-353.

Ambica, K., Mahendran, K., Talwar, S., Verma, M., Padmini, G. and Periasamy, R. (2013) 'Comparative evaluation of fracture resistance under static and fatigue loading of endodontically treated teeth restored with carbon fiber posts, glass fiber posts, and an experimental dentin post system: an in vitro study', J Endod, 39(1), pp. 96-100.

Anchieta, R. B., Rocha, E. P., Almeida, E. O., Freitas, A. C., Jr., Martin, M., Jr., Martini, A. P., Archangelo, C. M. and Ko, C. C. (2012) 'Influence of customized composite resin fibreglass posts on the mechanics of restored treated teeth', Int Endod J, 45(2), pp. 146-55.

Angmar-Mansson, B., Omnell, K. A. and Rud, J. (1968) 'Root fractures due to corrosion. 1. Metallurgical aspects', Odontol revy, 20(3), pp. 245-265.

Arvidson, k. and Wroblewski, R. (1978) 'Migration of metallic ions from screwposts into dentin and surrounding tissues', Eur J Oral Sci, 86(3), pp. 200-205.

Asmussen, E., Peutzfedt, A. and Heitmann, T. (1999) 'Stiffness, elastic limit, and strength of newer types of endodontic posts', J Dent, 27, pp. 275-278.

Asmussen, E., Peutzfeldt, A. and Sahafi, A. (2005) 'Finite element analysis of stresses in endodontically treated, dowel-restored teeth', J Prosthet Dent, 94(4), pp. 321-329.

Assif, D., Bitenski, A., Pilo, R. and Oren, E. (1993) 'Effect of post design on resistance to fracture of endodontically treated teeth with complete crowns', J Prosthet Dent, 69(1), pp. 36-40.

Assif, D. and Gorfil, C. (1994) 'Biomechanical considerations in restoring endodontically treated teeth', J Prosthet Dent, 71(6), pp. 565-7.

Atalay, C., Yazici, A., Horuztepe, A., Nagas, E., Ertan, A. and Ozgunaltay, G. (2016) 'Fracture resistance of endodontically treated teeth restored with bulk fill, bulk fill flowable, fiber-reinforced, and conventional resin composite', Oper Dent, 41(5), pp. E131-E140.

Athey, T. H. (1982) 'Systematic systems approach: An integrated method for solving systems problems', Englewood Cliffs NJ: Prentice-Hall, pp. 17-85.

Bajaj, D., Sundaram, N., Nazari, A. and Arola, D. (2006) 'Age, dehydration and fatigue crack growth in dentin', Biomaterials, 27(11), pp. 2507-2517.

Baraban, D. J. (1967) 'The restoration of pulpless teeth', Dent Clin North Am, Nov, pp. 633-653.

Barjau-Escribano, A., Sancho-Bru, J. L., Forner-Navarro, L., Rodríguez-Cervantes, P. J., Perez-Gonzalez, A. and Sanchez-Marin, F. T. (2006) 'Influence of prefabricated post material on restored teeth: fracture strength and stress distribution', Oper Dent, 31(1), pp. 47-54.

Barkhordar, R. A., Radke, R. and Abbasi, J. (1989) 'Effect of metal collars on resistance of endodontically treated teeth to root fracture', J Prosthet Dent, 61(6), pp. 676-678.

Barreto, B. C. F., Van Ende, A., Lise, D. P., Noritomi, P. Y., Jaecques, S., Vander Sloten, J., De Munck, J. and Van Meerbeek, B. (2016) 'Short fibre-reinforced composite for extensive direct restorations: a laboratory and computational assessment', Clin Oral Investig, 20(5), pp. 959-966.

Bartos, M., Suchy, T. and Foltan, R. (2018) 'Note on the use of different approaches to determine the pore sizes of tissue engineering scaffolds: what do we measure?', Biomed Eng online, 17(1), pp. 110.

Bassi, M. (2001) 'Light diffusion through double taper quartz-epoxy fiber posts', Am J Dent 13, pp. 19-21.

Batdorf, S. (2012) Strength of composites. Concise encyclopedia of composite materials: Elsevier.

Bateman, G., Ricketts, D. N. and Saunders, W. P. (2003) 'Fibre-based post systems: a review', Br Dent J, 195(1), pp. 43-48.

Bates, J., Stafford, G. and Harrison, A. (1975) 'Masticatory function—a review of the literature', J oral rehabil, 2(3), pp. 281-301.

Baudin, C., Osorio, R., Toledano, M. and de Aza, S. (2009) 'Work of fracture of a composite resin: Fracture-toughening mechanisms', J Bio Mater Res A, 89(3), pp. 751-758.

Bayne, S. C. and Thompson, J. Y. (2013) 'Biomaterials'. pp. e1-e97 (OnlinenVersion).

Belli, R., Petschelt, A. and Lohbauer, U. (2014) 'Are linear elastic material properties relevant predictors of the cyclic fatigue resistance of dental resin composites?', Dent Mater, 30(4), pp. 381-391.

Berger, H., Kari, S., Gabbert, U., Rodriguez Ramos, R., Bravo Castillero, J. and Guinovart Diaz, R. (2007) 'Evaluation of effective material properties of randomly distributed short cylindrical fiber composites using a numerical homogenization technique', J Mech of Mater Struct, 2(8), pp. 1561-1570.

Bergman, B., Lundquist, P. and Sjo, U. (1989) 'Restorative and endodontic results after treatment with cast posts and cores', J Prosthet Dent, 61(1), pp. 10-15.

Bicalho, A., Valdívia, A., Barreto, B. d. C., Tantbirojn, D., Versluis, A. and Soares, C. (2014) 'Incremental filling technique and composite material—part II: shrinkage and shrinkage stresses', Oper Dent, 39(2), pp. e83-e92.

Bier, C. A. S., Shemesh, H., Tanomaru-Filho, M., Wesselink, P. R. and Wu, M. K. (2009) 'The ability of different nickel-titanium rotary instruments to induce dentinal damage during canal preparation', J Endod, 35(2), pp. 236-238.

Bijelic, J., Garoushi, S., Vallittu, P. and Lassila, L. (2013) 'Short fiber reinforced composite in restoring severely damaged incisors', Acta Odontol Scand, 71(5), pp. 1221-31.

Bijelic, J., Garoushi, S., Lassila, L. and Vallittu, P. (2015a) 'Oxygen inhibition layer of composite resins: effects of layer thickness and surface layer treatment on the interlayer bond strength', Eur J oral sci, 123(1), pp. 53-60.

Bijelic, J., Garoushi, S., Vallittu, P. and Lassila, L. (2015b) 'Mechanical properties, fracture resistance, and fatigue limits of short fiber reinforced dental composite resin', J Prosthet Dent, 115(1):95-102.

Bijelic, J., Garoushi, S., Lassila, L., Keulemans, F. and Vallittu, P. (2016) 'Mechanical and structural characterization of discontinuous fiber-reinforced dental resin composite', J Dent, 52, 70-78

Bilgi, P., Shah, N., Patel, P. and Vaid, D. (2016) 'Comparison of fracture resistance of endodontically treated teeth restored with nanohybrid, silorane, and fiber reinforced composite: An in vitro study', J Conserv Dent, 19(4), pp. 364-7.

Bitter, K. and Kielbassa, A. M. (2007) 'Post-endodontic restorations with adhesively luted fiber-reinforced composite post systems: a review', Am J Dent, 20(6), pp. 353-60.

Blumer, L., Schmidli, F., Weiger, R. and Fischer, J. (2015) 'A systematic approach to standardize artificial aging of resin composite cements', Dent Mater, 31(7), pp. 855-863.

Bocalon, A. C. E., Mita, D., Narumyia, I., Shouha, P., Xavier, T. A. and Braga, R. R. (2016) 'Replacement of glass particles by multidirectional short glass fibers in experimental composites: Effects on degree of conversion, mechanical properties and polymerization shrinkage', Dent Mater, 32(9), pp. e204-e210.

Boey, F. (1990) 'Reducing the void content and its variability in polymeric fibre reinforced composite test specimens using a vacuum injection moulding process', Polym Test, 9(6), pp. 363-377.

Bonfante, G., Kaizer, O. B., Pegoraro, L. F. and do Valle, A. L. (2007) 'Fracture strength of teeth with flared root canals restored with glass fibre posts', Int Dent J, 57(3), pp. 153-60.

Boschian Pest, L., Guidotti, S., Pietrabissa, R. and Gagliani, M. (2006) 'Stress distribution in a post-restored tooth using the three-dimensional finite element method', J Oral Rehabil, 33(9), pp. 690-7.

Braem, M., Lambrechts, G., Davidson, C., Vansant, E. and Vanhoof, C. (1993) 'Derangement of composite filler distribution inside syringe-type delivery systems', Dent Mater, 9(1), pp. 23-27.

Braem, M., Lambrechts, P. and Vanherle, G. (1994) 'Clinical relevance of laboratory fatigue studies', J Dent, 22(2), pp. 97-102.

Braem, M., Lambrechts, P., Gladys, S. and Vanherle, G. (1995) 'In vitro fatigue behavior of restorative composites and glass ionomers', Dent Mater, 11(2), pp. 137-141.

Brighenti, R. and Scorza, D. (2012a) 'A micro-mechanical model for statistically unidirectional and randomly distributed fibre-reinforced solids', Math Mech Solids, 17(8), pp. 876-893.

Brighenti, R. and Scorza, D. (2012b) 'Numerical modelling of the fracture behaviour of brittle materials reinforced with unidirectional or randomly distributed fibres', Mech Mater, 52, pp. 12-27.

Brighenti, R., Carpinteri, A. and Scorza, D. (2016) 'Micromechanical model for preferentially-oriented short-fibre-reinforced materials under cyclic loading', Eng Fract Mech, 167, pp. 138-150.

Brunthaler, A., König, F., Lucas, T., Sperr, W. and Schedle, A. (2003) 'Longevity of direct resin composite restorations in posterior teeth: a review', Clin Oral Investig, 7(2), pp. 63-70.

Burke, F., Wilson, N., Cheung, S. and Mjör, I. (2001) 'Influence of patient factors on age of restorations at failure and reasons for their placement and replacement', J Dent, 29(5), pp. 317-324.

Burstone, C. J. and Kuhlberg, A. J. (2000) 'Fiber-Reinforced Composites in Orthodontics-Applications of state-of-the-art polymers are illustrated', J Clin Orthod, 34(5), pp. 271-279.

Butz, F., Lennon, A. M., Heydecke, G. and Strub, J. R. (2001) 'Survival rate and fracture strength of endodontically treated maxillary incisors with moderate defects restored with different post-and-core systems: an in vitro study', Int J Prosthodont, 14(1), pp. 58-64.

Callaghan, D. J., Vaziri, A. and Nayeb-Hashemi, H. (2006) 'Effect of fiber volume fraction and length on the wear characteristics of glass fiber-reinforced dental composites', Dent Mater, 22(1), pp. 84-93.

Callister, W. D. and Rethwisch, D. G. (2007) Materials science and engineering: an introduction. Wiley New York.

Campos, R. E., Soares, P. V., Versluis, A., Júnior, O. B., Ambrosano, G. M. and Nunes, I. B. (2015) 'Crown fracture: Failure load, stress distribution, and fractographic analysis', J Prosthet Dent.

Carrera, C. A., Lan, C., Escobar-Sanabria, D., Li, Y., Rudney, J., Aparicio, C. and Fok, A. (2015) 'The use of micro-CT with image segmentation to quantify leakage in dental restorations', Dent Mater, 31(4), pp. 382-390.

Cavel, W. T., Kelsey, W. P. and Blankenau, R. J. (1985) 'An in vivo study of cuspal fracture', J Prosthet Dent, 53(1), pp. 38-42.

Chambers, A., Earl, J., Squires, C. and Suhot, M. (2006) 'The effect of voids on the flexural fatigue performance of unidirectional carbon fibre composites developed for wind turbine applications', Int J Fatigue, 28(10), pp. 1389-1398.

Cheung, W. (2005) 'A review of the management of endodontically treated teeth. Post, core and the final restoration', J Am Dent Assoc, 136(5), pp. 611-9.

Chieruzzi, M., Rallini, M., Pagano, S., Eramo, S., D'Errico, P., Torre, L. and Kenny, J. M. (2014) 'Mechanical effect of static loading on endodontically treated teeth restored with fiber-reinforced posts', Appl Biomater, 102(2), pp. 384-94.

Choi, K., Ferracane, J., Hilton, T. J. and Charlton, D. (2000a) 'Properties of packable dental composites', J Esthet Rest or Dent, 12(4), pp. 216-226.

Choi, K., Condon, J. and Ferracane, J. (2000b) 'The effects of adhesive thickness on polymerization contraction stress of composite', J Dent Res, 79(3), pp. 812-817.

Chong, K.-H. and Chai, J. (2003) 'Strength and mode of failure of unidirectional and bidirectional glass fiber-reinforced composite materials', Int J Prosthodont, 16(2), pp. 161-166.

Christensen, G. J. (1996) 'Posts: necessary or unnecessary?', J Am Dent Assoc, 127(10), pp. 1522-1526.

Christensen, G. J. (2004) 'Post concepts are changing', J Am Dent Assoc, 135(9), pp. 1308-1310.

Chung, S., Yap, A., Chandra, S. and Lim, C. (2004) 'Flexural strength of dental composite restoratives: Comparison of biaxial and three-point bending test', Appl Biomater, 71(2), pp. 278-283.

Cormier, C. J., Burns, D. R. and Moon, P. (2001) 'In vitro comparison of the fracture resistance and failure mode of fiber, ceramic, and conventional post systems at various stages of restoration', J Prosthodont, 10(1), pp. 26-36.

Costa, M., De Almeida, S. and Rezende, M. (2005) 'Critical void content for polymer composite laminates', AIAA J, 43(6), pp. 1336-1341.

Craig, R. G. and Peyton, F. A. (1958) 'Elastic and mechanical properties of human dentin', J dent Res, 37(4), pp. 710-718.

da Veiga, A., Cunha, A., Ferreira, D., da Silva Fidalgo, T., Chianca, T., Reis, K. and Maia, L. (2016) 'Longevity of direct and indirect resin composite restorations in permanent posterior teeth: a systematic review and meta-analysis', J Dent, 54, pp. 1-12.

Dale, J. W. and Moser, J. (1977) 'A clinical evaluation of semiprecious alloys for dowels and cores', J Prosthet Dent, 38(2), pp. 161-164.

Davis, P., Melo, L. S., Foxton, R. M., Sherriff, M., Pilecki, P., Mannocci, F. and Watson, T. F. (2010) 'Flexural strength of glass fibre-reinforced posts bonded to dual-cure composite resin cements', Eur J Oral Sci, 118(2), pp. 197-201.

De Gee, A. (1979) 'Some aspects of vacuum mixing of composite resins and its effect on porosity', Quintessence Int, 10(7), pp. 69-74.

De Munck, J., Van Landuyt, K., Coutinho, E., Poitevin, A., Peumans, M., Lambrechts, P. and Van Meerbeek, B. (2005) 'Micro-tensile bond strength of adhesives bonded to Class-I cavity-bottom dentin after thermo-cycling', Dent Mater, 21(11), pp. 999-1007.

de Silva, N., Aguiar, G., Rodrigues, M., Bicalho, A., Soares, P., Verissimo, C. and Soares, C. (2015) 'Effect of Resin Cement Porosity on Retention of Glass-Fiber Posts to Root Dentin: An Experimental and Finite Element Analysis', Braz Dent J, 26(6), pp. 630-636.

Demarco, F. F., Correa, M. B., Cenci, M. S., Moraes, R. R. and Opdam, N. J. (2012) 'Longevity of posterior composite restorations: not only a matter of materials', Dent Mater, 28(1), pp. 87-101.

Derand, T. (1971) 'Corrosion of screwposts', Odontol revy, 22(4), pp. 371.

Dietschi, D., De Siebenthal, G., Neveu-Rosenstand, L. and Holz, J. (1995) 'Influence of the restorative technique and new adhesives on the dentin marginal seal and adaptation of resin composite Class II restorations: An in vitro evaluation', Quintessence Int, 26(10), pp.717-727.

Dietschi, D., Duc, O., Krejci, I. and Sadan, A. (2007) 'Biomechanical considerations for the restoration of endodontically treated teeth: a systematic review of the literature--Part 1. Composition and micro-and macrostructure alterations', Quintessence Int, 38(9), pp. 733-743.

Dietschi, D., Duc, O., Krejci, I. and Sadan, A. (2008) 'Biomechanical considerations for the restoration of endodontically treated teeth: a systematic review of the literature, Part II (Evaluation of fatigue behavior, interfaces, and in vivo studies)', Quintessence Int, 39(2), pp. 117-29.

Dikbas, I. and Tanalp, J. (2013) 'An overview of clinical studies on fiber post systems', The Scientific World Journal, 2013.

Donovan, T. E., Sulaiman, T. A., Oliveira, G. M., Bayane, S. C. and Thompson, J. Y. (2017) 'Dental Biomaterials', in Sturdevant's Art & Science of Operative Dentistry-E-Book. pp. 453-476.

Dowker, S. E., Davis, G. R. and Elliott, J. C. (1997) 'X-ray microtomography: nondestructive three-dimensional imaging for in vitro endodontic studies', Oral Surg Oral Med Oral Pathol Oral Radiol Endod, 83(4), pp. 510-6.

Draughn, R. A. (1987) 'Slow crack propagation in composite restorative materials', J Biomed Mater Res A, 21(5), pp. 629-642.

Drummond, J. L. (1989) 'Cyclic fatigue of composite restorative materials', J Oral Rehabil, 16(5), pp. 509-520.

Drummond, J. L. (2000) 'In vitro evaluation of endodontic posts', Am J Dent, 13(Spec No), pp. 5B-8B.

Drummond, J. (2008) 'Degradation, fatigue, and failure of resin dental composite materials', J Dent Res, 87(8), pp. 710-719.

Drummond, J. L., Lin, L., Al-Turki, L. A. and Hurley, R. K. (2009) 'Fatigue behaviour of dental composite materials', J Dent, 37(5), pp. 321-330.

Dunn, W. J. (2016) 'Microcomputed tomographic comparison of posterior composite resin restorative techniques: sonicated bulk fill versus incremental fill', Gen Dent, 64(5), pp. 20-23.

Duret, B., Reynaud, M. and Duret, F. (1990) 'New concept of coronoradicular reconstruction: the Composipost (1)', Chir Dent Fr, 60(540), pp. 13-141.

Dyer, S. R., Lassila, L. V., Jokinen, M. and Vallittu, P. K. (2004) 'Effect of fiber position and orientation on fracture load of fiber-reinforced composite', Dent Mater, 20(10), pp. 947-55.

Eapen, A. M., Amirtharaj, L. V., Sanjeev, K. and Mahalaxmi, S. (2017) 'Fracture Resistance of Endodontically Treated Teeth Restored with 2 Different Fiber-reinforced Composite and 2 Conventional Composite Resin Core Buildup Materials: An In Vitro Study', J Endod, 43(9), pp.1499-1504.

Elbishari, H., Satterthwaite, J. and Silikas, N. (2011) 'Effect of filler size and temperature on packing stress and viscosity of resin-composites', Int J Mol Sci, 12(8), pp. 5330-5338.

Elbishari, H., Silikas, N. and Satterthwaite, J. (2012) 'Filler size of resin-composites, percentage of voids and fracture toughness: is there a correlation?', Dent Mater J, 31(4), pp. 523-527.

Ellakwa, A. E., Shortall, A. C. and Marquis, P. M. (2002) 'Influence of fiber type and wetting agent on the flexural properties of an indirect fiber reinforced composite', J Prosthet Dent, 88(5), pp. 485-490.

Ellner, S., Bergendal, T. and Bergman, B. (2002) 'Four post-and-core combinations as abutments for fixed single crowns: a prospective up to 10-year study', Int J prosthod, 16(3), pp. 249-254.

Eskitascıoglu, G., Belli, S. and Kalkan, M. (2002) 'a', J Endod, 28(9), pp. 629-633.

Evans, S. (2006) 'Effects of porosity on the fatigue performance of polymethyl methacrylate bone cement: an analytical investigation', Proceedings of the Institution of Mechanical Engineers, Part H: J Eng Med, 220(1), pp. 1-10.

Fano, V., Ortalli, I. and Pozela, K. (1995) 'Porosity in composite resins', Biomaterials, 16(17), pp. 1291-1295.

Feilzer, A., De Gee, A. and Davidson, C. (1993) 'Setting stresses in composites for two different curing modes', Dent Mater, 9(1), pp. 2-5.

Fennis, W., Tezvergil, A., Kuijs, R. H., Lassila, L. V. J., Kreulen, C. M., Creugers, N. H. J. and Vallittu, P. K. (2005) 'In vitro fracture resistance of fiber reinforced cusp-replacing composite restorations', Dent Mater, 21(6), pp. 565-572.

Fernandes, A. S., Shetty, S. and Coutinho, I. (2003) 'Factors determining post selection: a literature review', J Prosthet Dent, 90(6), pp. 556-62.

Ferracane, J. and Greener, E. (1986) 'The effect of resin formulation on the degree of conversion and mechanical properties of dental restorative resins', J Biomed Mater Res, 20(1), pp. 121-131.

Ferracane, J. and Condon, J. R. (1992) 'Post-cure heat treatments for composites: properties and fractography', Dent Mater, 8(5), pp. 290-295.

Ferracane, J. (2005) 'Developing a more complete understanding of stresses produced in dental composites during polymerization', Dent Mater, 21(1), pp. 36-42.

Ferracane, J. (2011) 'Resin composite—state of the art', Dent Mater, 27(1), pp. 29-38.

Ferracane, J. (2013) 'Resin-based composite performance: are there some things we can't predict?', Dent Mater, 29(1), pp. 51-58.

Ferrari, M., Mason, P., Goracci, C., Pashley, D. H. and Tay, F. (2004) 'Collagen degradation in endodontically treated teeth after clinical function', J Dent Res, 83(5), pp. 414-419.

Fokkinga, W. A., Kreulen, C. M., Vallittu, P. K. and Creugers, N. H. (2004) 'A structured analysis of in vitro failure loads and failure modes of fiber, metal, and ceramic post-and-core systems', Int J Prosthodont, 17(4), pp. 476-82.

Fokkinga, W. A., Kreulen, C. M., Le Bell-Ronnlof, A. M., Lassila, L. V., Vallittu, P. K. and Creugers, N. H. (2006a) 'In vitro fracture behavior of maxillary premolars with metal crowns and several post-and-core systems', Eur J Oral Sci, 114(3), pp. 250-6.

Fokkinga, W. A., Kreulen, C. M., Le Bell., A. M., Lassila, L. V., Vallittu, P. K. and Creugers, N. H. (2006b) 'Fracture behavior of structurally compromised non-vital maxillary premolars restored using experimental fiber reinforced composite crowns', Am J Dent, 19(6), pp. 326-332.

Fonseca, R., Marques, A., Bernades, K., Carlo, H. and Naves, L. (2014) 'Effect of glass fiber incorporation on flexural properties of experimental composites', BioMed Res Int, 2014.

Fonseca, R., de Almeida, L., Mendes, G., Kasuya, A., Favarao, I. and de Paula, M. (2016) 'Effect of short glass fiber/filler particle proportion on flexural and diametral tensile strength of a novel fiber-reinforced composite', J prosthod Res, 60(1), pp. 47-53.

Forster, A., Sary, T., Braunitzer, G. and Fráter, M. (2017) 'In vitro fracture resistance of endodontically treated premolar teeth restored with a direct layered fiber-reinforced composite post and core', J Adhes Sci Technol, 31(13), pp. 1454-1466.

Fox, K. and Gutteridge, D. L. (1997) 'An in vitro study of coronal microleakage in root-canal-treated teeth restored by the post and core technique', Int Endod J, 30(6), pp. 361-368.

Frater, M., Forster, A., Kereszturi, M., Braunitzer, G. and Nagy, K. (2014) 'In vitro fracture resistance of molar teeth restored with a short fibre-reinforced composite material', J Dent, 42(9), pp. 1143-1150.

Fredriksson, M., Astbäck, J., Pamenius, M. and Arvidson, K. (1998) 'A retrospective study of 236 patients with teeth restored by carbon fiber-reinforced epoxy resin posts', J Prosthet Dent, 80(2), pp. 151-157.

Freedman, G. and Jain, C. (2008) 'Restoration of the endodontically treated tooth–a buyer's guide to pins and posts', Dent Today, 7, pp. 106-8.

Freilich, M. A., Duncan, J. P., Meiers, J. C. and Goldberg, A. J. (1998) 'Preimpregnated, fiber-reinforced prostheses. Part I. Basic rationale and complete-coverage and intracoronal fixed partial denture designs', Quintessence Int, 29(11), pp. 689-696.

Freiman, S., Mulville, D. and Mast, P. W. (1973) 'Crack propagation studies in brittle materials', J Mat Sci, 8(11), pp. 1527-1533.

Friedrich, K. and Karger-Kocsis, J. (1989) 'Fractography and failure mechanisms of unfilled and short fibre reinforced semicrystalline thermoplastics. ', in Roulin-Moloney, A. (1st ed.) Fractography and Failure Mechanisms of Polymers and Composites. Amsterdam. Elsevier, pp. 437-494.

Frykholm, K. O., Frithiof, L., Fernström, A. I., Moberger, G., Blohm, S. G. and Björn, E. (1968) 'Allergy to copper derived from dental alloys as a possible cause of oral lesions of lichen planus', Acta Derm venereol, 49(3), pp. 268-281.

Fusayama, T. and Maeda, T. (1969) 'Effect of pulpectomy on dentin hardness', J Dent Res, 48(3), pp. 452-460.

Gaintantzopoulou, M., Farmakis, E. and Eliades, G. (2018) 'Effect of Load Cycling on the Fracture Strength/Mode of Teeth Restored with FRC Posts or a FRC Liner and a Resin Composite', BioMed Res Int, 2018.

Galhano, G. A., Valandro, L. F., De Melo, R. M., Scotti, R. and Bottino, M. A. (2005) 'Evaluation of the flexural strength of carbon fiber-, quartz fiber-, and glass fiber-based posts', J Endod, 31(3), pp. 209-211.

Galhano, G. A., De Melo, R. M., Barbosa, S. H., Zamboni, S. C., Bottino, M. A. and Scotti, R. (2008) 'Evaluation of light transmission through translucent and opaque posts', Oper Dent, 33(3), pp. 321-324.

Garlapati, T. G., Krithikadatta, J. and Natanasabapathy, V. (2017) 'Fracture resistance of endodontically treated teeth restored with short fiber composite used as a core material-An in vitro study', J Prosthodont Res, 61(4), pp. 464-470.

Garoushi, S., Lassila, L. V. and Vallittu, P. K. (2006) 'Short fiber reinforced composite: the effect of fiber length and volume fraction', J Contemp Dent Pract, 7(5), pp. 10-17.

Garoushi, S., Lassila, L. V. and Vallittu, P. K. (2007a) 'Direct composite resin restoration of an anterior tooth: effect of fiber-reinforced composite substructure', Eur J Prosthodont Restor Dent, 15(2), pp. 61-66.

Garoushi, S., Vallittu, P. K. and Lassila, L. V. (2007c) 'Fracture resistance of short, randomly oriented, glass fiber-reinforced composite premolar crowns', Acta Biomater, 3(5), pp. 779-784.

Garoushi, S., Vallittu, P. K. and Lassila, L. V. (2007d) 'Use of short fiber-reinforced composite with semi-interpenetrating polymer network matrix in fixed partial dentures', J Dent, 35(5), pp. 403-408.

Garoushi, S., Vallittu, P. K. and Lassila, L. V. (2007e) 'Short glass fiber reinforced restorative composite resin with semi-inter penetrating polymer network matrix', Dent Mater, 23(11), pp. 1356-1362.

Garoushi, S., Vallittu, P. K. and Lassila, L. V. (2007b) 'Direct restoration of severely damaged incisors using short fiber-reinforced composite resin', J Dent, 35(9), pp. 731-736.

Garoushi, S., Vallittu, P. K. and Lassila, L. V. (2008a) 'Depth of cure and surface microhardness of experimental short fiber-reinforced composite', Acta Odontol Scand, 66(1), pp. 38-42.

Garoushi, S., Vallittu, P. K., Watts, D. C. and Lassila, L. V. (2008b) 'Polymerization shrinkage of experimental short glass fiber-reinforced composite with semi-inter penetrating polymer network matrix', Dent Mater, 24(2), pp. 211-215.

Garoushi, S., Vallittu, P. K. and Lassila, L. V. (2009) 'Continuous and short fiber reinforced composite in root post-core system of severely damaged incisors', Open Dent J, 3, pp. 36-41.

Garoushi, S., Vallittu, P. K. and Lassila, L. V. (2011) 'Fracture toughness, compressive strength and load-bearing capacity of short glass fibre-reinforced composite resin', Chin J Dent Res, 14(1), pp. 15-19.

Garoushi, S., Tanner, J., Vallittu, P. K. and Lassila, L. V. J. (2012) 'Preliminary clinical evaluation of short fiber-reinforced composite resin in posterior teeth: 12-months report', Open Dent J, 6, pp. 41–45.

Garoushi, S., Mangoush, E., Vallittu, M. and Lassila, L. (2013a) 'Short fiber reinforced composite: a new alternative for direct onlay restorations', Open Dent J, 7, pp. 181-185.

Garoushi, S., Sailynoja, E., Vallittu, P. K. and Lassila, L. (2013b) 'Physical properties and depth of cure of a new short fiber reinforced composite', Dent Mater, 29(8), pp. 835-841.

Gbadebo, O. S., Ajayi, D. M., Oyekunle, O. O. and Shaba, P. O. (2014) 'Randomized clinical study comparing metallic and glass fiber post in restoration of endodontically treated teeth', Indian J Dent Res, 25(1), pp. 58-63.

Garoushi, S., Hatem, M., Lassila, L. V. J. and Vallittu, P. K. (2015a) 'The effect of short fiber composite base on microleakage and load-bearing capacity of posterior restorations', Acta Biomater Odontol Scand, 1(1), pp. 6-12.

Garoushi, S., Vallittu, P. K., Shinya, A. and Lassila, L. (2015b) 'Influence of increment thickness on light transmission, degree of conversion and micro hardness of bulk fill composites', Odontology, pp. 1-7.

Garoushi, S., Sailynoja, E., Vallittu, P. K. and Lassila, L. (2016) 'Corrigendum to 'Physical properties and depth of cure of a new short fiber reinforced composite' [Dent Mater 29 (8) (2013) 835-841]', Dent Mater, 32(9), pp. 1196.

Garoushi, S., Vallittu, P. K. and Lassila, L. (2017) 'Mechanical Properties and Wear of Five Commercial Fibre-Reinforced Filling Materials', Chin J Dent Res, 20(3), pp. 137-143.

Garoushi, S., Gargoum, A., Vallittu, P. K. and Lassila, L. (2018) 'Short fiber-reinforced composite restorations: A review of the current literature', J Investig Clin Dent, 9(3), pp. 1-9.

Garoushi, S., Vallittu, P. K. and Lassila, L. (2019) 'Mechanical properties and radiopacity of flowable fiber-reinforced composite', Dent Mater J,83(2) pp. 169-202.

Ghavamnasiri, M., Maleknejad, F., Ameri, H., Moghaddas, M. J., Farzaneh, F. and Chasteen, J. E. (2011) 'A retrospective clinical evaluation of success rate in endodontic-treated premolars restored with composite resin and fiber reinforced composite posts', J Conserv Dent, 14(4), pp. 378.

Ghiorse, S. (1993) 'Effect of void content on the mechanical properties of carbon/epoxy laminates', SAMPE quarterly, 24, pp. 54-59.

Giovani, A. R., Vansan, L. P., de Sousa Neto, M. D. and Paulino, S. M. (2009) 'In vitro fracture resistance of glass-fiber and cast metal posts with different lengths', J Prosthet Dent, 101(3), pp. 183-8.

Goldberg, A. and Burstone, C. (1992) 'The use of continuous fiber reinforcement in dentistry', J Prosthet Dent, 8, pp. 197-202.

Goracci, C. and Ferrari, M. (2011) 'Current perspectives on post systems: a literature review', Aust Dent J, 56 Suppl 1, pp. 77-83.

Goracci, C., Cadenaro, M., Fontanive, L., Giangrosso, G., Juloski, J., Vichi, A. and Ferrari, M. (2014) 'Polymerization efficiency and flexural strength of low-stress restorative composites', Dent Mater, 60(3), pp. 688-694.

Grandini, S., Goracci, C., Monticelli, F., Borracchini, A. and Ferrari, M. (2005a) 'SEM evaluation of the cement layer thickness after luting two different posts', J Adhes Dent, 7(3), pp. 235-240.

Grandini, S., Goracci, C., Monticelli, F., Tay, F. R. and Ferrari, M. (2005b) 'Fatigue resistance and structural characteristics of fiber posts: three-point bending test and SEM evaluation', Dent Mater, 21(2), pp. 75-82.

Greenhalgh, E. (2009) Failure analysis and fractography of polymer composites. Elsevier.

Gulabivala, k. and Ng, Y. L. (2004) Endodontics. Elsevier.

Guo, Z., Liu, L., Zhang, B. and Du, S. (2009) 'Critical void content for thermoset composite laminates', J Compos Mater, 43(17), pp. 1775-1790.

Gurdal, Z., Tomasino, A. and Biggers, S. (1991) 'Effects of processing induced defects on laminate response-Interlaminar tensile strength', SAMPE quarterly, 27, pp. 39-49.

Gurel, M. A., Helvacioglu Kivanc, B., Ekici, A. and Alacam, T. (2016) 'Fracture Resistance of Premolars Restored Either with Short Fiber or Polyethylene Woven Fiber-Reinforced Composite', J Esthet Restor Dent, 28(6), pp.412-418.

Gutteridge, D. L. (1992) 'Reinforcement of poly (methyl methacrylate) with ultra-high-modulus polyethylene fibre', J Dent, 20(1), pp. 50-54.

Guzy, G. E. and Nicholls, J. I. (1979) 'In vitro comparison of intact endodontically treated teeth with and without endo-post reinforcement', J Prosthet Dent 42, pp. 39-44.

Habibzadeh, S., Rajati, H. R., Hajmiragha, H., Esmailzadeh, S. and Kharazifard, M. (2017) 'Fracture resistances of zirconia, cast Ni-Cr, and fiber-glass composite posts under all-ceramic crowns in endodontically treated premolars', J Adv Prosthodont, 9(3), pp. 170-175.

Hanson, E. C. and Caputo, A. A. (1974) 'Cementing mediums and retentive characteristics of dowels', J Prosthet Dent, 32(5), pp. 551-557.

Hayashi, M., Takahashi, Y., Imazato, S. and Ebisu, S. (2006) 'Fracture resistance of pulpless teeth restored with post-cores and crowns', Dent Mater, 22(5), pp. 477-485.

Hayashi, T. and Takahashi, J. (2017) 'Influence of void content on the flexural fracture behaviour of carbon fiber reinforced polypropylene', J Compos Mater, 51(29), pp. 4067-4078.

Hayes, M., Edwards, D. and Shah, A. (2015) Fractography in Failure Analysis of Polymers. Elsevier.

Heintze, S. D. and Rousson, V. (2012) 'Clinical effectiveness of direct class II restorations-a meta-analysis', J Adhes Dent, 14(5), pp. 407-431.

Heintze, S. D., Ilie, N., Hickel, R., Reis, A., Loguercio, A. D. and Rousson, V. (2017) 'Laboratory mechanical parameters of composite resins and their relation to fractures and wear in clinical trials—A systematic review', Dent Mater, 33(3), pp. e101-e114.

Helfer, A. R., Melnick, S. and Schilder, H. (1972) 'Determination of the moisture content of vital and pulpless teeth', Oral Surg, Oral Med, Oral Pathol, 34(4), pp. 661-670.

Helkimo, E., Carlsson, G. and Helkimo, M. (1977) 'Bite force and state of dentition', Acta Odontol Scand, 35(6), pp. 297-303.

Hiley, M. (1999) 'Fractographic study of static and fatigue failures in polymer composites', Plastics, Rubber and Composites, 28(5), pp. 210-227.

Hoeppner, M., Fonseca, R., Pfau, E., Justo, F. M., Favero, A. and Bremm, L. (2011) 'Rehabilitation of periodontally compromised teeth with fiber-reinforced composite resin: a case report', Quintessence Int, 42(2), pp.113-120.

Holmes, D., Diaz-Arnold, A. and Larry, J. I. (1996) 'Influence of post dimension on stress distribution in dentine', J Prosthet Dent, 75(2), pp. 140-7.

Hu, Y. H., Pang, L. C., Hsu, C. C. and Lau, Y. H. (2003) 'Fracture resistance of endodontically treated anterior teeth restored with four post-and-core systems', Quintessence Int, 34(5), pp. 349-53.

Hull, D. and Clyne, T. (1996) An introduction to composite materials. Cambridge university press.

Hunter, A., Feiglin, B. and Williams, J. (1989) 'Effects of post placement on endodontically treated teeth', J Prosthet Dent, 62(2), pp. 166-172.

Huysmans, M., van der Varst, P., Lautenschalger, E. P. and Monaghan, P. (1996) 'The influence of simulated clinical handling on the flexural and compressive strength of posterior composite restorative materials', Dent Mater, 12(2), pp. 116-120.

Ilie, N. and Hickel, R. (2009) 'Investigations on mechanical behaviour of dental composites', Clin Oral Investig, 13(4), pp. 427-38.

Ironside, J. and Makinson, O. (1993) 'Resin restorations: Causes of porosities', Quintessence Int, 24(12), pp.867-873.

Isidor, F. and Brondum, K. (1992) 'Intermittent loading of teeth with tapered, individually cast or prefabricated, parallel-sided posts', Int J Prosthodont, 5(3), pp.257-261.

Isidor, F., Odman, P. and Brondum, K. (1995) 'Intermittent loading of teeth restored using prefabricated carbon fiber posts', Int J prosthodont, 9(2), pp. 131-136.

Isidor, F., Brondum, K. and Ravnholt, G. (1999) 'The influence of post length and crown ferrule length on the resistance to cyclic loading of bovine teeth with prefabricated titanium posts', Int J prosthodont, 12(1),pp.78-82.

ISO, S. (2003) '11405 Dental materials—Guidance on testing of adhesion to tooth structure'.

Iwamoto, N. and Ruse, N. (2003) 'Fracture toughness of human dentin', J Biomed Mater Res A, 66(3), pp. 507-512.

Jain, L. K. and Wetherhold, R. C. (1992) 'Effect of fiber orientation on the fracture toughness of brittle matrix composites', Acta Mater, 40(6), pp. 1135-1143.

Jameson, M. W., Hood, J. A. A. and Tidmarsh, B. G. (1993) 'The effects of dehydration and rehydration on some mechanical properties of human dentine', J Biomech, 26(9), pp. 1055-1065.

Jokstad, A. and Mjor, I. (1996) 'Ten years' clinical evaluation of three luting cements', J Dent, 24(5), pp. 309-315.

Jollivet, T. and Greenhalgh, E. (2015) 'Fractography, a powerful tool for identifying and understanding fatigue in composite materials', Procedia Eng, 133, pp. 171-178.

Jordan, R. and Suzuki, M. (1992) 'The ideal composite material', J Can Dent Assoc, 58(6), pp. 484, 487.

Kakaboura, A., Rahiotis, C., Watts, D., Silikas, N. and Eliades, G. (2007) '3D-marginal adaptation versus setting shrinkage in light-cured microhybrid resin composites', Dent Mater, 23(3), pp. 272-278.

Kaleem, M., Satterthwaite, J. and Watts, D. (2009) 'Effect of filler particle size and morphology on force/work parameters for stickiness of unset resin-composites', Dent Mater, 25(12), pp. 1585-1592.

Kallio, T., Lastumäki, T. and Vallittu, P. (2001) 'Bonding of restorative and veneering composite resin to somepolymeric composites', Dent Mater, 17(1), pp. 80-86.

Kallio, T., Lastumaki, T., Lassila, L. and Vallittu, P. (2014) 'Influence of intermediate resin on the bond strength of light-curing composite resin to polymer substrate', Acta Odontol Scand, 72(3), pp. 202-208.

Kantor, M. E. and Pines, M. S. (1977) 'A comparative study of restorative techniques for pulpless teeth', J Prosthet Dent, 38(4), pp. 405-412.

Karacaer, O., Polat, T., Tezvergıl, A., Lassıla, L. and Vallıttu, P. (2003) 'The effect of length and concentration of glass fibers on the mechanical properties of an injection-and a compression-molded denture base polymer', J Prosthet Dent, 90(4), pp. 385-393.

Kardos, J. L. (1985) 'Critical issues in achieving desirable mechanical properties for short fiber composites', Pure and applied chemistry, 57(11), pp. 1651-1657.

Kelly, J. R., Campbell, S. D. and Bowen, H. K. (1989) 'Fracture-surface analysis of dental ceramics', J Prosthet Dent, 62(5), pp. 536-541.

Kelly, A. (2000) Test Methods, Nondestructive Evaluation and Smart Materials. Elsevier.

Kemaloglu, H., Emin Kaval, M., Turkun, M. and Micoogullari Kurt, S. (2015) 'Effect of novel restoration techniques on the fracture resistance of teeth treated endodontically: An in vitro study', Dent Mater J, 34(5), pp. 618-622.

Keulemans, F., Garoushi, S. and Lassila, L. (2017) 'Fillings and core build-ups', A Clinical Guide to Fibre Reinforced Composites (FRCs) in Dentistry: Elsevier, pp. 131-163.

Khan, A. S., Azam, M. T., Khan, M., Mian, S. A. and Rehman, I. U. (2015) 'An update on glass fiber dental restorative composites: A systematic review', Mater Sci Eng C Mater Biol Appl , 47, pp. 26-39.

Khera, S. C., Carpenter, C. W., Vetter, J. D. and Staley, R. N. (1990) 'Anatomy of cusps of posterior teeth and their fracture potential', J Prosthet Dent, 64(2), pp. 139-47.

Kim, K. H. and Okuno, O. (2002) 'Microfracture behaviour of composite resins containing irregular-shaped fillers', J Oral Rehabil, 29(12), pp. 1153-1159.

Kim, S. H. and Watts, D. C. (2004) 'Effect of glass-fiber reinforcement and water storage on fracture toughness (KIC) of polymer-based provisional crown and FPD materials', Int J Prosthodont, 17, pp. 318–22.

Kim, Paik, K. and Lee, S. (2007) 'Quantitative evaluation of the accuracy of micro-computed tomography in tooth measurement', Clin Anat, 20(1), pp. 27-34.

Kinney, J., Marshall, S. and Marshall, G. (2003) 'The mechanical properties of human dentin: a critical review and re-evaluation of the dental literature', Crit Rev Oral Biol Med, 14(1), pp. 13-29.

Kishen, A. and Asundi, A. (2005) 'Experimental investigation on the role of water in the mechanical behavior of structural dentine', J Biomed Mater Res A, 73(2), pp. 192-200.

Kohler, B., Rasmusson, C. and Odman, P. (2000) 'A five-year clinical evaluation of Class II composite resin restorations', J Dent, 28(2), pp. 111-116.

Krejci, I., Reich, T., Lutz, F. and Albertoni, M. (1990) 'An in vitro test procedure for evaluating dental restoration systems. 1. A computer-controlled mastication simulator', Schweiz Monatsschr Zahnmed,100(8), pp. 953-960. (Translated article obtained from Researchgate.net)

Krenchel, H. (1964) Fibre reinforcement: theoretical and practical investigations of the elasticity and strength of fibre-reinforced materials. Copenhagen : Akademisk Forlag.

Kuijs, R., Fennis, W., Kreulen, C., Barink, M. and Verdonschot, N. (2003) 'Does layering minimize shrinkage stresses in composite restorations?', J Dent Res, 82(12), pp. 967-971.

Kwon, Y., Ferracane, J. and Lee, I. B. (2012) 'Effect of layering methods, composite type, and flowable liner on the polymerization shrinkage stress of light cured composites', Dent Mater, 28(7), pp. 801-809.

Lagouvardos, P., Nikolinakos, N. and Oulis, C. (2015) 'Volume fraction and location of voids and gaps in ultraconservative restorations by X-ray computed micro-tomography', Dent Res J, 12(6), pp. 520-527.

Lambjerg-Hansen, H. and Asmussen, E. (1997) 'Mechanical properties of endodontic posts', J Oral Rehabil, 24(12), pp. 882-887.

Lamichhane, A., Xu, C. and Zhang, F. q. (2014) 'Dental fiber-post resin base material: a review', J Adv Prosthodont, 6(1), pp. 60-65.

Lang, R., Manson, J. and Hertzberg, R. (1987) 'Mechanisms of fatigue fracture in short glass fibre-reinforced polymers', J Mat Sci, 22(11), pp. 4015-4030.

Lange, F. (2016) 'Fracture of brittle matrix, particulate composites', in Broutman, L., Krock, R. 'Composite Material'. Elsevier.

Larson, T., Douglas, W. and Geistfeld, R. (1981) 'Effect of prepared cavities on the strength of teeth', Oper Dent, 6(1), pp. 2-8.

Lassila, L. V., Tanner, J., Le Bell, A. M., Narva, K. and Vallittu, P. K. (2004) 'Flexural properties of fiber reinforced root canal posts', Dent Mater, 20(1), pp. 29-36.

Lassila, L. V. and Vallittu, P. K. (2004) 'The effect of fiber position and polymerization condition on the flexural properties of fiber-reinforced composite', J Contemp Dent Pract, 5(2), pp. 14-26.

Lassila, L. V., Tezvergil, A., Lahdenpera, M., Alander, P., Shinya, A., Shinya, A. and Vallittu, P. K. (2005) 'Evaluation of some properties of two fiber-reinforced composite materials', Acta Odontol Scand, 63(4), pp. 196-204.

Lassila, L. V. J., Garoushi, S., Tanner, J., Vallittu, P. K. and Soderling, E. (2009) 'Adherence of Streptococcus mutans to fiber-reinforced filling composite and conventional restorative materials', Open Dent J, 3, pp. 227.

Lassila, L., Garoushi, S., Vallittu, P. K. and Sailynoja, E. (2016) 'Mechanical properties of fiber reinforced restorative composite with two distinguished fiber length distribution', J Mech Behav Biomed Mater, 60, pp. 331-338.

Lassila, L., Keulemans, F., Sailynoja, E., Vallittu, P. K. and Garoushi, S. (2018) 'Mechanical properties and fracture behavior of flowable fiber reinforced composite restorations', Dent Mater, 34(4), pp. 589-606.

Lastumaki, T., Kallio, T. and Vallittu, P. (2002) 'The bond strength of light-curing composite resin to finally polymerized and aged glass fiber-reinforced composite substrate', Biomaterials, 23(23), pp. 4533-4539.

Lastumaki, T. M., Lassila, L. V. J. and Vallittu, P. K. (2003) 'The semi-interpenetrating polymer network matrix of fiber-reinforced composite and its effect on the surface adhesive properties', J Mater Sci Mater Med, 14(9), pp. 803-809.

Lazari, P., Olivera, R., Anchieta, R., De Almeida, E., Freitas Junior, A., Kina, S. and Rocha, E. P. (2013) 'Stress distribution on dentin-cement-post interface varying root canal and glass fiber post diameters. A three-dimensional finite element analysis based on micro-CT data', J Appl Oral Sci, 21(6), pp. 511-517.

Le Bell-Ronnlof, A. M., Tanner, J., Lassila, L. V., Kangasniemi, I. and Vallittu, P. K. (2003) 'Depth of light-initiated polymerization of glass fiber-reinforced composite in a simulated root canal', Int J Prosthodont, 16(4), pp. 403-408.

Le Bell-Ronnlof, A. M., Tanner, J., Lassila, L. V., Kangasniemi, I. and Vallittu, P. K(2004) 'Bonding of composite resin luting cement to fiber-reinforced composite root canal posts', J Adhes Dent, 6(4), pp. 319-325.

Le Bell-Ronnlof, A. M., Lassila, L. V., Kangasniemi, I. and Vallittu, P. K. (2005) 'Bonding of fibre-reinforced composite post to root canal dentin', J Dent, 33(7), pp. 533-539.

Le Bell-Ronnlof, A., Lahdenpera, M., Lassila, L. and Vallittu, P. (2007) 'Bond Strength of Composite Resin Luting Cements to Fiber-reinforced Composite Root Canal Post ', J Contemp Dent Pract, 8(6), pp. 17-24.

Le Bell-Ronnlof, A. M., Lassila, L. V. J., Kangasniemi, I. and Vallittu, P. K. (2011) 'Load-bearing capacity of human incisor restored with various fiber-reinforced composite posts', Dent Mater, 27(6), pp. e107-e115.

Lee, S. (1992) Handbook of composite reinforcements. John Wiley & Sons.

Lee, J., Um, C. and Lee, I. (2006) 'Rheological properties of resin composites according to variations in monomer and filler composition', Dent Mater, 22(6), pp. 515-526.

Leprince, J. G., Palin, W. M., Vanacker, J., Sabbagh, J., Devaux, J. and Leloup, G. (2014) 'Physico-mechanical characteristics of commercially available bulk-fill composites', J Dent, 42(8), pp. 993-1000.

Lewinstein, I. and Grajower, R. (1981) 'Root dentin hardness of endodontically treated teeth', J Endod, 7(9), pp. 421-422.

Li, C., Wang, Y. and Backer, S. (1991) 'A micromechanical model of tension-softening and bridging toughening of short random fiber reinforced brittle matrix composites', J Mech Phys Solids, 39(5), pp. 607-625.

Li, X., Pongprueksa, P., Van Meerbeek, B. and De Munck, J. (2015) 'Curing profile of bulk-fill resin-based composites', J Dent, 43(6), pp. 664-672.

Libman, W. and Nicholls, J. (1995) 'Load fatigue of teeth restored with cast posts and cores and complete crown', Int J Prosthodont, 8(2), pp. 155-161.

Ling, R. S. M. and Lee, A. J. C. (1998) 'Porosity reduction in acrylic cement is clinically irrelevant', Clin Orthop Relat Res, 355, pp. 249-253.

Little, J. E., Yuan, X. and Jones, M. I. (2012) 'Characterisation of voids in fibre reinforced composite materials', NDT & E International, 46, pp. 122-127.

Liu, L., Zhang, B., Wang, D. and Wu, Z. (2006) 'Effects of cure cycles on void content and mechanical properties of composite laminates', Compos Struct, 73(3), pp. 303-309.

Lloyd, P. M. and Palik, J. F. (1993) 'The philosophies of dowel diameter preparation: a literature review', J Prosthet Dent, 69(1), pp. 32-36.

Lohbauer, U., von der Horst, T., Frankenberger, R., Kramer, N. and Petschelt, A. (2003) 'Flexural fatigue behavior of resin composite dental restoratives', Dent Mater, 19(5), pp. 435-440.

Loney, R. W., Moulding, M. B. and Ritsco, R. G. (1995) 'The effect of load angulation on fracture resistance of teeth restored with cast post and cores and crowns', Int J Prosthodont, 8(3), pp. 247-251.

Lovdahl, P. E. and Nicholls, J. I. (1977) 'Pin-retained amalgam cores vs. cast-gold dowel-cores', J Prosthet Dent, 38(5), pp. 507-514.

Love, R. and Purton, D. (1996) 'The effect of serrations on carbon fibre posts-retention within the root canal, core retention, and post rigidity', Int J Prosthodont, 9(5), pp. 484-488.

Love, R. and Purton, D. (1998) ' Retention of posts with resin glass ionomer and hybrid cements', J Dent, 26, pp. 599-602.

Maccari, P. C., Cosme, D. C., Oshima, H. M., Burnett, L. H., Jr. and Shinkai, R. S. (2007) 'Fracture strength of endodontically treated teeth with flared root canals and restored with different post systems', J Esthet Restor Dent, 19(1), pp. 30-36.

Magne, P. and Douglas, W. H. (1999) 'Rationalization of esthetic restorative dentistry based on biomimetics', J Esthet Restor Dent, 11(1), pp. 5-15.

Magne, P. (2007) 'Efficient 3D finite element analysis of dental restorative procedures using micro-CT data', Dent Mater, 23(5), pp. 539-548.

Mallick, P. K. (2007) 'Fiber-reinforced composites: materials, manufacturing, and design'. CRC press.

Mangold, J. T. and Kern, M. (2011) 'Influence of glass-fiber posts on the fracture resistance and failure pattern of endodontically treated premolars with varying substance loss: an in vitro study', J Prosthet Dent, 105(6), pp. 387-93.

Manhart, J., Kunzelmann, K.-H., Chen, H. and Hickel, R. (2000) 'Mechanical properties and wear behavior of light-cured packable composite resins', Dent Mater, 16(1), pp. 33-40.

Mannocci, F., Sherriff, M., Watson, T. F. and Vallittu, P. K. (2005) 'Penetration of bonding resins into fibre-reinforced composite posts: a confocal microscopic study', Int Endod J, 38(1), pp. 46-51.

Mannocci, F., Machmouridou, E., Watson, T. F., Sauro, S., Sherriff, M., Pilecki, P. and Pitt-Ford, T. R. (2008) 'Microtensile bond strength of resin-post interfaces created with interpenetrating polymer network posts or cross-linked posts', Med Oral Patol Oral Cir Bucal, 13(11), pp. 745-752.

Mattison, G. D., Delivanis, P. D., Thacker Jr, R. W. and Hassell, K. J. (1984) 'Effect of post preparation on the apical seal', J Prosthet Dent, 51(6), pp. 785-789.

McCabe, J. and Ogden, A. (1987) 'The relationship between porosity, compressive fatigue limit and wear in composite resin restorative materials', Dent Mater, 3(1), pp. 9-12.

McLaren, J. D., McLaren, C. I., Yaman, P., Bin-Shuwaish, M. S., Dennison, J. D. and McDonald, N. J. (2009) 'The effect of post type and length on the fracture resistance of endodontically treated teeth', J Prosthet Dent, 101(3), pp. 174-182.

McMillan, A. (2012) 'Material strength knock-down resulting from multiple randomly positioned voids', Journal of Reinforced Plastics and Composites, 31(1), pp. 13-28.

Mecholsky, J. (1995) 'Fractography: determining the sites of fracture initiation', Dent Mater, 11(2), pp. 113-116.

Mehdikhani, M., Gorbatikh, L., Verpoest, I. and Lomov, S. V. (2018) 'Voids in fiber-reinforced polymer composites: a review on their formation, characteristics, and effects on mechanical performance', J Compos Mater, 53(12), pp. 1579-1669.

Meiers, J. C., Duncan, J. P., Freilich, M. A. and Goldberg, A. J. (1998) 'Preimpregnated, fiber-reinforced prostheses. Part II. Direct applications: splints and fixed partial dentures', Quintessence Int, 29(12), pp. 761-768.

Meiers, J. C. and Freilich, M. A. (2000) 'Conservative anterior tooth replacement using fiber-reinforced composite', Oper Dent, 25(3), pp. 239-243.

Meiers, J. C. and Freilich, M. A. (2006) 'Use of a prefabricated fiber-reinforced composite resin framework to provide a provisional fixed partial denture over an integrating implant: a clinical report', J Prosthet Dent, 95(1), pp. 14-18.

Meira, J., Esposito, C., Quitero, M., Poiate, I., Pfeifer, C. C., Tanaka, C. and Ballester, R. (2009) 'Elastic modulus of posts and the risk of root fracture', Dent Traumatol, 25(4), pp. 394-398.

Mendoza , D. B., Eakle, W. S., Kahl, E. A. and Ho, R. (1997) 'Root reinforcement with a resin-bonded preformed post', J Prosthet Dent, 78(1), pp. 10-14.

Mentink, A. G., Meeuwissen, R., Kayser, A. F. and Mulder, J. (1993) 'Survival rate and failure characteristics of the all metal post and core restoration', J Oral Rehabil, 20(5), pp. 455-461.

Mezzomo, E., Massa, F. and Libera, S. (2003) 'Fracture resistance of teeth restored with two different post-and-core designs cemented with two different cements: an in vitro study. Part I', Quintessence Int, 34(4), pp. 301-306.

Miettinen, V., Narva, K. K. and Vallittu, P. K.(1999) 'Water sorption, solubility and effect of post-curing of glass fibre reinforced polymers', Biomaterials, 20(13), pp. 1187-1194.

Miettinen, V. and Vallittu, P. K(1997) 'Water sorption and solubility of glass fiber-reinforced denture polymethyl methacrylate resin', J Prosthet Dent, 77(5), pp. 531-534.

Miletic, V., Peric, D., Milosevic, M., Manojlovic, D. and Mitrovic, N. (2016) 'Local deformation fields and marginal integrity of sculptable bulk-fill, low-shrinkage and conventional composites', Dent Mater, 32(11), pp. 1441-1451.

Miletic, V., Pongprueksa, P., De Munck, J., Brooks, N. R. and Van Meerbeek, B. (2017) 'Curing characteristics of flowable and sculptable bulk-fill composites', Clin Oral Investig, 21(4), pp. 1201-1212.

Milnar, F. J. (2010) 'Aesthetic treatment of dark root syndrome', Dent Today, 29(9), pp. 74-76.

Milutinovic-Nikolic, A., Medic, V. and Vukovic, Z. (2007) 'Porosity of different dental luting cements', Dent Mater, 23(6), pp. 674-678.

Mohammadi, N., Kahnamoii, M., Yeganeh, P. K. and Navimipour, E. J. (2009) 'Effect of fiber post and cusp coverage on fracture resistance of endodontically treated maxillary premolars directly restored with composite resin', J Endod, 35(10), pp. 1428-1432.

Monticelli, F., Goracci, C. and Ferrari, M. (2004) 'Micromorphology of the fiber post–resin core unit: a scanning electron microscopy evaluation', Dent Mater, 20(2), pp. 176-183.

Monticelli, F., Toledano, M., Tay, F. R., Cury, A. H., Goracci, C. and Ferrari, M. (2006) 'Post-surface conditioning improves interfacial adhesion in post/core restorations', Dent Mater, 22(7), pp. 602-609.

Moreira, D. M., de Andrade Feitosa, J. P., Line, S. R. P. and Zaia, A. A. (2011) 'Effects of reducing agents on birefringence dentin collagen after use of different endodontic auxiliary chemical substances', J Endod, 37(10), pp. 1406-1411.

Morgano, S. M. and Milot, P. (1993) 'Clinical success of cast metal posts and cores', J Prosthet Dent, 70(1), pp. 11-16.

Morgano, S. M. (1996) 'Restoration of pulpless teeth: application of traditional in present and future contexts', J Prosthet Dent, 75(4), pp. 375-380.

Morgano, S. M. and Brackett, S. E. (1999) 'Foundation restorations in fixed prosthodontics:Current Knowledge and Future Needs', J Prosthet Dent, 82(6), pp. 643-657.

Morresi, A., D'Amario, M., Capogreco, M., Gatto, R., Marzo, G., D'Arcangelo, C. and Monaco, A. (2014) 'Thermal cycling for restorative materials: does a standardized protocol exist in laboratory testing? A literature review', J Mech Behav Biomed Mater, 29, pp. 295-308.

Mortazavian, S. and Fatemi, A. (2015a) 'Fatigue behavior and modeling of short fiber reinforced polymer composites including anisotropy and temperature effects', Int J Fatigue, 77, pp. 12-27.

Mortazavian, S. and Fatemi, A. (2015b) 'Fatigue behavior and modeling of short fiber reinforced polymer composites: a literature review', Int J Fatigue, 70, pp. 297-321.

Mulder, R., Mohammed, N., du Plessis, A. and le Roux, S. (2017) 'A pilot study investigating the presence of voids in bulk fill flowable composites', SADJ, 72(10), pp. 462-465.

Murphy, J. 1998. Reinforced plastics handbook. Elsevier.

Nagas, E., Cekic-Nagas, I., Egilmez, F., Ergun, G., Vallittu, P. and Lassila, L. (2017) 'Bond strength of fiber posts and short fiber-reinforced composite to root canal dentin following cyclic loading', J Adhes Sci Technol, 31(13), pp. 1397-1407.

Nagata, K., Garoushi, S., Vallittu, P., Wakabayashi, N., Takahashi, H. and Lassila, L. (2016) 'Fracture behavior of single-structure fiber-reinforced composite restorations', Acta Biomater Odontol Scand, 2(1), pp. 118-124.

Nalla, R. K., Imbeni, V., Kinney, J. H., Staninec, M., Marshall, S. J. and Ritchie, R. O. (2003) 'In vitro fatigue behavior of human dentin with implications for life prediction', J Biomed Mate Res A, 66(1), pp. 10-20.

Naumann, M., Blankenstein, F. and Dietrich, T. (2005a) 'Survival of glass fibre reinforced composite post restorations after 2 years-an observational clinical study', J Dent, 33(4), pp. 305-312.

Naumann, M., Blankenstein, F., Kiessling, S. and Dietrich, T. (2005b) 'Risk factors for failure of glass fiber-reinforced composite post restorations: a prospective observational clinical study', Eur J Oral Sci, 113(6), pp. 519-524.

Naumann, M., Sterzenbach, G. and Proschel, P. (2005c) 'Evaluation of load testing of postendodontic restorations in vitro: linear compressive loading, gradual cycling loading and chewing simulation', J Biomed Mater Res B: Appl Biomater, 74(2), pp. 829-834.

Naumann, M., Metzdorf, G., Fokkinga, W., Watzke, R., Sterzenbach, G., Bayne, S. and Rosentritt, M. (2009) 'Influence of test parameters on in vitro fracture resistance of post-endodontic restorations: a structured review', J Oral Rehabil, 36(4), pp. 299-312.

Naumann, M., Koelpin, M., Beuer, F. and Meyer-Lueckel, H. (2012) '10-year Survival Evaluation for Glass-fiber–supported Postendodontic Restoration: A Prospective Observational Clinical Study', J Endod, 38(4), pp. 432-435.

Nazari, A., Sadr, A., Saghiri, M. A., Campillo-Funollet, M., Hamba, H., Shimada, Y., Tagami, J. and Sumi, Y. (2013) 'Non-destructive characterization of voids in six flowable composites using swept-source optical coherence tomography', Den Mater, 29(3), pp. 278-286.

Neves, A., Jaecques, S., Van Ende, A., Cardoso, M., Coutinho, E., Lührs, A., Zicari, F. and Van Meerbeek, B. (2014) '3D-microleakage assessment of adhesive interfaces: exploratory findings by μCT', Den Mater, 30(8), pp. 799-807.

Newman, M. P., Yaman, P., Dennison, J., Rafter, M. and Billy, E. (2003) 'Fracture resistance of endodontically treated teeth restored with composite posts', J Prosthet Dent, 89(4), pp. 360-7.

Ng, C., Dumbrigue, H., Al-Bayat, M., Griggs, J. and Wakefield, C. (2006) 'Influence of remaining coronal tooth structure location on the fracture resistance of restored endodontically treated anterior teeth', J Prosthet Dent, 95(4), pp. 290-296.

Nicola, S., Alberto, F., Tempesta, R. M., Comba, A., Carlo, M. S., Pasqualini, D. and Berutti, E. (2016) 'Effects of fiber-glass-reinforced composite restorations on fracture resistance and failure mode of endodontically treated molars', J Dent, 53, pp. 82-87.

Nie, E. M., Chen, X. Y., Zhang, C. Y., Qi, L. L. and Huang, Y. H. (2013) 'Influence of masticatory fatigue on the fracture resistance of the pulpless teeth restored with quartz-fiber post–core and crown', Int J Oral Sci, 4(4), pp. 218-220.

Nissan, J., Dmitry, Y. and Assif, D. (2001) 'The use of reinforced composite resin cement as compensation for reduced post length', The Journal of prosthetic dentistry, 86(3), pp. 304-308.

Norman, D. A. and Robertson, R. E. (2003) 'The effect of fiber orientation on the toughening of short fiber-reinforced polymers', Journal of applied polymer science, 90(10), pp. 2740-2751.

O'Brien, W. J. (2002) 'Dental materials and their selection'.

Ogden, A. (1985) 'Porosity in composite resins—an Achilles' heel?', Journal of dentistry, 13(4), pp. 331-340.

Olejniczak, A. J. and Grine, F. E. (2006) 'Assessment of the accuracy of dental enamel thickness measurements using microfocal X-ray computed tomography', The Anatomical Record Part A: Discoveries in Molecular, Cellular, and Evolutionary Biology, 288(3), pp. 263-275.

Omran, T. A., Garoushi, S., Abdulmajeed, A. A., Lassila, L. V. and Vallittu, P. K. (2016) 'Influence of increment thickness on dentin bond strength and light transmission of composite base materials', Clinical Oral Investigations, pp. 1-8.

Opdam, N., Roeters, J., Peters, T. C., Burgersdijk, R. and Teunis, M. (1996a) 'Cavity wall adaptation and voids in adhesive Class I resin composite restorations', Dental Materials, 12(4), pp. 230-235.

Opdam, N., Roeters, J., Peters, T., Burgersdijk, R. and Kuijs, R. (1996b) 'Consistency of resin composites for posterior use', Dental Materials, 12(5-6), pp. 350-354.

Opdam, N., Feilzer, A., Roeters, J. and Smale, I. (1998) 'Class I occlusal composite resin restorations: in vivo post-operative sensitivity, wall adaptation, and microleakage', American journal of dentistry, 11(5), pp. 229-234.

Opdam, N., Roeters, J., Joosten, M. and Veeke, O. (2002) 'Porosities and voids in Class I restorations placed by six operators using a packable or syringable composite', Dental Materials, 18(1), pp. 58-63.

Opdam, N. J. M., Van de Sande, F. H., Bronkhorst, E. M., Cenci, M. S., Bottenberg, P., Pallesen, U., Gaengler, P., Lindberg, A., Huysmans, M. C. and Van Dijken, J. W. (2014) 'Longevity of posterior composite restorations: a systematic review and meta-analysis', Journal of dental research, 93(10), pp. 943-949.

Ozcan, M. and Valandro, L. F. (2009) 'Fracture strength of endodontically-treated teeth restored with post and cores and composite cores only', Operative dentistry, 34(4), pp. 429-436.

Ozsevik, A., Yildirim, C., Aydin, U., Culha, E. and Surmelioglu, D. (2016) 'Effect of fibre-reinforced composite on the fracture resistance of endodontically treated teeth', Australian Endodontic Journal, 42(2), pp. 82-87.

Papa, J., Cain, C. and Messer, H. H. (1994) 'Moisture content of vital vs endodontically treated teeth', Dental Traumatology, 10(2), pp. 91-93.

Papadogiannis, D., Kakaboura, A., Palaghias, G. and Eliades, G. (2009) 'Setting characteristics and cavity adaptation of low-shrinking resin composites', Dental Materials, 25(12), pp. 1509-1516.

Park, Y., Yi, K., Lee, I. K. and Jung, Y. (2005) 'Correlation between microtomography and histomorphometry for assessment of implant osseointegration', Clinical Oral Implants Research, 16(2), pp. 156-160.

Park, J., Chang, J., Ferracane, J. and Lee, I. B. (2008) 'How should composite be layered to reduce shrinkage stress: incremental or bulk filling?', Dental Materials, 24(11), pp. 1501-1505.

Patel, P., Shah, M., Agrawal, N., Desai, P., Tailor, K. and Patel, K. (2016) 'Comparative evaluation of microleakage of class II cavities restored with different bulk fill composite restorative systems: An in vitro study', J Res Adv Dent, 5(2), pp. 52-62.

Patnana, A. K., Vanga, V. N. R. and Chandrabhatla, S. K. (2017) 'Evaluating the Marginal Integrity of Bulk Fill Fibre Reinforced Composites in Bio-mimetically Restored Tooth', Journal of clinical and diagnostic research: JCDR, 11(6), pp. ZC24.

Pegoretti, A., Fambri, L., Zappini, G. and Bianchetti, M. (2002) 'Finite element analysis of a glass fibre reinforced composite endodontic post', Biomaterials, 23(13), pp. 2667-2682.

Perdigao, J., Gomes, G. and Lee, I. K. (2006) 'The effect of silane on the bond strengths of fiber posts', Dental Materials, 22(8), pp. 752-758.

Pereira, J. R., do Valle, A. L., Shiratori, F. K., Ghizoni, J. S. and Bonfante, E. A. (2014) 'The effect of post material on the characteristic strength of fatigued endodontically treated teeth', The Journal of prosthetic dentistry, 112(5), pp. 1225-1230.

Perel, M. L. and Muroff, F. I. (1972) 'Clinical criteria for posts and cores', J Prosthet Dent 28, pp. 405-11.

Peters, O., Laib, A., Rüegsegger, P. and Barbakow, F. (2000) 'Three-dimensional analysis of root canal geometry by high-resolution computed tomography', Journal of Dental Research, 79(6), pp. 1405-1409.

Peters, O., Laib, A., Göhring, T. and Barbakow, F. (2001) 'Changes in root canal geometry after preparation assessed by high-resolution computed tomography', Journal of Endodontics, 27(1), pp. 1-6.

Petersen, K. B. (1971) 'Longitudinal root fracture due to corrosion of an endodontic post', Journal of the Canadian Dental Association, 37(2), pp. 66-68.

Petersen, R. C. (2005) 'Discontinuous fiber-reinforced composites above critical length', Journal of dental research, 84(4), pp. 365-370.

Peutzfeldt, A. and Asmussen, E. (2004) 'Determinants of in vitro gap formation of resin composites', Journal of Dentistry, 32(2), pp. 109-115.

Pitel, M. L. and Hicks, N. L. (2003) 'Evolving technology in endodontic post', Compendium 24, pp. 13-29.

Plotino, G., Grande, N. M., Bedini, R., Pameijer, C. H. and Somma, F. (2007) 'Flexural properties of endodontic posts and human root dentin', dental materials, 23(9), pp. 1129-1135.

Purk, J., Dusevich, V., Glaros, A. and Eick, J. (2007) 'Adhesive analysis of voids in class II composite resin restorations at the axial and gingival cavity walls restored under in vivo versus in vitro conditions', Dental Materials, 23(7), pp. 871-877.

Qing, H., Zhu, Z., Chao, Y. and Zhang, W. (2007) 'In vitro evaluation of the fracture resistance of anterior endodontically treated teeth restored with glass fiber and zircon posts', J Prosthet Dent, 97(2), pp. 93-8.

Quinn, J. B. and Quinn, G. D. (2010) 'Material properties and fractography of an indirect dental resin composite', dental materials, 26(6), pp. 589-599.

Rantala, L. I., Lastumaki, T. M., Peltomaki, T. and Vallittu, P. K. (2003) 'Fatigue resistance of removable orthodontic appliance reinforced with glass fibre weave', Journal of oral rehabilitation, 30(5), pp. 501-506.

Reeh, E. S., Messer, H. H. and Douglas, W. H. (1998) 'Reduction in tooth stiffness as a result of endodontic and restorative procedure', Journal of Endodontics, 15, pp. 512–6.

Rengo, C., Spagnuolo, G., Ametrano, G., Juloski, J., Rengo, S. and Ferrari, M. (2014) 'Micro-computerized tomographic analysis of premolars restored with oval and circular posts', Clin Oral Investig, 18(2), pp. 571-8.

Rivera, E., Yamauchi, M., Chandler, G. and Bergenholtz, G. 'Dentin collagen cross-links of root-filled and normal teeth'. Journal of Endodontics, 195-195.

Roberts, D. H. (1970) 'The failure of retainers in bridge prostheses. An analysis of 2,000 retainers', British dental journal, 128(3), pp. 117.

Rocca, G., Saratti, C. M., Cattani-Lorente, M., Feilzer, A., Scherrer, S. and Krejci, I. (2015) 'The effect of a fiber reinforced cavity configuration on load bearing capacity and failure mode of endodontically treated molars restored with CAD/CAM resin composite overlay restorations', Journal of dentistry, 43(9), pp. 1106-1115.

Rodolpho, P., Donassollo, T., Cenci, M., Loguercio, A., Moraes, R., Bronkhorst, E., Opdam, N. and Demarco, F. (2011) '22-Year clinical evaluation of the performance of two posterior composites with different filler characteristics', Dental Materials, 27(10), pp. 955-963.

Rodriguez-Cervantes, P. J., Sancho-Bru, J. L., Barjau-Escribano, A., Forner-Navarro, L., Perez-Gonzalez, A. and Sanchez-Marin, F. T. (2007) 'Influence of prefabricated post dimensions on restored maxillary central incisors', J Oral Rehabil, 34(2), pp. 141-52.

Rosatto, C., Bicalho, A., Veríssimo, C., Bragança, G., Rodrigues, M., Tantbirojn, D., Versluis, A. and Soares, C. (2015) 'Mechanical properties, shrinkage stress, cuspal strain and fracture resistance of molars restored with bulk-fill composites and incremental filling technique', Journal of dentistry, 43(12), pp. 1519-1528.

Rosenstiel, S. F., Land, M. F. and Fujimoto, J. (2006) Contemporary fixed prosthodontics. 4th ed edn.: Elsevier Health Sciences, p. 336-378.

Roulin-Moloney, A. C. (1989) Fractography and failure mechanisms of polymers and composites. Elsevier applied science.

Rud, J. and Omnell, K. A. (1970) 'Root fractures due to corrosion diagnostic aspects', European Journal of Oral Sciences, 78(1-4), pp. 397-403.

Sadek, F. T., Monticelli, F., Goracci, C., Tay, F. R., Cardoso, P. E. C. and Ferrari, M. (2007) 'Bond strength performance of different resin composites used as core materials around fiber posts', Dental Materials, 23(1), pp. 95-99.

Sahafi, A., Peutzfeldt, A., Asmussen, E. and Gotfredsen, K. (2002) 'Bond strength of resin cement to dentin and to surface-treated posts of titanium alloy, glass fiber, and zirconia', The journal of adhesive dentistry, 5(2), pp. 153-162.

Salameh, Z., Sorrentino, R., Ounsi, H. F., Goracci, C., Tashkandi, E., Tay, F. R. and Ferrari, M. (2007) 'Effect of different all-ceramic crown system on fracture resistance and failure pattern of endodontically treated maxillary premolars restored with and without glass fiber posts', J Endod, 33(7), pp. 848-51.

Salvi, G. E., Siegrist Guldener, B. E., Amstad, T., Joss, A. and Lang, N. P. (2007) 'Clinical evaluation of root filled teeth restored with or without post-and-core systems in a specialist practice setting', Int Endod J, 40(3), pp. 209-15.

Santos, R., da Silveira, L., Moreira, L., Cardoso, M., da Silva, F., dos Santos Paula, A. and Albertacci, D. (2018) 'Damage identification parameters of dual-phase 600–800 steels based on experimental void analysis and finite element simulations', Journal of Materials Research and Technology.

Sapone, J. and Lorencki, S. F. (1981) ' An endodontic -prosthodontic approach to internal tooth reinforcement', J Prosthet Dent 45, pp. 164-70.

Schilder, H. (1966) 'The value of culturing in endodontic treatment', Dental clinics of North America, pp. 127-138.

Schmitter, M., Hamadi, K. and Rammelsberg, P. (2011) 'Survival of two post systems--five-year results of a randomized clinical trial', Quintessence Int, 42(10), pp. 843-50.

Schwartz, R. S. and Robbins, J. W. (2004) 'Post placement and restoration of endodontically treated teeth: a literature review', J Endod, 30(5), pp. 289-301.

Sedgley, C. M. and Messer, H. H. (1992) 'Are endodontically treated teeth more brittle?', Journal of Endodontics, 18(7), pp. 332-335.

Seefeld, F., Wenz, H., Ludwig, K. and Kern, M. (2007) 'Resistance to fracture and structural characteristics of different fiber reinforced post systems', Dental Materials, 23(3), pp. 265-271.

Shah, J., Raghavendra, S., Gathani, K. and Wadekar, S. (2016) 'A practical approach in conservative management of vertical coronal fracture in molar: A case report', IIOABJ, 7, pp. 42-44.

Shillingburg, H. T., Fisher, D. W. and Dewhirst, R. B. (1970) 'Restoration of endodontically treated posterior teeth', The Journal of prosthetic dentistry, 24(4), pp. 401-409.

Shillingburg, H. T. and Kessler, J. C. (1982) Restoration of the endodontically treated tooth. Chicago: Quintessence Publishing Co. , p. 13-44.

Shillingburg, H. T., Hobo, S., Whitsett, L. D., Jacobi, R. and Brackett, S. E. (1997) Fundamentals of fixed prosthodontics. 3rd edn.: Quintessence Publishing. co. inc, p. 181-210.

Shouha, P., Swain, M. and Ellakwa, A. (2014) 'The effect of fiber aspect ratio and volume loading on the flexural properties of flowable dental composite', Dental Materials, 30(11), pp. 1234-1244.

Signore, A., Benedicenti, S., Kaitsas, V., Barone, M., Angiero, F. and Ravera, G. (2009) 'Long-term survival of endodontically treated, maxillary anterior teeth restored with either tapered or parallel-sided glass-fiber posts and full-ceramic crown coverage', J Dent, 37(2), pp. 115-21.

Silness, J., Gustavsen, F. and Hunsbeth, J. (1979) 'Distribution of corrosion products in teeth restored with metal crowns retained by stainless steel posts', Acta Odontologica Scandinavica, 37(6), pp. 317-321.

Silva de Assis, F., Lima, L., Nogueira, S., Rodrigues Tonetto, M., Bhandi, S. H., Souza Pinto, S. C., Malaquias, P., Loguercio, A. D. and Coelho Bandeca, M. (2016) 'Evaluation of Bond Strength, Marginal Integrity, and Fracture Strength of Bulk-vs Incrementally-filled Restorations', Journal of Adhesive Dentistry, 18(4).

Siso, S., Hurmuzlu, F., Turgut, M., Altundasar, E., Serper, A. and Er, K. (2007) 'Fracture resistance of the buccal cusps of root filled maxillary premolar teeth restored with various techniques', International Endodontic Journal, 40(3), pp. 161-168.

Sisodia, S., Gamstedt, E., Edgren, F. and Varna, J. (2015) 'Effects of voids on quasi-static and tension fatigue behaviour of carbon-fibre composite laminates', Journal of composite materials, 49(17), pp. 2137-2148.

Skjorland, K., Hensten-Pettersen, A., orsta-Vik, D. and Soderholm, K. (1982) 'Tooth colored dental restorative materials: Porosities and surface topography in relation to bacterial adhesion', Acta Odontologica Scandinavica, 40(2), pp. 113-120.

Smith, D. C. (1962) 'Recent developments and prospects in dental polymers', The Journal of Prosthetic Dentistry, 12(6), pp. 1066-1078.

Smith, C. T. and Schuman, N. (1997) 'Restoration of endodontically treated teeth: a guide for the restorative dentist', Quintessence International, 28(7).

Soares, C., Valdivia, A., da Silva, G., Santana, F. and Menezes Mde, S. (2012) 'Longitudinal clinical evaluation of post systems: a literature review', Braz Dent J, 23(2), pp. 135-740.

Soares, R., Ataide, I., Fernandes, M. and Lambor, R. (2016) 'Fibre reinforcement in a structurally compromised endodontically treated molar: a case report', Restorative dentistry & endodontics, 41(2), pp. 143-147.

Soares, L. M., Razaghy, M. and Magne, P. (2018) 'Optimization of large MOD restorations: Composite resin inlays vs. short fiber-reinforced direct restorations', Dent Mater.

Sokol, D. (1984) 'Effective use of current core and post concept', J Prosthet Dent, 52, pp. 231-34.

Solnit, G. (1991) 'The effect of methyl methacrylate reinforcement with silane-treated and untreated glass fibers', Journal of Prosthetic Dentistry, 66(3), pp. 310-314.

Sorensen, J. A. and Martinoff, J. T. (1984a) 'Clinically significant factors in dowel design', The Journal of Prosthetic Dentistry, 52(1), pp. 28-35.

Sorensen, J. A. and Martinoff, J. T. (1984b) 'Intracoronal reinforcement and coronal coverage: a study of endodontically treated teeth', The Journal of prosthetic dentistry, 51(6), pp. 780-784.

Sorensen, J. and Engelman, M. J. (1990) 'Ferrule design and fracture resistance of endodontically treated teeth', The Journal of prosthetic dentistry, 63(5), pp. 529-536.

Sperling, L. and Mishra, V. (1996) 'The current status of interpenetrating polymer networks', Polymers for Advanced Technologies, 7(4), pp. 197-208.

Standlee, J., Caputo, A. and Hanson, E. (1978) 'Retention of endodontic dowels: effects of cement, dowel length, diameter, and design', The Journal of prosthetic dentistry, 39(4), pp. 400-405.

Steagall, L., Ishikiriama, A., de Lima Navarro, M. F. and Soares, F. B. (1980) 'Fracture strength of human teeth with cavity preparations', The Journal of Prosthetic Dentistry, 43(4), pp. 419-422.

Stern, N. and Hirshfeld, Z. (1973) 'Principles of preparing endodontically treated teeth for dowel and core restorations', Journal of Prosthetic Dentistry, 30(2), pp. 162-165.

Sterzenbach, G., Rosentritt, M., Frankenberger, R., Paris, S. and Naumann, M. (2012) 'Loading standardization of postendodontic restorations in vitro: impact of restorative stage, static loading, and dynamic loading', Oper Dent, 37(1), pp. 71-79.

Stewardson, D., Shortall, A., Marquis, P. and Lumley, P. (2010) 'The flexural properties of endodontic post materials', dental materials, 26(8), pp. 730-736.

Stockton, L. W. (1999) 'Factors affecting retention of post systems: a literature review', The Journal of prosthetic dentistry, 81(4), pp. 380-385.

Strand, G., Tveit, A., Gjerdet, N. and Eide, G. (1995) 'Marginal ridge strength of teeth with tunnel preparations', International dental journal, 45(2), pp. 117-123.

Strassler, H. E. (1999) 'Restoring endodontically compromised teeth with fiber-reinforced light transmitting anchors', Contemporary Esthetics and Restorative Practice, 3(3), pp. 58-60.

Suarez, J., Molleda, F. and Guemes, A. (1993) 'Void content in carbon fibre/epoxy resin composites and its effects on compressive properties', ICCM/9. Composites: Properties and Applications., 6, pp. 589-596.

Sun, J. and Lin-Gibson, S. (2008) 'X-ray microcomputed tomography for measuring polymerization shrinkage of polymeric dental composites', Dental materials, 24(2), pp. 228-234.

Sun, J., Eidelman, N. and Lin-Gibson, S. (2009a) '3D mapping of polymerization shrinkage using X-ray micro-computed tomography to predict microleakage', dental materials, 25(3), pp. 314-320.

Sun, J., Fang, R., Lin, N., Eidelman, N. and Lin-Gibson, S. (2009b) 'Nondestructive quantification of leakage at the tooth–composite interface and its correlation with material performance parameters', Biomaterials, 30(27), pp. 4457-4462.

Swain, M. V. and Xue, J. (2009) 'State of the art of Micro-CT applications in dental research', Int J Oral Sci, 1(4), pp. 177-188.

Tanaka, K., Taira, M., Shintani, H., Wakasa, K. and Yamaki, M. (1991) 'Residual monomers (TEGDMA and Bis-GMA) of a set visible-light-cured dental composite resin when immersed in water', J Oral Rehabil, 18(4), pp. 353-362.

Tang, J., Lee, W. and Springer, G. (1987) 'Effects of cure pressure on resin flow, voids, and mechanical properties', J Compos Mater, 21(5), pp. 421-440.

Tanner, J., Robinson, C., Soderling, E. and Vallittu, P. K. (2003) 'Early Plaque Formation on Fiber-reinforced Composites in vivo', 81st General Session of the International Association for Dental Research.

Tanner, J. and Le Bell, A. M. (2016) 'Fiber-Reinforced Dental Materials in the Restoration of Root-Canal Treated Teeth'. Springer, pp. 67-86.

Teixeira, E. C., Teixeira, F. B., Piasick, J. R. and Thompson, J. Y. (2006) 'An in vitro assessment of prefabricated fiber post systems', J Am Dent Assoc, 137(7), pp. 1006-1012.

Teixeira, C. S., Silva-Sousa, Y. C. and Sousa-Neto, M. D. (2008) 'Effects of light exposure time on composite resin hardness after root reinforcement using translucent fibre post', J Dent, 36(7), pp. 520-8.

Tekce, N., Pala, K., Tuncer, S., Demirci, M. and Serim, M. (2017) 'Influence of polymerisation method and type of fibre on fracture strength of endodontically treated teeth', Austr Endod J, 43(3), pp. 115-122.

Terry, D. A., Triolo Jr, P. and Swift Jr, E. J. (2001) 'Fabrication of direct fiber-reinforced posts: a structural design concept', J Esthet Restor Dent, 13(4), pp. 228-240.

Testori, T., Badino, M. and Castagnola, M. (1993) 'Vertical root fractures in endodontically treated teeth: a clinical survey of 36 cases', J Endod, 19(2), pp. 87-90.

Tezvergil, A., Lassila, L. V. and Vallittu, P. K. (2006) 'The effect of fiber orientation on the polymerization shrinkage strain of fiber-reinforced composites', Dent Mater, 22(7), pp. 610-616.

Titley, K, Chernecky, R, Rossouw, P & Kulkarni, G 1998, 'The effect of various storage methods and media on shear-bond strengths of dental composite resin to bovine dentine', Arch oral biol, 43 (4), pp. 305-311.

Torbjorner, A., Karlsson, S. and Odman, P. A. (1995) 'Survival rate and failure characteristics for two post designs', J Prosthet Dent, 73(5), pp. 439-444.

Torbjorner, A., Karlsson, S., Syverud, M. and Hensten-Pettersen, A. (1996) 'Carbon fiber reinforced root canal posts Mechanical and cytotoxic properties', Eur J Oral Sci, 104(5-6), pp. 605-611.

Torbjorner, A. (2000) 'Treatment management. Posts and cores', A Textbook of Fixed Prosthodontics. Stockholm: Gothia, pp. 173-186.

Torbjorner, A. and Fransson, B. (2004) 'A literature review on the prosthetic treatment of structurally compromised teeth', Int J Prosthodont, 17(3), pp. 369-76.

Totiam, P., Gonzalez-Cabezas, C., Fontana, M. and Zero, D. (2007) 'A new in vitro model to study the relationship of gap size and secondary caries', Caries Res, 41(6), pp. 467-473.

Trabert, K. C., Caputo, A. A. and Abou-Rass, M. (1978) 'Tooth fracture\ 3-A comparison of endodontic and restorative treatments', J Endod, 4(11), pp. 341-345.

Trope, M., Maltz, D. O. and Tronstad, L. (1985) 'Resistance to fracture of restored endodontically treated teeth', Endod Dent Traumatol 1, pp. 375-380.

Tsujimoto, A., Barkmeier, W., Takamizawa, T., Watanabe, H., Johnson, W., Latta, M. and Miyazaki, M. (2016a) 'Relationship between mechanical properties and bond durability of short fiber-reinforced resin composite with universal adhesive', Eur J Oral Sci, 124(5), pp. 480-489.

Tsujimoto, A., Barkmeier, W. W., Takamizawa, T., Latta, M. and Miyazaki, M. (2016b) 'Bonding performance and interfacial characteristics of short fiber-reinforced resin composite in comparison with other composite restoratives', Eur J Oral Sci, 124(3), pp. 301-308.

Tsujimoto, A., Barkmeier, W. W., Takamizawa, T., Latta, M. and Miyazaki, M. (2016c) 'Mechanical properties, volumetric shrinkage and depth of cure of short fiber-reinforced resin composite', Dent Mater J, 35(3), pp. 418-424.

Tuncer, S., Demirci, M., Tekce, N., Tuncer, A. K. and Bag, H. G. (2013) 'The Effect of Two Bulk Fill Resin Composites on Microleakage in Endodontically Treated Teeth', The Journal of Dentist, 1(1), pp.8-15.

Turner, C. H. (1982) 'The utilization of roots to carry post-retained crowns', J Oral Rehabil, 9(3), pp. 193-202.

Uzun, I., Malkoc, M., Keles, A. and Ogreten, A. (2016) '3D micro-CT analysis of void formations and push-out bonding strength of resin cements used for fiber post cementation', J Adv Prosthodont, 8(2), pp. 101-109.

Valderhaug, J., Jokstad, A., Ambjørnsen, E. and Norheim, P. (1997) 'Assessment of the periapical and clinical status of crowned teeth over 25 years', J Dent, 25(2), pp. 97-105.

Vallittu, P. K. (1993) 'Comparison of two different silane compounds used for improving adhesion between fibres and acrylic denture base material', J Oral Rehabil, 20(5), pp. 533-539.

Vallittu, P. (1994) 'Acrylic resin-fiber composite—Part II: The effect of polymerization shrinkage of polymethyl methacrylate applied to fiber roving on transverse strength', J Prosthet Dent, 71(6), pp. 613-617.

Vallittu, P., Lassila, V. and Lappalainen, R. (1994) 'Acrylic resin-fiber composite—Part I: The effect of fiber concentration on fracture resistance', J Prosthet Dent, 71(6), pp. 607-612.

Vallittu, P. (1995a) 'The effect of void space and polymerization time on transverse strength of acrylic-glass fibre composite', J Oral Rehabil, 22(4), pp. 257-261.

Vallittu, P. (1995b) 'Impregnation of glass fibres with polymethylmethacrylate using a powder-coating method', Applied Composite Materials, 2(1), pp. 51-58.

Vallittu, P. K. (1996) 'A review of fiber-reinforced denture base resins', J Prosthodont, 5, pp. 270–6.

Vallittu, P. K. (1997a) 'Glass fiber reinforcement in repaired acrylic resin removable dentures: preliminary results of a clinical study', Quintessence Int, 28(1), pp. 39-44.

Vallittu, P. (1997b) 'Oxygen inhibition of autopolymerization of polymethylmethacrylate–glass fibre composite', J Mater Sci Mater Med, 8(8), pp. 489-492.

Vallittu, P. K. (1998a) 'Compositional and weave pattern analyses of glass fibers in dental polymer fiber composites', J Prosthodont, 7(3), pp. 170-176.

Vallittu, P. K. (1998b) 'Some aspects of the tensile strength of unidirectional glass fibre–polymethyl methacrylate composite used in dentures', J Oral Rehabil, 25(2), pp. 100-105.

Vallittu, P. K. (1999) 'Flexural properties of acrylic resin polymers reinforced with unidirectional and woven glass fibers', J Prosthet Dent, 81(3), pp. 318-326.

Vallittu, P. K. (2001) 'Case report: a glass fibre reinforced composite resin bonded fixed partial denture', Eur J Prosthodont Restor Dent, 9(1), pp. 35-38.

Vallittu, P. (2009) 'Interpenetrating polymer networks (IPNs) in dental polymers and composites', J Adhes Sci Technol, 23(7-8), pp. 961-972.

Vallittu, P. K. (2014) 'Glass fibers in fiber-reinforced composites', in Matinlinna, J. P. 'Handbook of Oral Biomaterials'. CRC press, pp. 255-278.

Vallittu, P. K. (2015) 'High-aspect ratio fillers: Fiber-reinforced composites and their anisotropic properties', Dent Mater, 31(1), pp. 1-7.

Vallittu, P. k. and Ozcan, M. (2017) Clinical Guide to Principles of Fiber-reinforced Composites in Dentistry. Woodhead Publishing.

Vallittu, P. (2018) 'An overview of development and status of fiber-reinforced composites as dental and medical biomaterials', Acta Biomater Odontol Scand, 4(1), pp. 44-55.

Van Dijken, J. and Sunnegardh-Gronberg, K. (2006) 'Fiber-reinforced packable resin composites in Class II cavities', J Dent, 34(10), pp. 763-769.

Varvara, G., Perinetti, G., Di Iorio, D., Murmura, G. and Caputi, S. (2007) 'In vitro evaluation of fracture resistance and failure mode of internally restored endodontically treated maxillary incisors with differing heights of residual dentin', J Prosthet Dent, 98(5), pp. 365-372.

Wetherhold, R. C. and Jain, L. (1992) 'The toughness of brittle matrix composites reinforced with discontinuous fibers', Mater Sci Eng A, 151(2), pp. 169-177.

Wiskott, H. W. A., Meyer, M., Perriard, J. and Scherrer, S. S. (2007) 'Rotational fatigue-resistance of seven post types anchored on natural teeth', Dent Mater, 23(11), pp. 1412-1419.

Wolff, D., Geiger, S., Ding, P., Staehle, H. J. and Frese, C. (2012) 'Analysis of the interdiffusion of resin monomers into pre-polymerized fiber-reinforced composites', Dent Mater, 28(5), pp. 541-7.

Wu, M., Pehlivan, Y., Kontakiotis, E. and Wesselink, P. (1998) 'Microleakage along apical root fillings and cemented posts', J Prosthet Dent, 79(4), pp. 264-9.

Yadav, K., De Ataide, I., Fernandes, M., Lambor, R. and Alreja, D. (2016) 'Endodontic Management of a Mandibular First Molar with Radix Entomolaris and Conservative Post-endodontic Restoration with CAD/CAM Onlay: A Novel Clinical Technique', J Clin Diag Res, 10(11), pp.13-15.

Yamazaki, P., Bedran-Russo, A., Pereira, P. and Swift Jr, E. (2006) 'Microleakage evaluation of a new low-shrinkage composite restorative material', Oper Dent, 31(6), pp. 670-676.

Yang, Z., Hou, Y. F. and Pan, X. B. (2008) 'Fracture resistance and failure modes of endodontically treated human teeth restored with four different post-core systems', Abstract. Hua Xi Kou Qiang Yi Xue Za Zhi, 26(6), pp. 633-5, 639.

Yasa, B., Arslan, H., Yasa, E., Akcay, M. and Hatirli, H. (2016) 'Effect of novel restorative materials and retention slots on fracture resistance of endodontically-treated teeth', Acta Odontol Scand, 74(2), pp. 96-102.

Yenisey, M. and Kulunk, S. (2008) 'Effects of chemical surface treatments of quartz and glass fiber posts on the retention of a composite resin', J Prosthet Dent 99(1), pp. 38-45.

Zhang, Y., Du, W., Zhou, X. and Yu, H. (2014) 'Review of research on the mechanical properties of the human tooth', International journal of oral science, 6(2), pp. 61.

Zhu, Y., Blumenthal, W. and Lowe, T. (1997) 'Determination of non-symmetric 3-D fiber-orientation distribution and average fiber length in short-fiber composites', J Compos Mater, 31(13), pp. 1287-1301.

Zicari, F., Van Meerbeek, B., Debels, E., Lesaffre, E. and Naert, I. (2010) 'An up to 3-Year Controlled Clinical Trial Comparing the Outcome of Glass Fiber Posts and Composite Cores with Gold Alloy-Based Posts and Cores for the Restoration of Endodontically Treated Teeth', Int J prosthodont, 24(4), pp. 363-372.

Zicari, F., Van Meerbeek, B., Scotti, R. and Naert, I. (2012) 'Effect of fibre post length and adhesive strategy on fracture resistance of endodontically treated teeth after fatigue loading', J Dent, 40(4), pp. 312-321.

Zicari, F., Coutinho, E., Scotti, R., Van Meerbeek, B. and Naert, I. (2013) 'Mechanical properties and micro-morphology of fiber posts', Dent Mater, 29(4), pp. e45-e52.

Ziskind, D., Hasday, M., Cohen, S. and Wagner, H. (2011) 'Young's modulus of peritubular and intertubular human dentin by nano-indentation tests', J Struct Biol, 174(1), pp. 23-30.

Appendices

Appendix 1. everX Posterior SFRC (GC, Tokyo, Japan) parameters as reported by the manufacturer and as investigated by Bijelic et al., 2016

Manufacturer	Total filler load average 67 Wt%: Silicon dioxide particulate fillers Barium glass particulate fillers E-glass fibre fillers: max. 15 Wt_f%, average: 8.6 Wt_f%					
	E-glass fibres diameter (μm)	E-glass fibres length (mm)	E-glass fibres aspect ratio l/d	critical fibre length l_{fc}	Optimal fibre length l_{fo}	Fibre volume fraction V_f%
	16-17	0.3- 2	18-125	-	-	-
Bijelic et al., 2016	17	0.3–1.9	18–112	0.85-1.09	1.0–1.3	7.2

Wt%: total filler weiht fraction
$Wt_{f\%}$: fibre filler weight fraction

Appendix 2. Pairwise comparisons between variables of void location, distribution and size

2.1: Pairwise comparisons between closed, open and core voids volume and volume fraction

Void Location		Void volume(mm^3)				Void volume fraction (%)			
		Estimate	95% CI level		P-value	Estimate	95% CI level		P-value
			Lower	Upper			Lower	Upper	
Closed	**Open**	0.3237	0.1576	0.4897	0.0009	1.4205	0.7188	2.1222	0.0007
	Core	0.01093	-0.1888	0.2107	0.9082	1.9922	1.3827	2.6017	<0.00001
Open	**Core**	0.3127	0.07150	0.5540	0.0147	-0.5717	-1.1243	-0.0190	0.0435

2.2: Pairwise comparisons between coronal, middle and apical voids volume and volume fraction

Void distribution		Void volume(mm^3)				Void volume fraction (%)			
		Estimate	95% CI level		P-value	Estimate	95% CI level		P-value
			Lower	Upper			Lower	Upper	
Coronal	**Middle**	0.1133	0.02737	0.1993	0.0134	0.7350	-0.2349	1.7049	0.1264
	Apical	-0.1440	-0.2574	-0.03065	0.0164	-0.06667	-1.2064	1.0731	0.9019
Middle	**Apical**	-0.03067	-0.09841	0.03708	0.3481	0.6683	-0.0457	1.3824	0.0644

2.3: Pairwise comparisons between voids sizes number and percentage

Void size		Voids number				Voids percentage			
		Estimate	95% CI level		P-value	Estimate	95% CI level		P-value
			Lower	Upper			Lower	Upper	
Small	**Medium**	-297.00	-344.65	-249.35	<0.0001	-79.5267	-82.2208	-76.8327	<0.0001
	Large	-317.33	-365.63	-269.04	<0.0001	-85.2233	-87.0068	-83.4399	<0.0001
Medium	**Large**	-20.3333	-24.6669	-15.9997	<0.0001	-5.6966	-6.9394	-4.4538	<0.0001

Appendix 3. Colour-coded models of closed voids in XFP group specimens

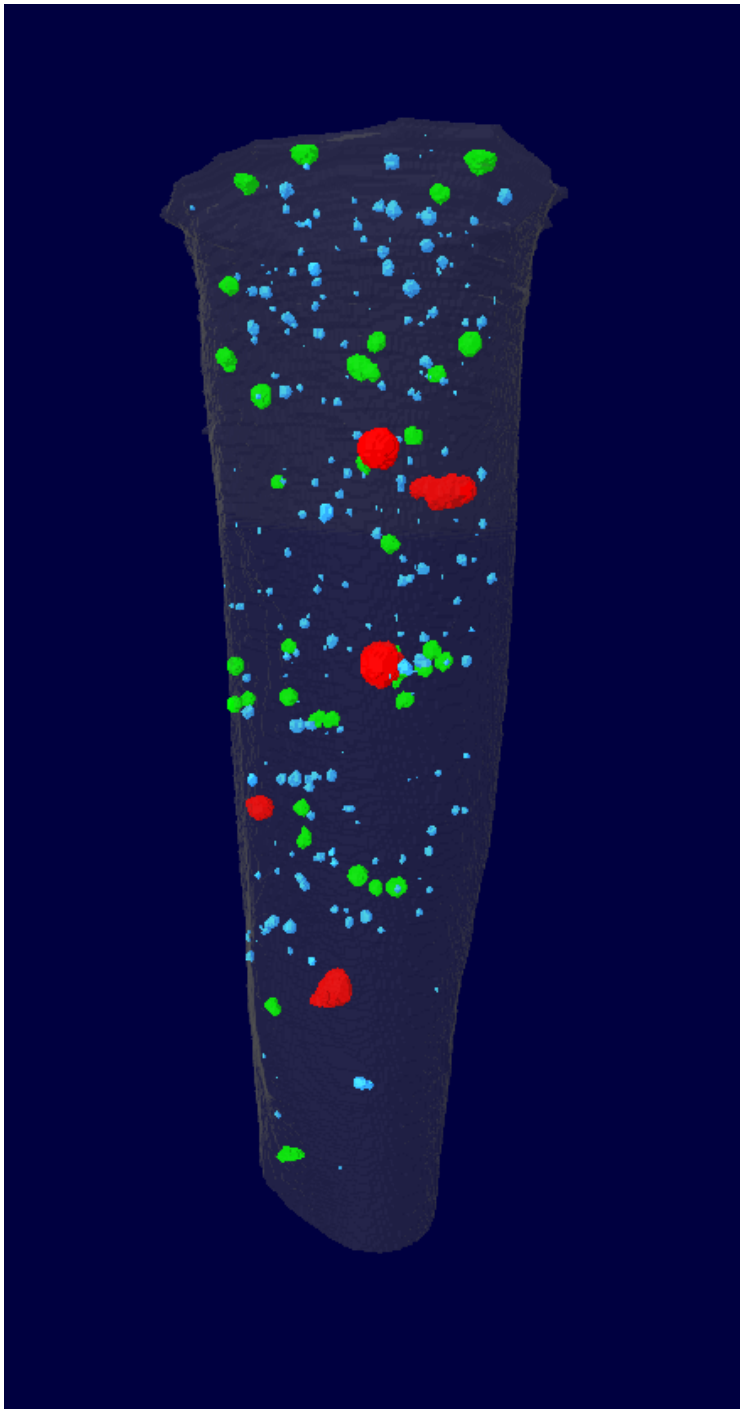

XFP specimen 1
Void volume:0.3 mm^3
Void volume fraction:1.3%

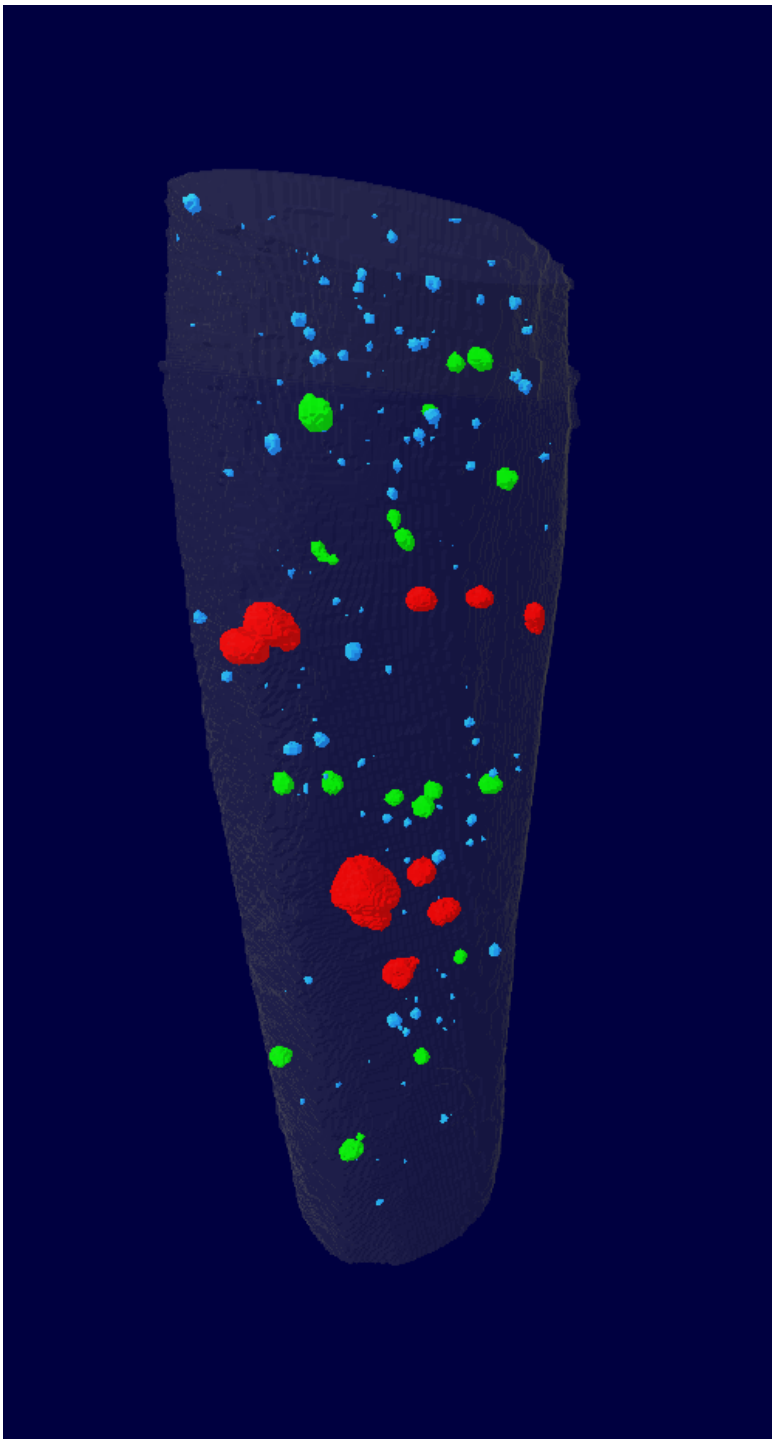

XFP specimen 2
Void volume:0.4 mm^3
Void volume fraction:1.4%

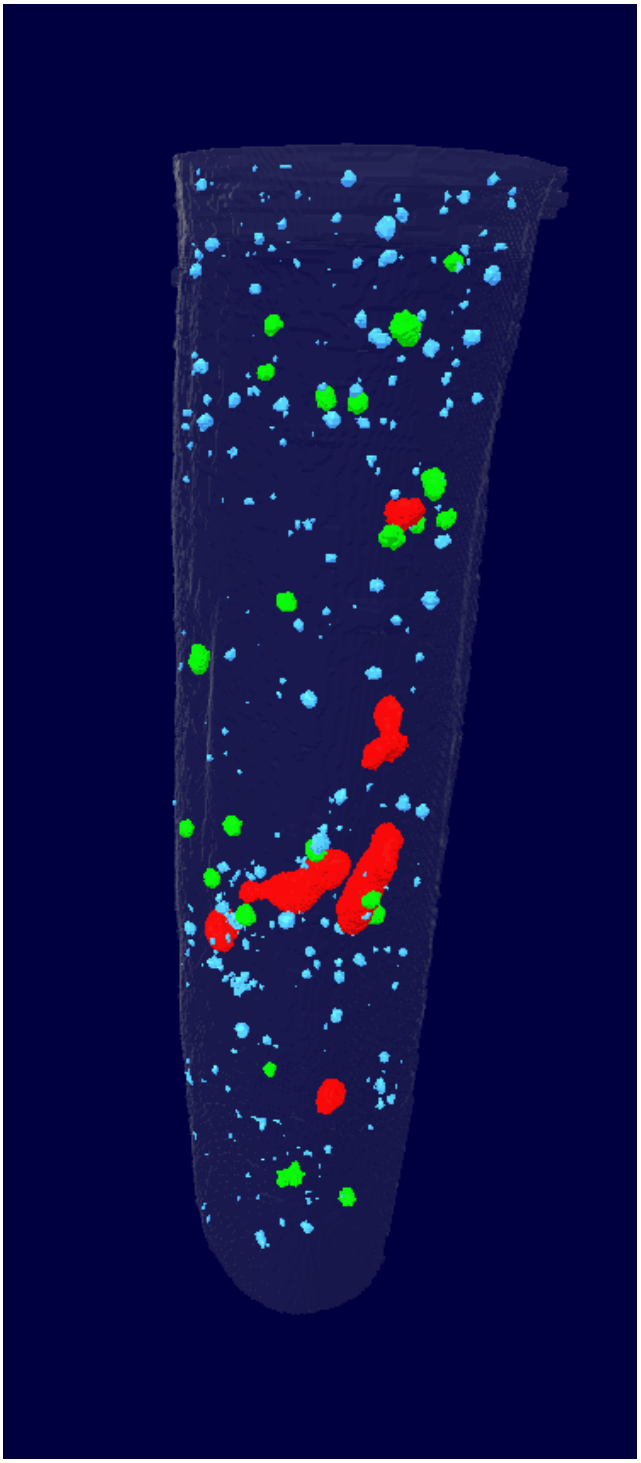

XFP specimen 3
Void volume: 0.7mm^3
Void volume fraction:2.9 %

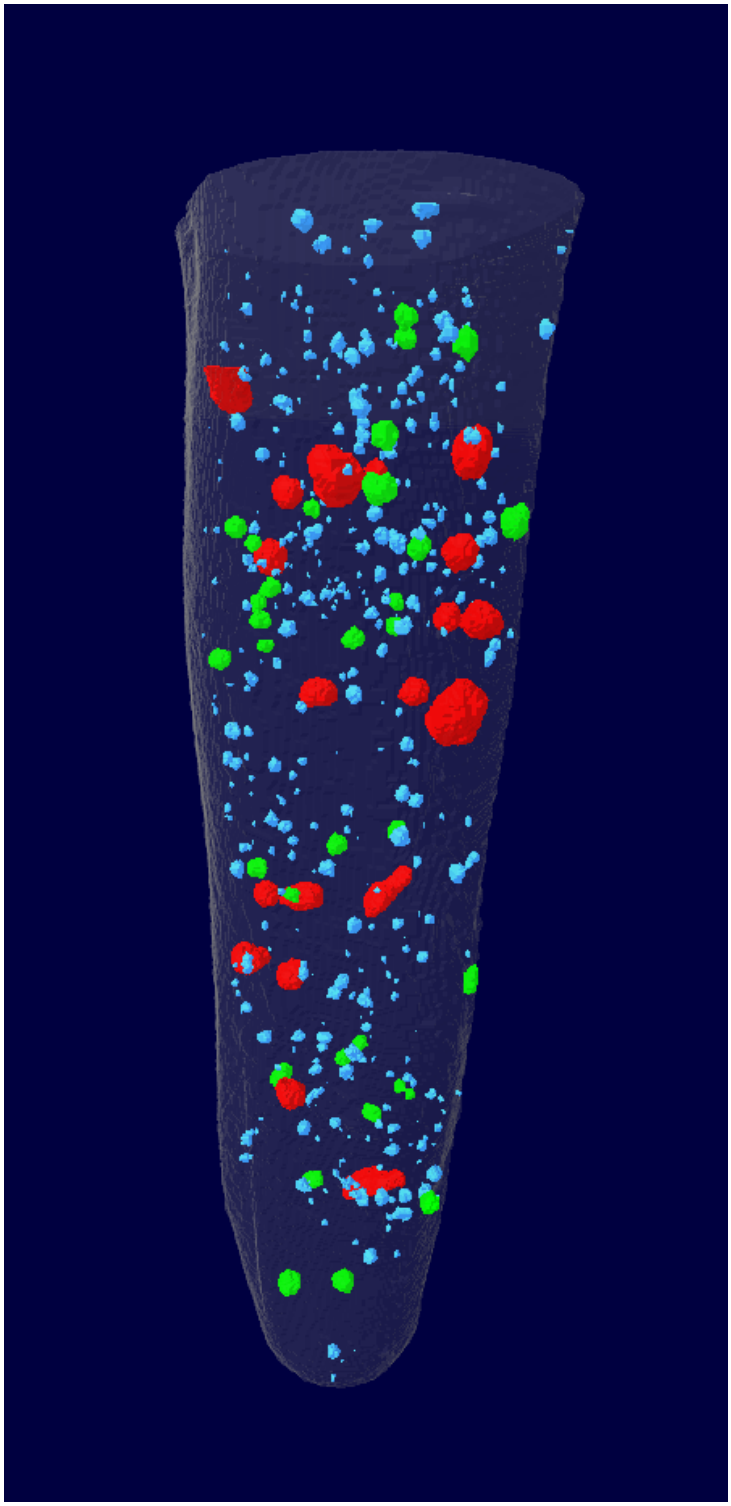

XFP specimen 4
Void volume: 0.4mm^3
Void volume fraction: 1.8%

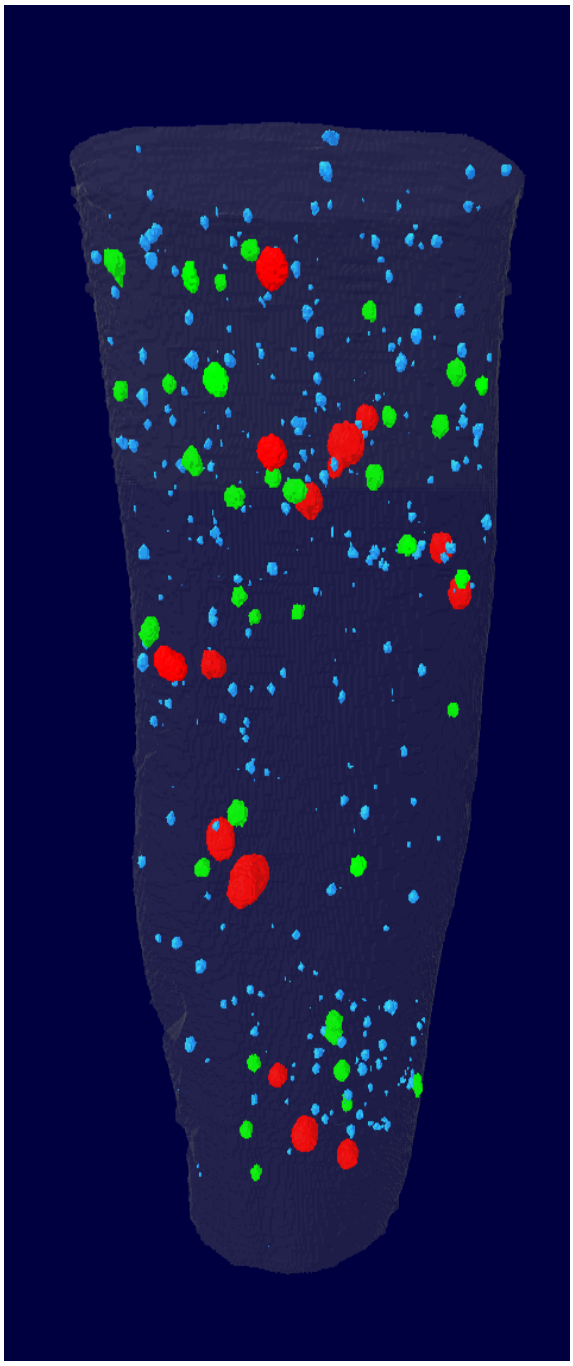

XFP specimen 5
Void volume: 0.5 mm^3
Void volume fraction: 1.9%

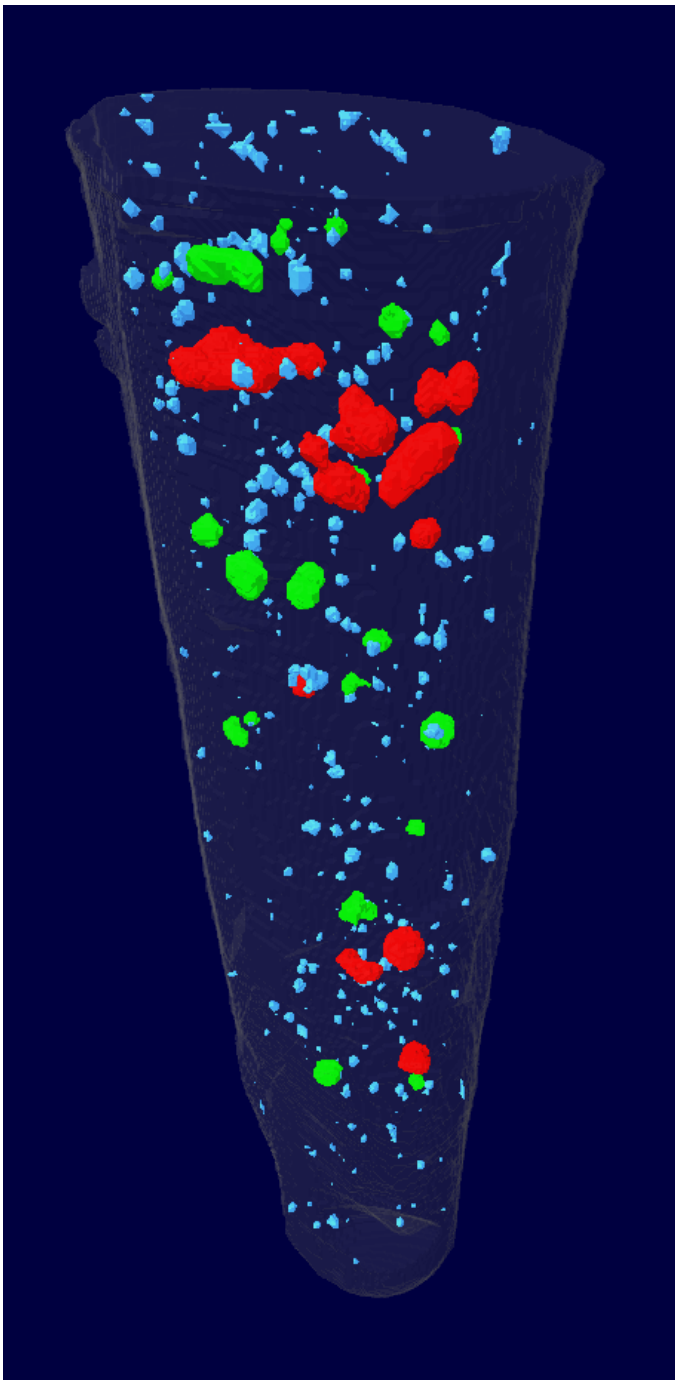

XFP specimen 6
Void volume: 0.6mm^3
Void volume fraction:2.5 %

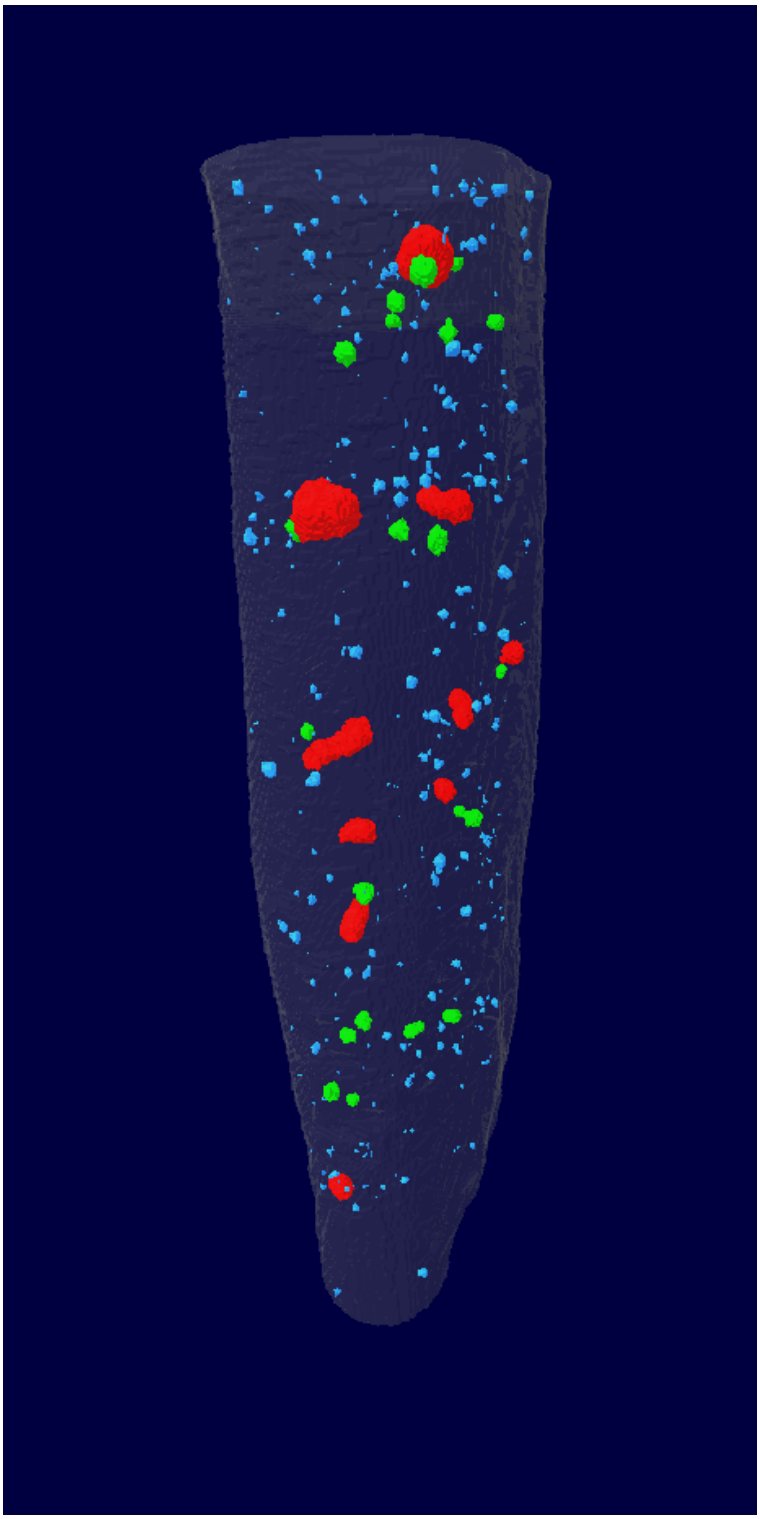

XFP specimen 7
Void volume: 0.5mm^3
Void volume fraction: 1.9%

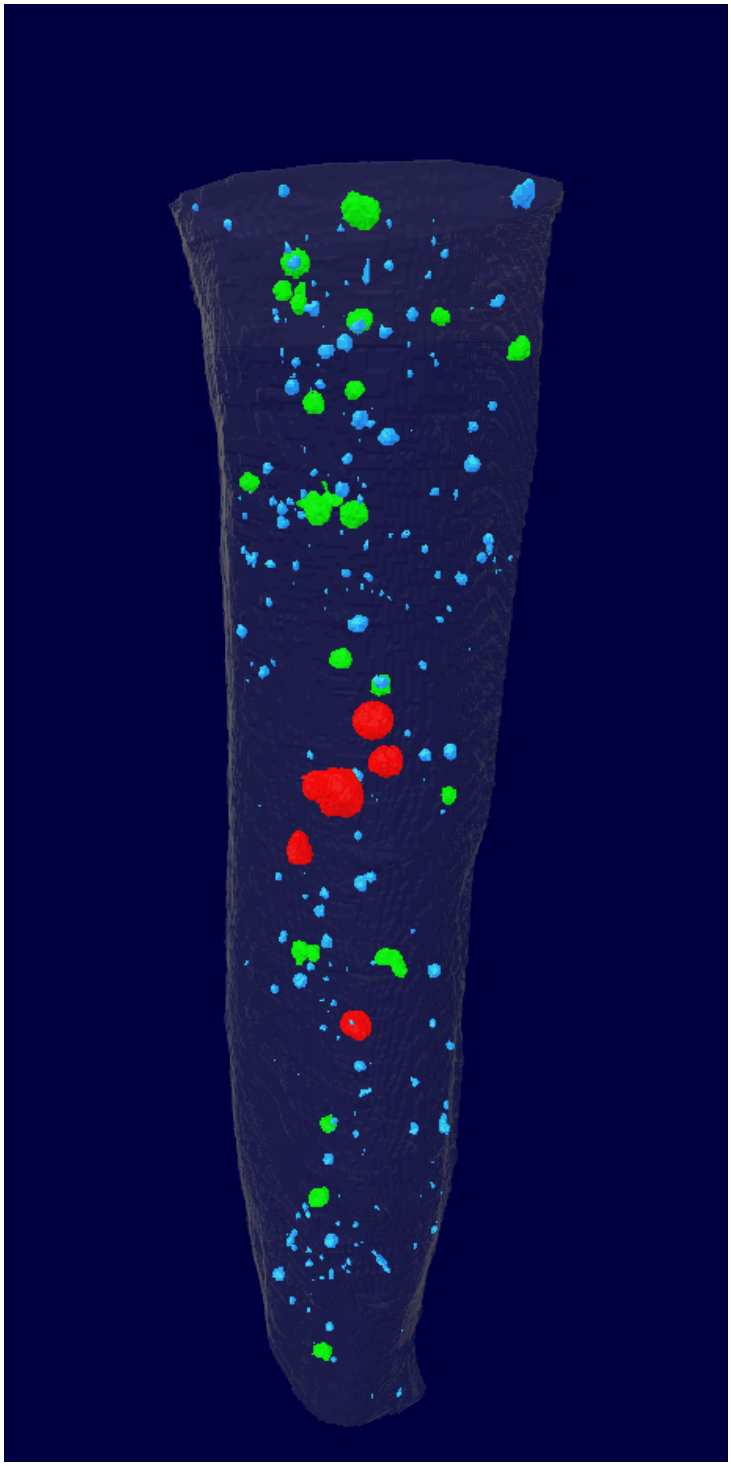

XFP specimen 8
Void volume: 0.9mm^3
Void volume fraction:3.9 %

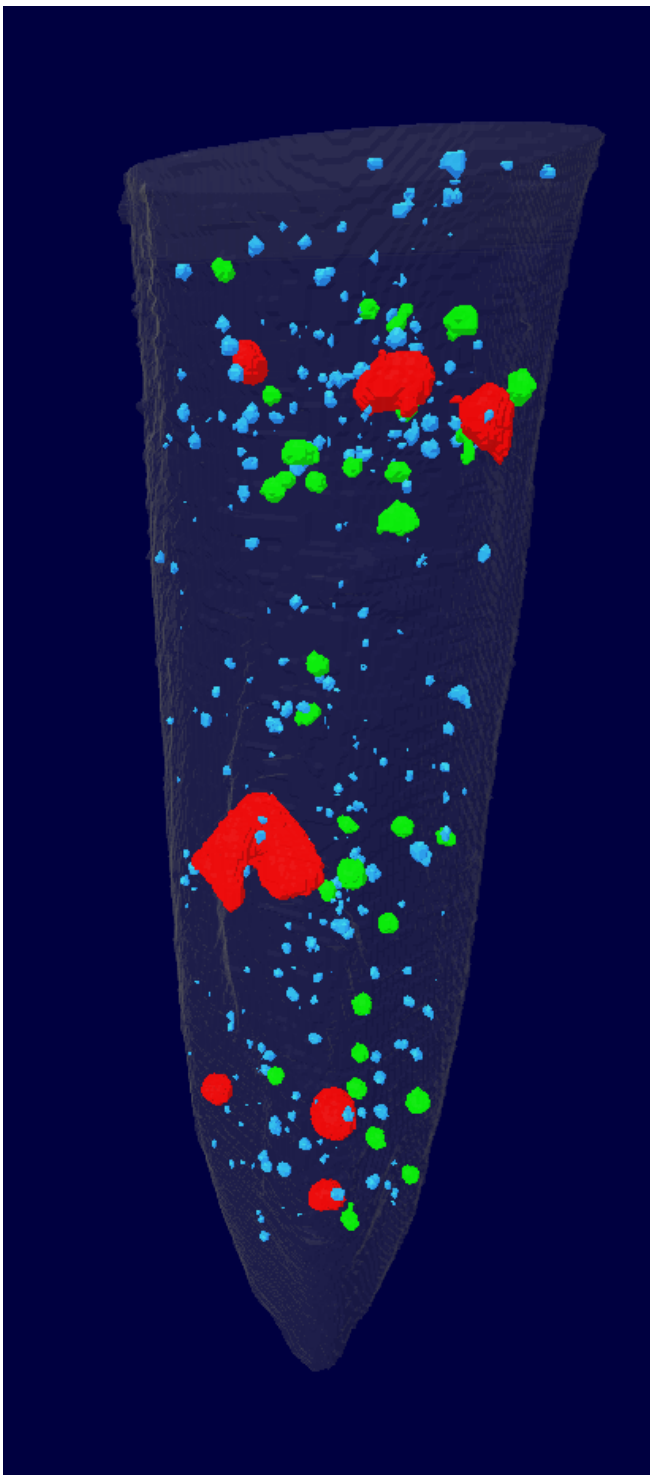

XFP specimen 9
Void volume: 0.5mm^3
Void volume fraction: 2.7%

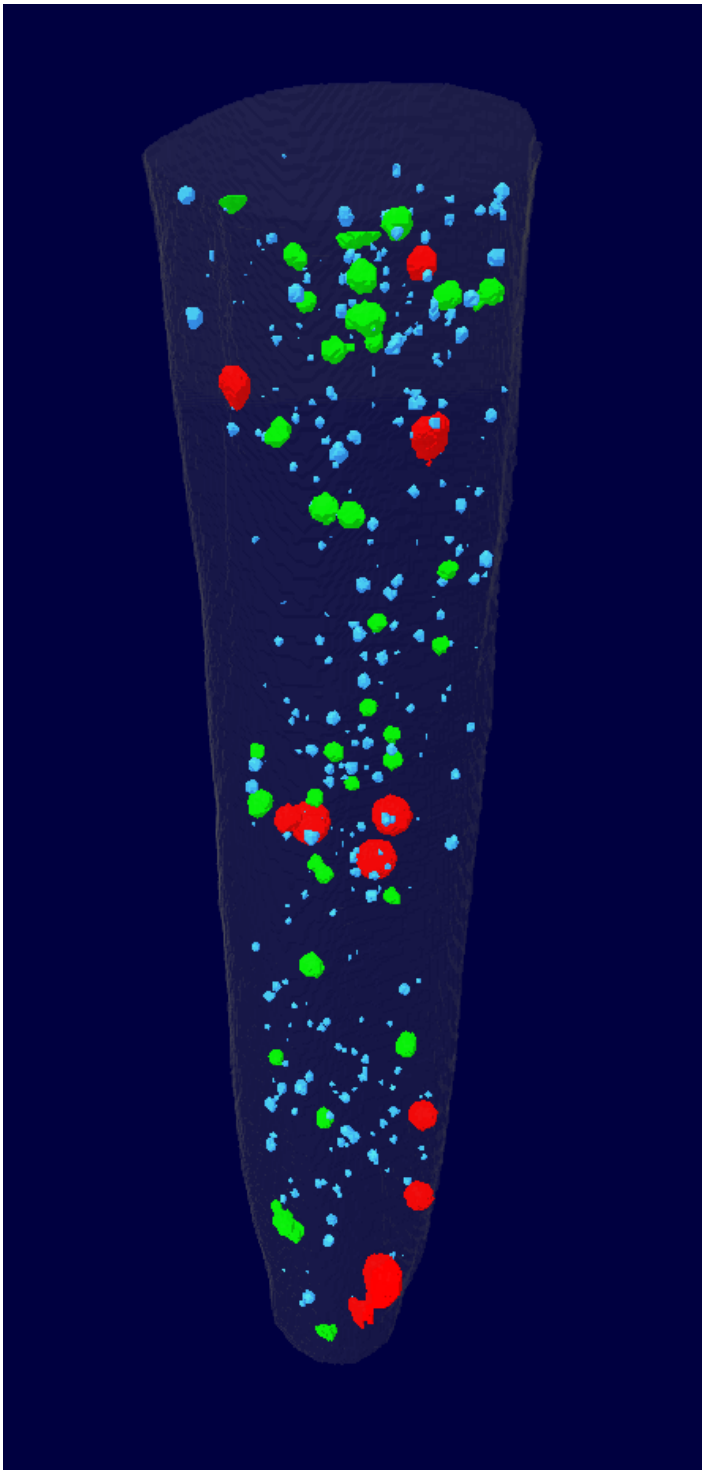

XFP specimen 10
Void volume: 0.3mm^3
Void volume fraction: 1.8%

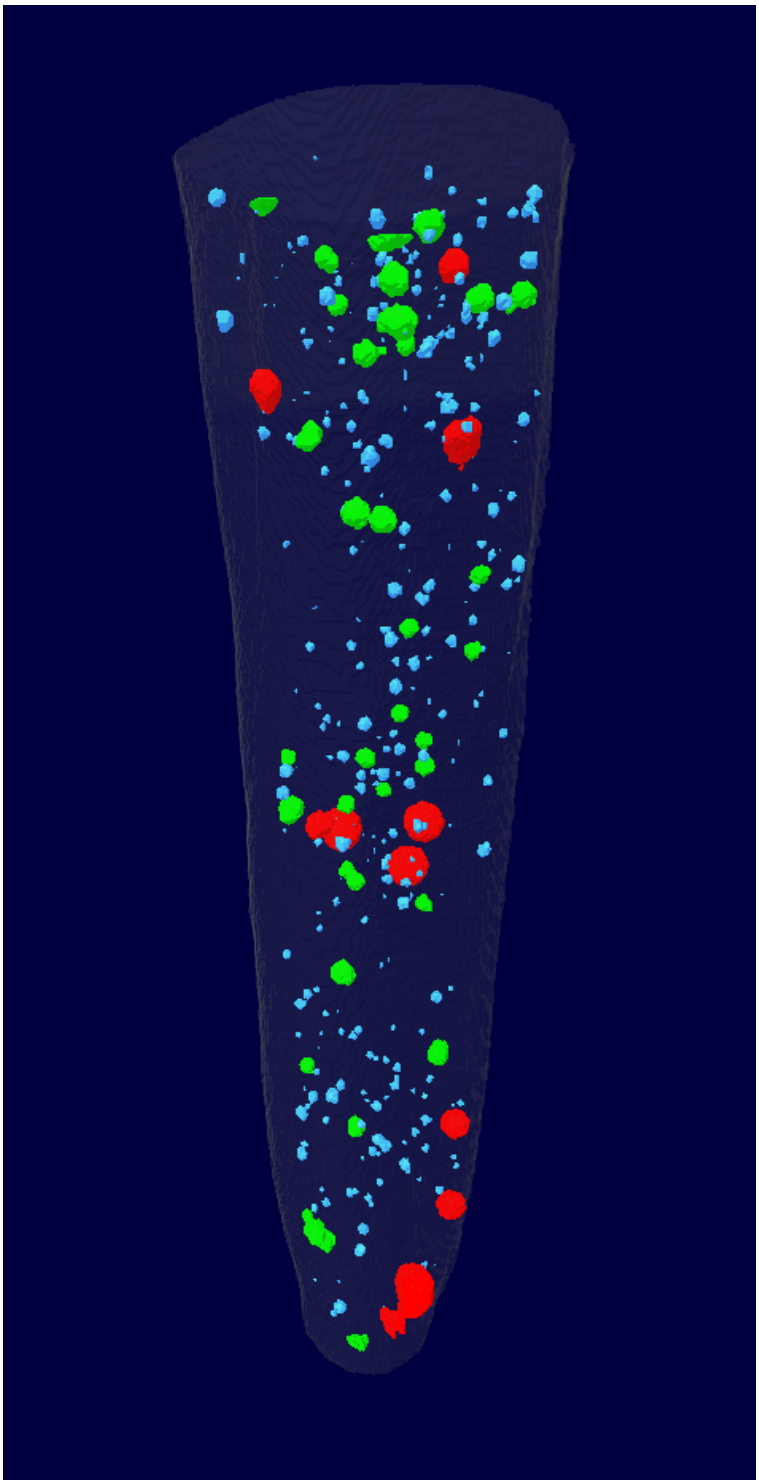

XFP specimen 11
Void volume: 0.6mm^3
Void volume fraction: 2.9%

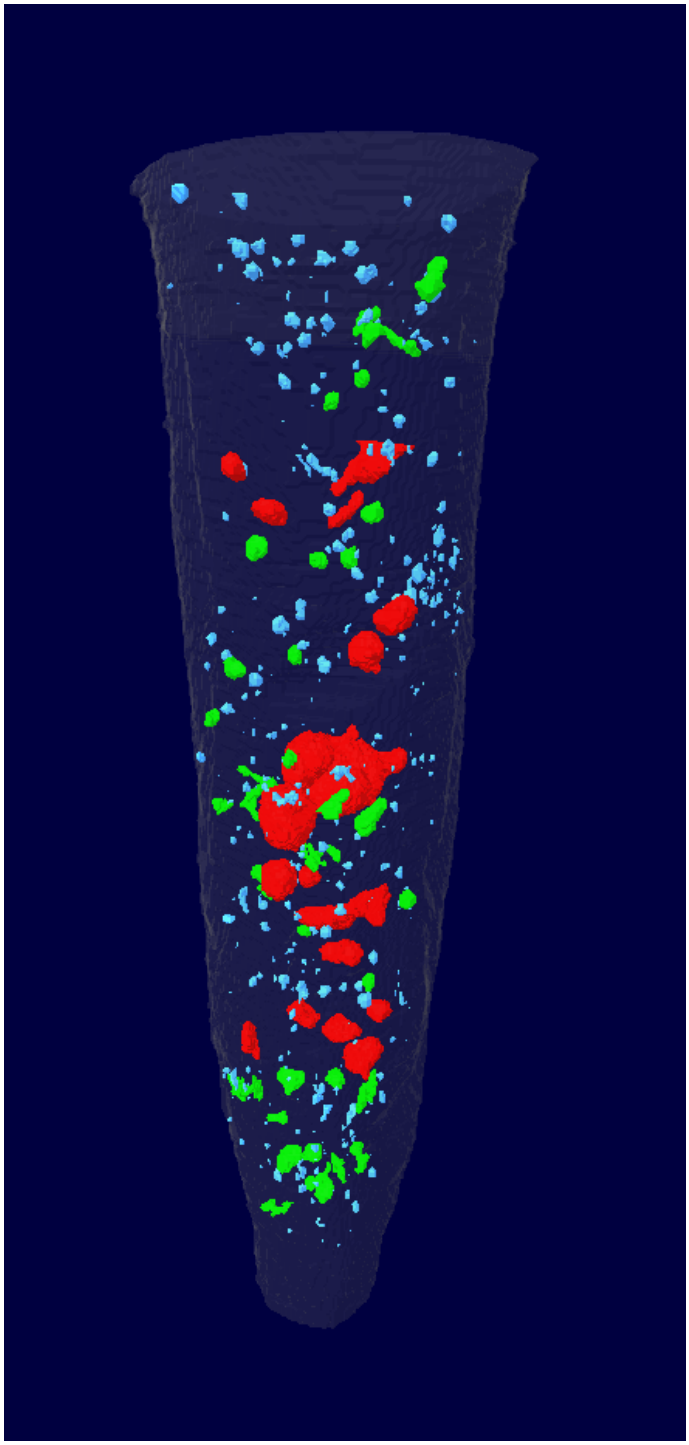

XFP specimen 12
Void volume: 1.1mm^3
Void volume fraction:4.9 %

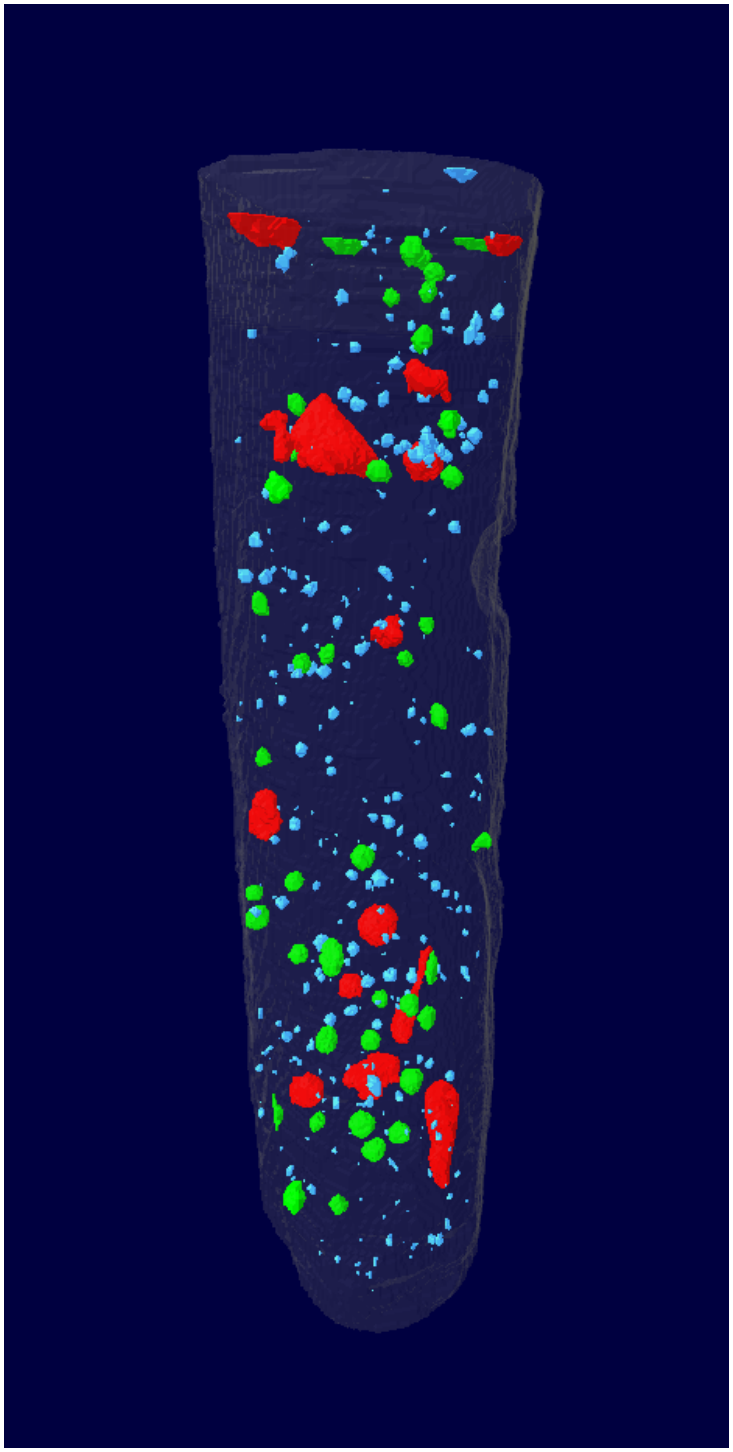

XFP specimen 13
Void volume: 0.8mm^3
Void volume fraction: 3.9%

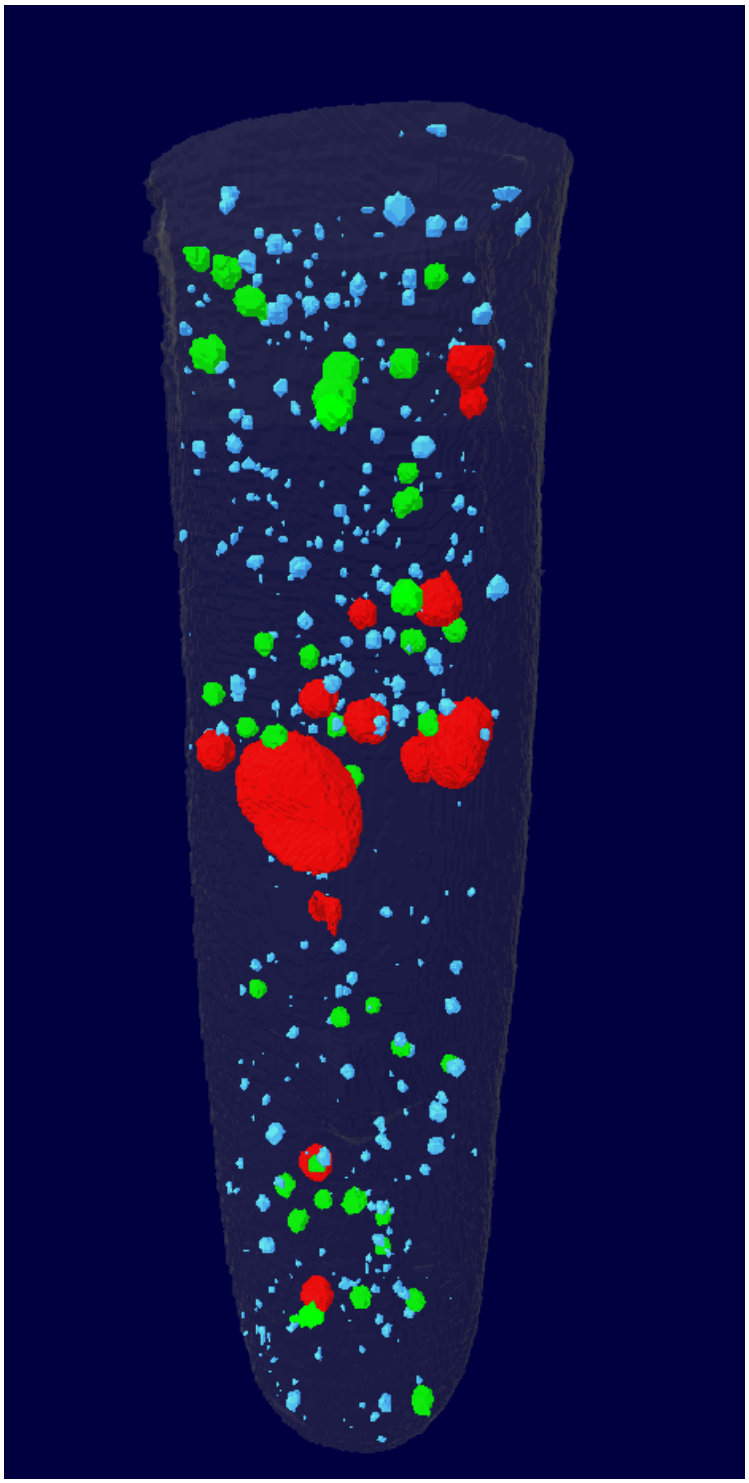

XFP specimen 14
Void volume: 0.6mm^3
Void volume fraction: 3.5%

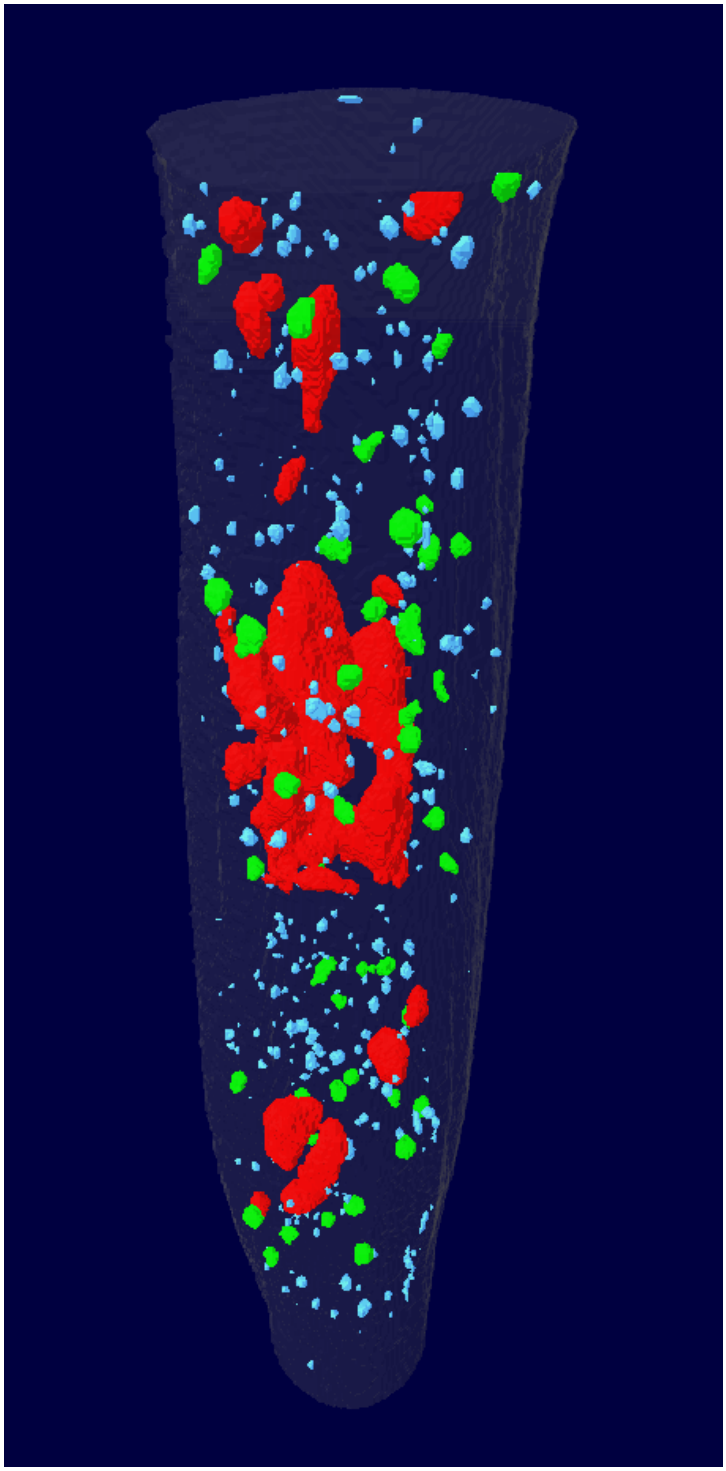

XFP specimen 15
Void volume: 1.3mm^3
Void volume fraction: 4.9%

Appendix 4. Publication:

AlZahrani, F. and Richards, L. (2018) 'Micro-CT evaluation of a novel periodontal ligament simulation technique for dental experimental models', Archives of Orofacial Science, 13(2).

This paper describes a work completed during an earlier phase (pilot study) of the PhD. It describes a simple technique to construct the tooth-PDL-bone experimental model with a reproducible PDL layer of a uniform width. This paper has been published in the Archives of Orofacial Science and attached in the next page.

Statement of contribution by the authors

Title: Micro-CT evaluation of a novel periodontal ligament simulation technique for dental experimental models

Authors: F AlZahrani and L Richards

F AlZahrani: was primarily responsible for this project. F AlZahrani designed and co-ordinated the study, conducted the experiments, and collected and interpreted the data.

L Richards: assessed in designing the study and interpreting the data. L Richards provided critical comments and general supervision.

F AlZahrani and L Richards were involved with the preparation of the manuscript.

L Richards gives written permission for this paper to be included in F AlZahrani thesis titled “An in vitro study of the failure of short glass-fibre reinforced composite post and core restoration of endodontically treated teeth”.

..

F AlZahrani **L Richards**

Archives of Orofacial Sciences
www.dental.usm.my/aos/ © Penerbit Universiti Sains Malaysia. 2018
print ISSN: 1823-8602
e-ISSN: 2231-7163

Arch Orofac Sci (2018), **13**(2): 93-103.

Original Article

Micro-CT evaluation of a novel periodontal ligament simulation technique for dental experimental models

Fawzia AlZahrani*, Lindsay Richards

Adelaide Dental School, Faculty of Health and Medical Sciences, The University of Adelaide, Adelaide, South Australia, 5005 Australia.

* Corresponding author: fawzia.alzahrani@adelaide.edu.au

Submitted: 19/08/2018. Accepted: 29/11/2018. Published online: 29/11/2018.

Abstract A reliable technique for simulation of the periodontal ligament (PDL) is required for *in vitro* studies. This paper proposes a simple technique to construct a tooth-PDL-bone experimental model with a reproducible PDL layer of a uniform width. In a preliminary study, two PDL simulation techniques were compared; transitional wax technique: wax layer was used to create a space for the PDL simulating material (light-body silicon) and direct rubber application technique: PDL simulating material (rubber die-spacer) was painted directly on the root surface. In both techniques, teeth were mounted in acrylic resin to simulate the supporting bone. The tooth-PDL-bone models were scanned using SkyScan 1076 micro-CT scanner and PDL-layer width was measured at selected sites on the roots using CTAn software. Based on the results of the preliminary study, 10 experimental models were constructed using the direct rubber application technique to confirm the reproducibility and consistency of the PDL layer width using micro-CT. Intra-class correlation coefficients (ICC) were calculated to assess the reproducibility. The transitional wax technique showed significantly greater variability in the PDL layer width when compared with the direct rubber application technique ($F=66.0$, $p<0.001$). The direct rubber application technique showed excellent reproducibility (ICC= 0.94; 95% confidence interval: 0.86, 0.98).

Keywords: Experimental model; micro-CT; periodontal ligament; rubber; simulation.

Introduction

Well-designed laboratory-based dental investigations permit a preliminary assessment of the likely clinical suitability of new dental products and procedures. *In vitro* investigations of teeth and dental restorative materials response to both static and dynamic occlusal loads have been extensively documented in the literature (Newman *et al*., 2003; Sahafi *et al*., 2005; Abdul Salam *et al*., 2006; Fokkinga *et al*., 2006a; Ambica *et al*., 2013; Adanir *et al*., 2015). Such investegations require construction of dental experimental models that simulate oral and clinical conditions. It has been recognized that mechanical behavior of the experimental models is influenced by parameters such as the physical and biomechanical properties of the tested material (Assif and Gorfil, 1994; Cheung, 2005), the nature of the applied load (Caplan *et al*., 2002; Naumann *et al*., 2005), the remaining tooth structure (Iqbal *et al*., 2003; Akkayan, 2004; Stankiewicz and Wilson, 2008), and the simulated supporting apparatus, namely PDL and bone (Soares *et al*., 2005; Brosh *et al*., 2011; Pérez-González *et al*., 2012; Marchionatti *et al*., 2014). Nevertheless, some, but not all, laboratory-based investigations simulate the PDL layer in the experimental models.

Evaluation of dental experimental model that comprise a simulated PDL layer in contrast to a model that lacks this feature has often appeared in the literature (Soares *et al*., 2005; Brosh *et al*., 2011; Pérez-González *et al*., 2012; Marchionatti *et al*., 2014). The results suggested that the presence of a PDL layer permits the realistic simulation of tooth movement with uniform stresses distribution within the artificial PDL material (Brosh *et al*., 2011). It has also been demonstrated that the presence of a PDL-simulating material modifies the mode of fracture when subjecting the models to occlusal loads (Soares *et al*., 2005). This has been supported by finite element modeling/analyses (FEM/FEA) that have evaluated different approaches to build

numerical computed dental models (Cattaneo *et al*., 2005; Chen *et al*., 2005; Aversa *et al*., 2009). These studies have shown that the inclusion of a simulated PDL modifies the stress (Chen *et al*., 2005) and strain (Aversa *et al*., 2009) distribution in the computed models. It has been concluded that PDL simulation is a crucial step in FEA models construction (Cattaneo *et al*., 2005; Chen *et al*., 2005; Aversa *et al*., 2009) and recommended to include a simulated PDL in experimental models (Rosentritt *et al*., 2011; González-Lluch *et al*., 2016).

The decision on whether or not to include a PDL layer in the experimental models varies among researchers. PDL was simulated in the experimental models in several *in vitro* studies that applied both linear (Akkayan and Gülmez, 2002; Newman *et al*., 2003; Fokkinga *et al*., 2006b; Krastl *et al*., 2014) and dynamic compressive loads (Rosentritt *et al*., 2004; Sahafi *et al*., 2005; Naumann *et al*., 2006; Balkenhol *et al*., 2011; Pereira *et al*., 2014). On the other hand, Naumann *et al.* (2009) reviewed the study designs of sixty-nine dental laboratory studies and found that 50% of the studies that applied a dynamic testing protocol and 72% of the studies that applied a linear compressive loads have not simulated the PDL (Naumann *et al*., 2009). Some researchers exclude the PDL simulation step to avoid complicating the test design (Cormier *et al*., 2001; Hu *et al*., 2003; Marchi *et al*., 2008). Other researchers believe that the presence of a PDL layer will cause dislodgement of the tooth during testing, which interferes with the accurate assessment of the material being investigated (Martínez-González *et al*., 2001; Al-Omiri and Al-Wahadni, 2006).

Natural PDL has irreplaceable functional and structural roles. Healthy PDL consists of collagen fiber bundles that are arranged in different directions around the tooth to provide attachment and support during mastication (Lindhe *et al*., 2008). The cellular content of the PDL facilitates fiber and bone remodeling in response to pathological conditions as in periodontal diseases or in response to orthodontic tooth movement (Lindhe *et al*., 2008). The extracellular fluid motion in the PDL provides a hydrostatic and damping reaction to protect the tooth in response to physiological forces (Natali *et al*., 2004; Komatsu, 2010). PDL mobility is determined largely by the PDL width, height and structural quality. The healthy PDL is situated within the alveolar bone proper and continuously surrounds the root with a width that ranges between 0.2 to 0.4 mm (average of 0.25mm) (Lindhe *et al*., 2008).

To represent the structural and functional features of the PDL, different simulating techniques and materials with variable PDL thicknesses have been documented in the *in vitro* studies (Bortoluzzi *et al*., 2007; Nishimura *et al*., 2008; Büttel *et al*., 2009; McLaren *et al*., 2009; Ayad *et al*., 2011; Rosentritt *et al*., 2011; Sterzenbach *et al*., 2011; Barcellos *et al*., 2013; Palamidakis *et al*., 2013; Marchionatti *et al*., 2014). The tooth-PDL-bone dental experimental model consists of the tooth root surrounded by a resilient material (representing the PDL) and embedded in a rigid material (representing the bone). The most commonly used technique to build this model involves several steps (Akkayan, 2004; Bortoluzzi *et al*., 2007; Marchionatti *et al*., 2014). It starts with covering the root with a transitional isolating material before mounting in the bone representative material. The transitional material acts as a spacer that is discarded and replaced with the resilient, PDL simulating material. While, petroleum jelly (Brosh *et al*., 2011), wax (Bortoluzzi *et al*., 2007; Marchionatti *et al*., 2014) and aluminum foil (Akkayan, 2004) have been used as transitional isolating materials, a wide range of PDL simulating materials with different properties and consistencies have been used by researchers. These include; addition silicone (Nishimura *et al*., 2008; Ayad *et al*., 2011), condensation silicone (Barcellos *et al*., 2013; Palamidakis *et al*., 2013; Pereira *et al*., 2014), polyether (Rosentritt *et al*., 2004; Balkenhol *et al*., 2011), polyvinyl siloxane (Fokkinga *et al*., 2006a; Krastl *et al*., 2014), polysulfide (Soares *et al*., 2005), polyurethane (Soares *et al*., 2005; Sterzenbach *et al*., 2011) and industrial rubber materials (Naumann *et al*., 2006; McLaren *et al*., 2009).

The documented artificial PDL width varies greatly between studies. While a very thin PDL layer of 0.1 mm width has been reported (Heydecke *et al*., 2001), a thick layer of 1.0 mm width has also been documented (Rosentritt *et al*., 2006). The majority of the documented simulated PDL layer widths

have been in the range of 0.2- 0.3 mm (Soares *et al.*, 2005; Büttel *et al.*, 2009; Balkenhol *et al.*, 2011; Krastl *et al.*, 2014). However, there is some uncertainty regarding the achievement of this width in experimental models. Despite its popularity, a major limitation of the transitional isolating material technique is the absence of confirmation that the purported material width has been achieved accurately and uniformly around the root. Simulating the natural PDL width and continuity is assumed to be a fundamental requirement to achieve a realistic response of the experimental model to the applied load in *in vitro* studies (Hu *et al.*, 2003; Al-Omiri and Al-Wahadni, 2006; Marchi *et al.*, 2008). Failure to achieve this could negatively affect the accuracy of the mechanical tests results and therefore, the PDL is considered as an unintended variable in the study design. Also, and more importantly, the reproducibility and consistency of the simulated PDL among experimental models often have been overlooked by researchers.

Therefore, this paper aims to evaluate the uniformity and reproducibility of the frequently applied PDL simulation technique that involves utilization of wax as a transitional isolating material and to compare it with an alternative, novel and simple PDL-simulation technique.

Materials and methods

Approval of the study was obtained from the Faculty of Health Science at the University of Adelaide (No. H2014-237). A preliminary study was first conducted to evaluate the PDL layer uniformity and root coverage quality for the transitional wax technique and a proposed PDL simulation technique. The transitional wax technique followed previous studies protocols (Soares *et al.*, 2005; Bortoluzzi *et al.*, 2007; Marchionatti *et al.*, 2014). The proposed PDL simulation technique involved a direct construction of the PDL layer around the root without a transitional isolating material step. Based on the results of the preliminary study, subsequent micro-CT verification was conducted on 10 experimental models to confirm the reproducibility of the PDL in the proposed simulation technique.

Single-rooted human teeth were used to construct tooth-PDL-bone experimental models for all investigatory procedures. All roots were cleaned from calculus, deposits and any attached soft tissue using an ultrasonic scaler before commencing the experimental models' construction. On all teeth, a line representing the simulated alveolar bone crest was placed on the root surface 1mm apical to the cemento-enamel junction (CEJ) as illustrated in figure 1. A second line was placed 2mm below the CEJ (1 mm below the first line) to mark the coronal limit of the PDL (Nugala *et al.*, 2012). All experimental steps were performed by one operator.

Tooth-PDL-bone experimental model construction

Transitional wax technique

In this PDL simulation technique, wax was used as the isolating medium to create a space for the PDL around the root. The root was immersed for two seconds into a liquefied (60°C) base-plate wax (Kerr Dental, Orange, CA, USA) until the root is completely covered with the wax up to the lower line marked on the root. This creates a wax layer around the root that is approximately 0.3 mm thick (Marchionatti *et al.*, 2014). A cylindrical brass mould was filled with autopolymerising acrylic resin (ProBase Cold, Ivoclar Vivadent, Schaan, Liechtenstein) to represent the alveolar bone surrounding the tooth. Using sticky wax, the tooth was attached to the vertical rod of the dental surveyor (J.M. Ney Company, Bloomfield, CT, USA) to maintain the tooth vertical orientation in the acrylic resin mould. The filled mould was placed on the surveyor-base directly below the tooth-vertical rod assembly. The tooth-rod assembly was lowered into the autopolymerising acrylic resin filled mould until the higher marking on the root is reached. The tooth was secured in this position until the acrylic resin is fully polymerized. A putty index of the mounted tooth in the acrylic resin mould was made to assess in tooth repositioning in the block at a later stage.

The tooth was removed from the fully polymerized acrylic resin and the wax spacer around the root was removed using hot water and hand instrument. A socket for the root

and the artificial PDL layer was created inside the acrylic resin block. A light-body silicon impression material (Imprint 4, 3M ESPE, MN, USA) was injected into the resultant root socket in the acrylic block to simulate the PDL layer. The tooth was relocated immediately into the socket and secured in the original place using the putty index. After setting of the impression material, the excess impression material was removed using a scalpel blade.

Novel PDL-simulation technique (Direct rubber application technique)

In this technique, an artificial PDL material, latex rubber die-spacer (Rubber-Sep, Kerr Dental, Orange, CA, USA) was applied directly to the root surface using the accompanying brush. The material was applied up to the lower line marked on the root in successive coats until the desired width was reached. According to the manufacturer, each coat has a thickness of 12 µm, and to achieve a selected PDL width of approximately 0.25 mm, twenty coats of the rubber material were applied. Each coat required few seconds to dry before the application of the next coat. The tooth was then mounted in the acrylic resin block as described previously. After setting of the acrylic resin, tooth-PDL-bone experimental model was created (Fig. 1).

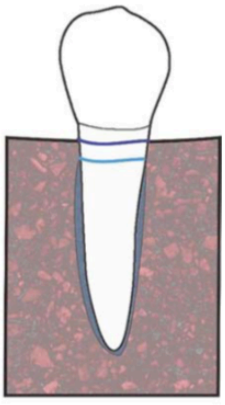

Fig. 1 A schematic drawing of the tooth-PDL-bone experimental model with two lines drown on the root; top line represents the simulated alveolar bone crest, and the bottom line represents the height of the simulated PDL.

Micro-CT scanning and analyses

Experimental models were scanned using a micro-CT SkyScan 1076 (Bruker Micro-CT, Kontich, Belgium) scanner. Before scanning, the fully polymerized acrylic resin blocks containing the teeth were removed from the brass cylinders to avoid radiographic artifacts. The tooth-PDL-bone model was secured to a mounting foam holder that facilitated proper positioning in the carbon-composite bed inside the micro-CT scanner chamber. The acquisition parameters were set and saved to ensure consistency of the scanning procedure of all teeth (voltage; 50 Kv, current; 160 MA, resolution; 9 µm, rotation step; 0.8°, rotation; 180°, frame averaging; 2). The projected raw images were saved as Tag Image File Format (TIFF) files.

NRecon software (SkyScan, version 1.6.9.4) was used to reconstruct and combine the projected images of the models. After importing to NRecon software, one cross-section was previewed to set the parameters to ensure maximum contrast and visualization of different parts of the viewed images. These parameters include smoothing, beam-hardening correction, malalignment compensation and thresholding. The same parameters were used for all cross-sections of all scanned models to create bitmap format (BMP) files.

The reconstructed BMP files of the scanned models were then visualized in three orthogonal views (coronal, sagittal and trans-axial) using Data-Viewer software (SkyScan, version 1.5.1.2). The dataset was saved for further analysis. CTvox software (SkyScan, version 3.0.0.0) was used for detailed three-dimensional reconstruction and assessment of the models.

Using the Data-Viewer software images dataset, CTAn software (SkyScan, version 1.14.4.1) was used to measure the width of the simulated PDL layer in both techniques. The measurements were performed at three predetermined sections on the root (coronal, middle and apical) in the sagittal plane images. The most coronal measurements were performed in the cross-section that was located three millimeters below the CEJ. The middle measurements were performed in the cross-section that was located three-

millimeter below the previous one and the apical measurements were performed in the cross-section that was located three-millimeter below the middle one. In each section, the measurements of the PDL material width were performed in the mid-buccal (M-B), mid-lingual (M-L), mid-distal (M-D) and mid-mesial (M-M) in the trans-axial plane images. All measurements were recorded in millimeters.

CTvox and Data-Viewer software images were inspected visually to evaluate the simulated PDL material adhesion to the root, uniformity and overall coverage quality. Mean (± SD) for the PDL layer widths were calculated for all points on root sections for experimental models of both techniques.

Direct rubber application technique reproducibility verification

On the basis of the preliminary data on both techniques, the transitional wax technique was not pursued, and micro-CT scanning and data analysis were performed for 10 experimental models constructed using the direct rubber application technique to verify the technique reproducibility.

Mean and the standard deviation for the CTAn software recorded widths were calculated for each point of every predetermined root section. To confirm the reproducibility of the PDL layer width, an Intra-class Correlation Coefficient (ICC) was calculated using Stata Statistical Software (Release 14. College Station, TX: StataCorp LP). This estimates correlations between individual and average PDL layer widths made by the same experimental model, “raters”. In this sense, “raters” are the four-point CTAn measurements recorded for the three root sections, in each experimental model (total of 12 “raters” /experimental model). The ICC measures the strength of inter-“raters” reliability. Cicchetti (1994) interpreted the ICC values less than 0.4 as “poor” inter-rater reliability, between 0.40 and 0.59 as “fair”, between 0.60 and 0.74 as “good” and between 0.75 and 1.00 as “excellent”.

Results

Preliminary results

The PDL layer simulated in the preliminary study was first visually assessed on micro-CT images. Figures 2a, 2b and 2c show root cross-sections of the transitional wax technique experimental model. Figures 3a, 3b and 3c show root cross-sections of the direct rubber application technique experimental model. The PDL layer in the direct rubber application technique is closely adherent to the root with a uniform and continuous coating, as displayed in the images. In the images of the transitional wax technique, the PDL layer is unevenly distributed on the root with loss of attachment between the PDL layer and the root, which appeared as spaces between the surfaces.

The results of the CTAn software measurements for the transitional wax technique and the direct rubber application techniques are presented in Table 1. The data shows that the PDL layer width was inconsistent in the transitional wax technique with PDL width ranging from 0.00-0.42 mm. On the other hand, the PDL layer simulated by direct rubber application technique shows less variation ranging from 0.20-0.27 mm. Interestingly the mean width for both groups across all sites was 0.24 mm but the transitional wax technique widths were significantly more variable ($F=66.0$, $p<0.001$).

Direct rubber application technique reproducibility verification results

Mean (±SD) of the PDL layer widths simulated by the direct rubber application technique are presented in Table 2. The mean of the PDL layer width was between 0.24±0.006 and 0.25±0.004 in the coronal section, 0.25± 0.003 and 0.25±0.005 in the middle section and 0.24±0.006 and 0.25±0.002 in the apical section. The calculated ICC value for the average width measurements was found to be 0.94 (95% confidence interval: 0.86-0.98). According to Cicchetti (1994) interpretation, 0.94 indicates an excellent inter-“raters” reliability.

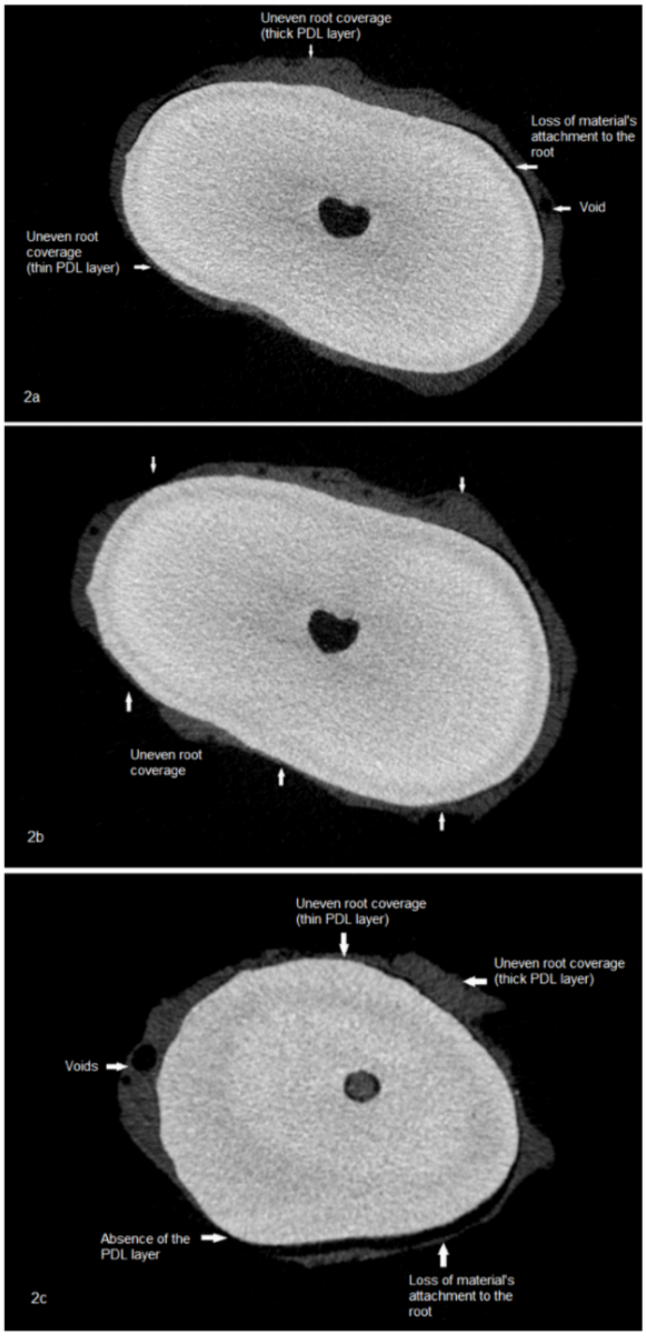

Figure. 2a, 2b and 2c Micro-CT images of PDL simulated with transitional wax technique at different trans-axial sections. Note the loss of material's attachment to the root surface in some areas (presented as a space between the PDL material and the root in all sections), voids and uneven root coverage.

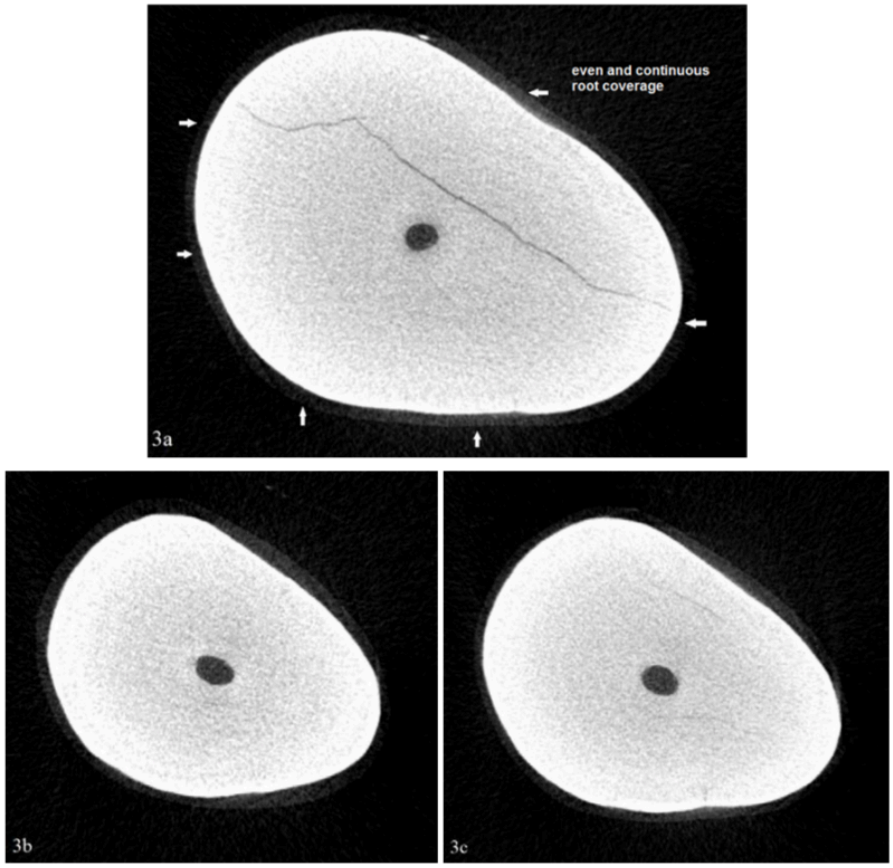

Figure. 3a, 3b and 3c Micro-CT images of PDL simulated with direct rubber application technique at different trans-axial sections. Note even root coverage in all sections.

Table 1 Width of PDL layer measured for both techniques in the preliminary study

Measurement levels		Coronal section				Middle section				Apical section				Mean ± SD
		M-B	M-L	M-M	M-D	M-B	M-L	M-M	M-D	M-B	M-L	M-M	M-D	
Transitional wax technique	model 1	0.35	0.41	0.02	0.38	0.20	0.28	0.00	0.35	0.22	0.40	0.35	0.16	0.24 ± 0.14*
	model 2	0.42	0.24	0.00	0.2	0.36	0.28	0.26	0.00	0.42	0.23	0.09	0.24	
Direct rubber application technique	model 1	0.20	0.22	0.25	0.25	0.25	0.25	0.25	0.24	0.25	0.25	0.26	0.25	0.24 ± 0.02
	model 2	0.27	0.25	0.25	0.24	0.21	0.24	0.24	0.23	0.26	0.26	0.26	0.24	

* Variation differs significantly; F=66.0, p<0.001. M-B: mid-buccal, M-L: mid-lingual, M-D: mid-distal and M-M: mid-mesial

Table 2 Mean and standard deviations of PDL layer width in direct rubber application technique

Sections	Coronal Section				Middle Section				Apical Section			
	M-B	M-L	M-M	M-D	M-B	M-L	M-M	M-D	M-B	M-L	M-M	M-D
Mean	0.25	0.24	0.25	0.25	0.25	0.25	0.25	0.25	0.25	0.20	0.24	0.25
SD	0.004	0.006	0.004	0.003	0.004	0.003	0.005	0.006	0.003	0.002	0.006	0.002

Discussion

When compared to clinical studies, laboratory-based dental studies permit standardization of specimens and testing parameters as well as control of experimental variables (Naumann *et al*., 2005; 2009). Additionally, laboratory studies can be conducted at a reasonable cost and over a shorter duration. However, creating an experimental protocol and model that simulates dental structures and oral cavity conditions is crucial to laboratory-based studies. The inclusion of a PDL layer in experimental models has been endorsed in the literature despite the acknowledged variability in techniques and materials (Soares *et al*., 2005; Brosh *et al*., 2011; Rosentritt *et al*., 2011; González-Lluch *et al*., 2016).

The direct PDL simulation technique proposed in this paper employs a latex rubber material that is originally designated as a die spacer for laboratory-constructed dental restorations. This material is supplied in a liquid form that allows direct application of controlled uniform thin coatings. According to the manufacturer, applying a thin coat using the accompanying brush results in approximately 12 μm thickness layer. This facilitates simulation of a planned PDL width and height on the root and ensures consistency and reproducibility among the experimental models.

The function of the wax layer in the transitional wax technique is to create a space between the root and the simulated alveolar bone that is to be filled with the PDL simulating material at a later stage. Therefore, the accuracy of wax layer thickness in this technique is a prerequisite for the accuracy of the PDL simulation. However, the consistency, thickness, and uniformity of the wax layer were difficult to control and verify. Furthermore, the technique is complicated and involves many steps and materials, which increases the chance of variation between the created experimental models.

Although the light-body impression material was the material of choice to simulate the PDL in most documented study designs (Akkayan, 2004; Soares *et al*., 2005; Brosh *et al*., 2011; Marchionatti *et al*., 2014), there was no guarantee of inter-specimens and intra-specimen uniformity in the PDL layer thickness. Due to the viscosity of the light-body impression material, shear thinning can occur when the root is placed in the impression material-filled socket (Pang and Chai, 1994). Therefore, the material's precise flow and height on the root surface are unknown. This could explain the uneven spread of the impression material on the root surface that was observed in this technique. This is particularly true when considered within the context of the natural unevenness of the root surface and the variation of the created wax thickness. In contrast, direct control of the material thickness was observed when the rubber die-spacer material was applied directly to the root. The paintable nature of the die-spacer permits application of a closely adherent layer on all root irregularities. In addition, the number of coats can be easily decreased or increased to establish a predetermined PDL width.

To date, PDL simulation lack standardization in terms of materials, techniques and dimensions. Most reports have focused on confirming the significance of incorporating a viscoelastic material to simulate the PDL (Natali *et al*., 2004; Cattaneo *et al*., 2005; Chen *et al*., 2005; Soares *et al*., 2005; Marchionatti *et al*., 2014). However, evidence of attaining a reproducible PDL layer in *in vitro* study designs has never been reported.

Micro-CT scanning and analyses were used in this paper to assess the width uniformity of the simulated PDL layer and

quality of root coverage. Micro-CT is an advanced, modern and non-destructive investigation tool that has been utilized recently in various contexts in dental research (Swain and Xue, 2009). It requires minimal specimen preparation but allows high- resolution qualitative and quantitative specimen assessments through the commercially available software. The CTAn software data indicated that the desired artificial PDL material width in the direct rubber application technique is achieved uniformly with insignificant variability. This can be explained by the simplicity of the simulation technique, which does not involve multiple steps, and materials. On the other hand, the transitional wax technique showed significantly variable PDL width along the root surface, and most importantly, absence of the material in some areas around the root. This was confirmed by the trans-axial micro-CT images of the experimental models of both techniques (Figures 2a, 2b, 2c, 3a, 3b and 3c).

ICC is an inferential statistical method, which evaluates how strongly experimental models resemble each other in terms of quantitative measurements. In other words, ICC allows the assessment of reproducibility of a procedure and/or consistency of measurements. The experimental models constructed following the direct rubber application technique indicated excellent resemblance to each other with regard to the PDL width around the root. This confirms the reproducibility of the PDL layer simulated by the direct rubber application technique.

Within the limitations of this study, it has been concluded that the technique and material used for PDL simulation for *in vitro* experimental models affect the accuracy and reproducibility of the simulated PDL layer. In addition to technique simplicity, the paintable rubber material that is coated directly on the root surface can produce a continuous, uniform and reproducible artificial PDL layer for dental experimental models. However, further research is recommended to evaluate the viscoelasticity of the die-spacer rubber material and its effect on the mechanical behavior of the experimental models.

Acknowledgments

The authors thank Ms. Ruth Williams in Adelaide Microscopy department, the University of Adelaide for her assistance in micro-CT scanning and image analysis, and Ms. Suzanne Edwards in Adelaide Health Technology Assessment department, the University of Adelaide for her aid with statistics.

Declaration

The authors declare no conflicts of interest.

References

Abdul Salam SN, Banerjee A, Mannocci F, Pilecki P, Watson TF (2006). Cyclic loading of endodontically treated teeth restored with glass fibre and titanium alloy posts: Fracture resistance and failure modes. *Eur J Prosthodont Restor Dent*, **14**(3): 98-104.

Adanir N, Ureyen Kaya B, Kececi AD (2015). Fracture resistance of roots restored with four different fiber-reinforced composite posts. *Med Princ Pract*, **24**(6): 538-543.

Akkayan B (2004). An in vitro study evaluating the effect of ferrule length on fracture resistance of endodontically treated teeth restored with fiber-reinforced and zirconia dowel systems. *J Prosthet Dent*, **92**(2): 155-162.

Akkayan B, Gülmez T (2002). Resistance to fracture of endodontically treated teeth restored with different post systems. *J Prosthet Dent*, **87**(4): 431-437.

Al-Omiri MK, Al-Wahadni AM (2006). An ex vivo study of the effects of retained coronal dentine on the strength of teeth restored with composite core and different post and core systems. *Int Endod J*, **39**(11): 890-899.

Ambica K, Mahendran K, Talwar S, Verma M, Padmini G, Periasamy R (2013). Comparative evaluation of fracture resistance under static and fatigue loading of endodontically treated teeth restored with carbon fiber posts, glass fiber posts, and an experimental dentin post system: An in vitro study. *J Endod*, **39**(1): 96-100.

Assif D, Gorfil C (1994). Biomechanical considerations in restoring endodontically treated teeth. *J Prosthet Dent*, **71**(6): 565-567.

Aversa R, Apicella D, Perillo L, Sorrentino R, Zarone F, Ferrari M *et al.* (2009). Non-linear elastic three-dimensional finite element analysis on the effect of endocrown material rigidity on alveolar bone remodeling process. *Dent Mater*, **25**(5): 678-690.

Ayad MF, Bahannan SA, Rosenstiel SF (2011). Influence of irrigant, dowel type, and root-reinforcing material on fracture resistance of thin-walled endodontically treated teeth. *J Prosthodont*, **20**(3): 180-189.

Balkenhol M, Rupf S, Laufersweiler I, Huber K, Hannig M (2011). Failure analysis and survival rate of post and core restorations under cyclic loading. *Int Endod J*, **44**(10): 926-937.

Barcellos RR, Correia DP, Farina AP, Mesquita MF, Ferraz CC, Cecchin D (2013). Fracture resistance of endodontically treated teeth restored with intra-radicular post: The effects of post system and dentine thickness. *J Biomech*, **46**(15): 2572-2577.

Bortoluzzi EA, Souza EM, Reis JM, Esberard RM, Tanomaru-Filho M (2007). Fracture strength of bovine incisors after intra-radicular treatment with MTA in an experimental immature tooth model. *Int Endod J*, **40**(9): 684-691.

Brosh T, Porat N, Vardimon AD, Pilo R (2011). Appropriateness of viscoelastic soft materials as in vitro simulators of the periodontal ligament. *J Oral Rehabil*, **38**(12): 929-939.

Büttel L, Krastl G, Lorch H, Naumann M, Zitzmann NU, Weiger R (2009). Influence of post fit and post length on fracture resistance. *Int Endod J*, **42**(1): 47-53.

Caplan DJ, Kolker J, Rivera EM, Walton RE (2002). Relationship between number of proximal contacts and survival of root canal treated teeth. *Int Endod J*, **35**(2): 193-199.

Cattaneo PM, Dalstra M, Melsen B (2005). The finite element method: A tool to study orthodontic tooth movement. *J Dent Res*, **84**(5): 428-433.

Chen WP, Lee BS, Chiang YC, Lan WH, Lin CP (2005). Effects of various periodontal ligament elastic moduli on the stress distribution of a central incisor and surrounding alveolar bone. *J Formos Med Assoc*, **104**(11): 830-838.

Cheung W (2005). A review of the management of endodontically treated teeth. Post, core and the final restoration. *J Am Dent Assoc*, **136**(5): 611-619.

Cicchetti DV (1994). Guidelines, criteria, and rules of thumb for evaluating normed and standardized assessment instruments in psychology. *Psychol Assess*, **6**(4): 284-290.

Cormier CJ, Burns DR, Moon P (2001). In vitro comparison of the fracture resistance and failure mode of fiber, ceramic, and conventional post systems at various stages of restoration. *J Prosthodont*, **10**(1): 26-36.

Fokkinga WA, Kreulen CM, Le Bell-Rönnlöf AM, Lassila LV, Vallittu PK, Creugers NH (2006a). In vitro fracture behavior of maxillary premolars with metal crowns and several post-and-core systems. *Eur J Oral Sci*, **114**(3): 250-256.

Fokkinga WA, Kreulen CM, Le Bell-Rönnlöf AM, Lassila LV, Vallittu PK, Creugers NH (2006b). Fracture behavior of structurally compromised non-vital maxillary premolars restored using experimental fiber reinforced composite crowns. *Am J Dent*, **19**(6): 326-332.

González-Lluch C, Rodríguez-Cervantes PJ, Forner L, Barjau A (2016). Inclusion of the periodontal ligament in studies on the biomechanical behavior of fiber post-retained restorations: An in vitro study and three-dimensional finite element analysis. *Proc Inst Mech Eng*, **230**(3): 230-238.

Heydecke G, Butz F, Strub JR (2001). Fracture strength and survival rate of endodontically treated maxillary incisors with approximal cavities after restoration with different post and core systems: An in-vitro study. *J Dent*, **29**(6): 427-433.

Hu YH, Pang LC, Hsu CC, Lau YH (2003). Fracture resistance of endodontically treated anterior teeth restored with four post-and-core systems. *Quintessence Int*, **34**(5): 349-353.

Iqbal MK, Johansson AA, Akeel RF, Bergenholtz A, Omar R (2003). A retrospective analysis of factors associated with the periapical status of restored, endodontically treated teeth. *Int J Prosthodont*, **16**(1): 31-38.

Komatsu K (2010). Mechanical strength and viscoelastic response of the periodontal ligament in relation to structure. *J Dent Biomech*, **2010**:502318.

Krastl G, Izquierdo A, Büttel L, Zitzmann NU, Schmitter M, Weiger R (2014). Does an intracanal composite anchorage replace posts? *Clin Oral Investig*, **18**(1): 147-153.

Lindhe J, Karring T, Araujo M (2008). The anatomy of periodontal tissues. In: Lindhe J, Lang NP, Karring T (eds.), *Clinical Periodontology and Implant Dentistry, Vol. 2*, 5th edn. Oxford: Blackwell Publishing, pp. 3-49.

Marchi GM, Mitsui FH, Cavalcanti AN (2008). Effect of remaining dentine structure and thermal-mechanical aging on the fracture resistance of bovine roots with different post and core systems. *Int Endod J*, **41**(11): 969-976.

Marchionatti AM, Wandscher VF, Broch J, Bergoli CD, Maier J, Valandro LF *et al.* (2014). Influence of periodontal ligament simulation on bond strength and fracture resistance of roots restored with fiber posts. *J Appl Oral Sci*, **22**(5): 450-458.

Appendix 5. Pairwise comparisons between test groups mean failure loads

Post-hoc multiple pairwise comparisons between test groups mean failure loads (n=45)

Groups multiple comparisons		Estimate	95% confidence interval		P-value
			Lower	Upper	
C	**XFP**	477.95	411.61	544.29	<0.0001
	PFP	835.34	769.00	901.68	<0.00001
XFP	**PFP**	357.39	291.05	423.73	<0.00001

C: Control group; **XFP**: ETT restored with SFRC post, **PFP**: ETT restored with prefabricated FRC post

Appendix 6. Cross tabulation of mode of failure versus tested groups

Mode of failure Row Percentage Colum Percentage	**Control group**	**PFP group**	**XFP group**	**Total**
Crack/chipping of the crown (natural or ceramic)	15 60.00 100.00	5 20.00 33.33	5 20.00 33.33	25
Decementation of the ceramic crown	0 0.00 0.00	5 55.56 33.33	4 44.44 26.67	9
Decementation of post and core	0 0.00 0.00	1 100.00 6.67	0 0.00 0.00	1
Restoration bulk fracture (tooth fracture above CEJ)	0 0.00 0.00	0 0.00 0.00	6 100.00 40.00	6
Deep tooth fracture (below CEJ)	0 0.00 0.00	4 100.00 26.67	0 0.00 0.00	4
Total	15	15	15	45

XFP: ETT restored with SFRC post, **PFP**: ETT restored with prefabricated FRC post
Fisher's Exact Test P-value = 0.0123

Appendix 7. SEM micrographs of fractured XFP specimens

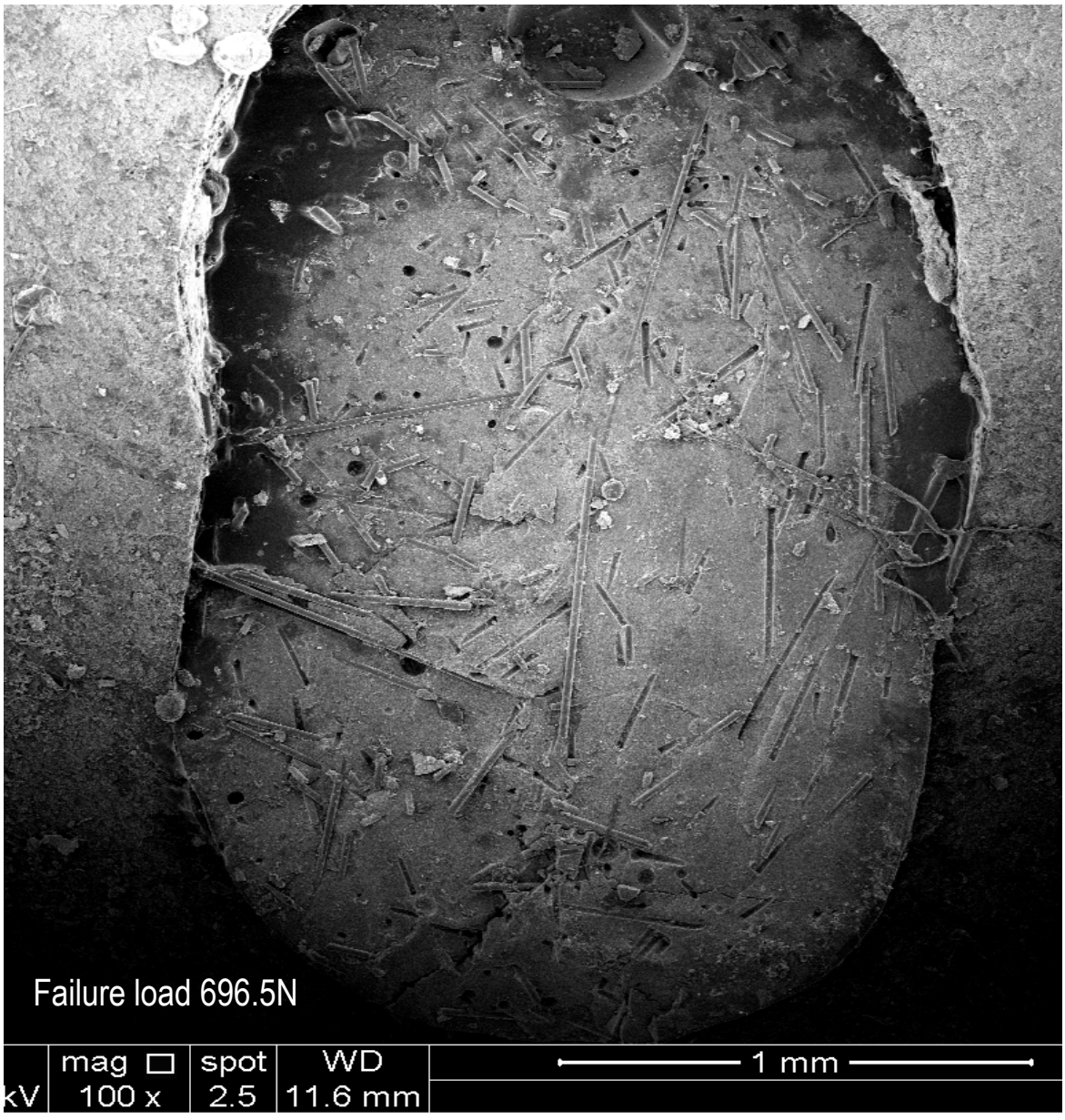

XFP specimen failed at 696.5N showing a fracture surface with relatively uniform fibres distribution that are present in high quantity with dominance of transversely oriented long fibres.

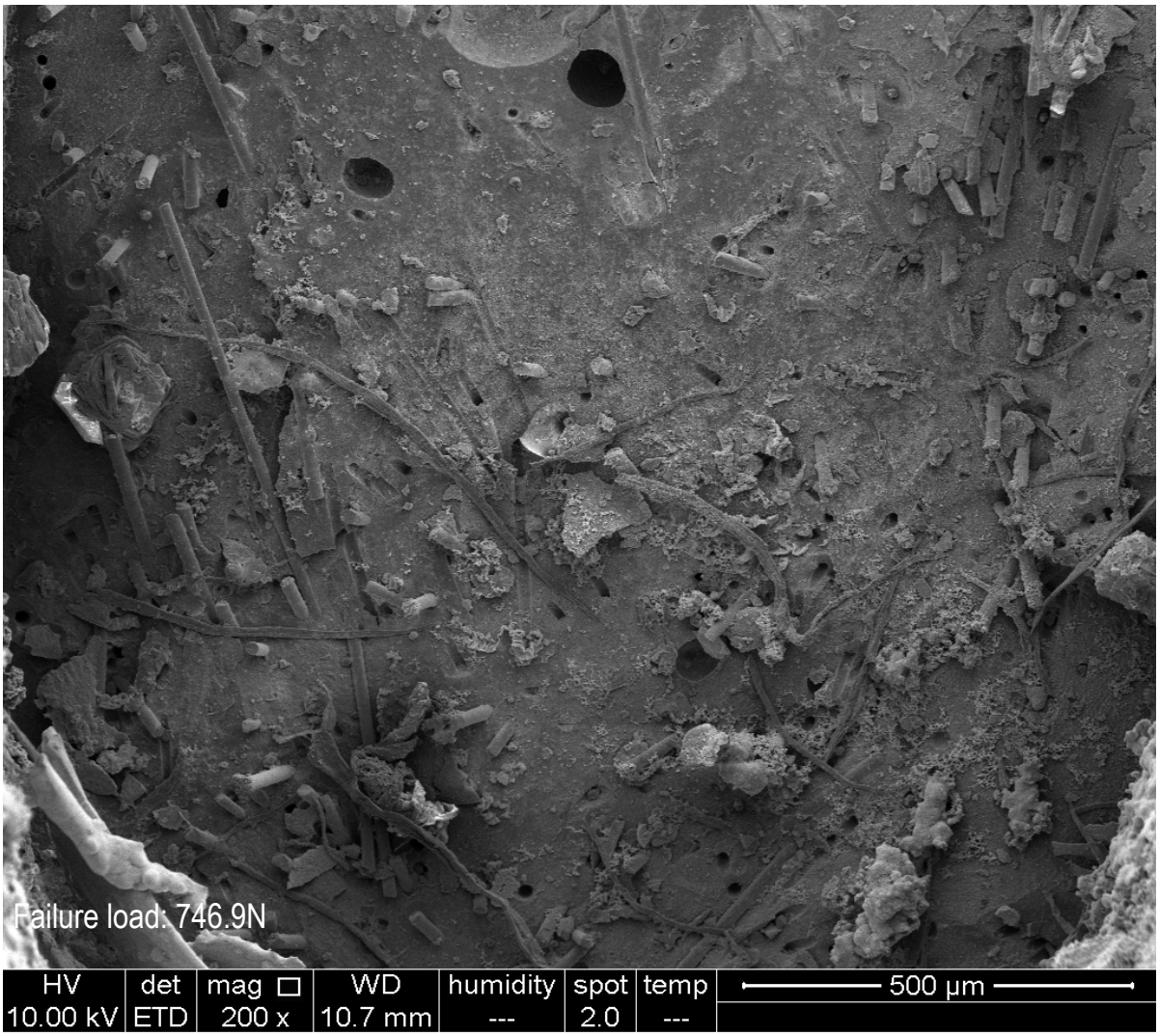

XFP specimen failed at 746.9N showing a fracture surface with dominance of multidirectional fibres that are unevenly distributed.

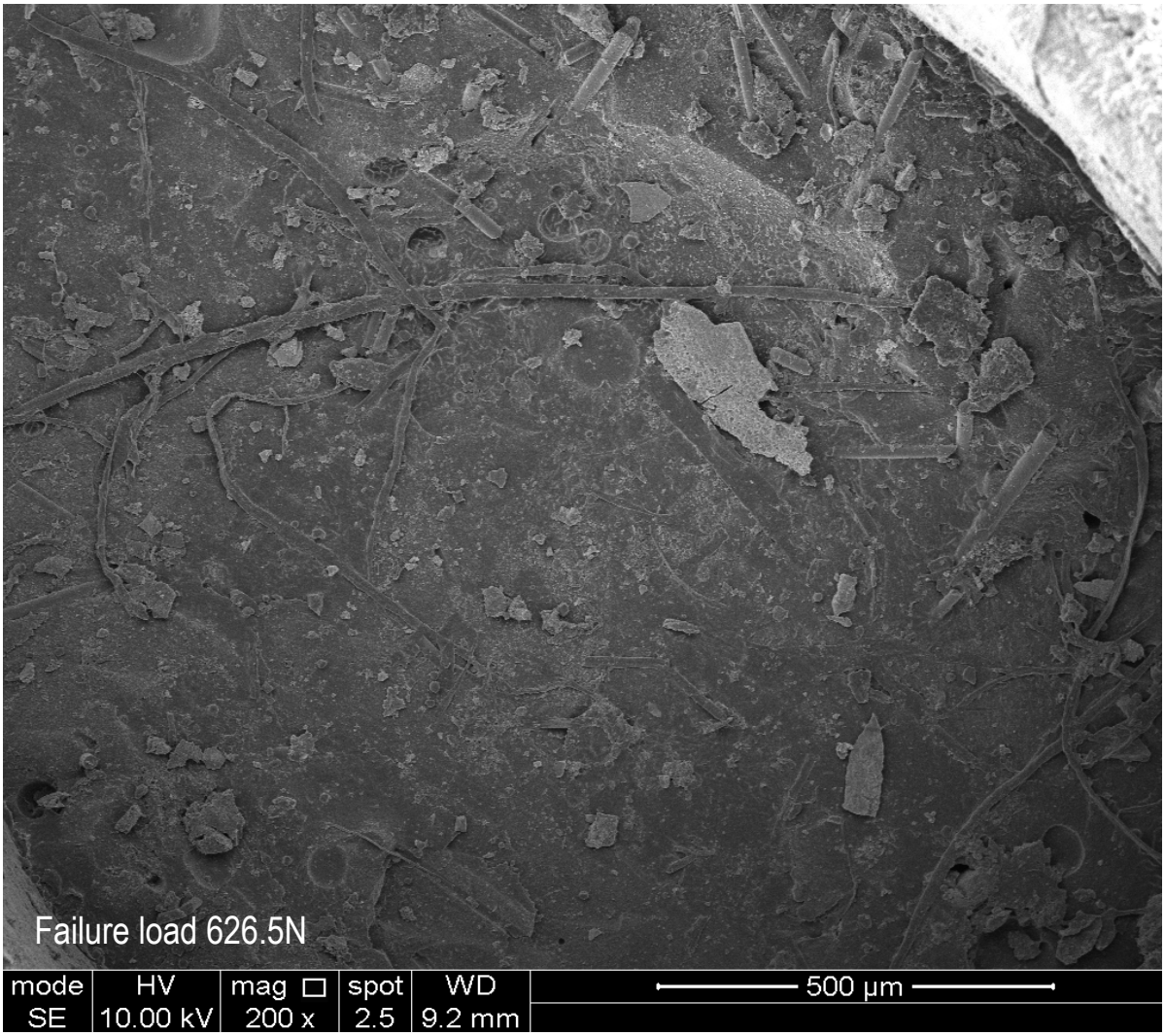

XFP specimen failed at 626.5N showing a fracture surface with multidirectional fibres that present in low quantity and are unevenly distributed

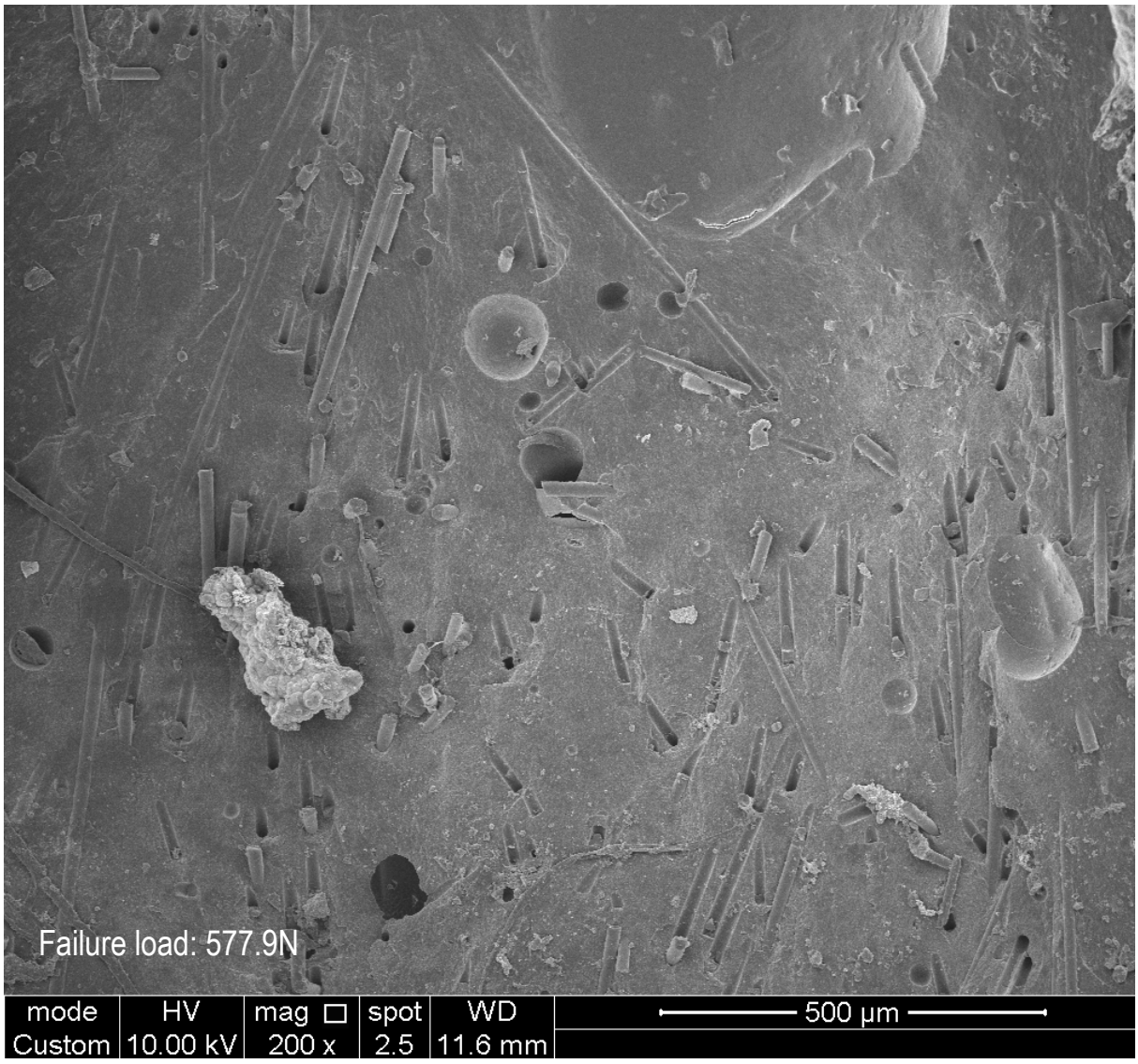

XFP specimen failed at 577.9N showing a fracture surface with low fibre content and dominance of transvers fibres orientation and debonded fibres.

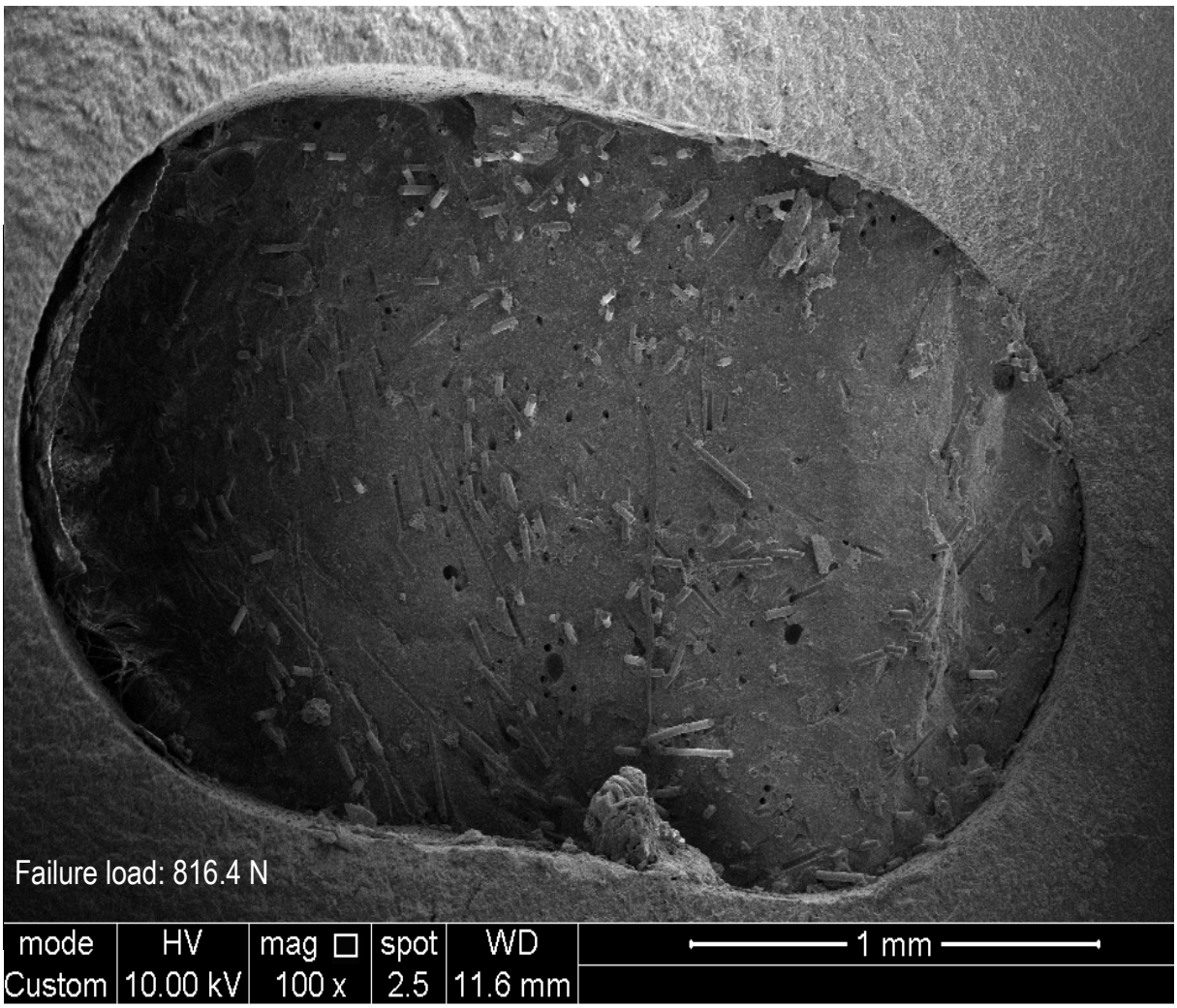

XFP specimen failed at 816.4N showing a fracture surface with uniform multidirectional fibres distribution that are present in high quantity.

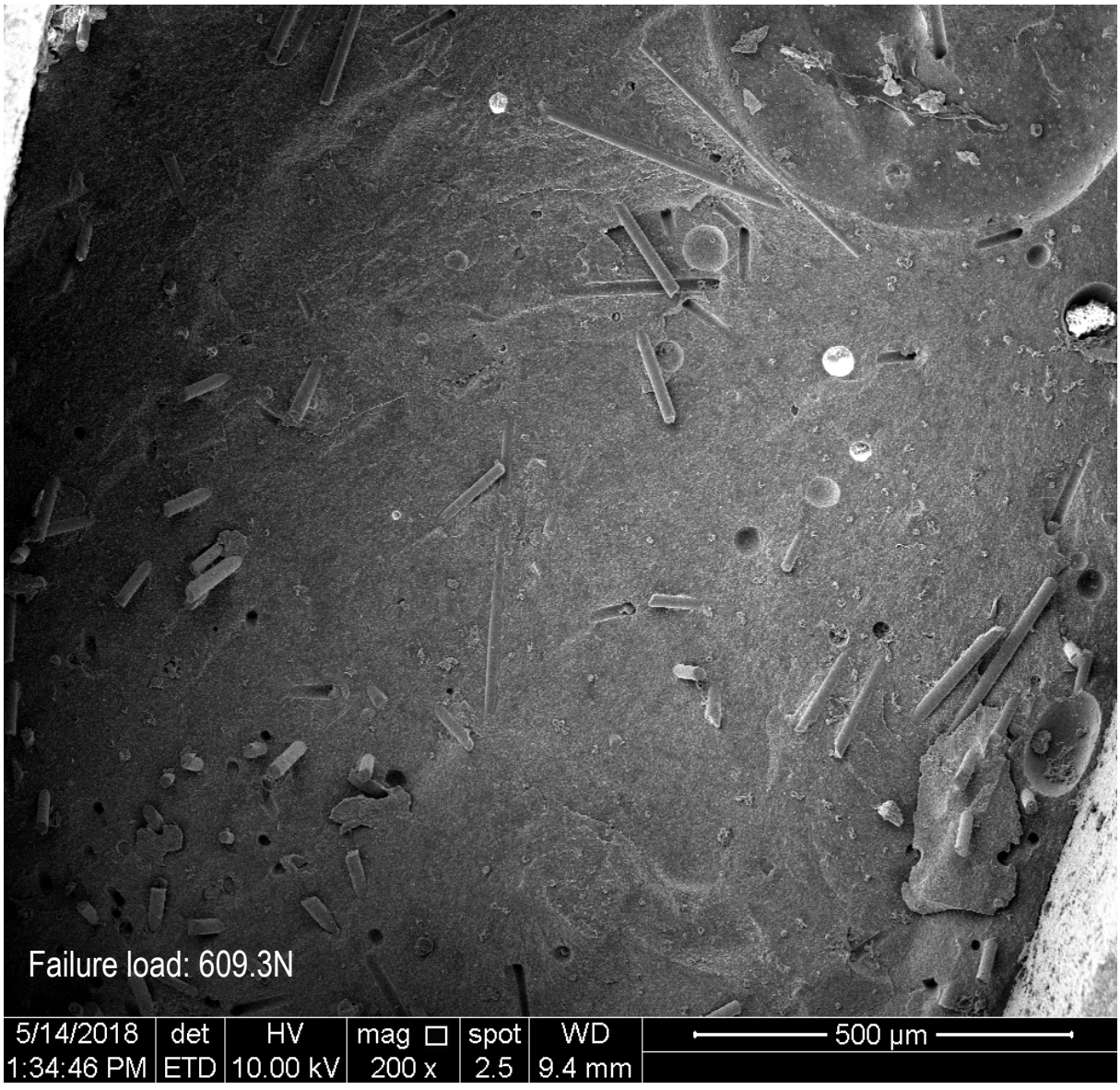

XFP specimen failed at 609.3N showing a fracture surface with low fibre content and dominance of transverse fibre orientation that are unevenly distributed